

LONDON
SCHOOL of
HYGIENE
& TROPICAL
MEDICINE



**INVESTIGATION OF THE RELATIONSHIP BETWEEN cGMP SIGNALLING
AND CALCIUM MOBILISATION IN *PLASMODIUM FALCIPARUM* WITH A
FOCUS ON THE ROLE OF PHOSPHODIESTERASES IN SEXUAL
DEVELOPMENT**

Eloise Maeve Walker

**Thesis submitted in accordance with the requirements
for the degree of Doctor of Philosophy**

University of London

August 2017

Department of Pathogen Molecular Biology

Faculty of Infectious and Tropical Diseases

LONDON SCHOOL OF HYGIENE AND TROPICAL MEDICINE

Supervisor: Professor David Baker



All of the time and work that has gone into this thesis is dedicated solely to my Mum, who we tragically lost to cancer at the end of 2015. My Mum always had faith in me even when I had no faith in myself and throughout this PhD journey, whenever I doubted my ability, was always the first person to tell me that I could do it.

Alexandra Louise Thompson

I hope that scientists, in the near future will be able to win the battle against devastating diseases such as cancer and malaria so that precious and much loved lives such as my Mums will no longer be lost before they should be.



DECLARATION OF OWN WORK

All students are required to complete the following declaration when submitting their thesis. A shortened version of the School's definition of Plagiarism and Cheating is as follows (*the full definition is given in the Research Degrees Handbook*):

"Plagiarism is the act of presenting the ideas or discoveries of another as one's own. To copy sentences, phrases or even striking expressions without acknowledgement in a manner which may deceive the reader as to the source is plagiarism. Where such copying or close paraphrase has occurred the mere mention of the source in a biography will not be deemed sufficient acknowledgement; in each instance, it must be referred specifically to its source. Verbatim quotations must be directly acknowledged, either in inverted commas or by indenting" (University of Kent).

Plagiarism may include collusion with another student, or the unacknowledged use of a fellow student's work with or without their knowledge and consent. Similarly, the direct copying by students of their own original writings qualifies as plagiarism if the fact that the work has been or is to be presented elsewhere is not clearly stated.

Cheating is similar to plagiarism, but more serious. Cheating means submitting another student's work, knowledge or ideas, while pretending that they are your own, for formal assessment or evaluation.

Supervisors should be consulted if there are any doubts about what is permissible.

DECLARATION BY CANDIDATE

I have read and understood the School's definition of plagiarism and cheating given in the Research Degrees Handbook. I declare that this thesis is my own work, and that I have acknowledged all results and quotations from the published or unpublished work of other people.

I have read and understood the School's definition and policy on the use of third parties (either paid or unpaid) who have contributed to the preparation of this thesis by providing copy editing and, or, proof reading services. I declare that no changes to the intellectual content or substance of this thesis were made as a result of this advice, and, that I have fully acknowledged all such contributions.

I have exercised reasonable care to ensure that the work is original and does not to the best of my knowledge break any UK law or infringe any third party's copyright or other intellectual property right.

To be completed by the candidate

NAME IN FULL (*Block Capitals*):

STUDENT ID NO:

SIGNED:

DATE

Abstract

Malaria kills almost half a million people every year and is a huge public health burden particularly in Sub-Saharan Africa. The current first line treatment is very effective but is threatened by the drug resistance that has been seen in the many effective compounds that have come before it. Consequently, there is a real need to develop new and novel compounds that target multiple stages of the parasite life cycle, as failure of our first line treatment could be devastating. Cell signalling pathways regulate essential events in the parasite lifecycle and as such, components of these pathways are potential targets for parasite disruption. The cyclic nucleotide and Ca^{2+} signalling cascades have essential functions at multiple stages in the parasite life cycle and often show overlap in their roles. This means that inhibition of one such pathway may disrupt the other. The relationship between 3'-5'-cyclic guanosine monophosphate and Ca^{2+} signalling is investigated here using Ca^{2+} assays on both schizont and gametocyte stages using a combination of genetic and pharmacological approaches. Results indicate that zaprinast-induced Ca^{2+} release through PDE inhibition is dependent upon PKG and in schizonts occurs via inositol triphosphate. Gametogenesis is an essential lifecycle event leading to transmission. The PDE *PfPDE δ* has been implicated in this event, however little is known about this enzyme. Using a *PfPDE δ* -ko line and the generation of a HA-tagged *PfPDE δ* line using the CRISPRCas9 gene editing system, this project seeks to confirm whether *PfPDE δ* is essential for gametogenesis and to understand more about the role that this protein plays in this event. This includes its cellular localisation, cyclic nucleotide specificity and its role in Ca^{2+} mobilisation, an event essential to the later stages of gametogenesis. The role of *PfPDE δ* in erythrocyte-infected gametocyte deformability is also investigated and the phenotype of a *PfPDE δ* -ko line is dissected. This information will eventually aim to determine whether *PfPDE δ* would be a good transmission-blocking target. Of particular interest to this thesis are compounds that would prevent transmission because currently the only licenced antimalarial to target transmission stages is Primaquine. A combination of a transmission-blocking agent with one that will inhibit asexual replicating stages would both alleviate clinical symptoms while preventing transmission. PDEs have already been identified and used as effective drug targets in humans. A small panel of Pfizer PDE inhibitors that have shown good activity in asexual blood stages has been tested against the gametocyte stages and this has led to the identification of a human PDE inhibitor that not only kills asexual blood stages in the low nM range, but also one that can kill gametocyte stages at similar concentrations. In addition to this, the mode of action of this compound has been determined.

Acknowledgements

First and foremost, I would like to thank my PhD supervisor, Professor David Baker who I respect as a scientist, a line manager and as a person. Thank you Dave for the invaluable advice and guidance throughout this PhD and more importantly, for giving me the opportunity to do this PhD in the first place. I would like to thank my friend, colleague and PhD advisor Dr Christian Flueck who has given me a lot of help and guidance particularly with my *PfPDE δ* -HA transgenic line. Thank you for all your help and advice and also, for the many helpful discussions related to my work over the years. Thank you also for being such fun company at work. I would like to extend my thanks to the rest of the Baker group past and present, particularly, Dr Avnish Patel and Stephanie Nofal who I really value as colleagues. I'm lucky to work with such nice, clever people and I always appreciate your advice. I would like to thank my friends and ex-Baker group colleagues Dr Laura Drought and Dr Christine Hopp, who are both wonderful, valued friends and who have been a huge support to me over the years. Many thanks to Mathieu Brochet and Catherine Lavazec with whom I collaborated to produce the phospholipid and deformability data respectively, both leading to publication. Thank you to both Elizabeth McCarthy and Rachel Gregory for help on the confocal microscope. This work wouldn't have been possible without the following lines and the people who worked hard to make them; *PfPDE α* -ko (Christian Flueck), *PfPDE β* conditional knock down (Laura Drought), *PfPDE δ* -ko and *PfPDE γ* -ko (Cathy Taylor), *PfPKG_{T618Q}* (Louisa McRobert), *PfPKG-dd* (Manoj Duraisingh and Jeffrey Dvorin). *3D7elo1-pfs16-CBG99* (Pietro Alano). I would also like to thank my dear friends Jessica Jones, Selina Bannoo and Colette Quan who are like sisters to me and never fail to offer love and support whenever I need it. Thank you to James, Richard and Babsey for kindly spending the time to read my introduction and to Dave for having to read the whole thing. I would also like to thank my dad, Michael Elkin, for his support and advice over the years and my much-loved brothers and sisters, Luke, Amber, Sam, Tabby and Georgia. I'm lucky to have such a wonderful, loving and supportive family. Lastly, but definitely not least (although I'm sure he thinks he should be first on the list!), I would like to thank my wonderful husband James, who has been so supportive and patient over the last years of my PhD. I wouldn't have been able to do this without you particularly given the circumstances in the last two years. Thank you for your love and support and for always giving me the 'you can do it' pep talk when I needed it. Thank you for being patient when you have a wife you hardly ever see and who is tired and stressed when you do. I am lucky to have you as my husband.

Table of Contents

Abstract.....	4
Acknowledgements.....	5
Contents.....	6
List of Figures and Tables.....	10
List of Abbreviations	14
Chapter 1: Introduction.....	17
1.1 Malaria	17
1.1.1 A brief history of malaria	19
1.1.2. The life cycle of <i>Plasmodium falciparum</i>	20
1.1.3. Key Interventions	24
1.1.3.A. Malaria diagnosis.....	24
1.1.3.B. Malaria vaccine development	24
1.1.3.C. Targeting the vector	26
1.1.3.D. Targeting the parasite: drug treatment and prophylaxis.....	26
1.2 Cell signaling.....	33
1.2.1. Cyclic nucleotide signalling	34
1.2.1.A. Key players in cyclic nucleotide signalling	36
1.2.2 Calcium (Ca ²⁺) signalling.....	55
1.2.3 Cell signalling in the asexual blood stages	59
1.2.4 Cell signalling in gametocytogenesis	62
1.2.5 Cell signalling in gametogenesis	65
1.2.6 A relationship between Ca ²⁺ signalling and PKG.....	69
1.3 Introduction summary	70
1.4 Aims and Objectives.....	71
Chapter 2: Materials and Methods.....	72
2.1. Parasite preparation	72
2.1.1. <i>P. falciparum</i> parasite culture.....	72
2.1.A. <i>P. falciparum</i> asexual culture	72
2.1.B. <i>P. falciparum</i> gametocyte initiation and culture	72
2.1.C. Preparation and Giemsa staining of thin blood films	73
2.2. <i>P. falciparum</i> synchronization and purification	74
2.2.A. <i>P. falciparum</i> sorbitol synchronization of early asexual stages.....	74
2.2.B. <i>P. falciparum</i> magnetic purification of mature asexual and gametocyte stages	74
2.2.C. <i>P. falciparum</i> Percoll purification of mature asexual stages and gametocytes.....	75
2.2.D. <i>P. falciparum</i> Compound 2 synchronization of mature asexual stages	75

2.3. Parasite sample preparation.....	76
2.3.A. Parasite sample preparation for immunoblotting and immunoprecipitation	76
2.3.B. Lipid extraction for electrospray mass spectrometry.....	77
2.3.C. Ring stage parasite sample preparation for transfection.....	77
2.4. Fluorescence techniques.....	78
2.4.A. Calcium release assay	78
2.4.B. Immunofluorescence assay	80
2.4.C. Luciferase Assay: Gametocyte viability assay.....	83
2.4.D. Live cell confocal microscopy	84
2.5. Gametocyte assays.....	85
2.5.A. Identifying the effect of PF9 on PKA-inhibited <i>PfPDEδ</i> -ko gametocytes.....	85
2.5.B. Identifying the effect of XA on PKA-inhibited <i>PfPDEδ</i> -ko gametocytes	85
2.5.C. PF9 dose response assay	86
2.5.D. PF9 time course assay	87
2.5.E. Rounding up assay	87
2.5.F. Microsphiltration assay.....	88
2.5.G. Phosphodiesterase assay	88
2.6. Molecular techniques	90
2.6.A. Transformation of competent <i>E. coli</i> cells	90
2.6.B. Miniprep for extraction of DNA.....	90
2.6.C. Restriction digest	91
2.6.D. DNA fragment clean up	91
2.6.E. DNA fragment ligation	92
2.6.F. Infusion cloning with oligos	92
2.6.G. MaxiPrep	93
2.6.H. Transfection.....	93
2.6.I. Polymerase chain reaction (PCR).....	94
2.7. <i>PfPDEδ</i> -HA line Assays	95
2.7.A. SDS-PAGE gel electrophoresis	95
2.7.B. Western blotting.....	95
2.7.C. Immunoprecipitation of <i>PfPDEδ</i> -HA	96
Chapter 3: Investigation into the relationship between cGMP signalling and Ca²⁺ release in <i>Plasmodium falciparum</i>	98
3.1. Introduction	98
3.2. Results.....	101
3.2.1 Zaprinast-induced Ca ²⁺ release in <i>P. falciparum</i> schizonts.....	101

3.2.2 Zaprinast-induced Ca ²⁺ release in stage V gametocytes.....	112
3.3. Discussion.....	119
Chapter 4: Investigation into the role of phosphodiesterases in distinct stages of gametocyte development using genetic and pharmacological approaches	127
4.1. Introduction	127
4.2. Results.....	130
4.2.1 Investigation into the effects of PDE inhibition on gametocyte deformability	130
4.2.2 Investigation into the effect of PDE inhibition on rounding up and emergence of <i>P. falciparum</i> gametocytes	132
4.2.3 Investigation into a possible link between the ‘stiff’ phenotype of the <i>PfPDEδ</i> -ko line and its inability to round up	140
4.2.4 Investigation into the effects of genetic and pharmacological phosphodiesterase disruption on Ca ²⁺ mobilisation	150
4.3. Discussion.....	155
Chapter 5: The mode of action of a gametocytocidal PDE inhibitor	165
5.1. Introduction	165
5.2. Results.....	168
5.2.1 The human PDE inhibitor PF9 shows potent activity against mature <i>P. falciparum</i> gametocytes.....	168
5.2.2 Investigation of the PDE target of PF9.....	172
5.2.3 PF9 causes rounding up of mature gametocytes and acts within 5 minutes of addition.....	181
5.2.4 Investigation into the mode of action of PF9	183
5.2.4.1. PF9 induces rounding up of wildtype stage V gametocytes.....	183
5.2.4.2. PF9 induces emergence of gametes from the host erythrocyte	193
5.2.4.3. PF9 induces exflagellation of 3D7a male gametes	196
5.2.4.4. PF9 induces PKG-dependent Ca ²⁺ release in stage gametocytes of the 3D7a line.....	197
5.3. Discussion.....	199
5.3.1 PF9 inhibition of viability	199
5.3.2 <i>PfPDE</i> target of PF9 in stage V gametocytes.....	200
5.3.3 PF9 mode of action on stage V gametocytes.....	203
5.3.4 Discussion summary	209
Chapter 6: Generation of a <i>PfPDEδ</i>-HA tagged transgenic line	210
6.1. Introduction	210
6.2. Results.....	212

6.2.1 The design and generation of a transgenic <i>PfPDEδ</i> -HA tagged line using the CRISPR-Cas9 gene editing system	212
6.2.2 <i>PfPDEδ</i> -HA gives a faint signal by immunofluorescence assay.....	217
6.2.3 <i>PfPDEδ</i> -HA partially co-localises with the Golgi marker ERD2	221
6.2.4 Purification of HA tagged <i>PfPDEδ</i> -HA by immunoprecipitation from gametocyte lysates	222
6.2.5 cGMP (but not cAMP) hydrolytic activity is detected in immunoprecipitated <i>PfPDEδ</i> -HA protein from stage IV/V gametocyte lysate	224
6.2.6 <i>PDE</i> inhibition reduces both cAMP and cGMP hydrolytic activity in mature gametocyte stages	226
6.3. Discussion.....	230
Chapter 7: General Discussion	233
7.1. Project overview	233
7.2. A relationship between cGMP signaling and calcium mobilisation	234
7.3. Generation of a <i>PfPDEδ</i> haemagglutinin- tagged transgenic line for use as a tool to study the role of <i>PfPDEδ</i> in gametocyte stages.....	239
7.4. A role for <i>PfPDEδ</i> in gametocyte infected erythrocyte deformability	241
7.5. A possible sex-specific role for <i>PfPDEδ</i> in gametogenesis	244
7.6. The Pfizer human PDE inhibitor, PF9 as a gametocytocidal compound	247
7.7. General summary of discussion	249
References	250
Appendix.....	282

List of Tables and Figures

Figure 1.1	The full lifecycle of <i>Plasmodium falciparum</i>	P21
Figure 1.2	Schematic of the basic cyclic nucleotide cascade	P35
Figure 1.3	Schematic of the structure and domain organisation of the 11 human PDE families[1]	P42
Figure 1.4	Detection of <i>PfPDE</i> α mRNA levels in <i>P. falciparum</i> parasite stages	P44
Figure 1.5	Detection of <i>PfPDE</i> β mRNA levels in <i>P. falciparum</i> parasite stages	P45
Figure 1.6	Detection of <i>PfPDE</i> γ mRNA levels in <i>P. falciparum</i> parasite stages	P46
Figure 1.7	Detection of <i>PfPDE</i> δ mRNA levels in <i>P. falciparum</i> parasite stages	P48
Figure 1.8	Chemical structures of C1 and C2	P52
Figure 1.9	Schematic depicting the generation of IP ₃ leading to Ca ²⁺ mobilisation from the ER	P56
Figure 2.1	Representative graph depicting measurement of levels of Ca ²⁺ with time in the Ca ²⁺ release assay.	P71
Figure 2.2	Schematic showing PDE-Delta-HA and PL6 plasmid digest and fragment ligation	P92
Figure 3.1	Ca ²⁺ release in Fluo-4 loaded 3D7a segmented schizonts stimulated with zaprinast	P102
Figure 3.2	Ca ²⁺ release in Fluo-4 loaded <i>PfPKG</i> _{T618Q} segmented schizonts stimulated with zaprinast	P103
Figure 3.3	The effects of C2 on zaprinast-stimulated Ca ²⁺ levels in Fluo-4-AM-loaded 3D7a line schizonts.	P104
Figure 3.4	Zaprinast-induced Ca ²⁺ release in the presence of C2 in Fluo-4-AM-loaded 3D7a schizonts over time.	P105
Figure 3.5	The effects of C2 on zaprinast-stimulated Ca ²⁺ levels in Fluo-4-AM-loaded <i>PfPKG</i> _{T618Q} line schizonts.	P106
Figure 3.6	Zaprinast-induced Ca ²⁺ release in the presence of C2 in Fluo-4-AM-loaded <i>PfPKG</i> _{T618Q} line schizonts over time.	P107
Figure 3.7	The effects of C2 on zaprinast-stimulated Ca ²⁺ levels in Fluo-4-AM-loaded <i>PfPKG</i> -DD line schizonts.	P109
Figure 3.8	Changes in levels of PIP ₂ and PIP ₃ over time in mature <i>P. falciparum</i> schizonts, in response to zaprinast treatment in the presence of C2 in the wildtype 3D7a line compared to the gatekeeper mutant <i>PfPKG</i> _{T618Q} .	P111
Figure 3.9	Changes in levels of PI and PIP over time in mature <i>P. falciparum</i> schizonts, in response to zaprinast treatment in the presence of C2 in the wildtype 3D7a line compared to the gatekeeper mutant <i>PfPKG</i> _{T618Q} .	P111
Figure 3.10	Ca ²⁺ release in Fluo-4-AM-loaded 3D7a stage V gametocytes.	p112

Figure 3.11	Ca ²⁺ release in Fluo-4-AM-loaded <i>Pf</i> PKG _{T618Q} line stage V gametocytes.	p115
Figure 3.12	C2 reduction of zaprinast or XA-induced Ca ²⁺ release in <i>Pf</i> PKG _{T618Q} gametocytes compared to gametocytes of the wildtype line.	p115
Figure 3.13	Live confocal microscopy of Fluo-4-AM loaded 3D7a stage V gametocytes before (A) and directly after (B) XA addition.	p116
Figure 3.14	Images from live confocal microscopy of fluo-4-AM loaded 3D7a stage V gametocytes.	p117
Figure 3.15	Schematic showing rough pattern of fluorescence seen in the live cell microscopy images	p118
Figure 3.16	Schematic showing a model of signalling pathways induced by zaprinast involved in asexual blood stage merozoite egress.	p125
Figure 3.17	Schematic showing a model of signalling pathways activated by XA (orange arrows) and zaprinast (green arrows) that induce gametogenesis.	p126
Figure 4.1	Retention rates of <i>Pf</i> PDEγ-ko and <i>Pf</i> PDEδ-ko stage V gametocytes filtered through a microsphiltration matrix.	p131
Figure 4.2	XA-induced rounding up and emergence in 3D7a gametocytes in the presence and absence of C2.	p133
Figure 4.3	Confocal Images of XA-induced rounding up and emergence in the 3D7a line +/- C2	p133
Figure 4.4	XA induced rounding up and emergence in the <i>Pf</i> PKG _{T618Q} line in the presence and absence of C2	p134
Figure 4.5	Confocal images of XA-induced rounding up and emergence in the <i>Pf</i> PKG _{T618Q} line +/- C2.	p135
Figure 4.6	XA induced rounding up and emergence in the <i>Pf</i> PDEγ-ko line in the presence and absence of C2.	p137
Figure 4.7	Confocal Images of XA-induced rounding up and emergence in the <i>Pf</i> PDEγ-ko line +/- C2	p137
Figure 4.8	XA induced rounding up and emergence in the <i>Pf</i> PDEδ-ko line in the presence and absence of C2.	p139
Figure 4.9	Confocal Images of XA-induced rounding up and emergence in the <i>Pf</i> PDEδ-ko line +/- C2	p139
Figure 4.10	Rounding up of <i>Pf</i> PDEδ-ko stage V gametocytes treated with 10 μM KT5720.	p142
Figure 4.11	Rounding up of <i>Pf</i> PDEδ-ko stage V gametocytes treated with 5 μM KT5720.	p143
Figure 4.12	Rounding up of <i>Pf</i> PDEδ-ko stage V gametocytes treated with 1 μM KT5720.	p144
Figure 4.13	Rounding up of <i>Pf</i> PDEδ-ko stage V gametocytes with no PKA inhibition	p145
Figure 4.14	Addition of KT5720 to stage V gametocytes of the 3D7a line.	p146
Figure 4.15	XA stimulation of <i>Pf</i> PDEδ-ko gametocytes.	p147
Figure 4.16	XA-stimulation of <i>Pf</i> PDEδ-ko gametocytes in the presence of KT5720.	p148
Figure 4.17	XA-stimulated 3D7a stage V gametocytes.	p148
Figure 4.18	Ca ²⁺ release in purified stage V gametocytes of the <i>Pf</i> PDEγ-ko line.	p151
Figure 4.19	Ca ²⁺ release in stage V <i>Pf</i> PDEδ-ko gametocytes.	p152

Figure 4.20	Ca ²⁺ release in stage V <i>PfPDEα</i> -ko gametocytes.	p154
Figure 4.21	Comparison between parasite lines of the <i>PfPKG</i> -specificity of the XA and zaprinast-induced Ca ²⁺ responses.	p154
Figure 4.22	Schematic showing a model of the relationships between cyclic nucleotide signalling, <i>PfPDEδ</i> , gametocyte deformability and gametocyte rounding up and gamete emergence.	p160
Figure 5.1	EC ₅₀ (μM) values of Pfizer PDE inhibitors tested against immature <i>P. falciparum</i> 3D7elo1-pfs16-CBG99 gametocyte stages (II/III) in a gametocyte viability assay.	p170
Figure 5.2	Representative image of a Giemsa-stained blood film taken prior to the start of an immature stage gametocyte luciferase assay.	p171
Figure 5.3	EC ₅₀ (μM) values of Pfizer PDE inhibitors tested against immature <i>P. falciparum</i> 3D7elo1-pfs16-CBG99 gametocyte stages (IV/V) in a gametocyte viability assay.	p171
Figure 5.4	Representative image of a Giemsa-stained blood film taken prior to the start of a mature stage gametocyte viability assay.	p172
Figure 5.5	Parasitaemia of stage IV/V NF54 gametocytes treated with PF9.	p175
Figure 5.6	Parasitaemia of stage IV/V <i>PfPDEγ</i> -ko line gametocytes treated with PF9. <i>PfPDEγ</i> -ko line	p176
Figure 5.7	Parasitaemia of stage IV/V <i>PfPDEα</i> -ko line gametocytes treated with PF9. <i>PfPDEα</i> -ko line	p177
Figure 5.8	Parasitaemia of stage IV/V <i>PfPDEδ</i> -ko line gametocytes treated with PF9.	p179
Figure 5.9	Reduction in number of stage V gametocytes treated with PF9 in the presence and absence of C2.	p180
Figure 5.10	Time course of PF9 treatment of stage V gametocytes from the 3D7a line.	p182
Figure 5.11	Images of Giemsa-stained blood films of 3D7a stage V gametocytes incubated ± PF9	p182
Figure 5.12	Comparison of PF9 treatment in wildtype (3D7a) and <i>PfPDEδ</i> -ko gametocytes.	p184
Figure 5.13	Comparison of XA and PF9 treatment of 3D7a stage V gametocytes.	p185
Figure 5.14	Morphology of 3D7a stage V gametocytes treated with either XA or PF9.	p186
Figure 5.15	Comparison of morphology of PF9 (10 μM) treated and XA-treated (30 μM) 3D7a stage V gametocytes	p187
Figure 5.16	Features of rounded-up parasites (A) compared to non-activated parasites (B)	p187
Figure 5.17	Comparison of XA and PF9 treatment of <i>PfPDEδ</i> -ko line stage V gametocytes.	p188
Figure 5.18	Morphology of <i>PfPDEδ</i> -ko stage V gametocytes treated with either XA or PF9	p189
Figure 5.19	Comparison of PF9 treatment of 3D7a stage V gametocytes to XA and zaprinast treatment.	p191
Figure 5.20	Comparison of PF9 treatment of <i>PfPDEδ</i> -ko line stage V gametocytes to XA and zaprinast treatment.	p192
Figure 5.21	Levels of emergence from host erythrocytes in 3D7a gametocytes treated with PF9 in the presence and absence of C2.	p194

Figure 5.22	Representative images of 3D7a stage V gametocytes stained with WGA coupled to Texas Red to detect emergence of parasites from erythrocytes.	P195
Figure 5.23	Exflagellating male gametocytes following treatment with PF9.	P196
Figure 5.24	Ca ²⁺ release in Fluo-4-AM-loaded 3D7a Stage V gametocytes stimulated with PF9.	P198
Figure 5.26	Schematic of predicted PF9-induced signalling pathways leading to gametogenesis in stage V gametocytes.	p208
Figure 6.1	Schematic showing the strategy to introduce a C-terminal triple HA tag into the <i>PfPDEδ</i> locus.	p213
Figure 6.2	<i>PfPDEδ</i> -HA integration PCR	p215
Figure 6.3	XA-induced rounding up in the <i>PfPDEδ</i> -HA transgenic line	p216
Figure 6.4	Immunofluorescence Assay of <i>PfPDEδ</i> -HA mature gametocytes	p218
Figure 6.5	Immunofluorescence Assay of <i>PfPDEδ</i> -HA mature gametocytes	p219
Figure 6.6	Immunofluorescence Assay of NF54 mature gametocytes	p220
Figure 6.7	Immunofluorescence Assay of <i>PfPDEδ</i> -HA mature gametocytes	p221
Figure 6.8	Western blot of Immunoprecipitated <i>PfPDEδ</i> -HA from stage IV/V gametocyte lysates	p223
Figure 6.9	Cyclic nucleotide hydrolysing activity of immunoprecipitated <i>PfPDEδ</i> protein	p225
Figure 6.10	The effect of PF9 and XA on <i>PfPDEδ</i> -HA cGMP hydrolysing activity	p227
Figure 6.11	The effect of PF9 and XA on <i>PfPDEβ</i> -HA cAMP hydrolysing activity	p229
Figure 6.12	The effect of PF9 and XA on <i>PfPDEβ</i> -HA cGMP hydrolysing activity	p229
Figure 7.1	Schematic presenting the relationship between cyclic nucleotide signalling molecules and Ca ²⁺ -dependent signalling proteins throughout the parasite lifecycle.	p238
Figure 7.2	The predicted cell signalling pathways in gametocyte infected erythrocyte deformability and gametogenesis.	p242
Figure A1	Sequence of synthetic gene	p282
Figure A2	Primer sequences for integration PCR and gRNA oligo sequences	p282
Figure A3	XA-induced Ca ²⁺ release in <i>P. falciparum</i> schizonts	p283
Figure A4	Predicted protein structure of <i>PfPDEδ</i>	p283

List of Tables

Table 2.1	An overview of the properties of Compound 2, KT5720, zaprinast, PF9 and XA.	P97
Table 4.1	Percentage retention rate (± SD) of 3D7a, <i>PfPDEδ</i> -ko and <i>PfPDEγ</i> -ko stage V gametocytes passed through a microsphere matrix.	p131
Table 5.1	EC ₅₀ values (μM) of 5 Pfizer PDE inhibitors in a gametocyte viability assay.	p170
Table 5.2	Counts of NF54, <i>PfPDEγ</i> -ko and <i>PfPDEδ</i> -ko	p179
Table 5.3	Comparison of PF9 treatment in wildtype (3D7a) and <i>PfPDEδ</i> -ko gametocytes.	p184
Table 5.4	Comparison of XA and PF9 treatment of 3D7a and <i>PfPDEδ</i> -ko line stage V gametocytes.	p189

List of Abbreviations

ABA	Abcisic acid
AB	Antibody
AC	Adenylyl cyclase
ACT	Artemisinin combination therapy
AMA1	Apical membrane antigen 1
ATP	Adenosine triphosphate
AMP	Adenosine 5'-monophosphate
AKAP	A-kinase anchoring protein
BP	Base pair
BSA	Bovine serum albumin
Ca ²⁺	Calcium ion
cAMP -	Cyclic adenosine monophosphate
cGMP	3'-5'-cyclic guanosine monophosphate
CDPK	Calcium-dependent protein kinase
CD	Catalytic domain
CRISPR/Cas9	Clustered regularly interspaced short palindromic repeat targeting of Cas9
CSP	Circumsporozoite protein
CNs	Cyclic nucleotides
C1	Compound 1
C2	Compound 2
DAG	Diacylglycerol
DBL	Duffy binding like
DD	Destabilising domain
DHFR	Dihydrofolate reductase
DHA	Dihydroartemisinin
DHPS	Dihydropteroate synthase
DMSO	Dimethyl sulfoxide
DNA	Deoxyribonucleic acid
EBA175	Erythrocyte-binding antigen 175
EC ₅₀	Half maximal effective concentration
EGTA	Ethylene glycol tetraacetic acid
ELISA	Enzyme-linked immunosorbent assay
EMP1	Epithelial membrane protein 1
EPA	Exoprotein A
EPAC	Exchange factor directly activated by cAMP
ER	Endoplasmic reticulum
GAF	Gametocyte activating factor
GAF Domain	cGMP-activated PDEs adenylyl cyclase and Fh1A domain
GC	Guanylyl cyclase
GEST	Gametocyte egress and sporozoite traversal
GMP	Guanosine 5'-monophosphate
GPCR	G-protein couples receptor
GSK	GlaxoSmithKline
gRNA	Guide RNA
GTP	G Guanosine-5'-triphosphate
G6PD	Glucose-6-phosphate dehydrogenase deficiency

HA	Haemagglutinin
HEPES	4-(2-hydroxyethyl)-1-piperazineethanesulfonic acid
hPDE	Human phosphodiesterase
HPLC	High performance liquid chromatography
IC ₅₀	Half maximal inhibitory concentrations
IFA	Immunofluorescence Assay
IMC	Inner membrane complex
IP	Immunoprecipitation
IPTp	Intermittent prevention treatment in pregnancy
IP ₃	Inositol triphosphate
IRS	Indoor residual spraying
ITN	Insecticide treated bed net
kDa	Kilodalton
LB	Luria-Bertani
mA	Milliamps
MACS	Magnetic cell separation
MAPK	Mitogen-activated protein kinase
MEF	Mosquito exflagellation factor
mGC	Mammalian guanylyl cyclase
MDR1	Multidrug resistance gene 1
Mg ²⁺	Magnesium Ion
MMV	Medicines for Malaria Venture
mPDE	Mammalian phosphodiesterase
ms	millisecond
MSP	merozoites surface protein
MVI	Malaria vaccine initiative
NaCl	Sodium chloride
nCi	Nanocurie
nM	Nanomolar
PAS	Per-ARNT-Sim domain
PBS	Phosphate buffered saline
PCR	Polymerase chain reaction
PDE	Phosphodiesterase
PDK1	Phosphoinositide-dependent protein kinase 1
Pf	<i>Plasmodium falciparum</i>
PKA	Protein kinase A
PKC	Protein kinase C
PKG	Protein kinase G
PI	Phosphatidyl-ID- <i>myo</i> -inositol
PI4P	phosphatidylinositol-4-phosphate
PI(4,5)	P ₂ -hosphatidylinositol(4,5)-biphosphate
PIP4K	Phosphatidylinositol-5-phosphate 4-kinase
PIP5K	Phosphatidylinositol-4-phosphate 5-kinase
PIP ₂	Phosphatidylinositol 4,5-bisphosphate
PI3K	Phosphoinositide3-kinase
PLC	Phospholipase C
PMCA	Plasma membrane Ca ²⁺ ATPases
RBC	Red blood cell
RDT	Rapid diagnostic test
RFU	Relative fluorescence units

Rh5	reticulocyte-binding protein homologue 5
RNA	Ribonucleic acid
RPKM	Reads per kilo base of exon model per million mapped reads
RT	Room temperature
sAC	mammalian soluble adenylyl cyclase
SDS	Sodium dodecyl sulphate
SDS-PAGE	Sodium dodecyl sulphate polyacrylamide gel electrophoresis
SEM	Standard error of the mean
SERA	Serine repeat antigen
SERCA	Sarcoendoplasmic reticular Ca ²⁺ ATPases
SOC	Substrate of CDPK4
SPA	Scintillation proximity assay
STEVOR	Sub-telomeric variable open reading frame
SUB1	Subtilisin-family serine protease
tmAC	Mammalian transmembrane adenylyl cyclase
TCP	Target candidate profile
TPP	Target product profile
UCR	Upstream conserved regulatory domain
UV	Ultraviolet
V	Volts
WHO	World Health Organisation
WT	Wild type
XA	Xanthurenic acid
Zap	Zaprinast
μM	Micromolar
μl	Microlitre
3D7a	Wildtype <i>P. falciparum</i>

Chapter 1

Introduction

1.1 Malaria

Malaria is a blood borne febrile illness resulting from a bite by a female *Anopheles* mosquito carrying apicomplexan parasites of the genus *Plasmodium*. The genus *Plasmodium* includes five different species of parasite that are known to infect humans. The most clinically relevant of these is *P. falciparum*. In 2015, 99 % of all estimated deaths from malaria were a result of *P. falciparum* infection[2]. 5 % of *P. falciparum* cases result in a severe form of the disease. Asymptomatic cases of *P. falciparum* do occur, but this is not as common an occurrence as with *P. vivax*[3]. *P. vivax* is the most widespread of the five species and although it is rarely fatal, malaria caused by infection of this species is still a major public health problem due to the morbidity it causes particularly in endemic areas and relapse of disease can occur with vivax infection due to dormant forms in the liver.

P. ovale and *P. malariae* malaria infections are less common and the disease they cause is of less clinical importance. *P. knowlesi* however, has the potential to cause severe disease in part due to its short 24-hour life cycle, which can quickly result in high parasitemias. This species is often mis-diagnosed as the benign *P. malaria*[4], and in certain parts of South east Asia, *P. knowlesi* is the dominant cause of malaria particularly in areas where other malaria species are diagnosed and treated effectively[5]. Due to the clinical importance of *P. knowlesi*, this can result in poor case management and improper treatment[6].

The clinical symptoms of malaria are caused by the asexual erythrocytic stage parasites that replicate in the bloodstream of the vertebrate host. This results in lysis and subsequent loss of host erythrocytes and a build-up of parasite derived waste products inside host erythrocytes, which are released into the blood stream. The host's immune system responds to this by activating immune cells such as macrophages, which release cytokines, and other soluble factors thus contributing to clinical symptoms of the disease, notably fever [7]:[8]. As observed by Golgi between 1886 and 1892, the characteristic symptom of periodic fever in malaria infection correlates with the lysis of erythrocytes and subsequent release of merozoites into the blood stream which induces an immune response leading to fever and other clinical symptoms [7].

The symptoms of malaria are many and varied depending on the severity and stage of disease, the patient profile and the species of *Plasmodium* causing the infection. Symptoms of

uncomplicated malaria include; fever, chills, nausea, sweats, vomiting, cough, abdominal pain, diarrhoea, headache and muscle aches, all common symptoms of a wide range of infectious diseases including the early symptoms of Ebola, influenza and other viral infections. As such, Malaria can often be diagnosed too late only when symptoms of severe disease manifest. Severe infection can lead to acute respiratory distress syndrome, which is an inflammatory reaction in the lungs, acute kidney failure and cerebral malaria, which can result in seizures, coma or other neurological abnormalities. If not treated soon enough (before 24 hours after onset of clinical symptoms) severe *P. falciparum* malaria may and does in many cases lead to death[8].

The incubation period of *Plasmodium* species ranges from 7 days to 30 days. *P. falciparum* generally establishes a clinical infection quicker than the other species, with *P. malariae* often presenting with a longer incubation period[8]. *P. malariae* can also cause latent infections, which have been known to last for many years in some people. However, this species rarely causes serious disease[9]. *P. vivax* and *P. ovale* differ from the other species in that they have the ability to remain dormant in the liver [10][11]. This stage of the lifecycle known as the hypnozoite stage derived from the Greek words *hypnos* for sleep and *zoon* for animal is a challenge to target with drugs and as yet primaquine is the only licenced antimalarial that kills these stages[12].

1.1.1. A brief history of malaria

Malaria has plagued the world for centuries. Records of this disease can be found in ancient Chinese text and symptoms of malaria had been described by Hippocrates[13]. The term Malaria is derived from the Italian for 'bad air' as disease had long been associated with swampy areas.

Malaria was first identified as a parasitic blood disease in 1880 when a French army surgeon, Charles Louis Alphonse Laveran observed what we now know as asexual blood stage forms in the blood of one of his patients. He named this parasite *Oscillaria malariae*. Laveran was not only successful in identifying that malaria is caused by a parasite found in the bloodstream, but he also observed that these parasites destroyed the blood cells of the host and produced particles of black pigment, known today as haemozoin, the product of haemoglobin digestion by the parasite, but identified by Laveran as 'melanins'; particles associated with the disease which were only observed in patients suffering from malaria. Studies by Laveran on these 'melanins' led to his discovery of the parasite[14]. Following Laveran's discovery, observations by the Italian neurosurgeon Camillo Golgi on periodicity of fevers identified that not only was there more than one form of this disease (one with a tertian pattern (2-day intervals between fevers) and the other with a quartan pattern (3-day intervals between fevers) of fever), but that these fever patterns corresponded with schizont rupture and release of merozoites into the blood stream. Golgi also observed that different forms of the disease resulted in different numbers of merozoites being released[15].

It was not until 1897, nearly 20 years after Laveran first discovered the malaria parasite, that it was demonstrated that this disease could be transmitted by mosquitoes. This was discovered by a British Army officer Ronald Ross who achieved transmission between birds[16]. However a connection of the disease to stagnant water had been known for some time, with the Romans using drainage programmes to control the disease, and scientists, including Laveran and Patrick Manson[17], hypothesising a role for the mosquito in facilitating this disease. Ross not only identified that this parasite could also infect birds and that the disease could be transmitted between birds via a mosquito vector, but he was the first to identify the oocyst stage in the mosquito mid gut[16]. A couple of years later, the role of the mosquito vector was confirmed further by the successful infection of two volunteers in London who were infected by mosquitoes fed previously on a malaria patient in Rome and sent over to the UK for the study[18].

1.1.2 The life cycle of *Plasmodium falciparum*

The liver and asexual blood stages

The life cycle of *P. falciparum* in the human host begins with the bite of an infected mosquito. While taking a blood meal, infectious sporozoites residing in the salivary glands can be introduced into the skin. These motile forms make their way to the bloodstream via the sinusoidal barrier of liver cells[19] to finally invade hepatocytes. Parasites then undergo schizogony, finally rupturing to release merozoites into the blood stream. Merozoites quickly invade host erythrocytes marking the start of asexual blood stage infection, the part of the life cycle responsible for the clinical symptom of malaria. Successful invasion leads to the development of ring stage forms. These early trophozoite stages mature into the 'feeding' trophozoite stages and the presence of parasite derived proteins such as *P. falciparum* epithelial membrane protein I (*PfEMP1*) on the host erythrocyte surface marks the switch from circulation in the blood stream to sequestration in the microvasculature of internal organs[20]. Trophozoite stages consume a large amount of haemoglobin with the formation of the waste product haemozoin, appearing as a large golden brown pigment in the food vacuole[21]. Haemozoin can be easily observed in Giemsa-stained blood films and the presence of this pigment can be used to separate early ring stages from mature asexual forms (section 2.2.B of methods). As trophozoite stages mature, they transport more parasite derived proteins to the erythrocyte surface and host erythrocyte membrane modifications by the parasite become more apparent, one such example is the increased permeability of host erythrocytes which allows parasites to obtain more nutrients from outside of the infected cell[21]. The start of nuclear division in the parasites marks the maturation of trophozoite stages into schizonts. Malaria parasites replicate their DNA by a process known as schizogony. This consists of a series of nuclear divisions to produce up to 32 daughter merozoites (this number varies depending upon the strain and species of parasite). Once nuclear division has occurred, individual merozoites are formed and retained within individual membranes. Schizonts then undergo the tightly regulated process of egress. Both the parasitophorous vacuolar membrane and the erythrocyte membranes rupture releasing fully mature (and competently invasive) merozoites into the blood stream. At this point, no longer hidden from the immune system, these invasive blood stages are now briefly open to attack by the host immune system. Merozoites rapidly invade new erythrocytes and the asexual cycle begins again (see Figure 1.1). This cycle varies between species and between strains of the different species, but for *P. falciparum* this cycle takes ~48 hours and corresponds to the characteristic fever peaks observed every 48 hours in malaria infected individuals.

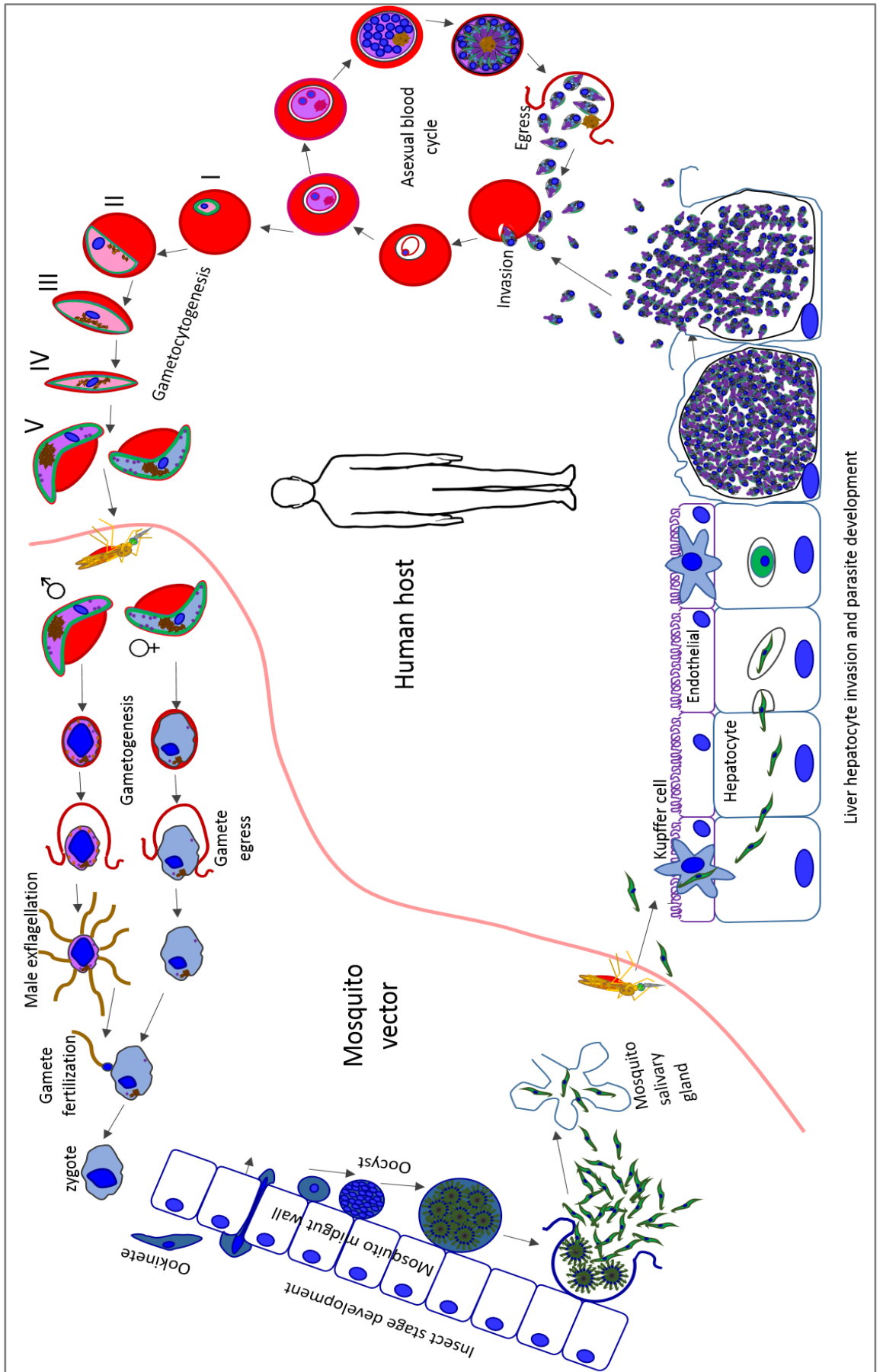


Figure 1.1. The full life cycle of *Plasmodium falciparum*

Sexual commitment and insect stage development

In order for the parasite to be transmitted to a mosquito, a small proportion of asexual stage parasites must commit to develop into the male and female sexual precursor cells known as gametocytes (see Figure 1.1). The process of this 'switch' from the asexual blood cycle to the sexual cycle and the subsequent development and maturation of these sexual stages to mature transmissible forms is known as gametocytogenesis. These mature forms are obligatory for transmission to the mosquito vector and thus essential for the survival and propagation of the malaria parasite and for disease. In *P. falciparum* infections, gametocytes are detectable after the asexual stages have established an infection in the blood stream of the human host. This is in part due to the long maturation period of *P. falciparum* gametocytes, which take 9-10 days to develop. There are many possible factors contributing to the 'decision' to switch to a transmission stage and cell signalling pathways may be involved in this process of gametocytogenesis. This will be discussed further in the cell signalling section of the introduction.

There are five morphologically distinct gametocyte stages (I-V) the last of which are mature male and female gametocytes primed for transmission to the mosquito vector [22][23]. The non-mature forms (stages I to IV) sequester in the bone marrow and are able to develop to maturity while avoiding splenic clearance [24]. Evidence suggests that these early stages exhibit a 'stiff' phenotype which is maintained by regulation of cAMP signalling[25] (this will be discussed further in the cell signalling section). The mature stages (Stage V) on the other hand, are distinct, crescent-shaped cells which circulate in the blood stream and can be taken up in the blood meal of a feeding mosquito. Once gametocytes reach full maturity (stage V) they become deformable. This change in phenotype coincides with their release from the bone marrow. This allows these transmission stages to transverse through the splenic slits while circulating in the host bloodstream, therefore avoiding spleen retention and thus clearance from the host circulation. On entering the mosquito mid gut, the dramatic change in environment and the reduction in temperature combined with the presence of a mosquito factor, xanthurenic acid (XA), (or a rise in pH in *in vitro* studies) triggers the cells to respond by 'rounding up' and emerging from the host erythrocyte. The mosquito factor inducing gametogenesis was identified as XA in 1998 by two separate groups. Billker et al[26] who carried out high-performance liquid chromatography (HPLC), high-voltage paper electrophoreses (HVPE), mass spectrometry (MS) and chemical derivatization assays on *Anopheles stephensi* pupae and activity assays using a read out of exflagellation events on *P. berghei* gametocyte stages, and Garcia et al[27], who used high

resolution electrospray MS from *Anopheles stephensi* mosquito tissue extracts, complemented by in vitro activity assays on *P. gallinaceum* and *P. falciparum*. On entering the mosquito midgut, emerged female macrogametes remain morphologically relatively unchanged. Males on the other hand exhibit a spectacular display known as exflagellation whereby the gametocyte undergoes 3 rounds of DNA replication and mitotic division producing 8 flagellated motile microgametes within 15 minutes which detach from the residual body and seek out the female macrogamete allowing fertilization to take place. This process of gametocyte 'activation', is known as gametogenesis and is by definition the 'formation of gametes'. Several studies have highlighted an important role for cell signalling, in the process of gametogenesis and this will be discussed later on in this report. Fertilization results in the formation of a zygote, which then develops into a motile ookinete, which transcends the mosquito gut wall followed by development into an oocyst. Once mature, oocysts rupture releasing many thousands of sporozoites into the salivary glands; these are transmitted to a human host when the mosquito takes a blood meal. Sporozoites establish an infection in the hepatocytes of the human host. This marks the first phase of human infection. However, there is some debate as to whether sporozoite infection of the skin is in fact the first phase of human infection rather than invasion of liver cells[28].

1.1.3 Key interventions

WHO estimated the number of recorded malaria cases in 2015 to have been 212 million, a 22 % decline since 2000[2]. A large proportion of this reduction in incidence can be attributed to malaria control interventions, namely the use of insecticide-treated bed nets [29] and still hugely important, but of a lesser impact over the last 5 years, the use of artemisinin based combination therapy[29] and indoor residual spraying[29]. However, despite this achievement in reduction of incidence, the number of people at risk of contracting malaria still remains high (3.2 billion)[29], as does the number of deaths per year attributed to this disease, which was estimated by WHO to be 429,000 in 2015[2]. The complex life cycle of the malaria parasite makes this a difficult disease to control and as such, the fight against this ancient disease must involve a combination of several key interventions not one alone.

1.1.3.A. Malaria diagnosis

Malaria is a deadly but treatable disease and if detected early, within 24 hours of onset of clinical symptoms (WHO) and treated in a timely fashion with the first line drug of choice, the mortality and serious complications of this disease can be prevented. Quick and affordable diagnosis and education of both health care professionals and patients, enables better case management and means that antimalarials are only used for those who actually have the disease promoting better treatment practices thus helping to prevent the spread of resistance. The WHO now recommends 'prompt malaria diagnosis either by microscopy or malaria Rapid Diagnostic Test (RDT) in all patients with suspected malaria before treatment is administered' (WHO).

1.1.3.B. Malaria vaccine development

The complex life cycle of the malaria parasite (Figure 1.1), coupled with its successful strategies enabling it to evade the host's immune system, poses huge challenges for the host in defeating the invading parasite. It does, however, present more targets for vaccine design and development. The ability of radiation-attenuated sporozoites to induce immunity has been recognised since the 1970's with protection being observed in both humans[30] and mice[31].

This demonstration that an immune response could be induced against malaria in addition to observations that individuals can develop progressive natural immunity with time[32][33], subsequently lead to important work on vaccine development. Despite the challenges to these projects, there has been recent progress with several candidates in the pipeline.

The most promising malaria vaccine candidate to date is the RTS,S/AS01 vaccine, which has been 30 years in the making and was initially developed by GlaxoSmithKline (GSK) in 1987 in collaboration with the Walter Reed Army Institute of research and more recently, PATH Malaria Vaccine Initiative (MVI). This pre-erythrocytic subunit vaccine targets the circumsporozoite protein (CSP) of *P. falciparum*, a protein that is presented on the surface of the sporozoite and is expressed by early liver stages. This vaccine candidate showed encouraging results in phase 3 clinical trials [34],[35]. However, the efficacy of this vaccine is limited with vaccine efficacy ranging from 25 % to 55 % in African children and as a result, this vaccine is still in the pipeline awaiting further clinical trials.

Other approaches include whole parasite sporozoite vaccines that involve challenge with aseptic, purified, radiation-attenuated *P. falciparum* sporozoites that have been cryopreserved (PfSPZ). This vaccine approach is well tolerated and has shown 100 % protection against challenge with malaria infection ten weeks post vaccination[36]. However, achieving high enough yields of irradiated sporozoites to support mass production of such a vaccine is a huge challenge.

Other vaccine targets include blood stage specific proteins such as apical membrane antigen-1 (AMA1)[37], merozoite surface proteins MSP1, MSP2 and MSP3[38][39][40], erythrocyte-binding antigen-175 (EBA175)[41], serine repeat antigen 5 (SERA5)[42] and reticulocyte-binding protein homologue (PfRh5)[43]. Blood stage vaccines are aimed at preventing invasion and therefore preventing clinical disease. However, these vaccine candidates are highly expressed on the surface of merozoites and exhibit high genetic diversity. This allows the parasite to escape attack by the host immune system and may also allow the parasite to evade vaccine-induced immunity[44].

Transmission blocking vaccines target antigens on the surface of gametes, zygotes and ookinetes with the aim of preventing development in the mosquito midgut. However a limitation to transmission blocking vaccines is that antigens used for inducing a transmission blocking response are not presented naturally to the host immune system. This means that the immune system will be unable to provide a natural boosting effect as a result of vaccination and this will be a likely limit to vaccine efficiency[35].

1.1.3.C. Targeting the vector

One of the most successful tools used for the fight against malaria in the last 15 years has been the distribution, increased access and increased use of insecticide treated bed nets (ITNs). WHO have estimated that use of ITNs has contributed greatly to the 18 % global decline in malaria cases estimated between 2000 and 2015[29]. This has been due to the impact of vector control being recognised through important research[45],[46] and subsequent effective implementation of vector control strategies as a result of this work. This ITN-led reduction in incidence can be attributed to an increased access to bed nets, coupled with a better understanding and use of bed nets in infected areas, with an increase of people sleeping under ITNs[2]. This reduction in incidence highlights that a simple action such as sleeping under a bed net can significantly reduce the burden of this disease and protect lives.

Indoor residual spraying (IRS) has been used as a vector control method against malaria as well as other vector borne diseases for many years with huge success and has proven instrumental to vector control. The insecticide dichloro-diphenyl-trichloroethane (DDT) was synthesized by a German student in 1874. However, the beneficial insecticidal properties of this compound were not known at the time and were not identified until many years later in 1939. This work, carried out by Swiss Scientist Paul Muller was fundamental to contributing to vector control and gained him the Nobel prize for medicine in 1948 (Nobel prize.org). Despite the progress seen with insecticide use, as with antimalarials, resistance has been observed and threatens to reverse the positive impact that this intervention has had on malaria control efforts[47],[48].

1.1.3.D. Targeting the parasite: Drug treatment and prophylaxis

In the fight against malaria, effective chemotherapy is essential, particularly for severe cases of the disease. With the current treatments, prophylaxis and interventions available, and with the often encountered issues with access to antimalarials not considered, malaria can be both prevented and treated easily. Treatments are currently effective, however, they do not inhibit transmission, and infected individuals are still able to transmit the parasite to the mosquito vector after clinical symptoms have ceased. Resistance has also emerged against all classes of antimalarials currently available excluding the artemisinin combination therapies (ACTs). However, slower parasite clearance times and an increased rate of treatment failure have been

observed for these drugs in Asia and recently in Africa[49], with some people calling this phenomenon resistance and others claiming that it is not and as such, there is some debate as to whether this is the start of emerging resistance. However, despite differing opinions, the slower clearance times remain a grave concern and the loss of this highly effective current treatment would be devastating to the fight against this disease. There is therefore need for new drugs that will target both the clinically relevant asexual blood stages and the transmission stages of this parasite, and particularly ones that would be active against all species in case the artemisinins fail.

Quinine

The naturally occurring compound quinine is an alkaloid compound isolated from the bark of the cinchona tree. This drug can now be made synthetically and in addition to exhibiting antimalarial properties, has also anti-inflammatory and analgesic effects. The medicinal benefits of cinchona bark were discovered hundreds of years ago when it was used in traditional medicine by native Peruvian Indians as a treatment for fever [50]. In fact, originally referred to as Peruvian bark, it was renamed in the 1700s after the countess of Chinchon was treated for a fever with this bark and was cured of her symptoms. It was successfully used as a first line treatment until the introduction of synthetic antimalarials in the 1920s [50]. Due to the toxicity of this drug, it is no longer used as a first line treatment. However, it is often used as a second line treatment in severe disease and is currently an important treatment for malaria in pregnancy particularly in the first trimester [50]. Quinine is also used to treat the related parasites of the *Babesia species*, which cause babesiosis.

Antifolates

Antifolates are synthetic compounds used to treat malaria infection and are subdivided into class 1 antifolates and class 2 antifolates by those that inhibit the parasite enzyme dihydropteroate synthase (DHPS) and those that inhibit the parasite enzyme dihydrofolate reductase (DHFR) respectively[51]. Combination of these two classes results in a synergistic effect so they are often used together[51]. Proguanil was the first compound of this class of antimalarials discovered. It is an inhibitor of DHFR and the partner drug to atovaquone in the drug combination used extensively as prophylaxis in travellers known as Malarone[51]. Chloroproguanil is synthesised by adding a chlorine group to the phenyl ring of proguanil. Both proguanil and chloroproguanil are metabolised into an active metabolite. Another class 2

antifolate is pyrimethamine, which was synthesised in the late 1940s and is another inhibitor of parasite DHFR. It is often used in combination with the DHPS inhibitor sulphadoxine. Although no longer widely used due to resistance, this combination is still often used for the intermittent prevention treatment of malaria during pregnancy (IPTp).

Quinoline antimalarials

The 4-aminoquinoline chloroquine was discovered in 1934 by the German Hans Andersag and originally named resochin[52]. It was used routinely as the first line treatment against *P. falciparum* infection, and was of particular value in 1955 to the WHO, who embarked on a global malaria eradication programme which also used the insecticide dichloro-diphenyl-trichloroethane (DDT) [53]. However, resistance of *P. falciparum* to chloroquine was confirmed in South East Asia in 1960[54] and as a consequence, this drug is no longer used to treat *P. falciparum* infections in areas where resistance has been recorded. It is however, still routinely used to treat *P. vivax* blood stage infections, and this treatment is still efficacious in most areas. Resistance to chloroquine is thought to be due to mutation in the *pfcr* gene and in some cases in the gene for *pfmdr1*[51]. The related compound Mefloquine has also been subject to resistance. This may be correlated with mutations in the *pfmdr1* gene. However, this has not been confirmed[51].

Artemisinin and the artemisinin derivatives

The herb *Artemisia annua*, also known as sweet wormwood, has been used in traditional Chinese medicine for centuries. Tea made from this plant was often used to treat fevers and it wasn't until the mid-20th century, 1971 in fact, that the active ingredient of sweet wormwood, or Qinghao as it was historically known, was isolated from this plant by Chinese scientists. This compound, artemisinin, proved to be a very efficient antimalarial and derivatives of it (Dihydroartemisinin (DHA), Artemether and Artesunate) are also very potent and effective drugs against malaria [55]. This important work gained the Chinese scientist Youyou Tu a Nobel Prize in 2015. As a result, since being licensed, Artemisinin combination therapy (ACT) has been the standard first line treatment for *P. falciparum* blood stage infection and is a very effective and widely used treatment regime which is effective against blood stage infections of all five species of malaria. However there has been some so-called resistance reported for artemisinin. Artemisinin resistance is defined by WHO as delayed parasite clearance following treatment with an artesunate monotherapy or with an artemisinin-based combination therapy (ACT)[56]. A slower clearance time is not necessarily an indication of resistance to artemisinin and may in

some cases reflect resistance to the partner drug. However, artemisinin resistance has been associated with a mutation in the propeller domain of the K13 (Kelch13, PF3D7_1343700) gene[56]. This can be used as a molecular marker to monitor the spread of artemisinin resistance as this mutation has been strongly correlated with reduced parasite clearance times. This has already been seen in Thailand, Vietnam, Cambodia and Myanmar. This emergence of resistance may be a result of one or more factors such as poor compliance, use of monotherapies, and substandard treatments[57]. Artemisinins are metabolised very quickly in the human body and as a result, the current regime is to treat the patient for three consecutive days. This highlights how poor compliance could promote resistance to the artemisinin component of the combination therapy used. Slow parasite clearance has been associated with increased presence of gametocytes. This is a concern as it facilitates a selective transmission advantage amongst drug resistant parasites[58]. To prevent the issues associated with fast metabolism of artemisinins, they must be partnered with a drug from a different class that has a longer half-life such as lumefantrine, mefloquine, amodiaquine, proguanil and sulphadoxine/pyrimethamine.

The observation of slow clearance with ACTs had prompted a need to investigate new targets and alternative drugs to treat malaria. Access to ACTs is also an issue, although the number of children under 5 years of age being treated with ACTs has increased (from less than 1 % in 2005 to 30 % in 2015)[2] and the proportion of ACTs used over alternative antimalarials for treatment of children has also increased in favour of ACT use. The recent identification of four imported cases of pfk13-independent treatment failure of artemether-lumefantrine in the UK[59] is a concern and emphasises the importance of identifying genetic markers in order to monitor the efficacy of this precious first line treatment.

Gametocytocidal compounds

Antimalarials that target asexual stages do not generally kill mature gametocyte stages. In fact, some compounds have even been documented to facilitate the production of gametocytes. Chloroquine was shown to stimulate a 5-fold increase in gametocytogenesis in *P. falciparum* in vitro[60]. This followed previous *in vivo* work on the murine species *P. chabaudi* which indicated an earlier peak of gametocytemia in mice treated with drug (pyrimethamine, quinine and mefloquine) 5 days post infection[61]. The combination drug sulphadoxine/pyrimethamine known as Fansidar, appeared to induce an almost 5-fold increase in *P. falciparum* gametocyte production in patients treated with this drug compared to those treated with chloroquine[62],

while others can kill the early gametocyte stages but not the late transmissible ones and vice versa. Artemisinin and its derivatives kill early stage gametocytes (I-III) but not mature stages. This reduces transmission efficiency but does not inhibit transmission as mature gametocytes still circulate in the blood stream[63]. As a result, drugs currently used to treat malaria will alleviate clinical symptoms but the individual will still be infectious to mosquitoes and therefore have the potential to spread disease.

Blocking transmission of malaria is an essential part of controlling this devastating disease. Developing new antimalarial compounds that target both the asexual blood stages that are responsible for the morbidity and mortality caused by malaria and at the same time killing gametocyte stages would both alleviate clinical symptoms and prevent the infection being passed on from the infected individual to other people. In the fight against malaria such a drug would be an invaluable weapon. However, there remains the concern that drugs targeting both the asexual stages and transmission stages of the life cycle would exhibit the same issues with the development of resistance and some argue that a transmission-only drug that targets the non replicating gametocyte stages would greatly reduce the selection for resistance. Such a drug, however, would not alleviate clinical symptoms but would be a good candidate for prophylaxis.

Primaquine (8-aminoquinoline)

The only available licenced drug that can kill mature *P. falciparum* gametocyte stages is the 8-aminoquinoline primaquine. This drug is hugely valuable as not only does it kill mature *P. falciparum* gametocytes, but it is also the only currently available drug that targets the *P. vivax* liver stages, including hypnozoites and as such is the only drug currently available to treat relapses.

Primaquine is currently used to treat vivax and ovale malaria, is used for prophylaxis and is also given as a single dose of between 0.5 mg/kg and 0.75 mg/kg to target the gametocyte stages[64]. However, primaquine cannot generally be used to treat people with G6PD (glucose-6-phosphate dehydrogenase deficiency), a common disorder in Africa and in some parts of Asia [65] as it results in severe haemolytic anaemia in persons deficient for this enzyme [66]. Aging erythrocytes become more and more G6PD deficient as they age. Oxidant haemolysis is a common effect of primaquine treatment but usually causes limited haemolysis in patients who have the normal enzyme. The health consequence of this limited haemolysis is outweighed by the treatment benefit in these patients and haemolysis tends to be much less severe than that caused by the malaria infection itself. However patients with G6PD are much more at risk of

severe haemolysis with subsequent anaemia, because although they produce the enzyme, it is unstable and degrades more rapidly thus resulting in higher levels of oxidant haemolysis of older erythrocytes which are more vulnerable to damage by oxidants and so more susceptible to lysis[12]. In these patients, treatment with primaquine can be life threatening and may lead to severe haemolysis and haemoglobinuric renal failure and in such cases the treatment efficiency does not outweigh the dangerous effect of the drug. Although there have been tests developed to identify people with G6PD deficiency, there is no current quick and simple test to identify the level of risk, it is therefore still too dangerous to treat with primaquine particularly in some areas of the globe where the more severe genetic variants are more common[12]. This has limited the use of this antimalarial despite it being a very valuable and unique compound in regards to its gametocytocidal and hypnozoitocidal activity. There is therefore a need to develop new compounds that target these stages of the lifecycle. The design of compounds that prevent transmission formed part of a proposal published by Medicines for Malaria Venture (MMV) in 2013[67], which outlined a list of target candidate profiles (TCP) and target product profiles (TPP). The aim of this was to provide a framework to channel research and development of antimalarial compounds in order to optimise malarial control efforts. An updated list published in 2016[68] includes molecules that clear asexual blood stages and with activity against hypnozoites (mainly *P. vivax*), hepatic schizonts, gametocytes and the insect vector[68].

Antibiotics

Several antibiotic compounds have been shown to be active against malaria parasites. A number of these compounds show differing modes of action to currently used antimalarials. This means that cross-resistance should not occur and these drugs have the potential to be good partner drugs in combination with current antimalarials. These compounds target the parasite apicoplast[69]. A large focus has been on two families of antibiotics, the tetracyclines and macrolides. Doxycycline is a synthetic tetracycline antibiotic originally developed in the 1960s by Pfizer Inc, but its potential as antimalarial compound wasn't discovered until the early 1970s[70]. Doxycycline has been shown to prevent the expression of apicoplast genes resulting in parasites devoid of functioning apicoplasts in the following cycle[71]. This compound can be used as a preventative measure in people travelling to malaria endemic areas[72]. Doxycycline exhibits slow acting activity against blood schizont stages and also shows partial efficacy against liver stages. When combined with another antimalarial compound exhibiting fast action against schizont stages, this treatment is very effective at preventing malarial infection[72].

The antimalarial quinolone Ciprofloxacin also causes formation of an abnormal apicoplast and a resulting delayed death of parasites[71]. It has been shown to have the ability to increase the anti-malarial activity of Primaquine[73]. However ciprofloxine has shown some off target toxicity[74].

Clindamycin is the semisynthetic derivative of the antimicrobial agent, Lincomycin[74]. Clindamycin is thought to target the apicoplast[74] and has been shown to be active against several apicomplexan parasites including *Toxoplasma*[75] and *P. falciparum*[76]. Most antibiotics present with a delayed activity and in studies with arithromycin, ciprofloxacin, clindamycin and docycycline on *P. falciparum* asexual blood stages, compounds appeared to be relatively inactive initially. However, a delayed death phenotype was observed and this was attributed to the progeny of treated parasites inheriting abnormal apicoplasts, leading to cell death and a subsequent inability of parasites to fully mature[68]. This emphasises a need for appropriate and faster acting partner drugs for these compounds when used in the treatment of malaria.

1.2 Cell signalling

The life cycle of *P. falciparum* is extremely complex. Tightly regulated and timely interactions between components of cell signalling cascades are likely required in order for the parasite to develop through all stages of its lifecycle and to successfully infect the host and transmit to the mosquito vector. Huge progress has been made in understanding signal transduction pathways in mammalian systems and although this knowledge has helped facilitate understanding in protozoan systems, there is still much more to learn and work on cell signalling in protozoans such as *P. falciparum* is still in its infancy. This has in part been due to the huge differences between mammalian and protozoan signalling pathway components, and due to a lack of reagents and the difficulties associated with growth and manipulation of the organisms both at the cellular and genetic level.

Signalling pathways are initiated when a stimulus is detected by a cell. This is followed by the coordination of an appropriate response. The presence of an external stimulus generally, but not always, involves the interaction of a molecule with its receptor on the surface of the cell. This interaction activates the receptor, which can then induce intracellular changes in concentrations of downstream secondary messengers. Changes in the concentrations of these secondary messengers amplify the original signal and activate downstream effector proteins leading to an appropriate and timely cellular response.

Several types of secondary messenger signalling pathways exist. In *P. falciparum*, previous research has shown that cyclic nucleotide and Ca^{2+} signalling are both important pathways involved in coordinating many cellular functions essential to the parasite life cycle. There is often an overlap of these two signalling pathways in several important stages of the parasite lifecycle and as such, a relationship between these two signalling pathways is thought to often occur. The following will from this point focus specifically on cyclic nucleotide and Ca^{2+} signalling in the context of the *Plasmodium* lifecycle. Specific interest will be focused towards such signalling interactions in the sexual stage of the life cycle but with additional reference to cyclic nucleotide signalling and Ca^{2+} signalling in other organisms in particular mammalian systems.

1.2.1 Cyclic nucleotide signalling

Cyclic nucleotide signalling regulates a wide range of cellular events in many different organisms. Ranging from regulation of heart function[77] and olfaction in mammals[78] to bacterial phytopathogenesis[79]. Cyclic nucleotide signalling has been well documented in mammalian systems with recognition that dysregulation of this signalling pathway leads to the pathology of a wide range of diseases and as such, components of this pathway have long since been recognised as good drug targets. Studies have also highlighted an essential role for this pathway in infectious organisms including apicomplexans such as *T. gondii* where it regulates gliding motility, invasion[80], cellular differentiation[81], gene expression and proliferation[82] and in *Eimeria* where inhibition of the cyclic nucleotide signalling pathway inhibits growth[83]. With relevance to this project, *Plasmodium* species require cyclic nucleotide signalling to regulate several key phases of their complex life cycle.

The cyclic nucleotide signalling cascade involves several key components that interact with each other in a systematic and highly organised manner to regulate downstream effector molecules that will vary depending upon the cellular response required and the initial signal. As such, this pathway can be activated by a range of different signals and can regulate many cellular responses across a diverse range of organisms and in a temporal and spatial manner. In mammalian cells, cyclic nucleotide signalling is predominantly initiated by activation of membrane bound G protein-coupled receptors (GPCRs), which can have both a stimulatory and inhibitory effect on levels of cyclic nucleotides. However, as yet, there has been no evidence of genes encoding GPCRs in *Plasmodium* species. The key components of this pathway include the secondary messengers 5'-cyclic adenosine monophosphate (cAMP) and 3'-5'-cyclic guanosine monophosphate (cGMP). Levels of these secondary messengers are regulated by the opposing action of two classes of enzymes, firstly, their synthesis by adenylyl cyclase (AC) and guanylyl cyclase (GC) respectively and secondly, their hydrolysis by a family of enzymes known as phosphodiesterases (PDEs). These secondary messengers activate their specific downstream effector molecules: cAMP activates PKA and cGMP activates PKG. Once activated these effector proteins can phosphorylate downstream target proteins leading to the desired cellular response (see Figure 1.2).

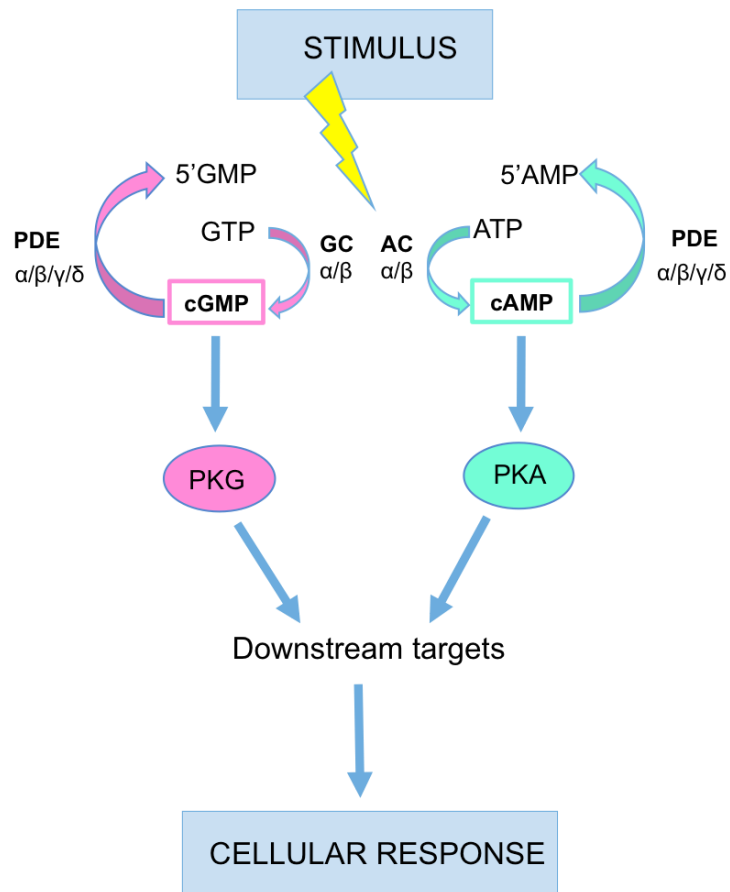


Figure 1.2: Schematic of the basic cyclic nucleotide cascade. To initiate the cascade, a stimulus is detected; in mammalian cells this is often by a receptor interaction on the cell surface. The stimulus could act on the cyclase or PDE and results in changes in levels of the cyclic nucleotides (CNs) cAMP and/or cGMP. These are regulated by opposing actions of cyclases and PDEs. Increased levels of CNs leads to activation of downstream effector proteins, the main ones being PKA and PKG for cAMP and cGMP respectively. PKA and PKG then phosphorylate downstream target proteins leading to a cellular response.

1.2.1.A. The key players in cyclic nucleotide signalling

The regulators: Phosphodiesterases (PDEs) and cyclases (GCs and ACs)

PDEs and cyclases are important signalling enzymes that work in a tightly coordinated partnership to regulate levels of cGMP and cAMP. Guanylyl cyclases convert guanosine-5'-triphosphate (GTP) to cyclic guanosine-3',5'-monophosphate (cGMP) and adenylyl cyclases convert adenosine triphosphate (ATP) to 3',5'-cyclic adenosine monophosphate (cAMP). PDEs are enzymes that hydrolyse the cyclic phosphate bond in cAMP and/or cGMP to produce the inactive products 5'-AMP and 5'-GMP respectively. These essential enzymes are good potential drug targets and in fact, in mammalian systems, these enzymes and in particular the PDEs have been used as drug targets to treat a range of health problems from sildenafil citrate that targets mammalian PDE5[84] to treat erectile dysfunction[85],[86] to the mammalian GC-C inhibitor linaclotide used to treat irritable bowel syndrome[87] and the mammalian PDE 4 inhibitor roflumilast-a to treat chronic obstructive pulmonary disease[88].

Adenylyl cyclases

Mammalian adenylyl cyclases

Adenylyl cyclases (ACs) are ubiquitous and important signalling enzymes. Mammalian ACs fall under the large category of class III cyclases which also contains all mammalian GCs[89]. The ten identified mammalian ACs exhibit differing tissue expression patterns and regulation and can be categorised into two main types, a single soluble isoform (sAC) first identified by Buck and colleagues in 1999 [90] which is expressed in many tissue types and can be directly activated by Ca^{2+} and bicarbonate[91],[92] and the nine better characterised and earlier identified heterotrimeric G protein-regulated membrane associated isoforms (tmAC)[93]. Mammalian tmACs have a short cytoplasmic amino acid terminus followed by two regions of six transmembrane domains separated by a catalytic domain. The second transmembrane domain is followed by a second catalytic domain[94]. The activity of mammalian tmACs is for the most part regulated by interaction of hormones and neurotransmitters with G protein-coupled receptors[95]. sACs lack the transmembrane domains that tmAC have but have the two catalytic domains which are located at the N-terminus of the protein connected by a linker[96]. The active site of these enzymes is formed by interaction between conserved catalytic residues in each of the two catalytic domains (C1 and C2), which in the active state of the enzyme, interact forming

a homodimer [96]. Conversion of ATP to cAMP only occurs when these two homologous cytoplasmic domains combine. Prior to interaction the domains are catalytically inactive[97]. TmACs have been associated with processes such as cardiac myocyte function[98] and brain functions[93]. The soluble isoform has been associated amongst other functions with apoptosis[99], glucose induced insulin release[100] and control of prostate cell proliferation[101]. The latter two roles indicate sAC to be a potential drug target in diseases such as prostate cancer and diabetes. Unlike tmACs, which are restricted to the cell membrane, sACs are able to localise to different areas of the cell depending on where cAMP regulation needs to occur[102]. This temporal and spatial distribution adds to the complexity of cAMP signalling and means that multiple AC isoforms can be expressed at any one time and can play different functions in a cell. This reflects the diversity and complexity of cyclic nucleotide signalling.

***Plasmodium* adenyl cyclases**

Genes encoding two ACs (*PfAC α* and *PfAC β*) have been identified in the *P. falciparum* genome. Unlike *Plasmodium* GCs, these are distinct from each other. However, both show similarity in their catalytic domains to mammalian soluble ACs[103]. *PfAC α* is predicted to be bifunctional and is thought to contain a predicted voltage-gated potassium channel domain suggesting that this enzyme may be sensitive to changes in the membrane potential and involved in ion conduction across the membrane[104]·[105]·[106]. It has a predicted structure of 6 transmembrane domains and a single carboxyl-terminal catalytic domain with amino acid residues required for substrate binding[106]. This differs from the currently less characterised *PfAC β* , which has no predicted transmembrane domains and two sAC-like AC catalytic domains. Unlike *PfAC β* , *PfAC α* has been heterologously expressed and characterised[105]. Transcripts appear at high levels in gametocyte stages suggestive of a role for this cyclase in the sexual stage of the parasite life cycle[106]. In further support of this, higher PKA activity has been reported in the gametocyte producing line LE5 compared to the non-producing line T9/96[107]. Like *PfGC β* , the *PfAC α* gene is intron rich[106]. A role for this cyclase in liver sporozoites has also been indicated[108]. *PfAC β* mRNA on the other hand is highly expressed in asexual blood stages (plasmodb.org) indicative of a role for this cyclase in the asexual erythrocytic stage of the life cycle. In fact, to date, unlike *PfAC α* , attempts to produce a *PfAC β* knockout line have been unsuccessful, highly indicative of an essential role in asexual blood stages. However, with the current ever advancing genetic techniques, a conditional knockout may not be far away and this would advance studies into the role of this cyclase. *PfAC β* mRNA transcript levels increase in the trophozoite stage reaching a rapid peak during schizogony[109]·[110]. This corresponds to

pharmacological data demonstrating that mammalian soluble AC inhibitors (thought to target *PfACβ*) are most effective 24-31 hours post invasion[111]. The same study also revealed a significant pH sensitivity of this cyclase leading to the prediction that *PfACβ* may act as a pH sensor for the parasite while it resides in the host erythrocyte.

Guanylyl cyclases

Mammalian guanylyl cyclases

In 1969, guanylyl cyclase (GC) was first identified in mammalian systems as being one of the enzymes responsible for cGMP regulation[112]:[113]. Since then genes encoding eleven mammalian GCs (mGCs) have been identified. Four of the eleven are soluble mGCs subunits termed $\alpha 1$, $\alpha 2$, $\beta 1$ and $\beta 2$ respectively. These exist as a heterodimers[114], each composed of one large α subunit and one small β subunit, are activated by nitric oxide[115] and require heme for activity[116]:[117]. They are located in most tissues including the brain, lung and kidney[118]:[119]. The remaining seven genes encode membrane-associated mGCs[119]. All encode functional proteins that have distinct structural and biochemical properties from the soluble forms apart from two (mGC-D and mGC-G), which are pseudogenes. mGC-A through to mGC-E exist as homodimers with the exception of mGC-C which exists as a homotrimer[119]. Unlike soluble mGCs, membrane-associated mGCs are activated by peptides[119] and require dimerization for activity[119]. The topology of all transmembrane mGC's consists of a ligand binding domain located extracellularly, suggestive of a receptor function for this domain, followed by a short transmembrane region containing two transmembrane domains and an intracellular catalytic domain responsible for cGMP synthesis[120]. Mg^{2+} or Mn^{2+} are required during GC synthesis to stabilise the negative charge of the molecule[94]:[121]. Disruption of mGCs can lead to many diseases including irritable bowel syndrome in the case of mGC-C disruption and congestive heart failure, as is the case for mGC-A disruption[122] and as such, mGCs are already targets for several inhibitors[87]:[123].

Plasmodium guanylyl cyclases

The genome of *P. falciparum* encodes two large guanylyl cyclases, *PfGCα* with a predicted molecular mass of 496kDa and *PfGCβ* with a predicted molecular mass of 370kDa[124],[125]. These cyclases are thought to be bifunctional[124] and the genes that encode them are located on different chromosomes[124]. The *PfGCβ* gene is located on chromosome 13 and is characterised by 13 introns, 12 of which are located in the ATPase-encoding area of the gene

whereas the *PfGCα* gene located on chromosome 11 is not subject to intron disruption[124]. In *Plasmodium* species guanylyl cyclases are predicted to be integral membrane proteins with 12 transmembrane domains in the cyclase region and a further 10 in the predicted type IV ATPase (flippase) domain[124]. Significant GC activity has been identified in membrane preparations of *P. falciparum* mature gametocytes[126] indicating a possible membrane localisation of one or both of the *P. falciparum* GCs. Compared to mammalian cyclases, *Plasmodium* cyclases exhibit unusual topological and structural features[125]. Both have an identical predicted topology with a paired C-terminal catalytic domain, which resembles mammalian G protein-dependent ACs with two catalytic domains each preceded by a region of six transmembrane helices[124] and an N-terminal P-type ATPase-like domain.

Both *PfGCα* (PF3D7a_1138400) and *PfGCβ* (PF3D7a_1360500) mRNA expression have been detected in the asexual blood stages, gametocytes and sporozoite stages of *P. falciparum*[127][110]. However, *PfGCα* mRNA expression is highest in asexual blood stage schizonts stages, whereas *PfGCβ* mRNA expression, although high in schizonts, is also high in gametocyte stages and sporozoites[110][124]. This is supported by RT PCR data on *P. berghei* which identifies *PbGCα* as the dominant cyclase in mixed asexual samples and *PbGCβ* as being additionally transcribed in enriched gametocytes[128]. This evidence reflects a likely stage specific role for these two GCs and in fact, evidence has pointed to a role for *PbGCβ* in ookinete motility. *P. berghei* parasites devoid of *PbGCβ* exhibited severely compromised ookinete motility[129][128]. These data were also indicative that at the ookinete stage *PbGCα* is unable to compensate for lack of *PbGCβ*. This knock out line was able to undergo gametogenesis indicating that *PbGCβ* is not essential for this process to occur. These data were consistent with a similar study in *P. falciparum* which showed a significantly reduced enzyme activity in a *PfGCβ* ko line but normal levels of gametogenesis[130]. Ability to knock *PfGCβ* out in this study was also indicative that this GC is not essential for the asexual blood stages or for gametocytogenesis or gametogenesis. Attempts to knock *PfGCα* out on the other hand have historically been unsuccessful[128][130], supportive of an essential role for this cyclase in asexual blood stages.

Phosphodiesterases

Mammalian phosphodiesterases

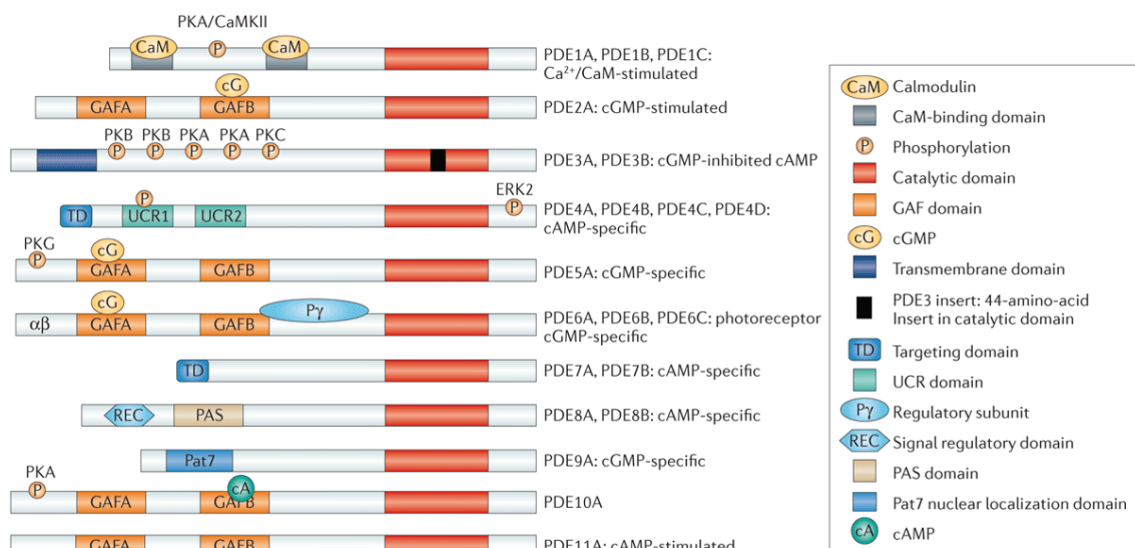
The PDE family of enzymes hydrolyse the 3'phosphoester bond of cAMP and/or cGMP. In mammals there are 11 different families of PDEs named PDE1 to PDE11 that are classified according to the substrates that they degrade. Whether they degrade cAMP specifically (PDE4, PDE7 and PDE8), cGMP specifically (PDE2, PDE5, PDE6 and PDE9), or whether they are dual specific as is the case for human PDE3, PDE10 and PDE11[131],[132]. Dual specific enzymes also differ in their preference for either cGMP or cAMP[132]. Each of the 11 gene families give rise to multiple isozymes resulting in more than 50 proteins. This in part is due to alternate splicing[132]. Mammalian PDEs (mPDEs) have two distinct domains, firstly an N-terminal regulatory domain, which as its name implies, is responsible for the regulatory function of the protein. This regulatory function differs between the PDE families due to the varying domain composition. Most mPDEs contain domains essential for kinase recognition and phosphorylation, ligand binding and domains required for dimerization. Some mPDEs (PDE2, PDE5, PDE6, PDE10 and PDE11) can be regulated by a cyclic nucleotide via an allosteric GAF (cGMP-activated PDEs adenyl cyclase and Eh1A) domain located in the N-terminal region to activate them to then hydrolyse another cyclic nucleotide. An example of this is the mPDEs in the heart that are regulated by cGMP leading to cAMP hydrolysis[133]. PDE 1 is unique in that its N-terminus contains calmodulin binding domains. PDE1, PDE3, PDE4, PDE5 and PDE10 have phosphorylation sites in their regulatory domain. Other differing regulatory and structural features include Per-ARNT-Sim (PAS) domains (which can bind small molecules and in a signalling system can function as a signalling sensor or play a role in protein-protein interactions), upstream conserved regulatory domains (UCR), transmembrane domains and anchoring domains (see figure 1.3).

PDEs are metal ion-dependent and require one zinc ion and an additional currently unknown metal ion, thought to be magnesium, for catalysis. The Zn^{2+} binding site is located in the catalytic domain, which is conserved and is also involved in cyclic nucleotide recognition and substrate binding. As such, this domain is important for pharmacological targeting. The domain is composed of 16 alpha helices made up of 3 sub domains. Differences in this binding pocket and the differing properties of mammalian PDEs reflect the different PDE drug targets[134]. Most isoforms are expressed in multiple tissues for example, PDE2 is expressed in the adrenal gland, heart, lung, liver, platelets, and endothelial cells, PDE5 is expressed in the lung, platelets, smooth muscle, heart, endothelial cells and the brain, and PDE8 is expressed in the testes, eye, liver,

skeletal muscle, heart, kidney, ovary, brain, T lymphocytes and the thyroid. PDE 6 differs from all other mammalian PDEs as it is less widely distributed and is only present in the rods and cones of the retina[135] and the pineal gland[136]. PDE3 and PDE4 constitute the majority of cAMP regulatory activity[132].

Mammalian PDEs have long been acknowledged to be good drug targets to treat a multitude of diseases resulting from an imbalance in cyclic nucleotide signalling required to regulate normal cellular processes. A well known example of a drug that targets a human PDE is sildenafil citrate more commonly known as Viagra. This compound and a related compound tadalafil target PDE5 to increase vasodilation for the treatment of erectile dysfunction[86]. Sildenafil citrate was originally developed to treat heart disease and is still used to treat pulmonary arterial hypotension[137]. However, due to homology between mammalian PDEs, adverse side effects can sometimes be associated with drug treatment. In regards to treatment with Viagra, blue vision is sometimes experienced due to the additional targeting of PDE6 which shows homology to PDE5, a PDE that is highly concentrated in the retina and involved in retinal photo-transduction[138]. Inhibitors such as roflumilast that targets PDE4 also often result in poor tolerance due to undesirable side effects[139]. However, as a whole, these drugs are generally well tolerated.

Comparison of the catalytic domains of *Plasmodium* PDEs and human PDEs led researchers to hypothesise that the PDE1, PDE5 and PDE9 isoforms showed most similarity to *Plasmodium* PDEs[140] . This has allowed more of a focus for the design of small molecules targeting *Plasmodium* PDEs as the structures of compounds aimed at targeting *Plasmodium* PDEs can be designed based on the structure of known active PDE1, PDE5 and PDE9 inhibitors.



Nature Reviews | Drug Discovery

Figure 1.3. Schematic of the structure and domain organisation of the 11 Human PDE families[1]

***Plasmodium* phosphodiesterases**

There are four cyclic nucleotide PDE enzyme paralogues encoded in the *P. falciparum* genome (*Pf*PDE α - δ), which show similarity to their human homologues. 13 of the 16 amino acid residues found to be conserved across the mammalian PDE families are conserved also in *Plasmodium* PDEs[140]. The mammalian amino acids involved in metal binding are also conserved in the *Plasmodium* PDEs[141]. The catalytic domain of *Plasmodium* PDEs shows some similarities to the catalytic domain of human PDEs and shares the HD(X₂)H(X₄)N binding pocket signature[141], although the catalytic domain of *Plasmodium* PDEs is thought to be divergent enough from that of humans to be a target for drug discovery efforts. All *Plasmodium* PDEs are thought to be integral membrane proteins as the N-terminal domain contains 4 to 6 predicted transmembrane domains and PDE activity has been shown to be associated with parasite membrane fractions but not the soluble fraction[141]. Expression of these enzymes in *Plasmodium* is developmentally regulated at the mRNA level (Plasmo DB) and research indicating roles for these enzymes at different stages of the parasite life cycle is supportive of this (Drought LD & Flueck CH unpublished)[130]:[128]:[142]. *Plasmodium* PDE active sites show most similarity to mammalian PDEs 1, 5 and 9 and modelling work has indicated that cGMP can bind to all *Pf*PDEs leading to the hypotheses that *Plasmodium* PDEs are more likely to be better at hydrolysing

cGMP than cAMP[140]. The catalytic domain of the *Plasmodium* PDEs closely resemble that of mammalian PDEs[141].

PfPDE α* and *PfPDE β

PfPDE α encoded by the gene PF3D7_1209500 has a predicted size of 115 kDa and is expressed in blood stages but at relatively low levels (see Figure 1.4)[143],[141],[25]. Two splice variants of the gene have been identified, *PfPDE α A* which is predicted to have 6 transmembrane domains in the N-terminus and *PfPDE α B* which is predicted to have 4[141]. The gene is located on chromosome 12[141]. The catalytic region is located at the C terminus[141] and catalytic activity of *PfPDE α* has been demonstrated by heterologous expression and this PDE is thought to be cGMP specific[141],[143]. In further support of this, a knock out line was observed to have 20 % lower cGMP-PDE activity but cAMP-PDE activity remained unchanged[141]. There is evidence to suggest that the *PfPDE α* catalytic domains of both splice variants are intracellular[141]. This is also predicted to be the case for *PfPDE γ* . Interestingly, this is thought not to be the case for the other two *Plasmodium* PDEs which are predicted to have their catalytic domains exposed to the lumen of the parasitophorous vacuole but this has not been demonstrated biochemically[141]. This different topology between the *Plasmodium* PDEs may in some part explain the differing roles of these PDEs in the cell[141]. Deletion of *PfPDE α* demonstrated that it is not essential during the asexual blood stage of the lifecycle[141]. It is thought that at least one other PDE is expressed at this life cycle stage[143],[141] and that it is likely to be dual specific. A likely candidate is *PfPDE β* (PF3D7_1321500) which has a predicted size of 133 kDa, as it is highly expressed in asexual stages (see Figure 1.5)[141],[25]. Attempts to knock out *PfPDE β* have until recently, historically been unsuccessful suggesting that it is essential in erythrocytic stages and in fact, mRNA levels of all PDEs in asexual stages indicate that both *PfPDE α* and *PfPDE β* are expressed in asexual stages and this, together with data indicating that that *PfPDE α* is not essential at that stage and that its absence is unlikely to be compensated for by another PDE, has indicated that *PfPDE β* is likely to be the predominant PDE in asexual stages[141]. In support of this, a recent conditional knockout system has been developed and used to demonstrate an essential role for *PfPDE β* in *P. falciparum* blood stage replication (Laura Drought, PhD Thesis, 2014). Work using this knockout line has indicated the phenotype affects merozoite invasion and very early ring stage development (Christian Flueck, LSHTM, unpublished). Dual specificity of *PfPDE β* has been confirmed using PDE assays on immunoprecipitated protein from asexual blood stages (Laura Drought, PhD Thesis, 2014). [141]. The *PfPDE β* protein shows a similar topology to that of *PfPDE α A* with 6 transmembrane helices at the N-terminus and a catalytic

domain located at the C-terminus[141]. The gene encoding *PfPDEβ* is located on chromosome 13[141]. Evidence suggests that *PfPDEα* does not affect gametocytogenesis as parasites lacking this PDE switch to the gametocyte stages efficiently with a resulting gametocytemia (my observations, unpublished) and sexual stages appear to grow and develop normally to maturity indicating that this PDE does not play an essential role in sexual stage switching or gametocyte growth and development. *PfPDEα* has been detected in mature gametocyte stages. Interestingly, in a proteomic analysis of *P. falciparum* gametocytes, more protein was detected in mature male gametocytes than mature females, suggesting a possible sex-specific function of *PfPDEα*. The only other *PfPDE* detected at the protein level in this study was *PfPDEδ*, which was identified at similar levels in both sexes, although slightly higher in females (17.8 % females to 5.9 % males), [144]. Although *PfPDEα* appears dispensable for both asexual and sexual blood stage growth and development, it is expressed at the mRNA level in both stages and at the protein level in sexual stages, therefore a role for *PfPDEα* in mature gametocytes *in vivo* cannot be ruled out. No data are available on the insect stages so there may be a possible role for *PfPDEα* at these stages. Future conditional knockout studies involving *PfPDEα/PfPDEβ* may shed some light on a possible compensatory role for *PfPDEα*.

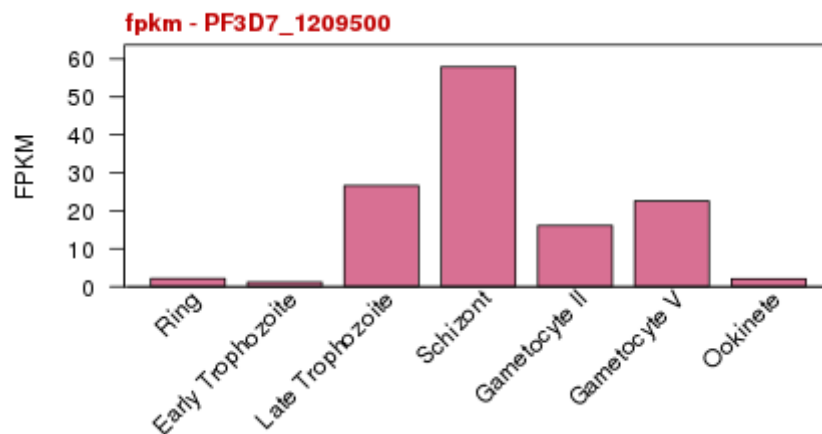


Figure 1.4. Detection of *PfPDEα* mRNA levels in *P. falciparum* parasite stages. Detection of *PfPDEα* mRNA in 7 life cycle stages of 3D7 by illumina sequencing. Measured as transcript levels of fragments per kilo base of exon model per million mapped reads (FPKM)[144].

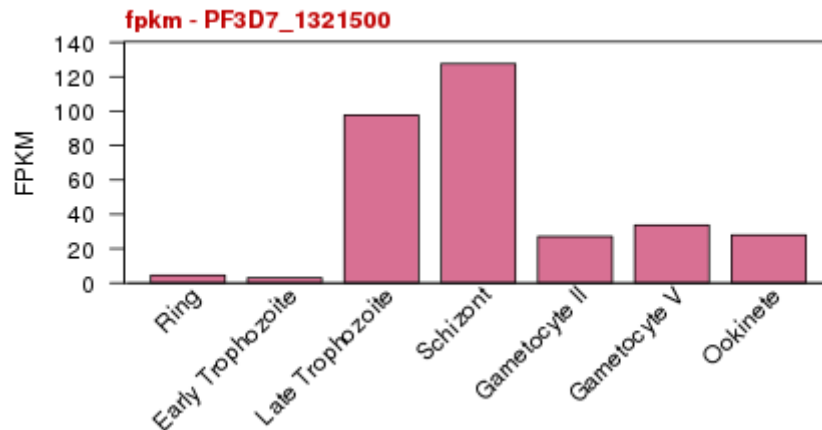


Figure 1.5. Detection of *PfPDEβ* mRNA levels in *P. falciparum* parasite stages. Detection of *PfPDEβ* mRNA in 7 life cycle stages of 3D7 by illumina sequencing. Measured as transcript levels of fragments per kilo base of exon model per million mapped reads (FPKM)[145].

PfPDEγ

PfPDEγ (PF3D7_1321600) is a 92 kDa protein that has been associated with sporozoite formation[142], (Cathy Taylor, PhD thesis, 2007). Its mRNA has been detected at low levels in asexual blood stages[141][25] and in gametocyte stages[145] (see Figure 1.6). This PDE has also been shown to be expressed in *P. yoelii* blood stages at a low level and at higher levels in the sporozoite stages[142]. The gene encoding *PfPDEγ* is located immediately adjacent to *PfPDEβ* on chromosome 13 but on the opposite strand[141]. The *PfPDEγ* protein consists of 6 transmembrane helices located at the N-terminal with a C-terminal catalytic domain[141]. Deletion of this PDE has been achieved in *P. falciparum*, *P. berghei* and *P. yoelii*[142], (Cathy Taylor, PhD Thesis, 2007). Parasite lines lacking *PfPDEγ* appear to grow and develop normally through the asexual blood cycle indicating that this PDE is not essential at this stage of the life cycle[130]. A knockout line of *PfPDEγ* was able to maintain the ability to switch from the asexual blood cycle to the sexual stage of the lifecycle and appeared to exhibit normal gametocytogenesis and gametogenesis indicative that *PfPDEγ* is not essential for the switch to the sexual cycle or for the growth and development of gametocytes to mature stages or for gametocyte activation (Cathy Taylor, PhD Thesis, 2007)[130]. *PbPDEγ* and *PyPDEγ* mutants also exhibit normal asexual growth and development and gametocyte initiation and development appeared unaffected, as seen in the *P. falciparum* line[142], (Cathy Taylor, PhD Thesis, 2007). These mouse models also showed that the oocyst development and development to the sporozoite stage was normal in the absence of PDEγ. However, in a study on *P. yoelii*, deletion

of *PyPDE γ* was shown to render sporozoites non-motile and unable to invade the salivary glands of the mosquito vector. *P. yoelii* sporozoites also exhibited elevated levels of cGMP. These data indicate an essential role for *PfPDE γ* in maintaining levels of cGMP required for sporozoite motility and subsequent salivary gland invasion in the mosquito vector, processes critical for transmission [142]. These data is supported by work on *P. berghei*, which showed high numbers of ookinetes and oocysts in a *PbPDE γ* -ko line, but very low number of sporozoites. Furthermore, in bite back assays (mosquitoes infected with the *PbPDE γ* -ko line were allowed to feed on uninfected mice), no transmission was seen suggesting that this line shows a defect in sporozoite production and infectivity (or invasion of liver cells). Although the exact cyclic nucleotide specificity of *PfPDE γ* is currently unknown, the highly elevated levels of cGMP observed in sporozoite stages are indicative that *PyPDE γ* hydrolyses cGMP. This was further supported by addition of the cGMP-specific inhibitor zaprinast that ablated sporozoite motility [142]. Levels of cAMP were not measured in this study and although the absence of *PfPDE γ* in *P. falciparum* stage V gametocytes did not appear to affect levels of cAMP or cGMP with levels comparable to the wildtype (Cathy Taylor, PhD Thesis, 2007), cAMP hydrolytic activity at the sporozoite stage cannot be ruled out and cAMP is known to be involved in sporozoite motility[146]. Interestingly, an RNA-Seq analysis of sporozoites of the *PyPDE γ* knock out line revealed greatly reduced transcript abundance of *PyPDE γ* as expected. However, levels of *PyPDE δ* and *PyPDE β* transcripts were increased whereas levels of *PyPDE α* remained the same[142]. This may indicate a compensatory role for *PyPDE δ* and *PyPDE β* when *PyPDE γ* is absent, although this is not enough to reverse the effect on sporozoite motility seen when *PyPDE γ* is absent.

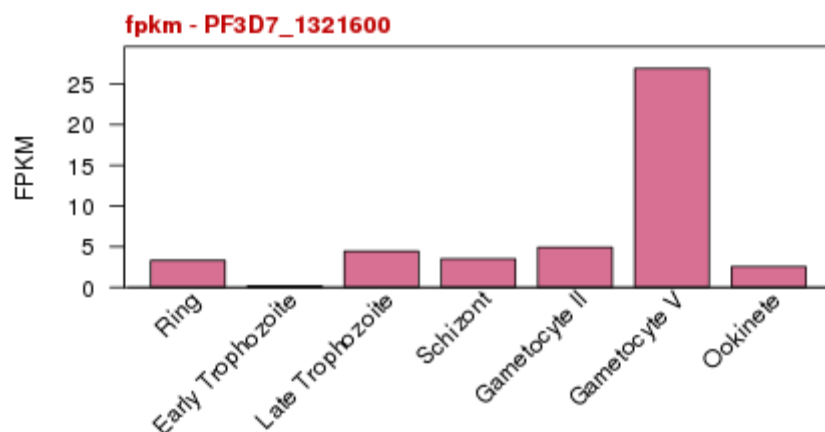


Figure 1.6. Detection of *PfPDE γ* mRNA levels in *P. falciparum* parasite stages. Detection of *PfPDE γ* mRNA in 7 life cycle stages of 3D7 by illumina sequencing. Measured as transcript levels of fragments per kilo base of exon model per million mapped reads (FPKM)[144].

PfPDEδ

PfPDEδ (PF3D7_1407500 Plasmo DB) is a 97 kDA protein with a predicted topology of 6 transmembrane helices located at the N-terminus followed by a catalytic domain[141]. The gene encoding *PfPDEδ* is located on chromosome 14. There is evidence using a *PfPDEδ*-ko line that this PDE appears to be essential for the process of gametogenesis to occur[130]. This is discussed in more detail in section 1.2.4 (p63). *PbPDEδ* has also been shown to regulate levels of cGMP in order to facilitate ookinete gliding through a *PfPKG*-dependent signalling pathway in *P. berghei*[128]. *PfPDEδ* mRNA is not expressed in asexual stages but is expressed at a high level in gametocyte stages[25] (Figure 1.7[144]). In a *PfPDEδ*-ko line, cGMP levels appeared elevated, reflected by a 50 % reduction in cGMP-PDE activity[130]. cAMP-PDE activity did not appear to be affected in this line suggesting that *PfPDEδ* may hydrolyse cGMP specifically[130]. However, later work on gametocyte-infected erythrocyte deformability has suggested a role for *PfPDEδ* in regulating levels of cAMP (although this may indirect). In this study, an increase in cAMP levels was observed in both stage II and stage V *PfPDEδ*-ko gametocytes compared to a wildtype line[25]. Given this information, a dual specific role for this enzyme cannot be ruled out. Given the striking level of *PfPDEδ* mRNA detected in mature gametocyte stages (Figure 1.7) and the evidence that this PDE is likely to be essential for the process of gametogenesis[130], this *Plasmodium* PDE is an interesting protein to study further and will be a dominant topic of this thesis. More evidence is needed to confirm the substrate specificity of *PfPDEδ* and its cellular localisation and as yet there are no data demonstrating that this PDE is actually present at the protein level in gametocyte stages (although given what we know so far, it is predicted to be). More investigation is required into the role of this PDE in the process of gametogenesis.

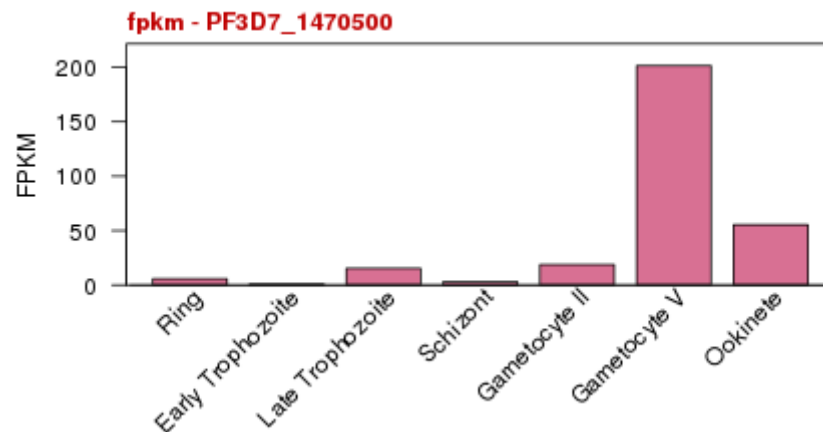


Figure 1.7. Detection of *PfpDEδ* mRNA levels in *P. falciparum* parasite stages. Detection of *PfpDEδ* mRNA in 7 life cycle stages of 3D7 by illumina sequencing. Measured in RNA-seq expression units as transcript levels of fragments per kilobase of exon model per million mapped reads (FPKM)[144].

The cyclic nucleotides: cGMP and cAMP

The cyclic nucleotides, cyclic adenosine monophosphate (cAMP) and 3'-5'-cyclic guanosine monophosphate (cGMP) are tightly regulated by the opposing actions of ACs and GCs respectively to synthesise them and by PDEs to hydrolyse them. The functions of cyclic nucleotides are mediated mostly by their respective effector kinases. In mammals, cGMP has additional cellular targets apart from PKG: cGMP-specific PDEs and cGMP-gated channels[147]. However, in *Plasmodia* there is currently only one known downstream effector protein for cGMP, PKG. In mammalian systems, although PKA is the main effector protein for cAMP, cyclic nucleotide-gated ion channels[148] and the exchange protein guanine nucleotide exchange factor (EPAC)[149] are also directly activated by cAMP. In mammals, there are two isoforms of EPAC that both contain a conserved cAMP-binding domain and bind cAMP with high affinity. This binding of cAMP to EPAC results in the direct activation of Ras-like small GTPases (Rap 1 and Rap 2) and plays an important role in signalling events required for the regulation of neurotransmitter release, Insulin secretion, cardiovascular function and cancer cell proliferation amongst other functions [150]:[151].

In *Plasmodium* species, known effector proteins of cAMP include the main effector PKA. EPAC has also been shown to be regulated by cAMP in *Plasmodium* and although divergent from mammalian EPAC, shares the putative cAMP binding sites[152].

cAMP was first identified as a signalling molecule in the 1950s prior to the identification of cGMP[153] where it was implicated in hormone-induced phosphorylation of proteins involved in the heart, liver, skeletal muscle and brain tissue[153]. cGMP was discovered in 1963 when it was isolated from rat urine[155]. It was subsequently demonstrated in 1969 that it is synthesised from guanosine triphosphate (GTP) by the enzyme guanyl cyclase (also known as guanylyl cyclase)[112].

In mammalian systems cross talk can occur between the cAMP and cGMP signalling pathways. An example of such cross-talk is the cGMP regulated PDE2-mediated hydrolysis of cAMP in the human heart[133]. cGMP can also competitively inhibit the hydrolysing activity of cAMP-PDEs[133]. This demonstrates the complexity of cyclic nucleotide signalling.

cAMP and cGMP regulate multiple cellular functions often in the same cell and as such signalling pathways involving these cyclic nucleotides must be tightly regulated and targeted to ensure the specificity of the required response. One of the ways that cells achieve this is to structurally and functionally restrict components of the signalling cascade by compartmentalising the proteins that regulate levels of cyclic nucleotides and effector proteins that are activated by cyclic nucleotides[156]. This allows components of the required signalling pathway only to be able to come into contact with each other to complete the signalling cascade when required. This can be achieved by spatial and temporal distribution of signalling components as well as targeting of proteins into complexes and the targeted localisation of components that restrict them to specific intracellular domains at very specific times.

In plasmodium cAMP signalling has been implicated in many important cellular processes including gametocyte-infected erythrocyte deformability[25], sporozoite migration through hepatocytes[108], cell cycle regulation[157], and merozoite invasion[152]. Similarly, cGMP also plays an essential roles across the parasite life cycle including late liver stage development[158], sporozoite invasion of mosquito salivary glands[142], gametogenesis[159], blood stage schizogony and invasion[160].

The effector proteins: cGMP-dependent protein kinase (PKG) and cAMP-dependent protein kinase (PKA)

Protein kinases phosphorylate target proteins by transferring a gamma phosphate from ATP phosphoryl groups to specific serine, threonine or tyrosine amino acids in the target protein[161]. This action can be reversed by protein phosphatases such as calcineurin that remove the phosphoryl groups[162]. Protein kinases such as PKA and PKG are involved in a range of different functions across a diverse array of organisms.

Protein kinase G (PKG)

Mammalian PKG

Human PKG is found in many parts of the body including, the brain, smooth muscle and platelets and was first isolated and purified from the human adrenal cortex in 1982[163]. Two types of mammalian PKG exist which are encoded by different genes, a 76 kDa soluble form (PKG I) which has two isoforms and a 87 kDa membrane bound form[164]. Mammalian PKG is structurally similar to PKA. However, it exists as a homodimer that has two distinct domains, a regulatory domain located at the N-terminus which contains two cGMP binding sites and a catalytic domain located at the C-terminus that binds substrates and Mg^{2+} /ATP[147]. Cyclic GMP interacts with PKG by binding to allosteric sites in the regulatory domain of PKG. This induces a conformational change resulting in exposure of the active site allowing phosphorylation of PKG substrate proteins to occur[165][166]. The two binding sites of PKG I exhibit differing affinity for cGMP binding[167].

***Plasmodium* PKG**

PKG has been identified in apicomplexans including *E. tenella*, *T. gondii* and *P. falciparum*[83][168][164]. *P. falciparum* expresses a single PKG, *Pf*PKG (Pf3D7_1436600), a 97.5kDa protein consisting of a C-terminal catalytic domain and an N-terminal regulatory domain, characterised by Deng and colleagues in 2002[164]. Unlike mammalian PKGs, *Pf*PKG is thought to exist as a monomer. cGMP binding to the regulatory domain of *P. falciparum* PKG has been determined by crystallography[169]. This protein kinase exhibits some structural similarities to mammalian PKG; however, it contains an additional two cGMP binding sites making a total of four, the last of which was shown to be degenerate[170]. *Pf*PKG is activated on binding to cGMP (in *Eimeria*, cGMP must be bound to all 3 functional cGMP binding domains

in order for full activation of the kinase[171],[170]) and its activation subsequently leads to cellular responses essential to parasite survival and life cycle progression including gametogenesis [159], ookinete gliding [128], late liver stage development[158], blood stage schizogony [160], merozoite invasion[172] and merozoite egress [173]. This protein kinase is the only known effector protein of cGMP in *Plasmodium* and phosphoproteomic analysis has indicated that it can phosphorylate many substrates[172]. PKG-dependent phosphorylation can lead to the mobilisation of an important signalling molecule, Ca^{2+} . PKG has been shown to be important for regulating the Ca^{2+} levels required for gametogenesis[159], *P. berghei* ookinete motility[174] and *P. falciparum* egress[175],[174]. As well as proteins involved in cell signalling, other targets of PKG include proteins involved in protein export, chromatin regulation, invasion, egress and transcriptional regulation amongst others[172]. Interestingly, studies of the *P. falciparum* phosphoproteome also indicated a possible feedback mechanism whereby the enzymes regulating the levels of cGMP could be phosphorylated by *Pf*PKG therefore possibly allowing *Pf*PKG to contribute to regulating cGMP hydrolysis and synthesis and therefore its own activation. There was also evidence to suggest that *Pf*PKG may phosphorylate *Pf*AC β indicating possible crosstalk between the cAMP and cGMP signalling pathways[172]. Such cross talk and feedback mechanism are seen in mammalian systems.

Investigation into *Pf*PKG expression and subcellular localisation in blood stages suggested a cytosolic localisation, with some endoplasmic reticulum (ER) overlap. *Pf*PKG was also shown to associate with the peripheral membrane fraction in subcellular fractionation experiments[176]. Mammalian PKG is able to translocate to the nucleus where it can regulate gene expression[177]. However, as yet there has been no evidence that *Plasmodium* PKG can do this and in fact, the sequencing of mRNA from ookinetes of a *gc* β *P. berghei* knock out mutant did not show any difference in gene expression compared to a wildtype control, indicating that in *P. berghei* ookinetes, there is no indication that *Pb*PKG can control transcription[174].

Apicomplexan PKGs differ from their mammalian orthologues at an important site adjoining the ATP-binding pocket [164],[83]. This makes them of particular interest as drug targets because compounds specifically targeted to apicomplexan PKG will act upon the parasite without disrupting host PKG. One such compound, the trisubstituted pyrrole 4-[2-(4-fluorophenyl)-5-(1-methylpiperidine-4-yl)-1H pyrrol-3-yl] pyridine; Compound 1 (C1), was developed by Merck as a treatment for *Eimeria* infection in chickens[83]. This compound, which is an ATP-competitive inhibitor, was subsequently shown to target apicomplexan PKG and exhibited activity against several apicomplexan parasites including *E. tenella*, *T. gondii* [178] and *P. falciparum* [179],[160].

A transgenic line resistant to C1 and the more potent C2 (4-[7-](dimethylamino)methyl)-2-(4-fluorophenyl)imidazo[1,2- α]pyridine-3-yl]pyrimidin-2-amine)[180] has been developed[159]. In this gatekeeper mutant, (*Pf*PKG_{T618Q}), a key threonine residue in the gatekeeper position of *Pf*PKG has been replaced by an amino acid with a more bulky side chain (glutamine) rendering this line resistant to C1 and C2. These compounds can no longer bind to the ATP binding site of the enzyme. This line in combination with the PKG inhibitors C1 and C2 is a valuable tool for confirming the specific involvement of *Pf*PKG in cellular events and to confirm that PKG is the primary target of the inhibitors in a particular cellular event[159]. These inhibitors have proved invaluable for functional studies on PKG[178]. C1 and C2 (Figure 1.8) although potent inhibitors of PKG, can target other kinases. One known non-PKG target for these compounds is the homologue of *Pf*CDPK4 in *T. gondii* *Tg*CDPK1[181]. A more specific PKG inhibitor (MRT00207065) has now been developed that has an IC₅₀ of 160 nM in a PKG assay and an EC₅₀ of 2.1 nM in a 72 hour *P. falciparum* growth assay and does not show any off-target effects when used at appropriate concentrations.

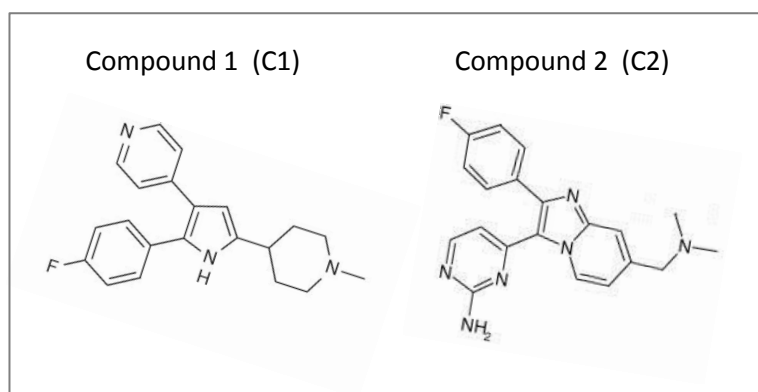


Figure 1.8. Chemical structures of C1 (4-[2-(4-fluorophenyl)-5-(1-methylpiperidin-4-yl)-1H-pyrrol-3-yl]pyridine)[182] and C2 (4-[7-](dimethylamino)methyl)-2-(4-fluorophenyl)imidazo[1,2- α]pyridine-3-yl]pyrimidin-2-amine)[181].

Protein Kinase A (PKA)

Mammalian PKA exists as a heterotetramer complex composed of two catalytic subunits (PKA-C) that bind to two regulatory subunits (PKA-R). Mammalian cells encode three isoforms of the catalytic subunit and four isoforms of the regulatory subunit[183]. The regulatory subunits are responsible for cellular localisation, which is achieved by association with A-kinase anchoring

proteins (AKAPs) which facilitate an association of the regulatory domain with other cellular components such as membrane associated proteins[184]. Both regulatory subunits contain two cAMP binding sites. When cAMP binds to the regulatory subunits of PKA it results in a conformational change in protein structure whereby the complex containing the catalytic and regulatory subunits dissociates. This releases the active catalytic subunit and enables it to phosphorylate target substrates[185][186][187]. PKA is subdivided into two classes depending on which regulatory subunit the protein contains. Type I PKA contains RI subunits whereas type II PKA contains RII regulatory subunits. The regulatory subunits exhibit differing affinity to cAMP binding and as such, the response to changing cAMP levels differs depending on which PKA isoform is present[185]. Differing tissue expression and therefore distribution of the different isoforms of the catalytic and regulatory subunits of PKA mean that PKA can mediate diverse cell signalling responses[183].

The regulatory subunit of PKA has also been characterised in *P. falciparum*[187]. *Pf*PKA activity has been detected in *P. falciparum* asexual blood stages and shows higher activity in schizont stages. Addition of the PKA inhibitor H89 blocks parasite growth[188]. However, it is unclear whether the PKA target is host or parasite derived as this inhibitor targets both and the IC_{50} for the human orthologue is much lower than that for the parasite PKA[189]. The domain allowing AKAP association, which is responsible for localisation and PKA function in mammals, is absent in Plasmodium (Baker et al; in press).

A homologue of the catalytic subunit of PKA has been identified in all plasmodium species[190][183][188] and is encoded by a single gene which has been cloned and characterised[188]. This gene is developmentally regulated[188] with higher levels detected in asexual blood stages than sexual stages initially indicating that PKA may not play a role in gametocyte stages. However, *Pf*PKA activity detected in gametocytes has been shown to be higher in gametocyte producing strains than non-gametocyte producing strains suggesting that in contrast to previous reports PKA may play a role in sexual stages[107], and in fact, recent work on gametocyte deformability[25] has identified a role for this protein kinase in sexual stages.

PKA phosphorylation of downstream substrates is known to regulate several key parasite processes. PKA is required for *P. berghei* sporozoite motility and liver cell invasion[108] and for *P. falciparum* erythrocyte invasion where it is required to phosphorylate the parasite adhesin apical membrane antigen 1 (AMA1)[191][192]. PKA has also been implicated in modulation of anion conductance in the host erythrocyte cell membrane in order to facilitate movement of nutrients required by the parasite into the infected cell[187]. PKA has recently been implicated

in *P. falciparum* merozoite invasion and ring formation (Christian Flueck, unpublished). A role for PKA in gametocyte-infected erythrocyte deformability has been identified. Regulation of levels of PKA are required for gametocytes to remain non-deformable while sequestering in the bone marrow (high PKA levels) and for mature gametocytes to become deformable once they are released into the peripheral circulation (low PKA levels)[25]. A phosphoproteome study suggested that phosphorylation events by PKA play an important role in *P. falciparum* schizont stages[193]. This same study also identified the merozoite glideosome motor proteins, myosin A, GAP45 and CDPK1, as potential substrates for PKA in *P. falciparum*[193].

In infected erythrocytes there is both host and parasite PKA present[188]. It is therefore not clear whether these parasite functions are a result of the host PKA, parasite PKA or both. This can complicate studies using pharmacological agents as tools to investigate the role of PKA in parasites as there is no chemical genetic tool available unlike for PKG.

1.2.2 Calcium (Ca²⁺) signalling

Ca²⁺ signalling in mammals

Calcium (Ca²⁺) is a ubiquitous intracellular signalling molecule that operates across a diverse range of organisms to regulate many different cellular functions ranging from organisation of cell polarity in plants [194] to muscle contraction in mammals [195]. Levels of Ca²⁺ in the cell are tightly regulated by stimulated release from internal stores, which increases the levels of Ca²⁺ in the cytoplasm. In mammals, Ca²⁺ levels in the cytoplasm are restored back to basal levels by removal into internal stores by pumps and exchangers. High levels of Ca²⁺ can be toxic to cells [196] so removal of Ca²⁺ is important to maintain Ca²⁺ gradients across cell membranes and to avoid prolonged elevated levels of Ca²⁺ in the cytosol. Sarcoendoplasmic reticulum Ca²⁺ ATPases (SERCA pumps) are P type ATPases that pump Ca²⁺ from the cytoplasm back into the ER by exchanging protons for two Ca²⁺ ions per ATP hydrolysed [161]. Similarly plasma membrane Ca²⁺ ATPases (PMCA pumps) pump Ca²⁺ out of the cytoplasm into the extracellular space by exchanging one Ca²⁺ ion for one ATP. Mammalian cells also use Na⁺/Ca²⁺ exchangers that exchange one Ca²⁺ ion for three Na⁺ ions. The inward movement of Na⁺ ions into the cell from the extracellular environment drives the movement of Ca²⁺ ions out of the cytoplasm [161]. In response to environmental cues and cell signalling cascades, Ca²⁺ ions are released from cellular stores such as the endoplasmic reticulum by Ca²⁺ channels such as inositol trisphosphate (IP₃) receptors and ryanodine receptors. Both are large channels located in the endoplasmic reticulum (ER) membrane and Ca²⁺ mobilisation out of the ER is thought to mainly occur through these two receptors. Ryanodine receptors are opened by changes in levels of Ca²⁺ whereas IP₃ channels are activated by interaction with signalling molecules such as inositol (1,4,5)-trisphosphate (IP₃) [161]. IP₃ is a secondary messenger produced by the hydrolysis of the phosphatidylinositol lipid, phosphatidylinositol (4,5)-bisphosphate (PI(4,5)P₂) by phospholipase C (PLC). PI(4,5)P₂ is a product of (PI4P) phosphorylation by the PIP5 kinase which is derived from the phosphorylation of phosphatidyl-1D-*myo*-inositol (PI) by the PI4 kinase (Figure 1.9). The generation of IP₃ is mediated by lipid kinases and leads to mobilisation of Ca²⁺ from the ER.

In mammalian cells three isoforms of ryanodine receptor exist. These have different tissue distribution with RYR1 being expressed in skeletal muscle, RYR2 in cardiac muscle and RYR3 which has a wider tissue distribution being found at low levels in several tissue types including the brain [197]. However, to date homologues of both the IP₃ and ryanodine receptors have not been identified in *Plasmodium* although there is evidence that they might exist through studies using pharmacological approaches [198]; [199]; [200].

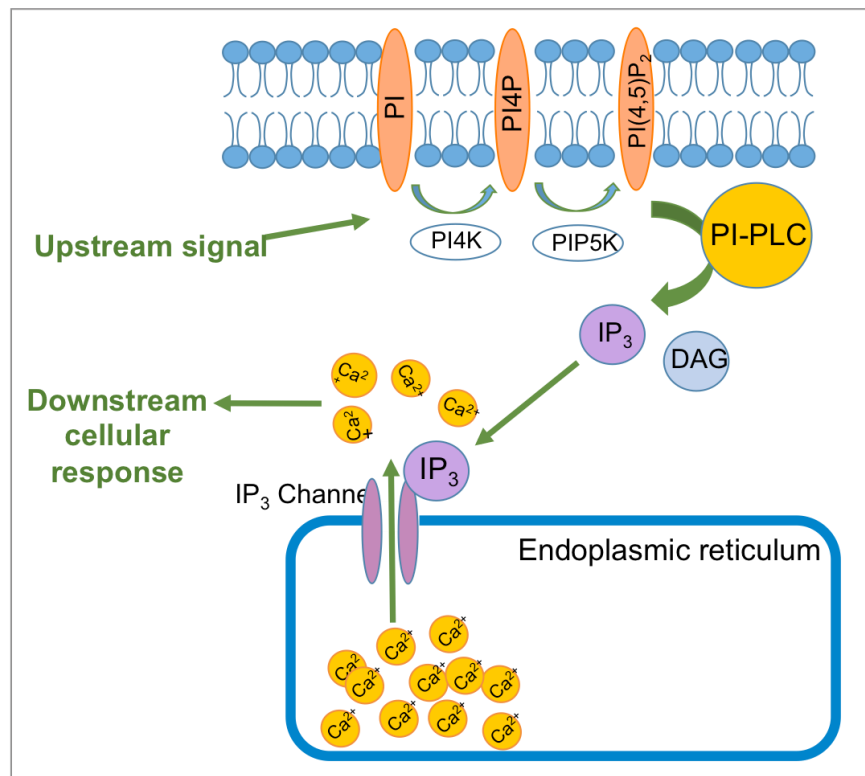


Figure 1.9: Schematic depicting the generation of IP₃ leading to Ca²⁺ mobilisation from the ER. Following an upstream signal, PI is phosphorylated by the lipid kinase PI4K to produce PI4P. The lipid kinase PIP5K then phosphorylates PI4P producing the phosphatidylinositol lipid PI(4,5)P₂, which undergoes hydrolysis by PI-PLC to produce the secondary messengers IP₃ and DAG. In mammalian cells IP₃ binds to its associate receptor on the ER membrane. Activation of the receptor leads to the mobilisation of Ca²⁺ out of the ER store and into the cytosol. This leads to the required downstream signalling response.

Ca²⁺ acts as a second messenger by binding to effector molecules. This often results in a change in the charge and/or shape of the protein and acts to regulate its function. The change in charge of some proteins when binding to the positive Ca²⁺ ion can allow them to translocate from the cytoplasm to the membrane[161]. Many proteins involved in Ca²⁺ signalling pathways such as protein kinase C (PKC) and phosphoinositide 3-kinase (PI3K) contain a domain known as a C2 domain that can bind Ca²⁺ ions and promote association with the plasma membrane[161] where they can interact with other signalling proteins and molecules. This allows spatial regulation of signalling molecules and acts to bring proteins into contact with their substrates. Binding of Ca²⁺ ions requires specific binding domains and one of the most common protein binding motifs is the EF hand domain. These domains capture Ca²⁺ ions between negatively charged oxygen

atoms within a loop of the helix-turn-helix structure and the affinity for Ca^{2+} can vary greatly between proteins [161].

In mammalian cells, calmodulin is an important signalling protein that is regulated by Ca^{2+} . Calmodulin is a small protein that amplifies the Ca^{2+} signal. The second messenger nucleotides cADPR and NAADP are important for controlling the release of Ca^{2+} from cellular Ca^{2+} stores. In plants, the phytohormone abscisic acid (ABA) acts to induce cADPR production, which results in Ca^{2+} mobilisation. Interestingly, this plant hormone is also present in the apicomplexan parasite *T. gondii*, where it governs the decision of the parasite to develop either to a dormant stage or to switch to lytic growth, and addition of exogenous ABA can trigger egress of *T. gondii* in a PKG-dependent manner, indicating that cADPR plays a role in the regulation of Ca^{2+} in this organism[201]. Although *T. gondii* is closely related to *Plasmodium* species, there has been no indication that ABA induced cADPR regulated Ca^{2+} pathways are present in *Plasmodium*. However an inhibitor of ABA synthesis fluridone, which is a registered pesticide has been shown to be active against malaria[202].

Ca^{2+} signalling in *Plasmodium*

Ca^{2+} signalling in apicomplexans is not well understood. However, Ca^{2+} is known to regulate many key events in apicomplexan parasites, including motility, development and protein secretion. Although several of the features of the Ca^{2+} signalling machinery found in mammals remain conserved in *Plasmodium*, there are many which are not, such as the classical mammalian Ca^{2+} effector proteins PKC and Ca^{2+} -calmodulin-dependent protein kinases and the ER Ca^{2+} receptors for ryanodine and IP_3 . A SERCA Ca^{2+} ATPase has been identified in *Plasmodium* as has a $\text{Ca}^{2+}/\text{H}^+$ exchanger. However, as yet no PMCA has been identified[203]. As seen in other organisms, in plasmodia levels of Ca^{2+} are tightly regulated. Unlike in mammals, however, calcium release in *Plasmodium* leads to activation of a family of calcium-dependent protein kinases (CDPKs). These kinases are key signalling molecules in plants, protozoa and fungi but are absent in humans which makes them an attractive therapeutic target in apicomplexans. These effector proteins bind calcium and are subsequently activated due to a change in conformation allowing the kinase to phosphorylate its substrates [204] [205]. The EF hand domain appears to be conserved in *Plasmodium* with around twenty proteins identified as containing this domain feature[206]. *Plasmodium* as with other apicomplexans, encodes an array of CDPKs. Several of these have been shown to play important roles in the life cycle of this parasite. *Pf*CDPK1 is expressed in all blood stages and is localised to the plasma membrane. It is thought to play an important role in invasion through discharge of micronemes [207]. It has been shown by

phosphoproteomics to be a direct cellular target of *Pf*PKG[172]. *Pf*CDPK2 is transcribed in late trophozoite stages, *Pf*CDPK3 is expressed in ookinetes and has been shown to be important for ookinete gliding motility [208], [209]. *Pf*CDPK4 has been shown to play an important role in regulating gametogenesis and is therefore important for transmission [210], and *Pf*CDPK5 is expressed in *P. falciparum* blood stages and is essential for merozoite egress and acts downstream of PKG[175]. *Pf*CDPK7 shows highest levels of transcription in ring stages. Disruption of the gene encoding *Pf*CDPK7 results in ablated development from the ring stages to trophozoite stages and fewer progeny generated from each subsequent schizont leading to an overall reduced growth rate[211].

The mitochondria [212], ER, food vacuole[213] and acidocalcisomes [214] are all reported intracellular Ca^{2+} stores in apicomplexans [198]. The ER is thought to be a major Ca^{2+} store in *Plasmodium*[213].

In *P. falciparum*, Ca^{2+} mobilization has been strongly implicated in the late stages of gametogenesis[159][215], in cell cycle development and progression [216][198][174], in ookinete gliding motility and invasion of the mosquito midgut [209][208][174], sporozoite development and invasion [217][218] and gamete formation [210][210][174]. The wide range of key events regulated by Ca^{2+} emphasises its critical importance as a signalling molecule in *P. falciparum*. Ca^{2+} must interact with many signalling and other downstream molecules in a timely and precise fashion, in order for the parasite to develop, survive and propagate.

1.2.3. Cell signalling in the asexual blood stages

Cell signalling in merozoite egress

Release of infectious merozoites from host erythrocytes is an essential step in the propagation of *P. falciparum* in the blood stream. This process must be tightly regulated in order for merozoites to be released only when they are fully mature and competent to invade new blood cells. Premature schizont rupture results in the release of merozoites which will not invade. This is seen in zaprinast-induced egress in which schizonts rupture in a *PfPKG*-dependent manner but merozoites are unable to invade new erythrocytes[173]. cGMP signalling has been shown to be essential for egress. Addition of the PKG inhibitor C1 to *P. falciparum* schizonts resulted in a block in schizont rupture which was not observed in parasites of the C1 insensitive line *PfPKG*_{T618Q}[160]. Mechanical shearing of C1-blocked schizonts resulted in merozoites that were invasively incompetent[175].

In order for schizont rupture and subsequent merozoite egress to occur, a protease cascade must be activated. A key player in this cascade is the subtilisin-family serine protease *PfSUB1*, which is expressed late in schizont maturation[219][173]. *PfSUB1* is stored in specialised organelles called exonemes from which it is released into the parasitophorous vacuole space[220]. *PfSUB1* proteolytically processes several proteins required for egress, one of which is the protein serine-repeat antigen 5 (SERA5)[220]. SERA5 is expressed abundantly in the parasitophorous vacuole of mature schizonts and appears to be indispensable for parasite growth[221]. Antibodies against SERA5 block egress[222]. *PfSUB1* has been shown to be refractory to deletion in blood stages identifying it as an essential protease in asexual blood stages[220].

Inhibition of *PfSUB1* results in a block in processing of SERA5, which also correlates with a block in egress and also invasion[220],[223]. In *P. falciparum*, *PfSUB1* also cleaves merozoite surface protein 1 (*PfMSP1*). During normal egress the cleaved forms of both MSP1 (shed from the merozoite surface) and SERA5 are shed into the surrounding medium. *PfSUB1*-mediated proteolytic processing of *PfMSP1* can be blocked by addition of C1[175]. C1 and C2 also block proteolytic processing of SERA5 and PKG inhibition was shown to have no effect on *PfSUB1* expression in the cell or for its maturation[173]. Instead, inhibition of *PfPKG* by C1 and C2 was shown to block the discharge of exonemes and micronemes and this block was shown to be reversible by removal of C1 or C2[173]. This observation explained the previous finding that mechanically ruptured *PfPKG* inhibited parasites produced non-invasive merozoites[175]. This can be explained by the fact that these merozoites have not been exposed to *PfSUB1*, which

stays trapped in exonemes due to PKG inhibition[173]. Addition of the PDE inhibitor zaprinast to mature schizonts induces premature egress and a rapid discharge of micronemes and exonemes and proteolytic processing of both *PfMSP1* and *PfSERA5*[173]. Zaprinast also induced a translocation of the protein *PfAMA1* (from micronemes) onto the surface of schizonts, this was inhibited by C1 treatment and was observed in both mature (segmented) schizonts and immature (non-segmented) schizonts[173].

Prior to blood stage egress a steady increase in cytoplasmic free Ca^{2+} occurs [224]. This was shown to be independent of external Ca^{2+} but dependent upon internal Ca^{2+} stores, as chelation with EGTA did not inhibit this Ca^{2+} release whereas the membrane-permeable chelator BAPTA-AM did. Furthermore, addition of the Ca^{2+} ionophore A23187 induced egress[224]. The related apicomplexan parasite *T. gondii* also requires mobilisation of Ca^{2+} for egress. Artificial stimulation of Ca^{2+} release using A23187 or ionomycin triggers microneme secretion and this process is blocked by disruption of Ca^{2+} release. This chelation of parasite Ca^{2+} also prevents *T. gondii* egress[225]. There is evidence that IP_3 is involved in mediating the Ca^{2+} response in *T. gondii*[226]. Ryanodine and caffeine (an agonist of ryanodine receptor Ca^{2+} release) also induced Ca^{2+} indicating that there may be a RYR-like receptor in *T. gondii*[226].

In *P. falciparum*, CDPK5 is present at the protein level in schizonts and invasive merozoites[110]. A conditional knock down line of CDPK5 using a destabilising domain system revealed an essential role for this protein in regulating merozoite egress[175]. Degradation of the CDPK5 protein using the DD system resulted in a block in egress. However, this block in egress differed to that seen with *PfPKG* inhibition in that the CDPK5 block occurred downstream of *PfSUB1* mediated proteolytic processing as processing of both *PfSUB1* and *PfMSP1* were unaffected by the absence of CDPK5[175], whereas inhibition of PKG results in a block in the proteolytic processing of *PfSUB1* substrates. The schizont block as a result of CDPK5 disruption also differed from that caused by PKG inhibition in terms of invasiveness of merozoites. Merozoites from schizonts derived from sheared CDPK5-deficient blocked schizonts were able to invade normally[175], whereas mechanically sheared C2 blocked schizonts were not[175]. However, removal of the C2 block releases invasive merozoites if allowed to egress naturally.

Cell signalling in merozoite invasion

Once merozoites are released into the harsh environment of the host bloodstream, they must quickly invade new erythrocytes in order to develop into ring stage forms and to develop through the subsequent asexual blood stage forms.

The first step of invasion involves an initial recognition of and contact with the erythrocyte. This primary contact is of low affinity and reversible[227]. Initial attachment is followed by reorientation of the parasite to bring its apical end into contact with the host erythrocyte membrane. This allows for a stronger interaction. The apical membrane protein 1 (AMA1) is translocated to the merozoite surface prior to invasion[227] and is essential for invasion[228]. Use of specific antibodies against *Pf*AMA1 did not block the initial attachment but prevented reorientation of the parasite[229]. *Pf*AMA1 has also been shown to be essential for invasion of *T. gondii*[230], where it is thought to be involved in forming the initial apical interaction and also in the regulation of rhoptry secretion[230].

Once the initial attachment has occurred, the parasite can start the process of entering the host cell. This entry involves the formation of a tight junction and the parasite is propelled forward by the action of an actin-myosin motor[231]. AMA1 is a key protein involved in formation of the tight junction[232]. The serine protease SUB2, which is released from micronemes at the apical end of the merozoites, acts to induce removal of the merozoite surface coat in a process known as 'shedding'[233]. During the process of invasion, the tight junction moves from the apical end of the parasite, which forms the initial attachment, to the posterior end of the parasite. As this occurs, a parasitophorous vacuole is formed enabling the parasite to reside within the host cell but in a compartment in which it has favourable conditions to survive. A possible role for *Pf*PDE β in erythrocyte invasion has been elucidated. Parasites devoid of *Pf*PDE β exhibited greatly reduced invasion and ring forms appeared to be unable to develop (Christian Flueck, LSHTM, unpublished).

1.2.4. Cell signalling in gametocytogenesis

Unlike the initiation of gametogenesis which requires a well-documented trigger resulting from the transition between the vertebrate host and mosquito vector, what makes a parasite decide to make the earlier transition from the asexual replication cycle to the transmission stages is presently not well understood. Very little is known about the signalling pathways involved in gametocytogenesis, although there are several factors that have come to light over the years and more recently, evidence of an epigenetic factor that is an important mediator of this process[234].

It has been known for some time that 'stress' is one such factor leading to the induction of gametocytogenesis *in vitro*. The use of spent medium to stress asexual cultures has been shown to result in the production of gametocytes[235]. Variations of this method are currently used as the 'gold standard' to produce gametocytes for *in vitro* studies. This observation that spent medium can trigger gametocytogenesis supports a hypothesis that the switch from the asexual cycle is one that allows the parasite to exit the increasingly unfavourable conditions of the host and to leave before host death occurs. However, the observation that *P. vivax* gametocytes appear early on in infection, sometimes prior to the observation of asexual stages calls this 'stress' hypothesis into question. However, stress induced initiation of gametocytogenesis *in vitro* may be different from what happens *in vivo*. The reason that *P. falciparum* gametocytes appear much later in the blood stream of the human host than the other human *Plasmodium* species could be due to their long maturation period (~10 days), and the ability of the immature stages to sequester means that *P. falciparum* gametocytes are only observed in the blood once they have fully matured. Despite this, the fact remains that *in vitro* stress can stimulate gametocytogenesis so must be an important factor at least *in vitro* when considering what initiates this process. However, the cell signalling pathways involved in this response to stress are currently unknown. There have been several other studies highlighting alternative *in vitro* triggers for gametocytogenesis. Carter et al, observed that lysed erythrocytes resulted in the formation of gametocytes[236]. Host reticulocytes have also been associated with increased gametocytemia[237] , as have host hormones such as steroids[238] [239]. Interestingly, *P. chabaudi* parasites converted to a much higher proportion of gametocytes when taken from their natural host, a mouse, and injected into a rat[240]. A publication in 1980[241] suggested a role for cAMP in the switch to gametocytes and data demonstrated that addition of cAMP to an asexual ring stage culture of *P. falciparum* resulted in nearly 100 % of asexual stages switching to gametocyte stages, although, this has yet to be replicated efficiently. However, prior to this

study in 1979, Hertelendy et al, described an increase in cAMP production in erythrocytes infected with *P. berghei* compared to uninfected erythrocytes[242]. Caffeine[243] and 8-bromo-cAMP[237], both of which inhibit the action of mammalian cAMP-PDEs, have both been reported to enhance the production of gametocytes. In addition to this, a comparison of a gametocyte producing and a non-gametocyte producing *P. falciparum* clone linked the loss of gametocyte-producing ability to a decrease in cAMP-dependent protein kinase activity[107], indicating a possible role for cyclic nucleotide signalling in gametocytogenesis. In further support of this, *PfAC α* is highly expressed in gametocyte stages[106] suggesting that PKA may play a role at this stage of the life cycle.

Recent studies have uncovered an epigenetic factor that regulates gametocyte induction leading many to believe that the switch from the asexual stages to the sexual stages is a stochastic event. The transcription factor *PfAP2-G* was identified in 2014 as an epigenetically regulated master switch of gametocytogenesis. It is encoded by a member of the *ApiAP2* gene family. In asexual blood stages, this gene appears to be epigenetically regulated[244][245] and spontaneously activated[246]. *ApiAP2* proteins are major transcriptional regulators in *Plasmodium* and have been shown to regulate several key developmental stages including liver stage development[247], ookinete formation[248] and sporozoite development[249]. However, until recently no link to the gametocyte stages had been seen and the use of both forward and reverse genetic approaches demonstrated a role for AP2G in gametogenesis and this has sparked a huge interest in this protein[250]. The early gametocyte markers *Pfg 14,744*, *Pfs16* and *Pfg 27/25* were all found in lower abundance in a *PfAp2-g* mutant line[250]. Furthermore, this mutant lost the ability to produce gametocytes completely, indicating that it directly activates the transcription of the early gametocyte genes required for gametocytogenesis. Interestingly two gametocyte non-producer clonal lines derived from 3D7a (F12 and A4) were found to have mutations in the *Pfap2-g* gene (*Pf3D7_1222600*, Plasmo DB). No other mutations associated with gametocyte formation were found in these lines and in particular, no disruptions in the sub telomeric region of chromosome 9 were found, the deletion of which has historically been known to be associated with gametocytogenesis[251]. Higher abundance of *PfAP2-G* transcripts was detected by RT-PCR in a high gametocyte producing clonal line (3D7B) compared to the lesser producer 3D7A[250]. HA tagging of *PfAP2-G* has indicated that this protein localises to the nuclear region[250].

It is not clear at which point in the asexual cycle gametocytogenesis is initiated, however, evidence has pointed to the switch occurring prior to the formation of segmented schizonts. In 1989, Bruce et al, used antibodies against the gametocyte specific marker *Pfg 27/25* and the

specific asexual marker MSA2 to show that in plaques obtained from erythrocyte monolayers, in a single segmented schizont all merozoites were either sexually committed or not[252]. In support of this, in *PfAP2-G* expressing schizonts, all merozoites in one schizont stained positive for *PfAP2-G*[250]. Interestingly, the work of Smith et al[253], showed that of those parasites that had committed to the sexual cycle, all merozoites from a single schizont were either all male or all female gametocytes.

A biased sex ratio in *P. falciparum* has already been identified and the ratio leans in favour of females. This female favoured sex ratio likely compensates for the fact that when gametogenesis occurs male gametocytes will produce 8 gametes whereas females will only produce one. Therefore more females are required to facilitate fertilisation efficiency. However, sex ratios do vary between strains and species[254]. In *P. falciparum* sex specificity can be distinguished by microscopy at stage V by Giemsa stain and earlier at stage III using the female sex specific antibody *Pf377* which highlights the higher number of osmiophilic bodies found in female gametocytes[255]. From stage III, females exhibit an increasing number of Golgi vesicles, mitochondria and ribosomes[23]. To specifically identify male gametocytes, α -tubulin II can be used. Females stain blue with Giemsa due to the presence of a higher density of ribosomes. In contrast, males tend to stain more pink in colouration using Giemsa. Nuclear size also differs between the sexes with females presenting with a smaller nucleus than males[256].

1.2.5. Cell signalling in gametogenesis

In *P. falciparum*, fully mature male and female stage V gametocytes circulating in the blood stream are primed for activation in the mosquito. This means that on entering the mosquito midgut they are ready for the process of gametogenesis to occur immediately. It's likely therefore that the components of the cell signalling pathways required for gametogenesis in the mosquito are already present in mature gametocytes circulating in the host bloodstream. In order for this process to be regulated efficiently and to avoid premature activation of gametocytes, processes and cell signalling cascades required for gametogenesis to be initiated in the mosquito vector must not be activated in the mammalian host. If this were to occur, transmission efficiency would be reduced due to premature initiation of gametogenesis leading to formation of gametes too early and prior to uptake of a blood meal. The key to this timely regulation of this switch to gametogenesis lies in the essential environmental and chemical triggers specifically induced by conditions in the mosquito vector, which are absent in the human host. Mature gametocytes may circulate in the blood stream for several days arrested in the G₀ phase of the cell cycle until eventually they may be taken up by a feeding mosquito taking a blood meal. This sudden and dramatic change in environment from the 37 ° C of the human host to the lower temperature of the vector, coupled with the presence of a mosquito-derived factor (and/or an increase in pH in *in vitro* settings), is known to initiate the process of gametogenesis. The pH change required *in vitro* to initiate gametogenesis along with a temperature decrease is bicarbonate-ion-dependent and requires a switch from pH 7.4 to between pH 8.0 and pH 8.3[257]. On exposure to the air, a decrease in the concentration of carbonic acid caused by loss of CO₂ from the blood is thought to result in this pH increase. The pH must be above pH 7.8 for exflagellation to be induced in a bicarbonate ion-dependent manner. Having observed that the pH of a blood meal rarely increases above this value and usually lies between pH 7.5 and pH 7.6[26], it was discovered through mosquito feeding assays using medium devoid of bicarbonate that a mosquito derived factor, uncharacterised at the time and named mosquito exflagellation factor (MEF)[26] or Gametocyte activating factor (GAF)[258] initiated gametogenesis in combination with the essential decrease in temperature *in vitro* rather than by a bicarbonate ion-dependent increase in pH[26]. This mosquito derived factor was later identified by HPLC and mass spectrometry to be a negatively charged small acidic substance and was shown to be the already identified tryptophan by-product of the ommochrome pathway in insects, xanthurenic acid (XA)[26]. The ommochrome pathway in insects is required for the synthesis of eye pigment. Using insect mutants which do not produce XA as a by-product it was demonstrated that MEF is

a product of the ommochrome pathway as homogenates of these mutants did not show MEF activity whereas wildtype homogenates did[26]. This was further confirmed by the fact that the mosquito vector responsible for malaria transmission, *A. gambiae*, uses this pathway and previous work prior to the discovery that MEF was in fact XA indicated MEF activity in mosquito heads[26]. XA can be found in mammalian serum at low concentrations[259], however, concentrations this low do not support exflagellation at blood meal pH and will only result in exflagellation between a narrow pH window. Addition of >3 μM XA to serum expanded this pH window thus increasing the likelihood of exflagellation occurring. This demonstrated that on transitioning to the mosquito in a blood meal, the presence of a higher concentration of XA than already present in the mammalian blood, could along with a small rise in pH and a temperature decrease, facilitate the process of gametogenesis[26].

With the use of increasingly sophisticated genetic and pharmacological tools, we are gaining more and more insight into the signalling pathways involved in the process of gametogenesis. However there is still much more that needs to be learned and although it is clear what the environmental signal for gametogenesis is, it is currently still unknown whether there is a receptor interaction at this initiation point and if so, what the receptor for XA is. The exact sequence of signalling events following the initial XA signal and identification of all the components involved in the signalling events regulating gametogenesis still remains unclear. However, the importance of certain signalling molecules is now apparent. XA coupled with a reduction in temperature can be used *in vitro* to stimulate gametogenesis. Studies using pharmacological and genetic tools have highlighted an important role for Ca^{2+} in this process[260], [210]. In fact, addition of XA to *P. berghei* gametocytes induces a rapid release of Ca^{2+} . This XA-induced Ca^{2+} release was gametocyte-specific and was not observed in mixed asexual stage preparations[210]. *P. falciparum* gametocytes were able to round up, and emergence was greatly reduced in the absence of Ca^{2+} as shown by studies using XA to induce gametogenesis in the presence of the intracellular Ca^{2+} chelator BAPTA-AM[159]. This study indicates that Ca^{2+} is not required for the early stages of gametogenesis to occur. The later stages of gametogenesis, specifically the male-specific process of exflagellation, do on the other hand require the presence of the Ca^{2+} . *P. berghei* gametocytes stimulated with XA in the presence of 100 μM BAPTA-AM were unable to exflagellate[210]. *P. falciparum* gametocytes were also unable to exflagellate in the absence of Ca^{2+} [159]. The essential role for Ca^{2+} in gametogenesis suggested the involvement of Ca^{2+} -dependent effector molecule. This led to the discovery that the Ca^{2+} -dependent protein kinase 4 (CDPK4) was required for exflagellation to occur. Regulation by CDPK4 was shown to be induced by XA and also by a rise in pH. A knockout of *PbCDPK4* in *P.*

berghei eliminated exflagellation completely and cells were still able to round up and emerge[210]. The requirement for CDPK4 only in the exflagellation stage of gametogenesis indicated a male-specific role for this kinase and in fact, CDPK4 is predominantly expressed in male stages (plasmodb.org). Further study into the specific role of *pbCDPK4* in exflagellation revealed a role in regulating cell cycle progression in activated male gametocytes. In *pbCDPK4* ko male parasites, no increase in DNA content was observed on stimulation with XA, this was in contrast to wildtype cells in which the DNA content of males increased by a factor of 5.5. In addition to this, the formation of axonemes and mitotic spindles, which usually occurs in microgametes on addition of XA, was inhibited in the knockout line[210]. More recent work in *P. berghei* gametocytes by Fang et al, has shown that CDPK4 plays a role in several distinct events of male gametogenesis and in a temporal manner. Within the first 30 seconds of gametocyte activation, and downstream of Ca^{2+} mobilisation, a myristoylated form of CDPK4 is activated by Ca^{2+} and phosphorylates the effector protein SOC1 (substrate of CDPK4 1) this leads to the recruitment of a complex containing MCM2-7/Cdt1 onto the ORC1-5/Cdc6 complex. This initiates the first of three rounds of DNA replication required for males gametocytes. This Ca^{2+} -activated myristoylated isoform of CDPK4 also plays another role independently of pre-complex loading and the subsequent first genome replication, by phosphorylating another effector protein, SOC2 (substrate of CDPK4-2). This is required to complete the first mitosis and for mitotic spindle formation. A non-myristoylated isoform of CDPK4 phosphorylates SOC3. This is down stream of all other processes required for male gametogenesis and is required for flagella motility[215].

Work by Kawamoto et al, also demonstrated an essential role for Ca^{2+} in exflagellation, this study also indicated that nitroprusside, a GC activator, enhanced exflagellation, as did 3-isobutyl-1-methylxanthine (IBMX), an inhibitor of both cAMP and cGMP, whereas, the GC inhibitor N-methyl-hydroxylamine prevented exflagellation. This indicated a role for both Ca^{2+} and cGMP in the later stages of gametogenesis. However, a pharmacological induced increase in cAMP did not affect exflagellation levels in this study, suggesting that gametogenesis is cGMP-dependent but not cAMP-dependent[260]. In support of this, studies using the cGMP-PDE inhibitor zaprinast have shown a role for cGMP signalling in gametogenesis. Increasing concentrations of zaprinast stimulated rounding up and exflagellation in a dose-dependent manner independently of XA, suggesting a role for cGMP in this process[159]. This led to the question of whether PKG was involved. Addition of the PKG inhibitor C1 to XA induced and zaprinast-induced gametocytes inhibited rounding up and subsequent exflagellation of gametocytes indicating an essential role for this signalling molecule in both XA and zaprinast-induced gametogenesis[159]. This was

verified further by the development of a *P. falciparum* line with insensitivity to C1. This *PfPKG_{T618Q}* gatekeeper mutant line was able to round up when stimulated with either XA or zaprinast both in the presence and absence of C2 indicating that the reversal of XA or zaprinast-induced rounding up and emergence observed in the wild type when C2 was added was in fact PKG-specific[159]. This work showed that PKG is the primary target of C1 and C2 and also that PKG has an essential role in gametogenesis/gametocyte activation. However, whilst C1 and C2 blocked exflagellation, this was also blocked in the *PfPKG_{T618Q}* gatekeeper mutant indicating that another C1/C2 sensitive kinase must have a role in this later stage of gametogenesis[159]. In fact, there is evidence that *TgCDPK1* is sensitive to C1[181]. In support of a role for cGMP signalling in gametogenesis, Muhia et al, measured cGMP levels as an indication of GC activity in mature *P. falciparum* gametocyte membrane preparations. They showed an increase in cGMP levels on addition of XA and concluded that XA could stimulate GC activity[126]. These assays were carried out in the presence of the non-selective cyclic nucleotide PDE inhibitor theophylline indicating that any increase in cGMP levels observed were not due to a reduction in PDE activity (however, this inhibitor has since been shown to be relatively inactive against *Plasmodium* PDEs with a > 100 μ M activity against C-terminal catalytic domain produced in *E. coli* compared to a 3.8 μ M activity for zaprinast [143]). To further support GC involvement, authors showed that cGMP increases were dependent upon Mg^{2+} or Mn^{2+} , which have been previously shown to be required for GC activity in other organisms.

PDE activity has also been implicated in the process of gametogenesis. Lines in which *PfPDE δ* had been disrupted showed elevated cGMP levels and a reduced rounding up at stage V and more strikingly, the majority of parasites failed to emerge from the host erythrocyte; these data suggest that the absence of *PfPDE δ* in this line leads to aberrant cGMP hydrolysis leading to increased levels of this cyclic nucleotide in gametocytes stages and as a consequence gametogenesis is disrupted[130]. Interestingly, Taylor et al[130], indicated that there is likely to be another cGMP-PDE in addition to *PfPDE δ* active in gametocyte stages as residual PDE activity seen in the *PfPDE δ* knockout line was more sensitive to the cGMP-PDE specific inhibitor zaprinast than *PfPDE δ* [130]. Interestingly, deletion of *PbPDE δ* in *P. berghei* does not lead to aberrant gametogenesis but rather affects the later insect stages[128] suggesting either differences between murine and human malaria parasites, or that unlike in *P. falciparum*, another PDE may be able to compensate for the absence of *PbPDE δ* and maintain cGMP at levels that allow gametogenesis to occur. Unlike *P. falciparum* lines lacking *PfPDE δ* , *P. berghei* parasites undergo normal gametogenesis and fertilisation takes place leading to the formation of ookinetes. However, it is at this stage in the parasite life cycle that disruption occurs due to

the absence *PfPDEδ*. Deletion of *PbPDEδ* results in a phenotypic change in ookinetes which impairs their ability to penetrate the mid gut epithelium leading to greatly reduced mosquito transmission [128]. This morphological change is reflected by ookinetes rounding up and is accompanied by breakdown of the inner membrane complex (IMC), a process that usually occurs later in the lifecycle at the point of oocyst formation once ookinetes have completed their transit through the midgut wall. Addition of the PKG inhibitor C1 was shown to reverse the ookinete phenotype in the *PbPDEδ*-ko line, indicating that the phenotype observed in the mutant line was due to disrupted levels of cGMP as a result of the absence of *PbPDEδ*. This phenotype is suggestive of a possible premature initiation of cellular events caused by aberrant cGMP signalling. Interestingly, this premature rounding up is what would be expected to occur in mature gametocytes of the *PfPDEδ*-ko line; however instead what is seen is a partial block in rounding up and a complete block in egress (this will be investigated in chapter 4).

1.2.6. A relationship between calcium (Ca²⁺) signalling and PKG

There is a clear symmetry between the role of *PfPKG* at various stages of the lifecycle and the role of Ca²⁺ release. Several cGMP-regulated signalling events appear to be dependent upon Ca²⁺ mobilisation from internal stores.

In *P. berghei*, PKG acts to maintain Ca²⁺ at levels required for ookinete gliding motility and sporozoite invasion of hepatocytes has been shown to require both PKG and CDPK4 [218]. PKG also controls levels of Ca²⁺ required for merozoite egress and activation of gametogenesis in both *P. berghei* and *P. falciparum*. It is thought that PKG induces calcium release through phosphoinositide metabolism and activation of PLC. This results in the production of IP₃ (and DAG) from PIP₂. Increased IP₃ production leads to displacement of Ca²⁺ from internal stores and as a subsequence, the induction of several critical stages of the malarial lifecycle [174].

PfPKG-induced rounding up of gametocytes appears to be independent of Ca²⁺ release [159]; however, in both *P. berghei* and *P. falciparum*, induction of exflagellation requires both cGMP and the release of Ca²⁺ suggesting that the later stages of gametogenesis are dependent on both signalling molecules and that a relationship exists between the two [210] [260] [174].

Gamete and merozoite egress can be blocked using the Ca²⁺ chelator BAPTA-AM. It can also be inhibited by *PfPKG* inhibitors and stimulated by zaprinast. This is reflective of an essential role for both Ca²⁺ and PKG in parasite egress. The observation that the PDE inhibitor zaprinast in *P. falciparum* can reverse this BAPTA-AM-induced egress block was suggested to reflect an

enhanced Ca^{2+} mobilisation induced by zaprinast in schizont stages which was able to overcome the activity of BAPTA-AM allowing egress to still occur in the presence of Ca^{2+} chelation (rather than indicating that *Pf*PKG acts downstream of Ca^{2+} release which is not thought to be the case) [173].

1.3. Introduction summary

The complex life cycle of *P. falciparum* makes malaria a very difficult disease to control. However, as a result of malaria control interventions particularly in the last 5 years, this ancient disease has gone from being the number one killer among children to the fourth highest cause of death in sub-Saharan African children[29]. Despite this accomplishment, malaria still remains a serious threat to the lives of adults and children, particularly in sub-Saharan Africa with the shocking reality that this disease currently kills a child every 2 minutes and remains a huge public health problem globally. Although our current first line treatments are good, eventual resistance is a real threat and if the development of new compounds with novel targets does not evolve fast enough, the consequence could be catastrophic and reverse efforts over the last 15 years, which have seen a downward trend in cases. Efforts must continue in the search to develop new antimalarial drugs preferably with different targets to succeed in the arms race against this organism. To achieve this, we must understand more about the cell signalling pathways involved in critical events of the parasite life cycle. The development of molecules that specifically target essential and conserved parasite proteins that play critical roles in cell cycle events such as schizogony and gametogenesis, and preferably compounds that target more than one part of the parasite life cycle, would be invaluable to the drug discovery effort. Cyclic nucleotide signalling in *Plasmodium* is essential for many stages in the parasite life cycle including cell cycle progression of asexual blood stages which cause the clinical symptoms of malaria and for transmission from the human host to the mosquito vector and as such, this is an attractive pathway to direct research efforts. Although not a priority in the past, targeting of the transmission stages of malaria is now seen as an important contribution to the fight against this ancient disease. The aims and objectives of this thesis are outlined below and seek to understand more about the role of cyclic nucleotide signalling and Ca^{2+} mobilisation in schizogony and gametogenesis and to investigate the possible gametocytocidal activity of compounds that target parasite PDEs.

Aims and objectives

- To explore the relationship between *Pf*PKG and Ca²⁺ mobilisation in *P. falciparum* schizont stages and mature gametocytes with the aim to determine the *Pf*PKG-specificity of the zaprinast-induced Ca²⁺ response in mature schizonts and both the zaprinast-induced and XA-induced Ca²⁺ responses in mature gametocytes.
- To investigate the biological effects of both pharmacological and genetic disruption of PDEs in *P. falciparum* gametocytes, with the aim to identify the effect of PDE absence on three important events in gametogenesis; rounding up, emergence and Ca²⁺ mobilisation.
- To dissect the two phenotypes of the *Pf*PDE δ -ko gametocytes which exhibit non-deformability and an inability to round up. With the aim to identify whether *Pf*PDE δ is required for XA-induced rounding up and emergence by using a PKA inhibitor to remove the PKA-induced 'stiff' phenotype.
- To design and create a *Pf*PDE δ triple HA tagged line and to use it to determine *Pf*PDE δ localisation in mature gametocyte stages.
- To pull down *Pf*PDE δ -HA protein from the *Pf*PDE δ triple HA tagged line and to use the material to carry out PDE assays with the aim to determine the cyclic nucleotide specificity of *Pf*PDE δ .
- To identify compounds with gametocidal activity from a panel of PDE inhibitors developed by Pfizer and to investigate the mode of action of candidates showing gametocyte inhibition from the screen.

Chapter 2

Materials and Methods

2.1. Parasite preparation

2.1.1. *P. falciparum* parasite culture

2.1. A. *P. falciparum* asexual stage culture

Cultures of *P. falciparum* NF54[261], *PfPDE γ -ko* and *PfPDE δ -ko* lines (Cathy Taylor PhD Thesis 2007), *PfPDE α -ko* line (Christian Flueck, LSHTM), *PfPKG^{T618Q}* (Louisa McRobert, LSHTM)[159], *PfPKG-DD* (kindly provided by Dr Manoj Duraisingh and Jeffrey Dvorin) and 3D7a [262] were grown and propagated using an adapted version of the Trager and Jensen method of *P. falciparum* culture[263]. Parasites were maintained in RPMI-1640 (Sigma) supplemented with (0.02 mg/ml) hypoxanthine (Sigma), 5 mg/ml Albumax II (Invitrogen), 2 mg/ml glucose (Sigma) and 0.3 mg/ml L-glutamine (Sigma) from here on referred to as culture medium (CM) or complete media and maintained in A+ human erythrocytes (whole blood, National Blood Service, Colindale) to a final haematocrit of between 1 % and 5 % and at parasitemias ranging from 0.5 % to 20 %. Cells were incubated at 37 °C in 5 % CO₂ (BOC) while shaking at 60 RPM (Eppendorf new Brunswick S41i CO₂ shaking incubator). In order to monitor growth and development of cultures, thin blood smears were made on glass slides (VWR) and stained with Giemsa (see section 2.1.C).

2.1.B. *P. falciparum* gametocyte initiation and culture

Spent culture medium (sCM) was removed from a high ring stage culture (8 % to 10 % parasitemia) and the culture then 'stressed' by addition of the sCM added back onto the culture in a ratio of 1:3 (10 ml sCM plus 20 ml new CM) (see 2.1.A for culture for culture media components). Cultures were incubated overnight at 37 °C with 5 % CO₂ (BOC). On day 2, cultures should appear as stressed late stage cultures. Blood smears of cultures were prepared in the morning, stained with Giemsa and examined by light microscopy (as described in section 2.1.C) to determine the level of stress. This was evaluated by comparing morphology of stressed cells to that of normal healthy cells of the same stage. Cultures were purified using a Percoll gradient (section 2.2.C). Very fresh whole blood (A+ preferred dependent on availability but other blood groups used as required) taken no more than 2 days prior (LSHTM blood service) was washed in

RPMI-1640 (Sigma) twice to remove all other blood components, leaving erythrocytes only and diluted in RPMI-1640 to a 50 % haematocrit. Washed blood was added to the purified schizont pellet to give a resulting parasitemia of ~ 3-5 % schizonts. Cultures were either stressed again using spent CM as described above or received a culture media change depending upon the level of stress observed previously by light microscopy. Cells were incubated overnight while shaking (60 RPM) at 37 °C in the presence of a modified gas mixture 3 % CO₂/1 % O₂/N₂ 200 bar (BOC) from now on referred to as 'gametocyte gas'. On day 3 cultures were examined by Giemsa smear. Cultures are expected to be high ring stage cultures at this point and a certain proportion should have committed to gametocytogenesis. Cultures above 5 % parasitemia were split into separate flasks and fresh RBC's added to make a parasitemia of ~ 5 % and a haematocrit of 0.5 % -1 %. After this point no erythrocytes were added to cultures for the remainder of the procedure. From this point onwards, until maturity at stage V, all cultures were continually maintained at 37 °C and received daily culture medium changes using a hot plate. Culture medium used was the same as described above but with an addition of 11.6 mg/ml N-Acetyl-D-Glucosamine (Sigma) to prevent asexual stage invasion. Cultures were gassed with gametocyte gas and incubated at 37 °C.

2.1.C. Preparation and Giemsa staining of thin blood films

Parasite samples were pelleted by centrifugation at 8000 rpm for 30 seconds. The supernatant was removed to leave a haematocrit of ~ 50 - 80 %. ~ 5 µl of sample was placed on a glass slide (VWR) using a Gilson pipette. A second glass slide was used to smear the sample across the slide. Samples were air dried at room temperature for ~ 2- 5 minutes then fixed in 100 % methanol (VWR). A 1:10 dilution of Giemsa R66 (Gurr-Azur-Eosin-methylene blue, VWR) was prepared in tap water. Slides were laid face down on a tray and Giemsa solution injected underneath using a syringe with a blunt ended needle. Slides were left to stain for 15-20 minutes. Once stained, slides were washed gently in tap water and left to air dry. Samples were viewed by light microscopy (Leitz LaborLux 8) using a x100 oil immersion lens. Counts were carried out using a 24 mm diameter miller square graticule (Pyser-SGI Ltd) to determine percentage parasitemia and the stage composition of cultures.

2.2 *P. falciparum* synchronisation and purification

2.2.A. *P. falciparum* sorbitol synchronisation of early asexual stages

Asexual blood stage cultures were synchronized using a method of (5 %) sorbitol (Sigma) treatment to remove all late stage asexual parasites leaving only ring stages. Parasite lines were cultured as indicated in section 2.1.A to a mostly ring stage parasitemia. Cultures were pelleted by centrifugation for 2 minutes at 500 xg. 5 % sorbitol (2.5 g of sorbitol (Sigma) added to 50 ml of purified water) pre-warmed to 37 °C was added to the pellet in a ratio of 1:6 (6 ml sorbitol to 1 ml parasite pellet). Samples were incubated for 10 min at room temperature then washed in pre-warmed RPMI-1640 (Sigma) followed by centrifugation at 500 xg for 2 min. This wash step was repeated to ensure all sorbitol had been removed. Samples were maintained at 37 °C in 5 % CO₂ (BOC) in line with the asexual stage culture methods indicated in section 2.1.A.

2.2.B. *P. falciparum* magnetic purification of mature asexual stages and gametocyte stages

Parasite lines were cultured as indicated in section 2.1.A to a predominantly schizont parasitemia, or were induced to produce gametocyte stage culture as indicated in section 2.1.B. Cultures were pelleted at 500 xg for 2 minutes (in a centrifuge pre-warmed to 37 °C for gametocyte samples). The supernatant was removed and samples prepared to a ~10 % haematocrit using warm RPMI. The MACS® cell separation column type CS (Miltenyl Biotec) was attached to the magnet and washed through with warm RPMI to wet the column (at this point onwards the column was not allowed to run dry). The parasite sample was loaded on top of the column and the regulator adjusted to allow a flow rate of ~2 drops per second. The sample was allowed to run through the column into a 50 ml tube (if early stages were not needed to be kept, this sample was discarded), after which, warm RPMI was flushed through the column at a flow rate of ~ 4 drops per second to remove all unbound material from the column. Once the flow through ran clear, the column was removed from the magnet and 20-30 ml of warm RPMI added and the regulator opened fully to allow all bound material to wash off the column. Flow through was collected in a 50 ml tube and pelleted by centrifugation at 500 xg for 2 minutes (in a centrifuge pre-warmed to 37 °C for gametocyte samples). The pellet should be purified late asexual stage parasites or stage II-V gametocytes (all stages containing haemozoin) and should contain no uninfected erythrocytes. Parasite samples were either used for further experiments

or put back into culture (see section 2.1.A) with fresh erythrocytes (for late asexual stages) and culture medium.

2.2.C. *P. falciparum* Percoll purification of mature asexual stages and gametocytes

Asexual stage cultures were synchronized using a method of (70 %) Percoll (90 ml Percoll (Sigma), 10ml 10x RPMI (1.04 g), 13.3 % sorbitol (3.724 g) in 1x phosphate buffered saline (PBS) (28 ml)) gradient to separate mature stage asexual parasites from early stages. Cultures were pelleted by centrifugation at 500 xg for 2 minutes. The supernatant was removed and the cell pellet layered gently onto 3 ml of Percoll pre-warmed to 37 °C. The Percoll gradient was centrifuged at 2500 xg for 10 minutes with no brake. The mature stage layer of cells containing purified mature stages located at the top of the gradient was removed and placed into 6 ml of pre-warmed RPMI-1640 (Sigma) and pelleted by centrifugation for 2 minutes at 500 xg to wash. Purified parasites were either used or placed back into culture with fresh erythrocytes (see section 2.1.A) and were incubated while shaking (60 RPM) at 37 °C to allow invasion to occur. The lower fraction of the Percoll gradient consisting of early asexual stages and uninfected erythrocytes was either discarded or synchronized further using sorbitol treatment (see section 2.2.A). To separate gametocyte stages from uninfected erythrocytes (all stages from stage II will be retained in the upper fraction), the above protocol was used and gametocytes were maintained at 37 °C at all times during this process.

2.2.D. *P. falciparum* Compound 2 synchronisation of mature asexual stages

Compound 2 (C2) blocks schizont egress (see section 1.3 of introduction for more details) and as such can be used to synchronise asexual blood stage cultures by allowing parasites to accumulate at the mature segmented schizont stage. Removal of C2 releases the block and allows egress within a short time period. To achieve highly synchronous cultures with a tight window of under 4 hours, asexual stage cultures were synchronised using a method of compound 2 (C2) (4-{7-[(dimethylamino)methyl]-2-(4-fluorophenyl)imidazo[1,2-*a*]pyridine-3-yl}pyrimidin-2-amine gifted from Merck & Co., Inc) block combined with the methods of sorbitol treatment and Percoll gradient (sections 2.2.A and 2.2.C respectively). Predominantly ring stage cultures of a high parasitemia (5 %- 10 %) were treated with sorbitol to remove all late stage parasites and incubated in fresh culture medium (section 2.1.A) over night at 37 °C. Parasites were monitored the next day by Giemsa stained smears (section 2.1.C). Once parasites

developed into segmented schizonts they were purified on a Percoll gradient (section 2.2.C). Purified parasites were put into pre-warmed culture medium and when schizonts appeared segmented they were incubated with (1 μ M to 2 μ M) C2 at a haematocrit of <0.5 %. A small control sample of un-blocked parasites was removed prior to addition of C2 to monitor schizont rupture. Parasites were incubated with C2 at 37 °C in 5 % CO₂ until most of the parasites in the control sample had ruptured. Parasites were incubated with C2 for no longer than 6 hours to avoid loss of parasites due to toxicity. Once incubated, parasites were washed once in pre-warmed RPMI-1640 (to remove the C2 and to release the schizont block) and immediately put into 25 ml of pre-warmed culture medium with fresh RBCs (volume depending upon the size of the schizonts pellet and desired resulting ring stage parasitemia). Cells were incubated while shaking (60 RPM) at 37 °C in 5 % CO₂ for 2 hours, after which an additional Percoll gradient was performed to remove any un-ruptured schizonts from the sample. The lower ring fraction was washed once in pre-warmed RPMI and a sorbitol treatment carried out to ensure removal of late stages in the early stage sample. Cells were either used or put into culture (as described in section 2.1.A) and allowed to grow to the required stage.

2.3. Parasite sample preparation

2.3.A. Parasite sample preparation for immunoblotting and Immunoprecipitation

Parasite samples were purified by Percoll gradient as described in sections 2.2.C and 2.2.D. Purified parasite pellets were re-suspended in 0.15 % saponin (Sigma-Aldrich) containing a cocktail of protease inhibitors- (1x protease inhibitor cocktail (inhibits a broad spectrum of cysteine, serine and metalloproteases and calpains, Roche), 2 mM EDTA and 1 mM PMSF (inhibits serine proteases and the cysteine protease papain, Sigma-Aldrich) to a ratio of 1:4 or less. Samples were incubated on ice for 5 minutes and vortexed intermittently until the whole pellet appeared lysed. Lysed samples were pelleted in a micro centrifuge at 8000 rpm for 30 seconds and then washed once in 1 % PBS (80 g NaCl, 2 g KCl, 14.4 g Na₂HPO₄, 2.4 g KH₂PO₄ in 1L H₂O) containing the same protease inhibitors as described above. Samples were snap frozen in a dry ice and ethanol (100 %) bath then stored at - 80 °C until use.

2.3.B. Lipid extraction for electrospray-mass spectrometry

Sample preparation for electrospray mass spectrometry was carried out at LSHTM in collaboration with Mathieu Brochet (Sanger institute). *P. falciparum* schizonts were synchronised using a combination of MACS purification (section 2.2.B) and sorbitol treatment (section 2.2.A). Lipids were extracted from 50 µl packed cell volume purified schizonts per replicate. Samples were washed in 1x PBS then suspended in 100 µl 1x PBS and transferred to a glass tube. A chloroform:methanol mix was prepared to a ratio of 1:2. 375 µl of this mix was added to cells to lyse them. Samples were vortexed thoroughly for 15 minutes. 125 µl CHCl₃ (chloroform) and 125 µl H₂O were added in order to make samples biphasic. This was followed by centrifugation at 1,000 xg for 5 minutes at room temperature. The lower phase was carefully removed from samples and transferred to a new glass vial and dried under nitrogen (BOC). In preparation for mass spectrometry (carried out by collaborator Terry K Smith at the university of St Andrews), lipids were dissolved in a 1:2 chloroform:methanol mix and acetonitrile:propanol:water (6:7:2). Samples were analysed and phospholipids identified by collaborators (Terry K Smith at the university of St Andrews) using a triple quadrupole mass spectrometer with a Nano electrospray source (Absceix 4000 QTrap). Phospholipid peak identity was verified using the LIPID MAPS (Nature Lipidomics gateway-www.lipidmaps.org).

2.3.C. Ring stage parasite sample preparation for transfection

Parasites were grown to a high ring stage parasitemia using an adapted version of the Trager and Jensen method as indicated in section 2.1.A and synchronised using a method of sorbitol treatment (Section 2.2.A) to remove late asexual parasite stages followed by a Percoll treatment the following day when parasites were segmented schizont stages (section 2.2.C). Fresh RBCs taken no more than 2 days prior (LSHTM blood service) were added to purified schizont stages and cells incubated while shaking (60 RPM) at 37 °C in 5 % CO₂ for 2 hours to give a high ring stage culture of 5 % to 10 % parasitemia. An additional Percoll gradient was then performed to remove any un-ruptured schizonts from the sample. The lower ring fraction was washed once in pre-warmed RPMI and parasites were put back into CM at 37 °C in 5 % CO₂ until required.

2.4. Fluorescence techniques

2.4.A. Calcium release assay

This assay was developed by Christine Hopp (LSHTM) and relies on the cell permeable, labelled calcium indicator Fluo-4-AM (Sigma, M22426). The AM ester allows access into the cell through membranes. Once in the cytoplasm, the AM ester gets cleaved, trapping the Fluo-4 inside the cell. Pharmacological treatments can then be used to release Ca^{2+} from internal stores into the cytoplasm. Fluo-4 will specifically bind Ca^{2+} ions and upon doing so will fluoresce. Levels of fluorescence can be measured as an indirect indicator of calcium release.

Changes in the levels of intracellular free Ca^{2+} were measured using Fluo-4-AM loaded segmented schizonts or mature gametocytes which had been cultured as previously indicated in sections 2.1.A and 2.1.B of these methods. Parasites were purified by Percoll gradient (as described in sections 2.2.C and 2.2.D) and pelleted by centrifugation for 2 min at 500 xg. Parasites were re-suspended in warm 10x Ringer Buffer (122.5 mM NaCl, 5.4 mM KCl, 0.8 mM MgCl_2 , 11 mM HEPES, 10 mM D-Glucose, 1 mM NaH_2PO_4) to $1\text{-}2 \times 10^8$ parasites/ml (25 μl pcv parasites per 1 ml Ringer buffer). 2 μl of 5 mM Fluo-4-AM was added per 1 ml of parasite preparation. Cells were incubated in the dark with Fluo-4-AM at 37°C for 45 min. Cells were then washed twice in warm Ringer buffer and incubated for 20 min to allow for de-esterification of the AM ester. This was followed by a further two washes. The pellet was re-suspended in Ringer buffer at $1\text{-}2 \times 10^8$ parasites/ml and plated out on the bottom half of a 96 well plate. Test compounds were diluted from DMSO stock concentrations to the required working concentration and transferred to the top half of the plate (dilutions were calculated to result in a final dilution in the well of 1:20 resulting in addition of 5 μl of compound per well). The excitation of the cells (bottom half of the plate) was measured at 488 nm using a SPECTRAMax M3 microplate fluorimeter (Molecular Devices) at 20 second intervals for a period of 3 minutes to achieve a baseline read (Figure 2.1). The plate was removed from the plate reader onto heat blocks and the cells rapidly transferred onto the test compounds using a multi-channel pipette. The plate was placed back in the plate reader and read for a further 5 minutes at 20 second intervals at the same excitation (see blue arrow in Figure 2.1). Levels of free internal Ca^{2+} were compared to the baseline read measured immediately prior to the addition of a test reagent. Data for test compounds were analysed in Microsoft Excel in reference to a DMSO control (0.5 %), a buffer only control and an ionophore control A23187 (20 μM in DMSO, Sigma). A23187 increases levels of Ca^{2+} in intact cells by allowing Ca^{2+} ions to cross cell membranes which are

usually impermeable to them. This allows a large unspecific release of Ca^{2+} from internal stores and can therefore be used as a positive control in Ca^{2+} release assays. Results are presented in this report as percentage of ionophore control or Ca^{2+} release in relative fluorescence units (RFU).

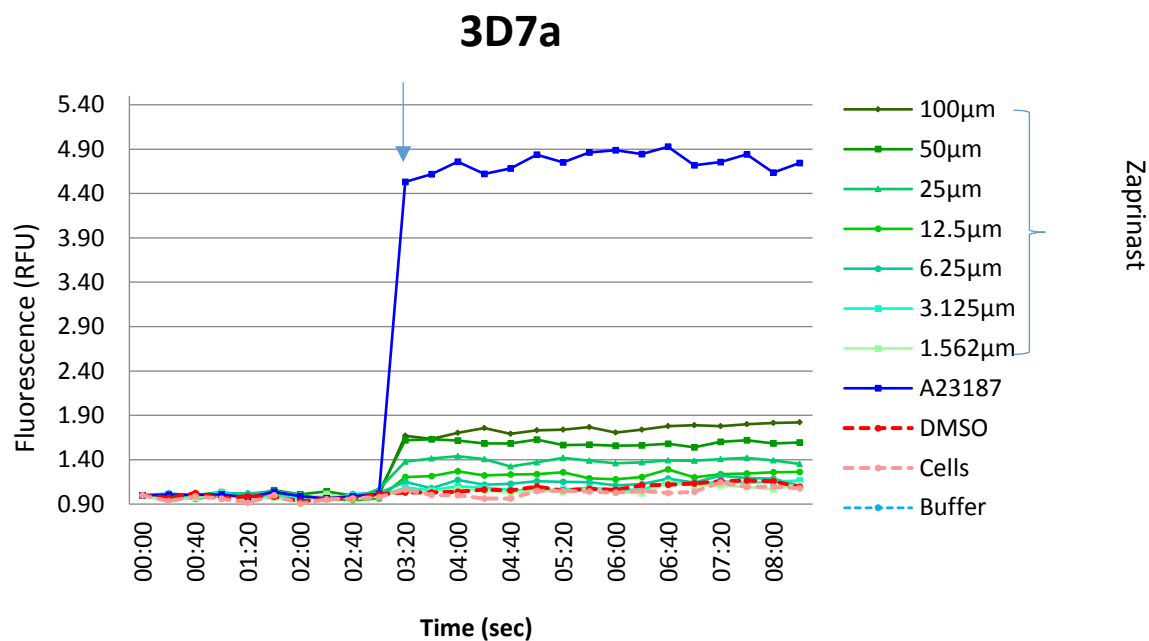


Figure 2.1. Representative graph depicting measurement of levels of Ca^{2+} with time in the Ca^{2+} release assay. Test samples (green) are compared to an ionophore control (Blue). Fluorescence of the DMSO control (red) and the baseline values for each samples (time points 00:00 to 02:40) are deducted from post read (time points 03:20 to 08:00) test sample values.

2.4.B. Immunofluorescence assay (IFA)

General protocol

Late stage schizonts or gametocyte stages were purified by Percoll gradient as described in section 2.2.C and 2.2.D. The purified suspension was pelleted by centrifugation for 2 minutes at 8000 rpm. Cells were re-suspended to roughly 50 % haematocrit and thin blood films prepared on glass slides (VWR). Samples were left to air dry for 2 hours or overnight. To make the wells, 2 circles of roughly 0.5 cm to 1 cm in diameter were drawn on each slide using a hydrophobic wax pen (Sigma). Slides were placed in a slide box and were fixed by either method A: 4 % formaldehyde diluted in PBS from a 16 % stock concentration (Thermo scientific), with or without 0.001 % glutaraldehyde (Sigma) for 30 minutes at room temperature then rinsed in 1 x PBS. Or method B: fixed in cold methanol (VWR) (-20 °C) for 2 minutes then left to air dry. Slides were then permeabilised in 0.1 % Triton (x100 Sigma) for 10 minutes at room temperature followed by a 1x PBS wash. Slides were blocked in 3 % bovine serum albumin (BSA), (diluted in 1x PBS, Sigma) overnight at 4°C. The following day, the required primary antibodies were diluted to the required concentration in BSA. Slides were removed from the 3 % BSA and all areas dried excluding the wells which remained wet at all times. ~50-100 µl of the primary antibody was pipette onto each well and mixed. Samples were incubated with the primary antibody for 1 hour at room temperature. Slides were then washed briefly with 1x PBS then shaken gently in fresh 1x PBS at room temperature for 30 minutes with three 1x PBS buffer changes at 10 minute intervals. The same process was repeated for the secondary antibody. After the final PBS wash, the slides were dried. One drop of Hydromount containing DAPI (1.5 µg/ml Dapi in glycerol based mounting medium Vectarlabs) was placed onto a coverslip and the coverslip placed gently over the sample with the hydromount situated on top of the wells. The coverslip was pressed gently onto the slide and the edges sealed with nail varnish.

Unless stated otherwise, samples were viewed using an EVOS FL cell imaging system (Thermo Fisher Scientific), which uses LED light cubes to deliver fluorophore excitation, and a Sony ICX445 monochrome CCD camera. α -HA antibody coupled to Alexa Fluor 594 was detected at an excitation of 585/29 nm and an emission peak of 624/40 nm, α -HA antibody coupled to α -rat biotin coupled to Alexa Fluor 488 conjugated streptavidin was detected at an excitation of 470/22 nm and an emission peak of 510/41 nm. WGA-TR was imaged using 592 nm excitation: 615 emission. Hoechst 33342 was imaged at 347 nm excitation and 483 emission.

Images were analysed using Adobe photoshop elements.

Immunofluorescence assay: Band 3 rounding up and emergence of gametocytes

Gametocytes were cultured as described in section 2.1.B and purified by Percoll gradient (section 2.2.D). Parasites were kept at 37 °C using a heat block. The purified parasite sample was mixed with uninfected erythrocytes to a ratio of roughly 2:1 (parasites:erythrocytes) and diluted in warm complete media (see section 2.1.A) to a final volume of 100 µl per sample. Test compounds were added to 1.5 ml tubes (Star lab) to give a final concentration of 10 µM or 30 µM XA, 2 µM C2, 1 µM MRT00207065, 100 µM zaprinast and 10 µM PF9. Control tubes contained 0.5 % DMSO. 100 µl of parasite sample was added to each tube and samples incubated for 30 minutes at room temperature. Samples were then washed once in warm RPMI followed by removal of the supernatant to leave a final haematocrit of ~50 %. Samples were smeared on glass slides and left to air dry for at least 2 hours. Samples were fixed in cold methanol and the general IFA protocol was followed as indicated above. The α -human Band 3 antibody (Abcam, Mouse monoclonal), which recognises specifically the cytoplasmic amino acid terminal of the integral erythrocyte glycoprotein Band 3, was diluted 1:5000 in BSA. The secondary antibody used to identify Band 3 binding (Molecular Probes goat anti mouse Alexa Flour 594) was diluted to 1:1000 in BSA. Slides were read using a confocal microscope (Zeiss LSM 510 laser scanning confocal microscope). DAPI was imaged at wavelength 405nm using laser diode and rhodamine at 594 nm using a HeNe 1 laser and images were analysed using Zeiss LSM image browser.

Immunofluorescence Assay: PDE δ -NF54 triple HA tag line: HA detection

Plasmodium falciparum gametocytes of the *Pf*PDE δ -HA transgenic line (see chapter 6 for details of the line) and an NF54 control were initiated and cultured as described in section 2.1.B to stage IV/V gametocyte stages and purified by Percoll gradient (See section 2.2.D). Parasites were kept at 37 °C continually using a heat block, and were prepared to a haematocrit of ~ 50- 80 % then smeared on glass slides and left to air dry for at least 2 hours. Samples were fixed in 4 % formaldehyde (diluted in 1x PBS from a 16 % stock, Thermo Scientific) and the general IFA protocol was followed as indicated above. α -HA antibody (High affinity rat monoclonal, stock 100 µg/ml, Roche) was diluted 1:100 in BSA and incubated for 1 hour followed by a wash step as indicated in the general protocol. Two conditions were used; the first was addition of the secondary antibody (Alexa Fluor 594 goat α -rat, Invitrogen), diluted to 1:1000 in BSA and incubated for 1 hour followed by a wash step. The second was the addition of biotinylated goat

α -rat IgG (1:200, vector labs Inc, Lot Z032). This was incubated for 1 hour at room temperature followed by 3 1x PBS wash steps as indicated in the general IFA method. This was followed by 1 hour incubation at room temperature with Alexa Fluor 488 conjugated streptavidin (diluted 1:500, vectorlabs inc, Lot Z032). This was followed by 3 1x PBS wash steps. IFA samples were prepared for microscopy as indicated in the general IFA section (above).

Note: For detection of ERD2, α -ERD2 (rabbit) diluted 1:1000 was followed by goat α -rabbit Alexa Fluor 594.

Immunofluorescence Assay: Wheat germ agglutinin rounding up and emergence of gametocytes

Wheat germ agglutinin (WGA) is a lectin that binds to sialic acid and N-acetylglucosaminyl residues. When conjugated to a fluorescent probe, it can be used to visualise the erythrocyte membrane by fluorescent microscopy. Gametocytes were initiated and cultured as indicated in section 2.1.B and purified by Percoll gradient (See section 2.2.D). Parasites were kept at 37 °C at all times using a heat block. Gametocyte stages do not purify efficiently with a 60 % Percoll gradient, with ~ 20 % of erythrocytes remaining in the sample. Uninfected erythrocytes are required in the sample to identify effective erythrocyte labelling. If the uninfected erythrocytes portion of the sample was lower than 5 % it was adjusted to ~ 5-20 % by addition of fresh uninfected erythrocytes. Purified parasite pellets were diluted in warm CM (see section 2.1.A) to ~ 1-5 % haematocrit (HC). For DNA staining of live parasites 20 μ M Hoechst 33342 (Cell Signalling Technology, diluted from 10 mg/ml stock in DMSO, stored in the dark) was added to parasite samples and incubated for 45 minutes at 37 °C (in the dark). Wheat germ agglutinin (5 μ g/ml, diluted from stock: 1 mg/ml in H₂O) conjugated to Texas red (excitation/emission maxima ~595/615 nm (WGA-TR) (Thermo Fisher Scientific)) was added to parasite samples and incubated for a further 15 minutes at 37 °C in the dark. Samples were washed 3x in warm RPMI-1640 and fresh CM added to the pellet to make a HC of ~ 1- 5 %. Test compounds were made to a working concentration of 1 μ M MRT00207065 and 10 μ M PF9 from DMSO stocks. Parasite samples were separated into three tubes (DMSO, PF9 and PF9 + MRT00207065) to a volume required to make a final drug dilution of 1:20 (5 μ l of compound added per 100 μ l of parasite samples). DMSO (0.05 %) was added to the control sample. Samples were incubated with compounds for 20 minutes at room temperature in the dark. Samples were washed once in warm RPMI-1640 (Sigma) followed directly by addition of 1 % formaldehyde diluted in 1x PBS (Thermo Fisher Scientific) containing 0.001 % glutaraldehyde (Sigma Aldrich) and incubated for

30 minutes to fix the cells. Samples were pelleted at 8000 xg for 30 seconds. The supernatant was removed and discarded leaving a pellet of ~ 60 -80 % HC and 2-5 µl of the pellet dropped onto a glass slide and a cover slip placed on top. The coverslip was sealed with nail varnish to prevent it drying up and the slide turned over to allow the cells to settle onto the coverslip. Images were taken (as indicated in the general protocol using an Evos FL microscope). The number of emerged (Hoechst 33342 staining but no WGA-TR staining) and non-emerged cells (Hoechst staining and WGA-TR staining) were counted from images. Bright field images were also taken of each sample to identify a morphological change from a crescent shape to a rounded form.

2.4.C. Luciferase Assay: Gametocyte viability assay

Bioluminescence is the emission of light from a living organism and involves a reaction in which a luciferase enzymes catalyses the oxidation of a specific substrate (in this case D-luciferin), this releases photons in the visible light spectrum which can be measured. This method can be used to quantitatively assess the viability of a parasite culture. The transgenic line 3D7*elo1-pfs16*-CBG99 (green emitting luciferase, 537 nm) kindly provided by Grazia Camarda and Pietro Alano[264] expresses the enzyme luciferase (CBG99 from the click beetle, *Pyrophorus plagiophthalmus*) under the control of the sexual stage specific *pfs16* gene promoter. This means that only gametocyte stages will express the enzyme. Synchronised gametocyte cultures of this line at early or late stages were used in gametocyte viability assays as described below to assess the stage specificity of pharmacological compounds by bioluminescence.

This line was used to measure the viability of gametocytes after addition of several possible gametocytocidal candidates. To achieve either an immature stage culture (Stages II to III) or a mature sexual stage culture (Stage V), parasites were induced and cultured as specified in section 2.1.B to either stage II or stage IV/V. Samples were prepared to a 2 % gametocytemia at 1 % haematocrit in complete CM.

The test compounds (PF9, PF10, PF11, PF12 and PF14) were diluted from a DMSO stock solution of 20 mM (in DMSO) into CM to a concentration of double the final concentration required and a 1:3 serial dilution for each compound in triplicate was carried out across the plate resulting in a final volume of 100 µl of test compound per well (10 µM, 3.33 µM, 1.11 µM, 0.37 µM, 0.123 µM, 0.041 µM, 0.013 µM, 0.0045 µM). The following controls were included in this assay: 0.5 % DMSO, no D-luciferin and uninfected erythrocyte control. 100 µl of parasite suspension was

added to each well excluding the erythrocyte only control wells. The plate was incubated for 48 hours at 37 °C in 1 % O₂/3 %CO₂/N₂ 200 bar.

Citrate buffer (developed by Cevenini et al[264]), was prepared using a combination of two solutions, 25.5 ml solution A (0.1 M citric acid monohydrate, Sigma Aldrich) + 74.5 ml solution B (0.1M trisodium citrate dehydrate, Sigma Aldrich) and adjusted to pH 5.4. This buffer was used to prepare 1 mM D-luciferin (Beetle Luciferin Potassium salt, Promega, Lot 0000153923, 50 mg, Ref E1602 MW 318.4). After the 48 hour incubation, 100 µl of 1 mM D-luciferin was added to each well excluding the Luciferase free control and the bioluminescence read immediately on a Spectramax M3 plate reader (Molecular Devices). Determination of the number of viable cells was measured in relative fluorescent units and is determined by quantification of ATP. Data were collected in Softmax Pro and analysed in GraphPad, Prism.

2.4.D. Live cell confocal microscopy

Gametocytes were initiated and cultured as indicated in section 2.1.B and purified by MACS purification (section 2.2.B). Parasites were kept at 37 °C at all times using a heat block. Purified samples were pelleted by centrifugation for 30 seconds at 8000 rpm and re-suspended in warm 10x Ringer Buffer (122.5 mM NaCl, 5.4 mM KCl, 0.8 mM MgCl₂, 11 mM HEPES, 10 mM D-Glucose, 1 mM NaH₂PO₄) to 1-2x10⁸ parasites/ml. 2 µl of 5 mM Fluo-4-AM was added per 1 ml of parasite preparation. Cells were incubated with Fluo-4-AM at 37°C for 45 min. Cells were then washed twice in warm Ringer buffer and incubated for 20 min to allow for de-esterification followed by a further two washes. Samples were resuspended in complete CM (section 2.1.A) to a haematocrit of ~ 50 %. 10 µl of sample was loaded onto a Poly-lysine (Sigma Aldrich) coated coverslips in a small petri dish (PELCO®, Ted Pella Inc). Cells were incubated for 2 minutes to enable binding to the cover slip. Cells were viewed by confocal microscopy (Zeiss LSM 510 laser scanning confocal microscope) and imaged in real time with sequential pictures taken 1 ms apart to produce multiple frames. After ~ 5/10 seconds, 5 µl XA was added to the sample to make a final concentration of 30 µM. Changes in fluorescence before and after addition of XA were observed and captured in real time. Green imaging read at a wavelength of 488 nm using an argon laser.

2.5. Gametocyte assays

2.5.A. Identifying the effect of PF9 on PKA-inhibited *PfPDE δ* -ko gametocytes

Stage V gametocytes of the *PfPDE δ* ko transgenic line (see chapter 6) and 3D7a wildtype parasites were purified on a Percoll gradient (see section 2.2.D) and mixed with uninfected erythrocytes to obtain a gametocytemia of between 2 % and 5 % (parasite samples with a parasitemia higher than 2 % were not purified). Samples were diluted in gametocyte culture media (section 2.1.B) to achieve a 0.5 % to 1 % haematocrit (referred to from here on as parasite preparation). The *PfPDE δ* -ko transgenic line was split into eight samples in a 24 well plate to a total culture volume of 1 ml per well at a final haematocrit of 2 %. DMSO (0.05 %) was added to two control samples. KT5720 was added to wells to make duplicates of the following final concentrations; 10 μ M, 5 μ M and 1 μ M. Concentrations of KT5720 were calculated to result in the same volume of all drug samples added to each well. 1 μ M of MRT00207065 was added to one of each of the two duplicates give the following samples: DMSO, DMSO + 065, KT5720 10 μ M, KT5720 10 μ M + 065, KT5720 5 μ M, KT5720 5 μ M + 065, KT5720 1 μ M, KT5720 1 μ M + 065. The 3D7a control sample was split into 4 samples and KT5720 was added to a final concentration of 10 μ M, 5 μ M and 1 μ M. 0.05 % DMSO was added to the last sample. All samples were incubated for 3 hours at 37°C / 5 % CO₂ (BOC). After incubation, each of the *PfPDE δ* -ko transgenic line samples was split into two. PF9 was added to one of each of the duplicates to a final concentration of 10 μ M. The equivalent percentage of DMSO was added to the other duplicate of each sample. Samples were incubated at room temperature for 20 minutes. All (*PfPDE δ* ko and 3D7a) samples were then pelleted by centrifugation at 8000 rpm for 30 seconds. The supernatant was removed to leave a final haematocrit of ~ 80 %. Blood films were prepared and stained with Giemsa as indicated in section 2.1.C. Numbers of stage IV/V gametocytes, rounded parasites and abnormal forms were counted by light microscopy as described in section 2.1.C. Samples were counted in duplicate and analysed in Excel. Graphs and statistics for each sample were generated in GraphPad, Prism.

2.5.B. Identifying the effect of XA on PKA-inhibited *PfPDE δ* -ko gametocytes

Stage V gametocytes of the *PfPDE δ* ko transgenic line and 3D7a wildtype line were prepared as indicated in section 2.5.A. The *PfPDE δ* -ko transgenic line was split into two samples (to a final volume of 100 μ l per sample). DMSO (0.05 %) was added to one of the *PfPDE δ* -ko samples and

to the 3D7a sample. KT5720 was added to the remaining *PfPDEδ*ko sample to a final concentration of 5 μ M. Samples were incubated for 12 hours at 37 °C / 5 % CO₂ (BOC). After incubation, each sample was split into duplicates. XA was added to one of each of the duplicates to a final concentration of 30 μ M. The equivalent percentage of DMSO was added to the other duplicate of each sample. Samples were incubated at room temperature for 30 minutes. All samples were then pelleted by centrifugation at 8000 rpm for 30 seconds, the supernatant was removed to leave a final haematocrit of ~ 80 %. Blood films were prepared and stained with Giemsa as indicated in section 2.1.C. Numbers of crescent shaped gametocytes and rounded parasites were counted by light microscopy. Samples were counted in duplicate and percentage parasitemia values generated using Excel. Graphs and statistics for each sample were generated in GraphPad, Prism.

2.5.C. PF9 dose response assay

Stage V gametocytes of the *PfPDEδ*ko transgenic line and 3D7a wildtype line were initiated and cultured to stage V as described in section 2.1.B. Stage V gametocytes were purified on a Percoll gradient (see section 2.2.D) and mixed with uninfected erythrocytes to obtain a gametocytemia of 1 % to 3 % depending upon the number of gametocytes (parasite samples with a parasitemia higher than 2 % were not purified). Samples were diluted in gametocyte culture media (section 2.1.B) to achieve a 0.5 % to 1 % haematocrit. Samples were then incubated for 12 hours at 37 °C / 5 % CO₂ (BOC) with 0.2 μ M, 2 μ M or 20 μ M PF9 or with < 1 % DMSO (control), all in the presence and absence of C2 (2 μ M). After incubation, all samples were pelleted by centrifugation at 8000 rpm for 30 seconds, the supernatant was removed to leave a final haematocrit of ~ 80 %. Blood films were prepared and stained with Giemsa as indicated in section 2.1.C. Numbers of crescent shaped gametocytes and abnormal forms were counted by light microscopy. Samples were counted in triplicate and percentage parasitemia values generated using Excel. Graphs and statistics for each sample were generated in GraphPad, Prism. Images of samples were generated using an Olympus BX51 light microscope with an Olympus SC30 camera.

2.5.D. PF9 time course assay

Stage V gametocytes of the 3D7a wildtype line were initiated and cultured to stage V as described in section 2.1.B. Stage V gametocytes were purified on a Percoll gradient (see section 2.2.D) and mixed with uninfected erythrocytes to obtain a gametocytemia of 1 % to 4 % depending upon the number of gametocytes (parasite samples with a parasitemia higher than 2 % were not purified). Samples were diluted in gametocyte culture media (section 2.1.B) to achieve a 0.5 % to 1 % haematocrit. Samples were split into 10 samples of 100 μ l each in eppendorf tubes and kept in a heat block at 37 °C. PF9 (final concentration 10 μ M) was added to 5 of the samples and < 1 % DMSO to the other 5 samples. Samples were incubated for 30 minutes at 37 °C. Every 5 minutes blood films were prepared from one PF9 sample and one DMSO control sample as follows; samples were pelleted by centrifugation at 8000 rpm for 30 seconds, the supernatant was removed to leave a final haematocrit of ~ 80 %. Blood films were prepared and stained with Giemsa as indicated in section 2.1.C. Numbers of crescent shaped gametocytes or rounded forms were counted by light microscopy. Samples were counted in triplicate and percentage parasitemia values generated using Excel. Graphs and statistics for each sample were generated in GraphPad, Prism. Images of samples were generated using an Olympus BX51 light microscope with an Olympus SC30 camera.

2.5.E. Rounding up assay

Stage V gametocytes were initiated and cultured to stage V as described in section 2.1.B. Gametocytes were purified on a Percoll gradient (see section 2.2.D) and mixed with uninfected erythrocytes to obtain a gametocytemia of 1 % to 4 % depending upon the number of gametocytes (parasite samples with a parasitemia higher than 2 % were not purified). Samples were diluted in gametocyte culture media (section 2.1.B) to achieve a 0.5 % to 1 % haematocrit. Mature gametocyte samples were treated with test compounds for a designated period of time (see individual experiments for more specific assay conditions). In all assays unless stated otherwise, treated samples were then pelleted by centrifugation at 8000 rpm for 30 seconds, the supernatant was removed to leave a final haematocrit of ~ 80 %. Blood films were prepared and stained with Giemsa as indicated in section 2.1.C. Numbers of crescent shaped gametocytes or rounded forms were counted by light microscopy. Samples were counted in triplicate and percentage parasitemia values generated using Excel. Graphs and statistics for each sample were generated in GraphPad, Prism. Images of samples were generated using an Olympus BX51 light microscope with an Olympus SC30 camera.

2.5.F. Microspheration assay

This assay uses a microsphere matrix to mimic splenic retention. A matrix was prepared using calibrated metal microspheres of two different size distributions (5 to 15 μm diameter and 15- to 25 μm diameter) made up of the following percentage of metals: 96 % tin, 3 % silver and 0.5 % copper (Industrie des Poudres Spheriques). Gametocyte samples were cultured as described in section 2.1.B to produce synchronous stage V gametocyte cultures. Samples were prepared to a parasitemia of 1 % to 5 %. Gametocyte cultures under 1 % were purified by MACS separation (see section 2.2.B) and diluted to the required percentage parasitemia using uninfected erythrocytes. Gametocytes were suspended in warm complete medium or RPMI-1640 to 1- 5 % haematocrit and perfused through the microsphere matrix at a flow rate of 60 mL/h using an electric pump (Syramed sp6000, Arcomed Ag). This was followed by 5 ml of complete medium to wash. Both the upstream and downstream samples were collected and blood smears prepared as described in section 2.1.C. Parasitemia of samples was determined by counts (2000 erythrocytes counted per sample) of Giemsa stained blood films.

2.5.G. Phosphodiesterase activity assay

This assay was developed by Laura Drought (Laura Drought, PhD Thesis, 2014) and is based on a scintillation proximity assay (SPA). This is a bead-based assay technology used to detect and quantify radioactivity and was adapted to measure the PDE activity of a protein sample. When a ^3H radioisotope decays it will release β particles. The distance that these β particles travel through an aqueous solution is dependent upon their energy. If the β particle is in close enough proximity to the SPA bead it will stimulate the stimulant within the bead (in the case of the assay this is yttrium (YSi)). This will generate light that can be detected using a scintillation counter. If the radioactive molecule does not come into close enough proximity to the SPA bead, the β particles will have insufficient energy to reach the bead and no light will be emitted.

Laura Drought has adapted this assay using SPA beads with an YSi core (Perkin Elmer, RPNQ0150). This assay relies on the fact that the cyclic nucleotides cAMP and cGMP are unable to bind to the SPA beads but when hydrolysed by a PDE, the linear nucleotide products 5'AMP or 5'GMP will bind SPA beads in the presence of zinc sulphate by an ion chelation mechanism. Higher levels of PDE hydrolysis will result in more binding and the light detected can be measured and quantified. PDE assays were carried out on immunoprecipitated HA tagged

PfPDE δ and immunoprecipitated HA tagged *PfPDE β* protein (see section 2.7.C for immunoprecipitation method).

PDE Assay on immunoprecipitated HA-tagged *PfPDE δ* and HA-tagged *PfPDE β*

Assays were conducted in a flexible 96 well plate (Perkin Elmer, 1450-401) in a final volume of 100 μ l. 90 μ l of immunoprecipitated (IP) sample diluted in 1x PDE assay buffer (10x buffer contains 17 mM EGTA, 500 mM Tris-HCL, 83 mM MgCl₂) was added per well. Test samples were added to the appropriate wells (PF9, 5 μ M and 200nM, and XA, 1 μ M and 10 μ M, stock solutions prepared in DMSO and working concentrations diluted in PDE assay buffer). The no-compound sample was diluted 1:10 in PDE assay buffer from the concentrated IP sample. [³H] cyclic nucleotides were diluted to 500nM in 1ml. To start the reaction, 10 μ l of either [³H]-cAMP or [³H]-cGMP [³H]cyclic nucleotide (Perkin Elmer cAMP-NET275250UC, cGMP-NET337250UC diluted in 1x PDE assay buffer) was added to wells. Samples were incubated for one hour at 37 °C. To terminate the reaction, 50 μ l of resuspended SPA beads (reconstituted to 20 mg/ml in distilled H₂O) were added to each well. The plates were sealed with plateseal (Perkin Elmer), briefly shaken and then incubated for a further 20 minutes at room temperature to allow the beads to settle. Scintillation was measured using a Wallac 1450 Microbeta™ scintillation counter (Perkin Elmer). Each well was counted for 30 seconds. Data was analysed in Excel and graphs generated in GraphPad, Prism.

2.6. Molecular techniques

2.6.A. Transformation of competent *E.coli* cells: General method

A method of artificial transformation is used to introduce recombinant DNA into chemically competent bacterial cells. Unless stated otherwise, the following method was used; plasmid DNA was added to chemically competent *E. coli* cells and incubated on ice for 30 minutes followed by a heat shock treatment in a water bath at 42 °C for 45 seconds. Samples were then placed on ice for 2 minutes followed by addition of 0.9 ml pre warmed SOC recovery medium (2 % tryptone, 0.5 % yeast extract, 10 mM NaCl, 2.5 mM KCL, 10 mM MgCL₂ and 20 mM glucose). Samples were placed on a shaker at 225 rpm at 37 °C for 1 hour after which they were diluted 1:10 with SOC medium. SOC medium was spread on an agar plate containing either ampicillin at a concentration of 100 µg per ml or Kanamycin at a concentration of 30 µg/ml. Plates were incubated over night at 37 °C. The following day colonies were picked from the agar plate and each put into Luria-Bertani (LB) broth (1 % tryptone, 0.5 % yeast extract, 1 % NaCl and 1.5 % agar) containing an antibiotic. Samples were incubated over night at 225 rpm at 37 °C.

For amplification of the plasmid containing the synthetic gene DH5α *E. coli* cells were used. Antibiotic used was kanamycin. After the last step described above DNA from competent cells was extracted as described in section 2.6.D.

For amplification of the PL6-δ-HA plasmid XL10 Gold *E. coli* cells were used. Antibiotic used was Ampicillin. After the last step described above, further colonies were picked and put into SOC medium containing ampicillin and incubated over night at 225 rpm at 37 °C. Mini preps were carried out on all samples (see method below).

2.6.B. Mini prep for extraction of DNA

The miniprep procedure is based on alkaline lysis of the bacterial cells. In the presence of high salt, DNA from lysed cells is then absorbed onto a silica membrane. This can then be eluted to produce a purified DNA sample. A QIAprep®spin mini prep kit (Qiagen, Lot 27104) was used to purify the DNA and the method followed as indicated by the manufacturer's instructions. DNA content was measured in each sample by nanodrop.

2.6.C. Restriction digest

Restriction digest of PDE δ -HA and PL6 plasmids

The method of restriction digest uses specialist enzymes (restriction endonucleases) that will selectively cut at specific DNA sequences to produce fragments which can be separated on an agarose gel to determine size. This method is used to prepare DNA for analysis or other processing such as ligation, which requires the generation of compatible ends to allow insertion of the required sequence of DNA into a compatible plasmid.

The method of restriction digest was used to firstly remove the synthetic gene from the plasmid in which it arrived and then to cut the PL6 plasmid in order to ligate the synthetic gene into it. Further restriction digests were then carried out throughout the construction process of the plasmid to ensure that the synthetic gene has inserted into the PL6 plasmid correctly. In all instances unless stated otherwise, a mastermix was prepared made up of the required restriction enzymes, PCR grade water and restriction digest buffer. Digestion preparations were prepared by adding plasmid samples to the mastermix followed by incubation at 37 °C for 1.5 hours. Digested samples were run on a 1 % agarose gel at 100V/13w/137MA for 1 hour to determine fragment sizes. All restriction endonucleases were supplied by Fermentas or New England Biolabs and in all instances restriction digest buffer was prepared unless stated otherwise as follows: (10x Cutsmart™ Buffer #B77045 with added bovine serum albumin (BSA), diluted in 1x PBS, Sigma).

2.6.D. DNA fragment clean up

PDE-Delta-HA and PL6 fragment DNA clean up

A miniElute® reaction clean up kit (Qiagen 28204) was used to clean up the DNA of digested plasmids. And the method was followed as per the supplier's instructions. Samples were eluted in 10 μ l elution buffer.

2.6.E. DNA fragment ligation

PDE-Delta-HA and PL6 fragment ligation (to ligate synthetic gene into PL6 plasmid)

DNA fragment ligation involves the joining of two DNA fragments through the action of an enzyme (see Figure 2.2 for schematic).

The transformed, cleaned and digested DNA fragments of PDE δ -HA and the pL6 repair template plasmid (sections 2.6.E) were incubated at room temperature for 2 hours in T4 ligase (enterobacteria phage T4), x10 ligase buffer (50 mM Tris-HCL, 10 mM MgCl₂, 1 mM ATP, 10 mM DTT, pH 7.5 at 25°C) and PCR water to give a total volume of 10 μ l. This was followed by an inactivation step at 65 °C for 10 minutes to inactivate the ligase.

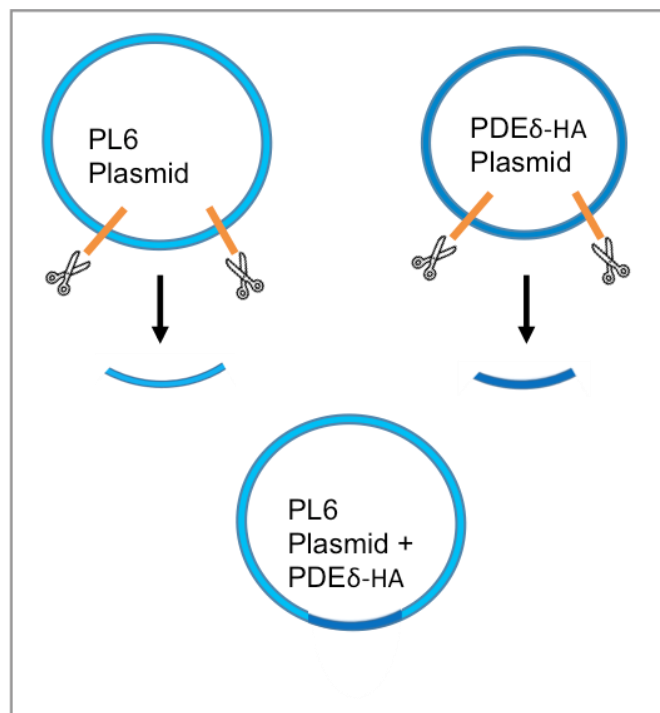


Figure 2.2: Schematic showing PDE-Delta-HA and PL6 plasmid digest and fragment ligation

2.6.F. Infusion cloning with oligos

Oligos (see appendix A2 for sequences) were firstly annealed. Both were diluted in PCR grade H₂O to prepare a stock concentration of 100 μ M. 10 μ M was made in a total volume of 100 μ l annealing reaction (10 μ l of each oligo, 10 μ l buffer (NE buffer D70025 10x Bio labs) and 70 μ l PCR H₂O). The reaction was incubated at 95 °C for 5 minutes to annealed oligos.

Infusion cloning was carried out by Avnish Patel, (LSHTM) using the pre-infusion cloning pL6 repair plasmid containing PDE δ -HA synthetic gene insert. The infusion cloning reaction was prepared on ice to result in a 5 μ l total reaction as follows: 1 μ l 5x enzyme mix, 5 μ l cut plasmid, 1.5 μ l of 0.5 μ M annealed oligos and 1.5 μ l PCR grade H₂O. The reaction was incubated at 50 °C for 15 minutes.

2.6.G. Maxi prep

Maxi prep on PL6 containing PDE δ HA plasmid sample 2b post-infusion cloning.

The post infusion cloning sample was put into LB broth. A Maxi kit (Qiagen plasmid *plus* maxi kit, cat 12963) was used to extract the DNA as indicated in the manufacturer's instructions. The DNA content of the Maxi prep product was measured by nanodrop. 1 μ l of sample was loaded onto the nanodrop to measure DNA content.

A restriction digest was carried out by Christian Flueck, LSHTM. This sample was used for transfection.

2.6.H. Transfection

Genetic manipulation of a *P. falciparum* NF54 parasite line (with good gametocyte producing capabilities) was achieved using a standard ring stage transfection protocol. In short, parasites were prepared as indicated in section 2.3.C. The co-precipitation was prepared using 85 μ l of precipitated PL9 high fidelity Cas9 blasticidin + gRNA DNA (measured as 176 ng/ μ l using a nanodrop, and 26 μ l of pL6 repair template containing the PDE δ -HA insert. 500 μ l 100 % EtOH was added and 60 μ l sodium acetate. Samples were incubated at - 80°C for 30 minutes then pelleted at 15300 xg in a cold centrifuge for 15 minutes. The supernatant was removed and the sample washed in 70 % EtOH. Samples were briefly pelleted and left to air dry.

DNA co-precipitation was resuspended in 10 μ l 1x TE buffer (1 mM Na₂EDTA, 10 mM Tris-HCL (pH 8)). This was followed by addition of 100 μ l PE primary cell solution. Samples were mixed well.

Parasite samples were pelleted at 8000 rpm for 30 seconds and all of the supernatant removed. The DNA-cytomix preparation was added to the parasite pellet and immediately transferred to a 0.2 cm cuvette (Bio-Rad). Cells were transferred gently using a pipette. The sample was

electoporated using a Lonza 4D-Nucleofector™ at 0.31 kilovolts (KV) and 950 microfarad (μF). Parasites were gently transferred to 10 ml pre-warmed CM (section 2.1.A) in a 25 ml culture flask with 0.5 ml very fresh blood (< 2 days old). Parasites were incubated at 37 °C / 5 % CO₂ (BOC) as indicated in section 2.1.A. 2.5 μg/ml blasticidin was added for 10 days and the parasites regularly monitored by Giemsa stained blood film (section 2.1.C) until parasites were detectable by microscopy. A PCR analysis of parasites (section 2.6.K) was carried out and samples analysed by SDS PAGE (section 2.7.A) and western blot (section 2.7.B) to confirm integration.

2.6.I. Polymerase chain reaction (PCR)

Polymerase chain reaction (PCR) is a technique that uses a method of thermal cycling in order to exponentially amplify a segment of DNA. This involves an initial denaturation step at a high temperature (94°C to 96°C) to break apart the double stranded DNA. This is followed by a decrease in temperature to allow annealing of specific primers to each strand of the DNA (this is usually 40-60 °C and varies depending on the optimal temperature required for the primer used). The last step involves a further increase in temperature to 72 °C to allow for elongation of the complementary strand of DNA which enables an enzyme, polymerase, to add nucleotides to the primer sequence. This extends both complementary strands, resulting in two segments of double stranded DNA. This cycle is repeated on average around 30 times leading to an amplification of the sequence of interest.

PCR to determine integration of the HA-tagging plasmid into the *PfPDEδ* locus

To confirm integration of the HA-tagging plasmid (NF54-*PfPDEδ*-HA) into the correct locus, the following PCR protocol was followed: DNA was extracted from whole blood from predominantly schizont stage cultures of the NF54-*PfPDEδ*-HA line using a Qiagen, DNeasy Blood & tissue kit, (Qiagen, cat 09504). Wildtype NF54 line parasites were used as a control. DNA was measured using a nanodrop giving a quantity of 43.2 ng/μl for NF54 sample and 134.1 ng/μl for the NF54-*PfPDEδ*-HA line DNA. A master mix was prepared using 100 μl BIOMix™ Red DNA polymerase (Bioline) and 100 μl PCR grade H₂O. Primer pairs (1 μl each primer) were added to 8 tubes as indicated as follows: tubes 1 and 2: WT specific (p1 + p2), tubes 3 and 4: Integration specific (p3 + p4), tubes 5 and 6: Episome and integrated specific (p4 + p5) and tubes 7 and 8: a DNA control (13'PKG-BC1F + PKG-CRD). See appendix A2 for primer sequences. 0.5 μl parasite DNA (NF54-*PfPDEδ*-HA line or NF54 control for each primer set) was added to primer pairs. 22.5 μl of master mix was added to each tube. The PCR reactions were cycled as follows: 94 °C for 3 minutes, 60

°C for 30 seconds, 65 °C for 30 seconds, 94 °C For 30 seconds, 60 °C for 30 seconds, 65 °C for 30 seconds, steps 4-6 cycles 30 times, then 65 °C for 3 minutes.

Samples were run on an agrose gel ((1g agrose in 100 ml TAE), 100v/13w/137ma for 1 hour).

2.7. *Pf*PDE δ -HA line assays

2.7.A. Sodium dodecyl sulphate polyacrylamide gel electrophoresis (SDS-PAGE)

Polyacrylamide gel electrophoresis is a method used to separate proteins based on their charge, size, electrophoretic mobility and conformation. In this project SDS-PAGE was used to separate proteins based on size by denaturing proteins leading to linearization. The SDS in the buffer results in an overall negative charge of the protein. Smaller proteins will travel further along the gel and sizes of proteins can be estimated based on comparison to proteins with an already known molecular weight. The molecular weight ladder used was Precision Plus protein™ Standards (BioRad, cat 161-0373). A tris/glycine based gel (Bio Rad mini-protean®TGX stain-Free™ gel) was placed in a gel tank with 1x SDS-PAGE running buffer. 15ul of each sample was loaded into the wells and the gel run for 40 minutes at 200V.

2.7.B. Western blotting

After completion of SDS-PAGE (section 2.7.A), the gel was blotted onto a nitrocellulose membrane (Bio Rad Trans-Blot® turbo™ mini sized transfer stacks) at 2.5 amps, 25V for 20 minutes. Once transfer had occurred, the nitrocellulose membrane was blocked in 5 % milk powder (Marvel dried skimmed milk in 1x PBS with 0.1 % Tween (Sigma Aldrich)) for an hour while shaking gently. The blot was then incubated with a 1:2000 dilution primary antibody (α -HA high affinity rat monoclonal 100 μ g/ml, clone 3F10, Roche) overnight while gently shaking. Samples were washed twice for 15 minutes in 1x PBS with 0.1 % Tween and stained with a secondary antibody (polyclonal rabbit α -rat Alexa Fluor 595 (Dako) 1.3 g/l stock, lot: 00076525, diluted in milk block to 1:6000) for 1 hour at room temperature while shaking. The blot was washed twice for 15 minutes in 1x PBS with 0.1 % Tween. Supersignal™ West Femto maximum sensitivity substrate (Thermo Scientific, cat 34095, enhanced chemiluminescent (ECL) substrate

with horseradish peroxidase) was added to the blot and ECL hyper film (GE healthcare) and the protocol followed according to the manufacturer's instructions.

2.7.C. Immunoprecipitation of *Pf*PDE δ -HA

An immunoprecipitation assay was carried out on the HA-tagged *Pf*PDE δ line using an anti-HA affinity matrix composed of immobilised anti-HA high affinity rat monoclonal antibodies (clone 3F10) (Roche, Diagnostics, Lot 10167700) to pull down *Pf*PDE δ protein from mature gametocyte samples (see section 2.3 A for gametocyte sample preparation). Parasite pellets were resuspended in 250 μ l ice cold PDE lysis buffer (150mM NaCl, 0.5 % Nonidet P-40, 10 mM Tris-HCL pH 7.5 and EDTA-free protease inhibitors) per 50 μ l of sample. Samples were incubated on ice for 30 minutes with occasional mixing followed by a 20 minute centrifugation step at 16000 \times g/4 ° C. The supernatant was transferred to a pre-cooled tube and the pellet discarded. A 15 μ l sample of supernatant was removed for immunoblotting and labelled 'undiluted input'. The volume of the remaining supernatant sample was adjusted to 500 μ l with PDE dilution buffer (150mM NaCl, 10 mM Tris-HCL pH 7.5 and EDTA-free protease inhibitors) to give a final detergent concentration of < 0.2 %. A sample of supernatant was saved for immunoblotting and labelled 'diluted input'. To equilibrate the anti-HA affinity matrix, 20 μ l was transferred to an eppendorf tube containing 500 μ l PDE dilution buffer. This was centrifuged at 8000 rpm for 30 seconds. The supernatant was removed and this wash step was repeated. After the second wash the supernatant was removed from the beads and discarded. The supernatant sample (all 500 μ l) was added to the equilibrated anti-HA affinity matrix and incubated at room temperature for 2 hours with constant mixing. After incubation, the anti-HA affinity matrix was pelleted by centrifugation at 8000 rpm for 30 seconds. The supernatant was removed to a new tube and a 40 μ l sample saved for immunoblotting and labelled as 'wash 1'. 500 μ l ice cold PDE dilution buffer was added to the pelleted Anti-HA affinity matrix and a 1000 μ l sample removed for immunoblotting and labelled 'bound beads'. The Anti-HA affinity matrix and the sample labelled 'bound beads' were then pelleted by centrifugation at 8000 rpm for 30 seconds. Tubes were then turned with the opposite side facing into the centrifuge and the matrix was centrifuged again at 8000 rpm for 30 seconds. The supernatant from the Anti-HA affinity matrix sample was removed to a new tube and a 40 μ l sample saved for immunoblotting and labelled as 'wash 2'. The remaining beads were saved for analysis by PDE assay (see section 2.5.G p88).

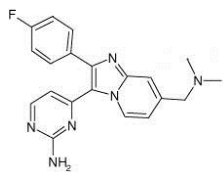
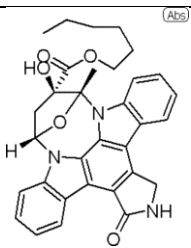
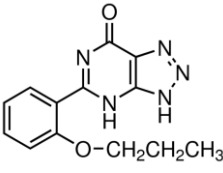
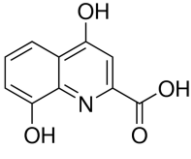
Compound name	Molecular weight	Structure	IC ₅₀ on Asexual stages (μM)	IC ₅₀ on gametocytes stages (μM)	Cellular Target	references
Compound 2	362.41		2.70 ± 0.17	unknown	PKG	Gurnett et al, 2001 McRobert et al, 2008
KT5720	537.61		2.5	unknown	PKA	(Christian Flueck, unpublished)
Zaprinast	271.27		3.0 ± 1.2	33.7 ± 1.3	PDE	McRobert et al, 2008
PF9		Pfizer compound. Restricted access to information.	0.14	0.052 ± 0.41	PDE	(Laura Drought, PhD Thesis)
XA	205.17		N/A	IC ₅₀ Unknown active on gametocytes above 3 μM. Working conc used: 3 μM to 30 μM	unknown	Bilker et al, 1998. Garcia et al, 1998

Table 2.1. An overview of the properties of C2, KT5720, zaprinast, PF9 and XA.

Chapter 3

Investigation into the relationship between cGMP signalling and Ca²⁺ release in *Plasmodium falciparum*

3.1. Introduction

*Pf*PKG plays an essential role in asexual blood stage schizogony. This tightly regulated process can be blocked by the *Pf*PKG inhibitors C1 and C2 with merozoites unable to egress[160]. *Pf*PKG is known to regulate the discharge of *Pf*SUB1 from the micronemes required for the proteolytic processing of proteins required for egress and invasion[173]. *Pf*PKG inhibition also leads to subsequent block in the release of proteins from the micronemes[173]. The PDE inhibitor zaprinast can induce premature egress of merozoites and does so in a *Pf*PKG-dependent manner[173]. This evidence suggests that the natural trigger for egress is likely to involve a signal that leads to elevated levels of cGMP. *Pf*PKG is also essential for XA-induced gametogenesis and this process can be blocked at the very earliest stages by addition of C1 and C2[159] with gametocytes unable to round up. In the absence of XA, zaprinast can stimulate gametogenesis and does so in a *Pf*PKG-dependent manner[159].

The mobilisation of Ca²⁺ into the cytosol from as yet unidentified internal stores plays a key role in many cellular processes within the parasite. In asexual blood stages a steady increase in Ca²⁺ occurs prior to blood stage merozoite egress[224]. This rise in cytosolic Ca²⁺ is an essential signalling event required for egress to occur and chelation of intracellular Ca²⁺ results in a block in egress[224]. Ca²⁺ mobilisation from internal stores is required for the secretion of microneme and rhoptry proteins[265], and for the activation of a Ca²⁺-dependent protein kinase, CDPK5, which is critical for merozoite egress and evidence suggests it acts downstream of *Pf*PKG regulated proteolytic processing[175].

Ca²⁺ is also an important signalling molecule in gametocyte stages where a rapid rise in cytosolic Ca²⁺ occurs in response to XA (and a concomitant decrease in temperature)[210]. In *P. berghei* gametocytes, this Ca²⁺ response occurs within 20 seconds of XA addition and is essential for exflagellation[260][210]. In gametocytes, Ca²⁺ mobilisation leads to the activation of a Ca²⁺-dependent protein kinase, CDPK4, which is required for male gametocyte cell cycle progression[210]. In *P. berghei*, Ca²⁺ activates a myristoylated isoform of CDPK4 enabling it to control two important events in male gametogenesis, which occur within the first 30 seconds of

gametocyte activation. Firstly, phosphorylation of the substrate SOC1 (substrate of CDPK4-1) leading to replication of the parasite genome from a haploid state enabling entry into the S phase. This involves recruitment of a complex to the origin of replication required to initiate the first genome replication and secondly, mitotic spindle assembly and formation, enabling chromosome segregation allowing duplicated genetic material to be separated into new cells. This involves phosphorylation of the CDPK4 substrate SOC2[215]. In addition to these two roles, a non-myristoylated isoform of CDPK4 plays a third role in male gametogenesis, by phosphorylating a third substrate SOC3, which acts downstream of genome replication, mitotic spindle assembly and axoneme assembly to activate flagella motility[215]. Interestingly, Ca^{2+} is required for all constituent events of gametogenesis in *P. berghei* and this has been explored in detail[210], but evidence using pharmacological inhibition of *Pf*PKG using C1 and chelation of Ca^{2+} using BAPTA-AM suggests that Ca^{2+} is only required for the later stages of gametogenesis in *P. falciparum*[159]. This may reflect possible species-specific differences.

There is a clear symmetry between the role of *Pf*PKG at various stages of the *Plasmodium* lifecycle and the role of Ca^{2+} in merozoite egress[175] and gametogenesis[210]·[215] as mentioned here, but also in merozoite invasion[207], ookinete gliding motility[209]·[208] and more recently, *P. berghei* sporozoite invasion of hepatocytes[218] . Zaprinast presumably bypasses the natural trigger for merozoite egress by elevating levels of cGMP through cGMP-*Pf*PDE inactivation. In gametocytes the natural trigger for gametogenesis (XA) is already known and in 2001, Muhia *et al* identified that XA could induce elevated levels of cGMP in gametocyte membrane preparations[126], suggestion that zaprinast and XA may act through the same pathway, but that zaprinast likely bypasses the initial XA signal.

In *Plasmodium* species phosphatidylinositol lipids are important secondary messengers in signalling cascades and also play an important role in vesicle trafficking[266]. Their synthesis is controlled by *Pf*PKG which targets the lipid kinases (PIP4K and PIP5K) that mediate their phosphorylation[174]. The regulation of phosphoinositide synthesis mediated by *Pf*PKG, specifically the production of IP_3 which occurs through activation of phospholipase C (PLC) results in the release of Ca^{2+} [174]. In gametocytes of the murine malaria parasite *P. berghei*, XA triggers the hydrolysis of PIP_2 which results in IP_3 production[200]. Two global analyses by mass spectrometry of the *P. berghei* phosphoproteome in ookinetes were carried out[174]. The first approach looked at the effect on the proteome of altered cGMP signalling using a *Pb*GC-ko mutant cell line and the second study used *Pb*PKG inhibition by C2 of both the wildtype and

gatekeeper mutant cell lines to determine changes in phosphorylation of proteins when *Pb*PKG was inhibited. Both of these approaches revealed several signalling pathways, which appear to operate downstream of *Pb*PKG. Interestingly, one of these was phosphoinositide metabolism and given the already identified link between XA stimulation and IP₃ production in gametocytes, this pathway was selected for further validation. Phosphoinositide lipid analysis on *P. berghei* ookinetes revealed that inhibition of *Pb*PKG led to a marked increase in levels of phosphatidylinositol (PI) and a concomitant increase in phosphatidylinositol 4-phosphate (PI4P) and phosphatidylinositol (4,5)-bisphosphate (PI(4,5)P₂) in gliding ookinetes. Indicating that *Pb*PKG controls lipid kinases to regulate phosphoinositide synthesis in motile ookinetes of *P. berghei*. Further studies showed that *Pb*PKG is also required to raise levels of cytosolic Ca²⁺ in both *P. berghei* ookinetes and *P. berghei* gametocytes (in response to XA stimulation).

In collaboration with the authors as part of this publication[174], we sought to investigate this link between *Pf*PKG, phosphatidylinositol synthesis and Ca²⁺ mobilisation in blood mature stages. As this has already been identified for *P. berghei*[174], we sought to identify whether this association between Ca²⁺ and cGMP signalling was conserved in the human parasite *P. falciparum*.

3.2. Results

3.2.1. Zaprinast-induced Ca²⁺ release in *P. falciparum* schizonts

Zaprinast induces Ca²⁺ release in segmented schizonts in a dose-dependent manner.

The *Pf*PKG inhibitor C2 and the C2-insensitive *Pf*PKG_{T618Q} line were used in Ca²⁺ release assays as tools to determine firstly whether the PDE inhibitor zaprinast can stimulate Ca²⁺ release in *P. falciparum* late schizonts, and secondly, to determine whether zaprinast-induced Ca²⁺ mobilisation is *Pf*PKG specific. Ca²⁺ levels were measured in Fluo-4-loaded schizonts over time both prior to and after addition of test compounds.

In the wildtype 3D7a line, the PDE inhibitor zaprinast induced Ca²⁺ mobilisation in mature, segmented schizonts in a dose-dependent manner (Figure 3.1). Elevation of Ca²⁺ levels was measurable at a zaprinast concentration of as low as 6.25 µM and was detectable within 20 seconds of addition of zaprinast to cells, indicating a rapid mobilisation of Ca²⁺ from internal stores in response to addition of this PDE inhibitor. No Ca²⁺ release was detected using this assay when cells were treated with 3.125 µM zaprinast, the lowest concentration tested. At the highest concentration tested (100 µM), Ca²⁺ release reached ~30 % of the ionophore control (A23187). The results imply that elevated cGMP levels induced by zaprinast stimulate Ca²⁺ release.

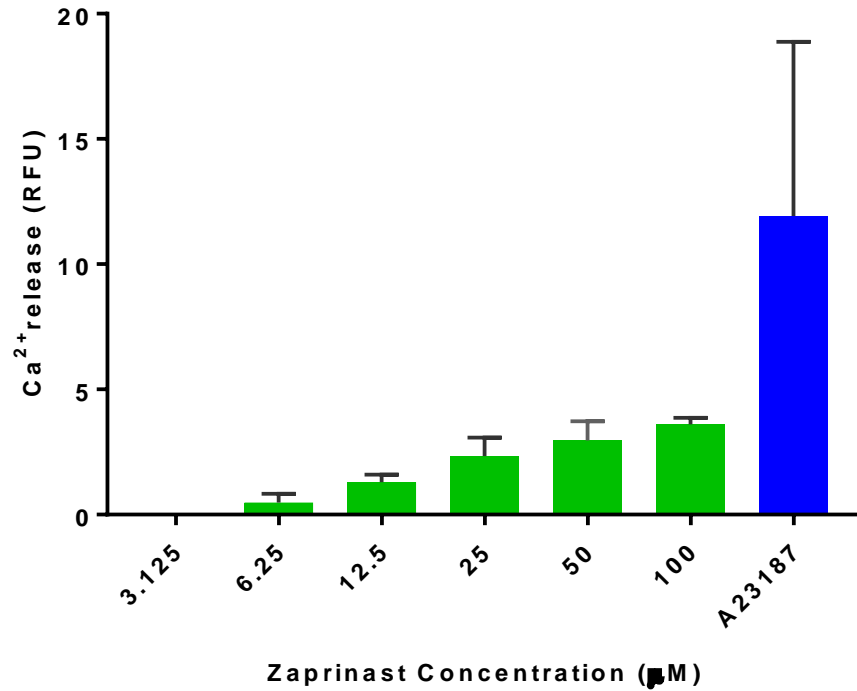


Figure 3.1. Ca²⁺ release in Fluo-4-AM-loaded 3D7a segmented schizonts stimulated with zaprinast. Data are presented as Ca²⁺ release measured as relative fluorescent units (RFU) minus the baseline fluorescence and fluorescence of the DMSO control sample. The ionophore (A23184) was used as a positive control. The bar chart was generated in GraphPad, Prism and shows the mean of 3 experiments each carried out in triplicate. Error bars represent SD.

In mature, segmented schizonts of the *Pf*PKG_{T618Q} line, zaprinast induced Ca²⁺ release in a dose-dependent manner (Figure 3.2) as was seen in the 3D7a line (Figure 3.1). Ca²⁺ release was detected at the lowest concentration of zaprinast tested (3.125 μM). At the highest concentration tested (100 μM), zaprinast induced Ca²⁺ mobilisation to ~ 27 % of the ionophore-treated control, a comparable level to that induced by 100 μM zaprinast in the 3D7a line (~ 30 %). As seen in the 3D7a wildtype line, 100 μM zaprinast induced Ca²⁺ release within 20 seconds of addition to schizonts of the *Pf*PKG_{T618Q} line (Figure 3.6). Zaprinast stimulation of the *Pf*PKG_{T618Q} line therefore exhibits a comparable pattern of Ca²⁺ mobilisation to that seen in the 3D7a wildtype line confirming that the genetically manipulated line does not have a reduced ability to release calcium in response to zaprinast.

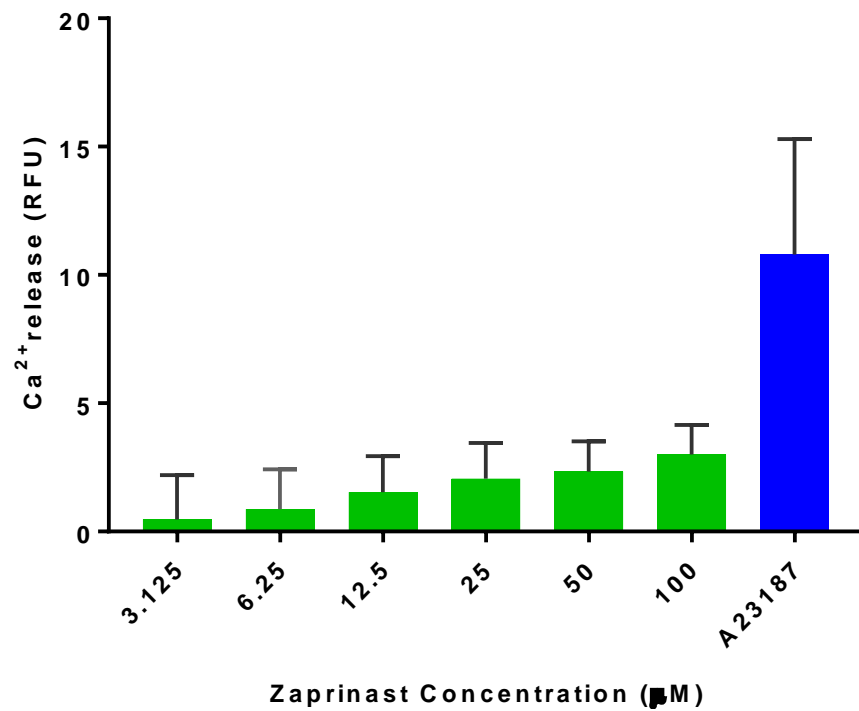


Figure 3.2. Ca²⁺ release in Fluo-4-AM-loaded *PfpPKG*_{T618Q} segmented schizonts stimulated with zaprinast. Data are presented as Ca²⁺ release measured as relative fluorescent units (RFU) minus the baseline fluorescence and fluorescence of the DMSO control sample. The ionophore (A23184) was used as a positive control. The bar chart was generated in GraphPad, Prism and shows the mean of 3 experiments each carried out in triplicate. Error bars represent SD.

Zaprinast-induced Ca^{2+} release in segmented schizonts is *Pf*PKG dependent

To investigate whether *Pf*PKG plays a role in zaprinast-induced calcium release, the previous experiments were repeated in the presence of the PKG inhibitor C2.

In segmented schizonts of the wildtype 3D7a line induced with 100 μM zaprinast, a dose-dependent decrease in fluorescence was measured with increasing concentrations of C2 (Figure 3.3: data shown as percentage of ionophore control and Figure 3.4: data shown as change in Ca^{2+} levels over time). Zaprinast induced Ca^{2+} release was completely reversed by 8 μM C2 ($P = 0.0434$, Welch's unpaired t test). Zaprinast treatment in the presence of 4 μM C2 reduced Ca^{2+} levels by ~85 % compared to zaprinast treatment alone (normalised to 100 %). 2 μM C2 reduced zaprinast induced Ca^{2+} release by ~ 60 %. At the lowest C2 concentration (1 μM), zaprinast-induced Ca^{2+} release was reversed by ~ 40 % compared to the zaprinast only sample ($P = 0.0295$, Welch's unpaired t test). The data suggests that zaprinast-induced Ca^{2+} release in schizonts is a *Pf*PKG-dependent event.

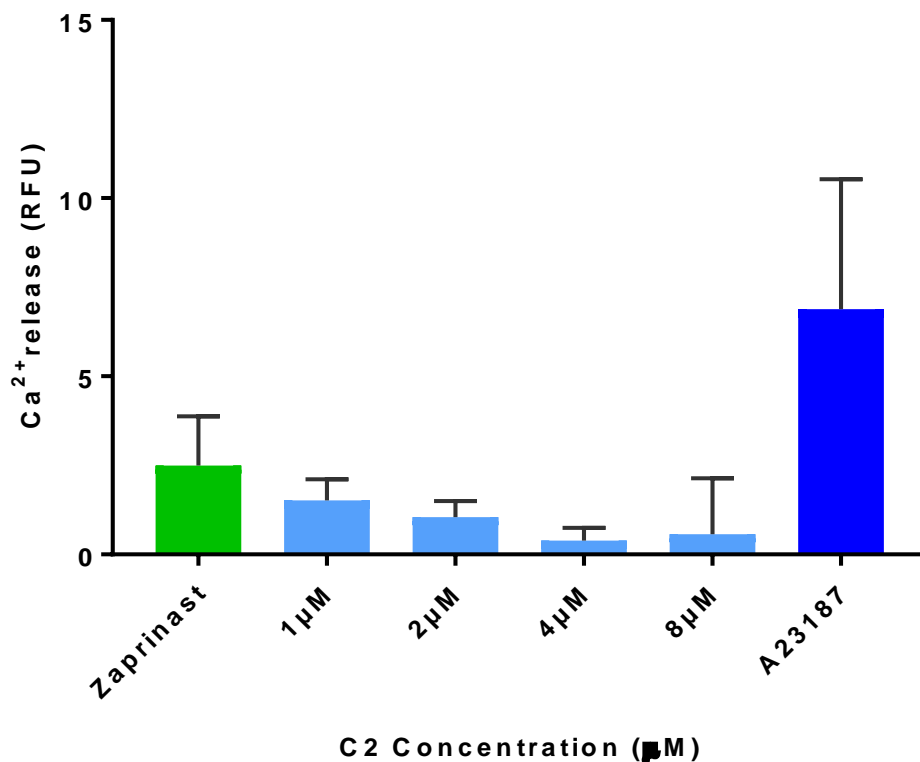


Figure 3.3. The effects of C2 on zaprinast-stimulated Ca^{2+} levels in Fluo-4-AM-loaded 3D7a line schizonts. A zaprinast only sample (green) is compared to zaprinast-treated samples in combination with a serial dilution of C2 (light blue). All samples are compared to an ionophore control (A23187). Data are

presented as Ca^{2+} release measured as relative fluorescent units (RFU) minus the baseline fluorescence and fluorescence of the DMSO (0.05 %) control sample analysed in Excel. The bar chart was generated in GraphPad, Prism and shows the mean of 3 experiments each carried out in triplicate. Error bars represent SD.

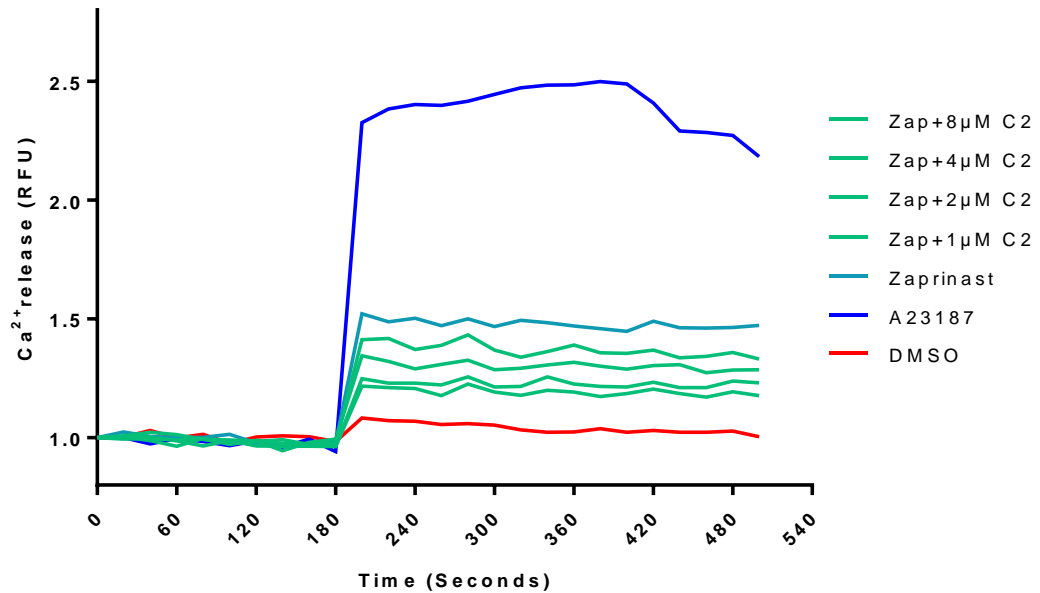


Figure 3.4. Zaprinast-induced Ca^{2+} release in the presence of C2 in Fluo-4-AM-loaded 3D7a schizonts over time. A zaprinast only sample (light blue) is compared to zaprinast-treated samples in combination with a serial dilution of C2 (green). All samples are compared to an ionophore control (A23187). Data are Ca^{2+} release measured every 20 seconds and presented as relative fluorescent units (RFU). Compounds were added to cells at the 2 minute time point (purple star). Data are normalised to the first baseline read of each sample (0 second time point) and minus the buffer only control. The graph generated in GraphPad, Prism. The data are from 1 experiment carried out in triplicate.

To confirm the on-target effects of C2 on Ca^{2+} release, this experiment was repeated with the C2-insensitive gatekeeper mutant line. In *PfPKG_{T618Q}* segmented schizonts, C2 was unable to reverse zaprinast-induced Ca^{2+} release at all four concentrations tested (Figure 3.5: data shown as percentage of ionophore control and Figure 3.6: data shown as change in Ca^{2+} levels over time). Levels of fluorescence induced by 100 μM zaprinast remained at a similar level regardless of the concentration of C2 added. This confirms that zaprinast-induced Ca^{2+} mobilisation is indeed *PfPKG* dependent.

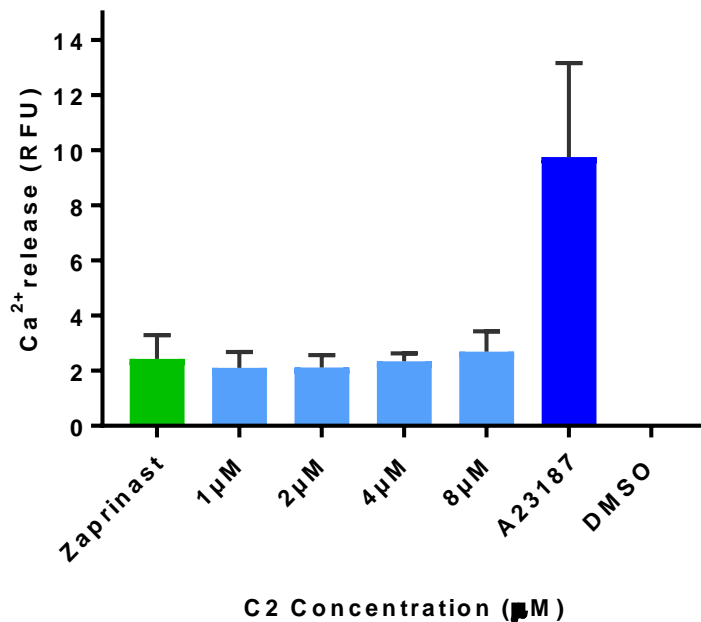


Figure 3.5. The effects of C2 on zaprinast-stimulated Ca^{2+} levels in Fluo-4-AM-loaded *PfPKG_{T618Q}* line schizonts. A zaprinast only sample (green) is compared to zaprinast treated samples in combination with a serial dilution of C2 (light blue). All samples are compared to an ionophore control (A23187). Data are presented as Ca^{2+} release measured as relative fluorescent units (RFU) minus the baseline fluorescence and fluorescence of the DMSO (0.05 %) control sample analysed in Excel. The bar chart was generated in GraphPad, Prism and shows the mean of 3 experiments each carried out in triplicate. Error bars represent SD.

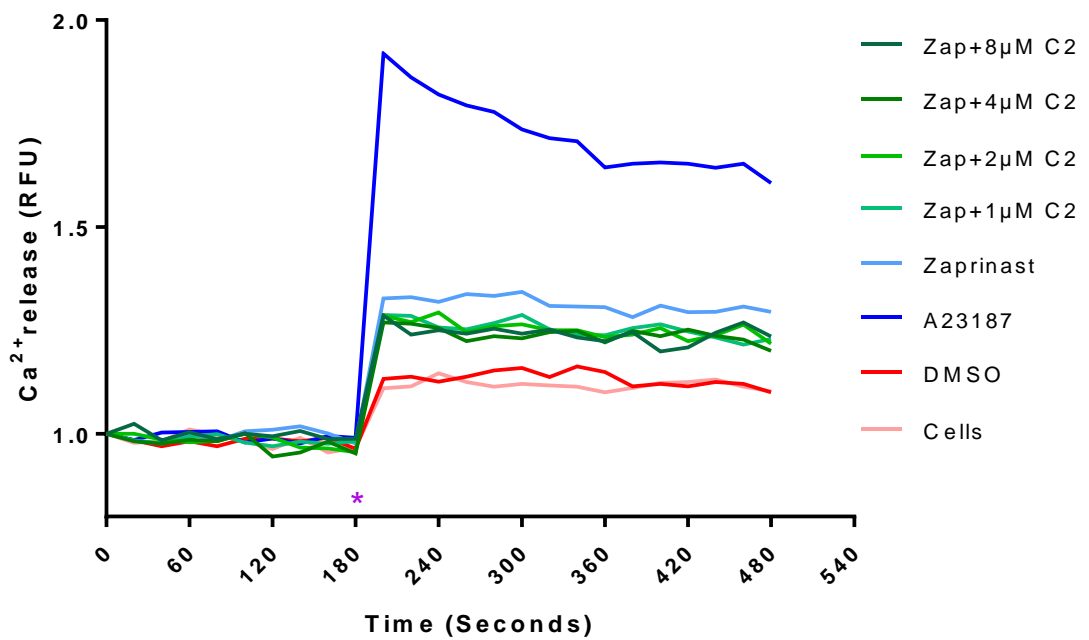


Figure 3.6. Zaprinast-induced Ca²⁺ release in the presence of C2 in Fluo-4-AM-loaded *Pf*PKG_{T618Q} line schizonts over time. A zaprinast-only sample (light blue) is compared to zaprinast-treated samples in combination with a serial dilution of C2 (green). All samples are compared to an ionophore control (A23187). Data are Ca²⁺ release measured every 20 seconds and presented as relative fluorescent units (RFU). Compounds are added to cells at the 2 minute time point (purple star). Data are normalised to the first baseline read of each sample (0 second time point). Minus the buffer only control. Data are analysed in Excel and the graph generated in GraphPad, Prism and shows the data from 1 experiment carried out in triplicate.

Use of a *Pf*PKG-DD line further confirms that zaprinast-induced Ca^{2+} release in schizonts is *Pf*PKG dependent

To further confirm that zaprinast-induced Ca^{2+} mobilisation is PKG specific, a *Pf*PKG conditional knockdown line (kindly provided by Dr Manoj Duraisingh and Jeffrey Dvorin) utilising a destabilising domain (DD) system was used to regulate the levels of *Pf*PKG. In this line a DD protein is fused to the C-terminus of *Pf*PKG. This fusion protein is rapidly degraded in the absence of the ligand shield-1 but is stabilised in its presence. Removal of shield-1 from cultures results in degradation of *Pf*PKG essentially producing a knockdown line of *Pf*PKG. Shield-1 was removed from cultures at the ring stage and parasites were allowed to develop to the segmented schizont stage. This was to ensure that, by the time the parasites reached the mature schizont stage, prior to egress, that most and if possible, all of the *Pf*PKG protein was absent from samples.

Zaprinast treatment induced Ca^{2+} release in the *Pf*PKG-DD line in the presence of Shield-1 (Figure 3.7 Purple bars). This sample is essentially the same as the wildtype line as *Pf*PKG is present at presumably comparable levels to the wildtype and *Pf*PKG_{T618Q} lines indicating (although levels of *Pf*PKG were not measured) that this genetically manipulated line has not affected its ability to release calcium in response to addition of zaprinast. Similarly to the results obtained with the wildtype 3D7a line, the zaprinast-induced Ca^{2+} release was reduced by ~ 85 % on addition of 2 μM C2 to the *Pf*PKG-DD line in the presence of Shield-1. This reduction in Ca^{2+} release on addition of C2 was shown to be significant ($P = 0.0063$, Welch's unpaired t test).

By contrast, in the absence of Shield-1 (Figure 3.7, blue bars) and therefore at reduced levels of *Pf*PKG (where *Pf*PKG has been degraded), much lower levels of fluorescence were measured in response to zaprinast treatment compared to the plus Shield-1 zaprinast-treated sample, indicative of much lower levels of Ca^{2+} release in this sample in response to zaprinast (Figure 3.7). The difference in zaprinast-induced Ca^{2+} release in samples grown in the presence and absence of Shield-1 was significant ($P = 0.0446$, Welch's unpaired t test). The levels of zaprinast-induced Ca^{2+} release in the minus Shield-1 samples (blue bars) plus and minus C2 (~7 % and ~ 6 % of ionophore control respectively), were comparable to C2 treatment of the plus shield-1 sample in which *Pf*PKG was present but inhibited (~ 4.5 % ionophore control). The small level of calcium release induced by zaprinast in the minus Shield-1 sample was not altered by addition of C2 ($P = 0.9333$, Welch's unpaired t test). These data provides independent confirmation that in asexual blood stage schizonts, zaprinast-induced Ca^{2+} mobilisation is *Pf*PKG dependent.

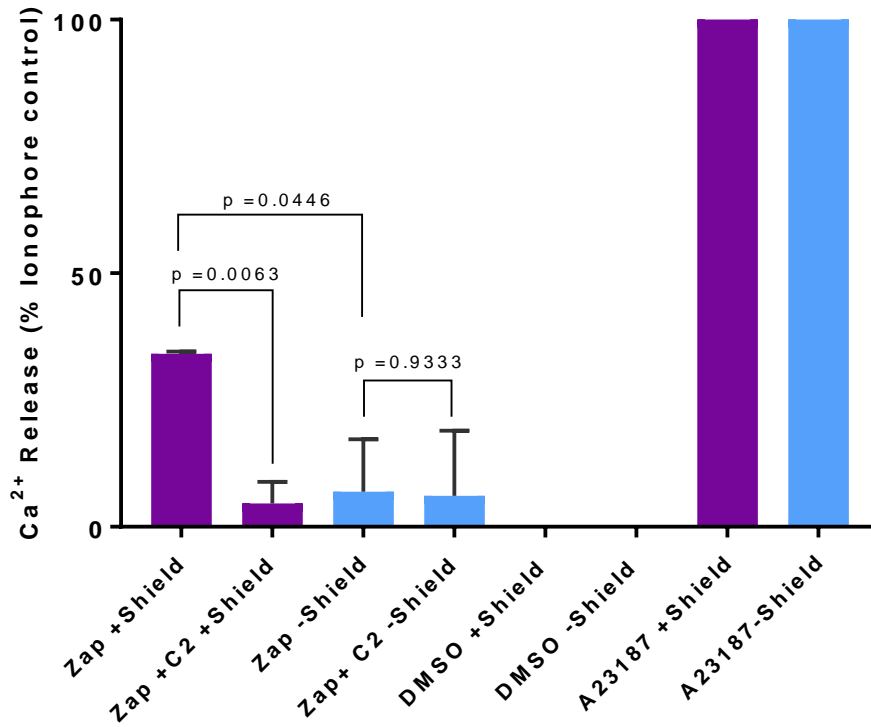


Figure 3.7. The effects of C2 on zaprinast-stimulated Ca²⁺ levels in Fluo-4-AM-loaded *Pf*PKG-DD line schizonts. Plus Shield-1 samples (*Pf*PKG stable: purple bars) ± C2, compared to minus Shield-1 samples (*Pf*PKG degraded: blue bars) ± C2. Data are presented as Ca²⁺ release, measured as percentage of ionophore control (both +/- shield-1). Minus the baseline fluorescence and fluorescence in the DMSO (0.05 %) control sample (both +/- shield-1). Data are analysed in Excel and the graph generated in GraphPad, Prism and is the average of 3 experiments each carried out in triplicate. Error bars represent SD.

Zaprinast triggers a rapid depletion in phospholipids in a *Pf*PKG-dependent manner

Lipid extractions were carried out on zaprinast-treated purified schizonts of the 3D7a and *Pf*PKG_{T618Q} lines either pre-incubated with C2 or with no C2 treatment. This was followed by analysis of the schizont lipidome by Electrospray-mass spectrometry to look at changes in levels of phospholipids in relation to *Pf*PKG inhibition (the mass spectrometry was carried out by Terry K Smith in schools of Biology and Chemistry, University of St Andrews). The relative abundance of the phospholipids PI, PIP, PIP₂ and PIP₃ were measured over time after addition of zaprinast to C2 pre-treated purified schizonts from the 3D7a and *Pf*PKG_{T618Q} lines.

Addition of zaprinast to the *Pf*PKG_{T618Q} line pre-incubated with C2 (this sample should reflect what would occur in the wildtype line with no C2 treatment) resulted in a rapid depletion in both PIP₂ and PIP₃ compared to the C2-treated wildtype (3D7a) control in which *Pf*PKG had been inhibited (Figure 3.8). This change in levels of phospholipids in zaprinast-induced *Pf*PKG_{T618Q} schizonts was accompanied by a reduction in levels of PIP and a concomitant increase in levels of PI (Figure 3.9). 3D7a schizonts treated with zaprinast showed no changes in levels of PI or PIP in the presence of C2. *Pf*PKG inhibition therefore prevented zaprinast-induced changes in levels of PI, PIP, PIP₂ and PIP₃ in the 3D7a wildtype line but not in the *Pf*PKG_{T618Q} lines, indicative that regulation of phosphoinositide levels by zaprinast is a *Pf*PKG-dependent event. These changes in levels of phospholipids occurred within 10 seconds of treatment.

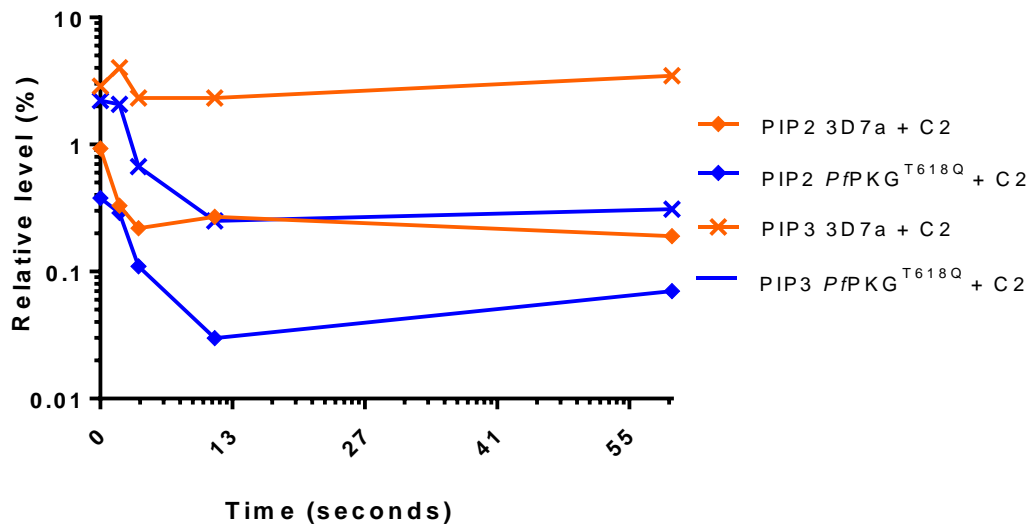


Figure 3.8. Changes in levels of PIP₂ and PIP₃ over time in mature *P. falciparum* schizonts, in response to zaprinast treatment in the presence of C2 in the wildtype 3D7a line compared to the gatekeeper mutant *PfPKG*^{T618Q}. Cells were pre-incubated with C2 (1 μM) then treated with 100 μM zaprinast followed by lipid extraction using chloroform-methanol and relative levels measured by nano-electrospray mass spectrometry. Data are 1 replicate. Graph was generated in Graphpad, Prism. This figure is a modified version of data presented in Brochet *et al* 2014[174].

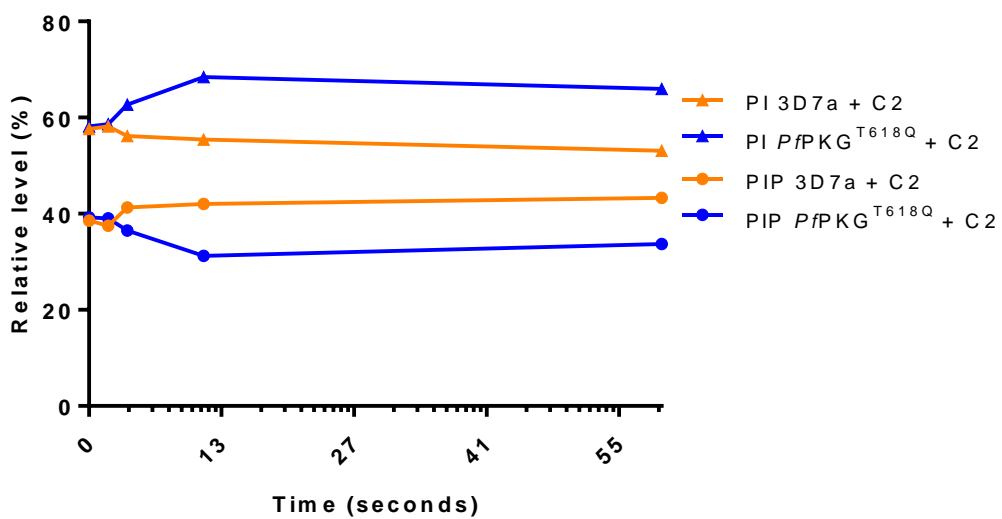


Figure 3.9. Changes in levels of PI and PIP over time in mature *P. falciparum* schizonts, in response to zaprinast treatment in the presence of C2 in the wildtype 3D7a line compared to the gatekeeper mutant *PfPKG*^{T618Q}. Cells were pre-incubated with C2 (1 μM) then treated with 100 μM zaprinast followed by lipid extraction using chloroform-methanol and relative levels measured by Nano electrospray mass spectrometry. Data are 1 replicate. The graph was generated in GraphPad, Prism. This figure is a modified version of data presented in Brochet *et al* 2014[174].

3.2.2. Zaprinast-induced Ca²⁺ release in stage V gametocytes

Both XA and zaprinast induce Ca²⁺ release in stage V gametocytes

In stage V gametocytes of the 3D7a wildtype line, zaprinast induced Ca²⁺ release to ~ 38 % of the ionophore control (Figure 3.10). This was reversed to ~ 5 % of the ionophore control by addition of C2. C2 did not reverse the zaprinast-induced Ca²⁺ release fully, but levels were reduced by ~ 85 % of zaprinast-treated samples and this was significant (P= 0.0155, Welch's unpaired t test) indicating that the majority of zaprinast-induced Ca²⁺ mobilisation is likely to be *Pf*PKG dependent. XA also induced Ca²⁺ levels to ~ 44 % of the ionophore control, levels comparable to that induced by zaprinast. This Ca²⁺ release was also reduced by addition of C2 but not fully (Figure 3.10), with levels of Ca²⁺ reduced by ~ 71 % compared to XA alone (normalised to 100 %). This reduction in XA-induced Ca²⁺ release was also significant (P=0.0363, Welch's paired t test).

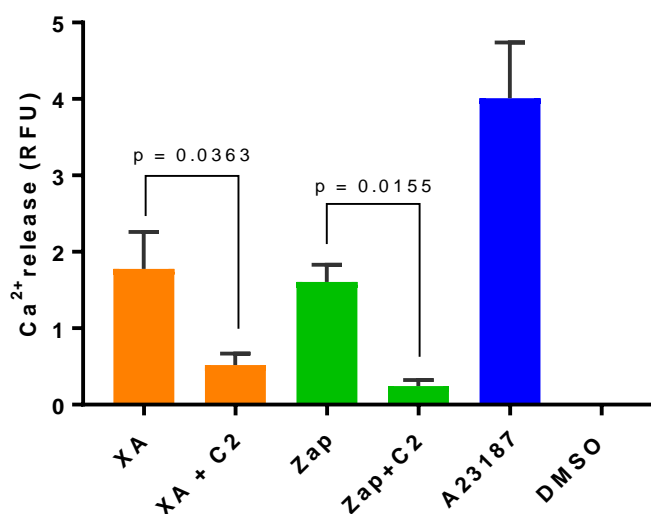


Figure 3.10. Ca²⁺ release in Fluo-4-AM-loaded 3D7a stage V gametocytes.

Parasites stimulated with XA (10 μ M) and zaprinast (100 μ M) in the presence and absence of 2 μ M C2. Data are presented as Ca²⁺ release measured as relative fluorescent units (RFU) minus the baseline fluorescence and fluorescence of the DMSO (0.05 %) control sample analysed in Excel. The ionophore (A23184) was used as a positive control. The bar chart was generated in GraphPad, Prism and shows the mean of 3 experiments each carried out in triplicate. Error bars represent SD.

Zaprinast induces Ca²⁺ release in stage V gametocytes in a *Pf*PKG-dependent manner

In order to investigate whether the reduction in Ca²⁺ release seen in both the zaprinast and XA-treated gametocyte samples was due to an on-target effect of *Pf*PKG inhibition by C2 (i.e. that Ca²⁺ release is PKG dependent), the *Pf*PKG_{T618Q} gatekeeper mutant line was used.

In the *Pf*PKG_{T618Q} cell line, zaprinast-induced Ca²⁺ release was not reversed by addition of either C2 or a more specific inhibitor MRT00207065 (EC₅₀ *Pf*PKG_{T618Q}/WT ratio in 72 h hypoxanthine incorporation assays = > 1,100. For C2 the ratio is 15 (Baker *et al*, NComms, in press)) indicating that in mature gametocytes zaprinast-induced Ca²⁺ mobilisation is likely to be a PKG-dependent event (Figure 3.11). A comparison of XA and zaprinast induced Ca²⁺ release in the wildtype and *Pf*PKG_{T618Q} gatekeeper mutant lines is presented in Figure 3.12. The difference between the Ca²⁺ release measured in zaprinast only samples compared to zaprinast samples also treated with C2 or MRT00207065 was shown to be not significant using a Welch's unpaired t-test with values of P=0.1470 and P=0.2103 respectively. This indicates that in contrast to the wildtype line, PKG inhibition in gametocyte samples treated with zaprinast did not significantly alter the level of zaprinast-induced Ca²⁺ release, therefore indicating that zaprinast-induced Ca²⁺ mobilisation in stage V gametocytes is likely to be a *Pf*PKG-dependent event.

XA-induced Ca²⁺ release appears to be by both a *Pf*PKG-dependent and a non *Pf*PKG-dependent manner

In the *Pf*PKG_{T618Q} gatekeeper mutant line, roughly half of the XA-induced Ca²⁺ release appeared to be reversed by addition of C2 with a ~ 54 % decrease in Ca²⁺ levels in C2-treated samples compared to the XA only sample (Figure 3.11). This was compared to a ~70 % decrease in Ca²⁺ levels in XA treated samples on addition of C2 to the wildtype line (Figures 3.10 and 3.12). This difference between the percentage decrease of Ca²⁺ levels in the wildtype line on addition of C2 vs the percentage decrease in the *Pf*PKG_{T618Q} cell line was not significant (P=0.3199, Welch's unpaired t test). This indicates that addition of C2 to the *Pf*PKG_{T618Q} gatekeeper mutant line does not significantly decrease the levels of Ca²⁺ induced by XA compared to the wildtype control, indicating that in the C2 resistant line, C2 can still reduce the Ca²⁺ levels and this may be explained by C2 targeting a different kinase that is not *Pf*PKG. (A comparison of XA and zaprinast induced Ca²⁺ release in the wildtype and *Pf*PKG_{T618Q} gatekeeper mutant lines is presented in Figure 3.12). However, unlike the wildtype line in which the decrease in Ca²⁺ levels on addition

of C2 was shown to be significant, in the *Pf*PKG_{T618Q} cell line, the difference in Ca²⁺ levels between XA treatment alone compared to XA-treatment in the presence of C2 was shown to be not significant (P= 0.1706, Welch's unpaired t test). Although these data are preliminary and require repeating, they indicate that the reduction in Ca²⁺ release in samples stimulated with XA in the presence of C2 in the *Pf*PKG_{T618Q} cell line is not significantly different to levels of Ca²⁺ in samples treated with XA alone. This preliminary data indicates that XA-induced Ca²⁺ release may be a *Pf*PKG-dependent event as there is a significant decrease in Ca²⁺ levels with addition of C2 in the wildtype line but this difference is not significant in the gatekeeper line.

Addition of MRT00207065 to XA- treated gametocytes of the *Pf*PKG_{T618Q} cell line appeared to reverse Ca²⁺ mobilisation less than C2. However, the difference between C2 and MRT00207065 treatment in XA-stimulated samples of this line was shown to be not significant (Welch's unpaired t test, P=0.7536). The difference in Ca²⁺ levels in XA treated samples compared to samples treated with both XA and MRT00207065 was shown to be not significant (Welch's unpaired t test, P= 0.2861). This indicates that the more specific PKG inhibitor MRT00207065 does not significantly reduce levels of XA-induced Ca²⁺ in stage V gametocytes.

Overall, these data points towards a possibility that XA induces Ca²⁺ mobilisation in mature gametocytes is through more than one pathway: through both a *Pf*PKG-dependent pathway and also through a pathway that is not *Pf*PKG-dependent. Data on Zaprinast-induced Ca²⁺ release in gametocytes on the other hand, appears clearer, with Ca²⁺ mobilisation likely to be induced through a *Pf*PKG-dependent pathway only.

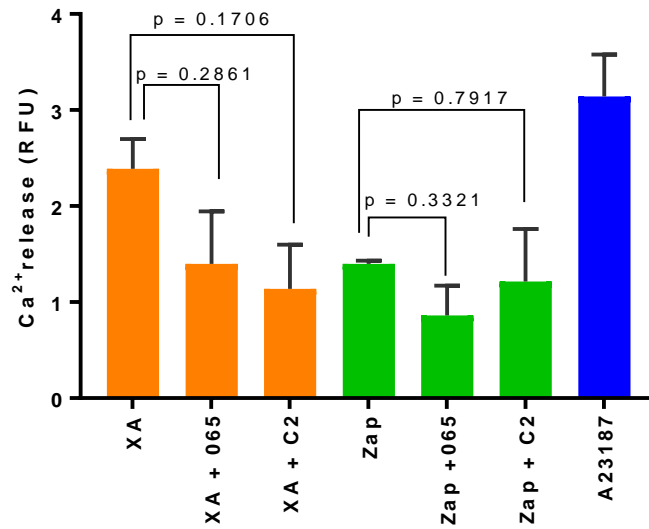


Figure 3.11. Ca²⁺ release in Fluo-4-AM-loaded *PfkPKG*_{T618Q} line stage V gametocytes. Parasites stimulated with XA (30 μ M) and zaprinast (100 μ M) in the presence and absence of 2 μ M C2 or 1 μ M MRT00207065 (065). Data are presented as Ca²⁺ release measured as relative fluorescent units (RFU) minus the baseline fluorescence and fluorescence of the DMSO (0.05 %) control sample analysed in Excel. The ionophore (A23184) was used as a positive control. The bar chart was generated in GraphPad, Prism and shows the mean of two technical replicates from 1 experiment. Error bars represent SEM.

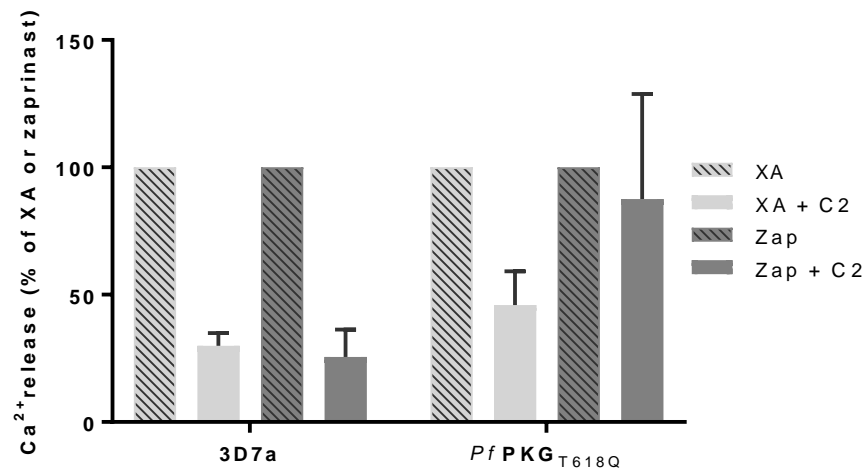


Figure 3.12. C2 reduction of zaprinast or XA-induced Ca²⁺ release in *PfkPKG*_{T618Q} gametocytes compared to gametocytes of the wildtype line. Data from figures 3.10 and 3.11 presented as percentage of either XA (light grey bars) or zaprinast (dark grey bars) with both XA and zaprinast normalised to 100 %. Data are the average of three repeats from three experiments for 3D7a and two repeats from 1 experiment for *PfkPKG*_{T618Q}. Error bars represent the SEM of the mean.

XA induces an immediate and rapid release of Ca²⁺ in 3D7a stage V gametocytes

In an attempt to visualise Ca²⁺ release in real time, 3D7a stage V gametocytes were loaded with Fluo-4-AM and observed by confocal microscopy. XA was added and the resulting fluorescence viewed in real time.

Prior to XA addition, Fluo-4-AM loaded gametocytes did not fluoresce (Figure 3.13 panel A). On addition of XA, a sudden and rapid increase in fluorescence was observed within milliseconds (ms) (Figure 3.13 panel B and Figure 3.14 and 3.15). This appeared to gradually decrease over a short period of time (~75 ms) with no fluorescence being observed after ~170 ms (Figure 3.14 and 3.15). At the ~95 ms time point, there appeared to be another wave of fluorescence which increased in intensity then gradually decreased. This fluorescence lasted for ~75 ms (see Figure 3.15 for schematic of these two peaks).

Interestingly, the majority of fluorescence appeared to be concentrated in circular foci at the two tips of the gametocyte (Figure 3.13).

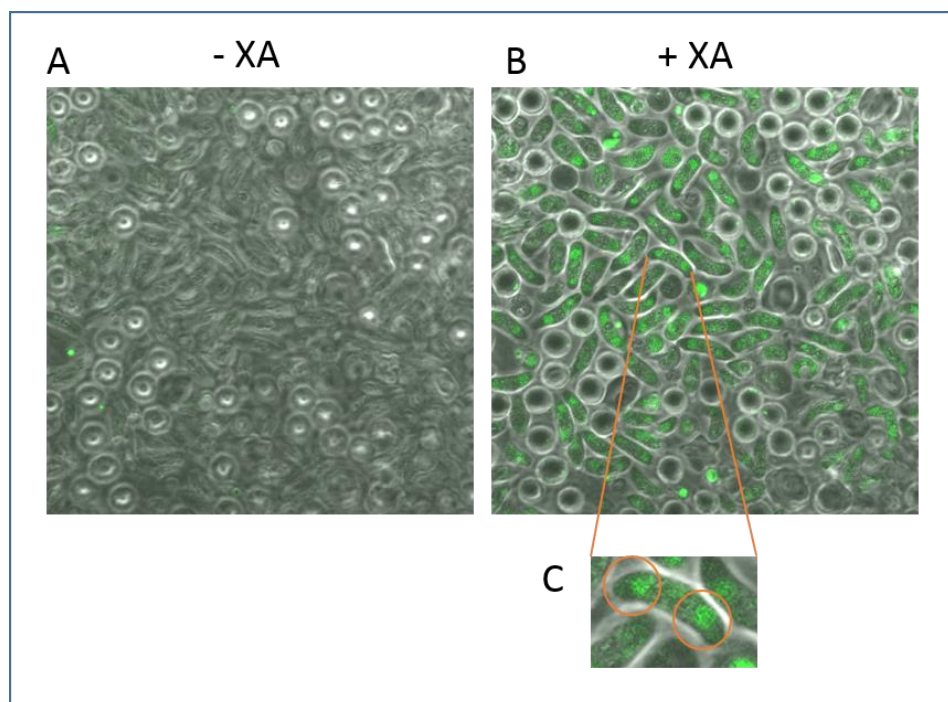


Figure 3.13. Live confocal microscopy of Fluo-4-AM loaded 3D7a stage V gametocytes before (A) and directly after (B) XA addition. Focal points of fluorescence (circled in orange) were identified towards both ends of gametocytes (C). Green fluorescence.

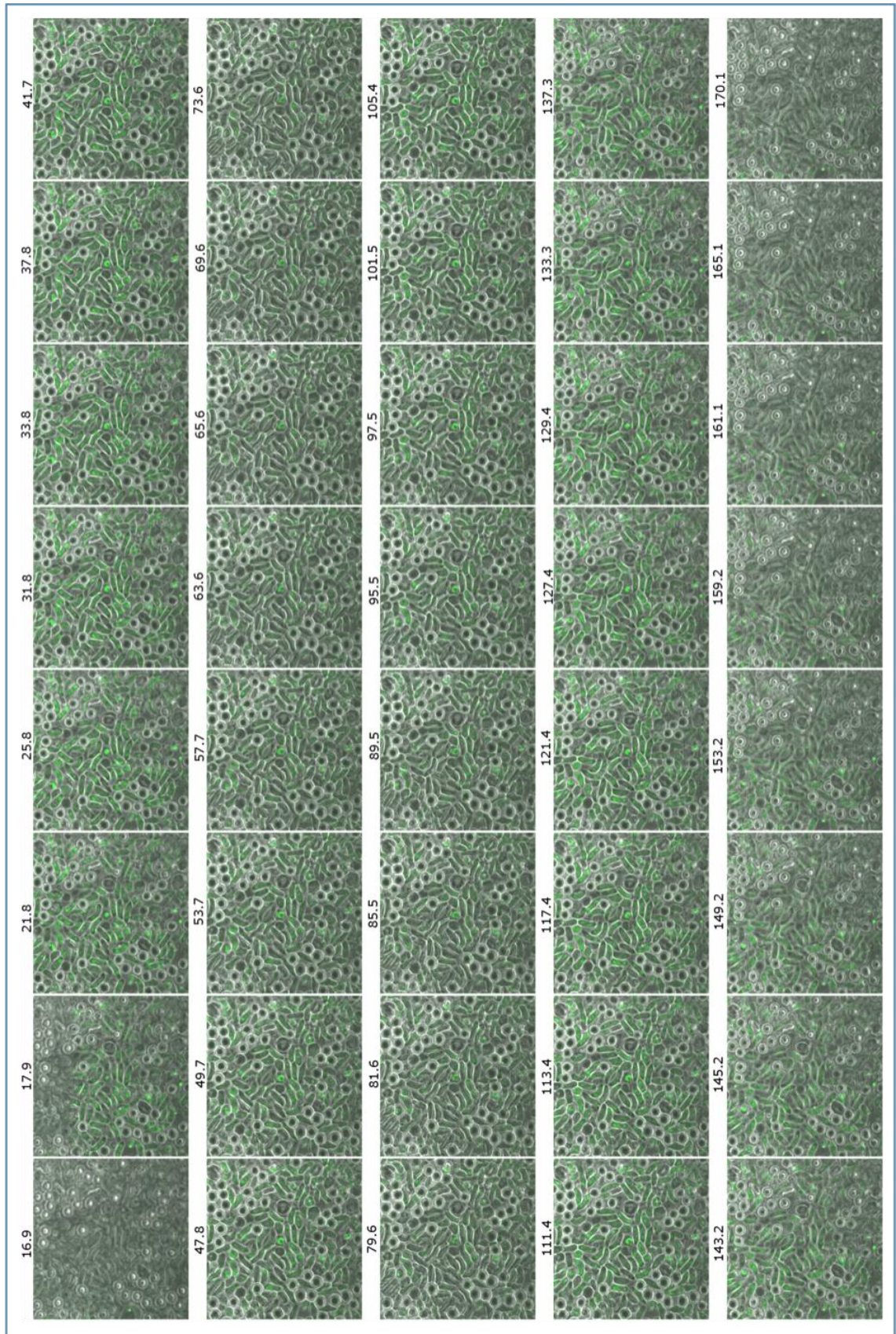


Figure 3.14. Images from live confocal microscopy of fluo-4-AM loaded 3D7a stage V gametocytes. Images generated in Zeiss image browser taken 1ms apart.

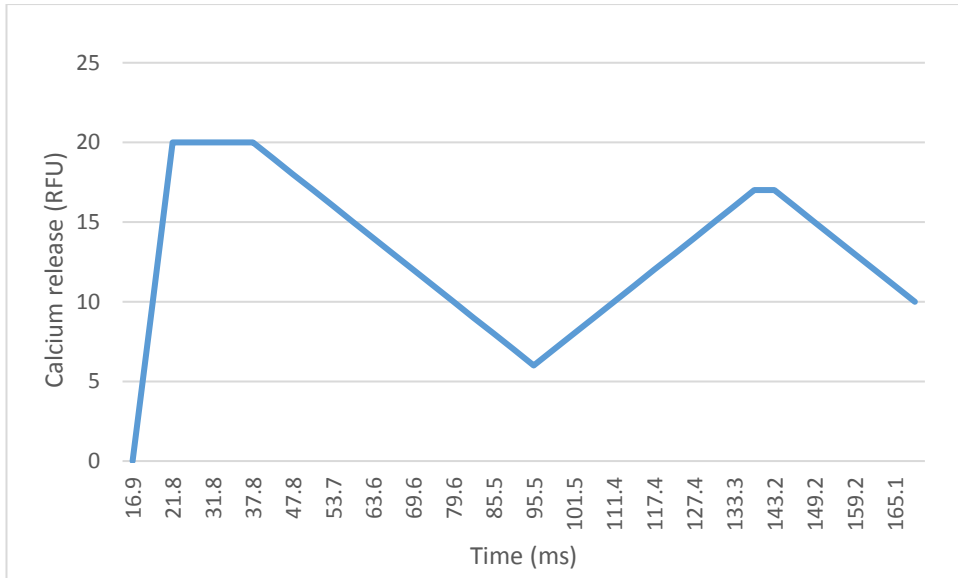


Figure 3.15. Schematic showing predicted pattern of fluorescence seen in the live cell microscopy images represented in Figure 1.12. XA induces a rapid increase in fluorescence in mature gametocytes followed by a gradual decrease in intensity. This is followed by what appears to be another wave of fluorescence, which is less rapid but reaches similar levels to the first peak. Levels of fluorescence then gradually decrease.

3.3. Discussion

The data obtained from these experiments have indicated that the PDE inhibitor zaprinast can induce Ca^{2+} mobilisation in both mature schizont stages and mature gametocyte stages of *P. falciparum*. The zaprinast Ca^{2+} response in both asexual and sexual stages appears to be a *Pf*PKG-dependent event. This supports data in the literature demonstrating that zaprinast is known to elevate cGMP levels in *P. falciparum*[159][173]. This was determined using the PKG inhibitor C2 (and a more potent and selective PKG inhibitor MRT00207065) on the wild type line and in combination with gatekeeper mutant *Pf*PKG_{T618Q} line, which is resistant to C2. An additional tool, a PKG conditional knockdown line, further confirmed the PKG specificity of the Ca^{2+} response in the blood stage schizonts. The data indicate that zaprinast induces Ca^{2+} mobilisation through the cGMP signalling pathway, by inhibition of cGMP hydrolytic PDE activity, which in turn leads to elevated levels of cGMP and subsequent activation of *Pf*PKG (for schematic see Figures 3.16 and 3.17). Zaprinast (a synthetic compound) is not the natural trigger of these events so it is not necessarily representative of what is happening *in vivo*. Indeed in gametocytes, the signalling events induced by XA do not appear as clear as those induced by zaprinast. There is evidence that XA may elevate cGMP levels in gametocyte stages[126] leading to the hypothesis that zaprinast essentially bypasses the initial XA interaction.

XA induced Ca^{2+} mobilisation in *P. falciparum* wildtype line stage V gametocytes. This is unsurprising as Ca^{2+} has been shown to be required for the late stages of male gametogenesis in *P. falciparum*[159]. The data presented here both in calcium assays and live cell imaging are consistent with the findings from studies in the literature which have shown that addition of XA to *P. berghei* gametocytes induces a rapid mobilisation of Ca^{2+} [210]. The data presented here also indicate that in *P. falciparum*, XA induces a Ca^{2+} response within 20 seconds of addition. In the wild type line, the Ca^{2+} response was reduced by addition of C2 but not fully reversed. The reason for this incomplete reversal of Ca^{2+} levels in the wild type line may be explained by the fact that both C2 and XA were added at the same time in this assay, so XA may be reaching its target to induce Ca^{2+} mobilisation before C2 can reach PKG to inhibit it fully. A small amount of residual Ca^{2+} was also measured in the zaprinast-treated wildtype line and this may be explained in the same way. This assay needs to be repeated with parasites pre-incubated with C2 to determine whether the residual Ca^{2+} levels seen in the C2-treated samples are due to experimental design.

In gametocytes of the gatekeeper mutant line, C2 inhibition of XA-induced Ca^{2+} mobilisation was not significant. This taken with wildtype data, indicating that C2 inhibition of XA-induced Ca^{2+}

release is significant, suggests that in stage V gametocytes, XA-induces the release of Ca^{2+} in a *Pf*PKG-dependent manner. However, although, data on the wildtype line are reproducible, initial data on the gatekeeper mutant line need to be interpreted with caution. This assay needs to be repeated as the data were from a single experiment carried out only in duplicate. Repeat experiments will be needed to confirm the PKG specificity of the XA response in gametocytes. The PKG_{T618Q} gatekeeper mutant is a poor gametocyte producer and it is consistently a challenge to produce a high enough yield of purified gametocytes from this line to carry out Ca^{2+} release assays. It would therefore be useful to use gametocytes from the *Pf*PKG-DD line plus and minus Shield-1 as an additional tool to look at the PKG specificity of the zaprinast and XA-induced Ca^{2+} responses in gametocytes. An alternative would be to make a new gatekeeper mutant using the NF54 line, which is a much more efficient gametocyte producer. It would also be beneficial to use the more PKG-specific inhibitor MRT00207065 in Ca^{2+} release assays on the wild type line as this would confirm that the decrease in Ca^{2+} levels seen with C2 inhibition of *Pf*PKG are in fact on target. If MRT00207065 treatment reduced the XA-induced Ca^{2+} release in the wildtype line by less than C2, this would indicate that part of the Ca^{2+} response is due to a C2-sensitive protein kinase that is not PKG. However, this result needs to be taken with caution as this inhibitor was used at 1 μM which may be too high a concentration to prevent an off target effect.

The initial stage of gametogenesis, rounding up, is PKG dependent but in *P. falciparum* this event is not dependent upon Ca^{2+} since addition of BAPTA-AM to mature *P. falciparum* gametocytes does not prevent rounding up[159], whereas the later stages of male gametogenesis require Ca^{2+} and are blocked by BAPTA-AM. However, there is evidence to suggest that at least some of the later events of male gametogenesis (post rounding up) are PKG independent but still C2 sensitive as exflagellation can be inhibited by C2 in both the wildtype and gatekeeper mutant lines[159], suggesting that another C2-sensitive protein kinase may regulate events required for exflagellation[159]. It was suggested that a likely candidate could be CDPK4[159] and in fact, not only does it have a small gatekeeper residue (conferring sensitivity to imidazopyridine (C2 + 065) and pyrrole (C1) PKG inhibitors)[267], this calcium-dependent protein kinase has been shown to be essential for the male specific events of genome replication, mitotic spindle assembly and flagella motility[215]-[210] leading to exflagellation. Therefore, it's essential that the PKG specificity of XA-induced Ca^{2+} release is determined and the additional and more in depth experiments listed above will be crucial for identifying whether this Ca^{2+} response is completely PKG dependent, or whether a proportion of the Ca^{2+} released in response to XA is PKG independent but C2 sensitive. If the latter is the case, this may indicate that another protein kinase such as CDPK4 could contribute to the Ca^{2+} response. Given the recent findings on CDPK4

in *P. berghei* by Fang *et al*[215], an interesting hypothesis would be that an initial PKG-dependent increase in Ca^{2+} levels is required to activate the myristoylated form of CDPK4 which is required to regulate DNA replication and mitotic spindle assemble, events that occur within the first 30 seconds of activation. This then leads to another wave of Ca^{2+} mobilisation, which is induced either directly or indirectly through phosphorylation of substrates by the myristoylated form of CDPK4, which then leads to activation of the non-myristoylated isoform of CDPK4 required for flagella motility about 9 minutes post activation. It may be possible to investigate this hypothesis using a knockout line of CDPK4, which uses the *Pf*PKG_{T618Q} gatekeeper mutant line as a background. This transgenic line could then be used in Ca^{2+} release assays in combination with PKG inhibition to determine whether levels of Ca^{2+} can be completely reversed by C2 when CDPK4 is absent. If part of the Ca^{2+} response in gametocytes is due to a PKG-dependent pathway and the other part due to CDPK4 induced Ca^{2+} release, it would be expected that in the *Pf*PKG_{T618Q} gatekeeper mutant line, as seen in data presented here, Ca^{2+} levels would be reduced by C2 targeting CDPK4 but the PKG-dependent proportion of Ca^{2+} would not be altered compared to the 3D7a wildtype line in which both PKG and CDPK4-induced Ca^{2+} levels would be reduced significantly by C2. However, in the absence of CDPK4 in a *Pf*PKG_{T618Q} gatekeeper mutant line (i.e. if CDPK4 is absent from the line and the line is also resistant to C2 targeting of PKG), it would be expected that the CDPK4 portion of Ca^{2+} release would be absent, therefore there should be no reduction in levels of Ca^{2+} on addition of C2 because the two targets of C2, PKG, and CDPK4 would have been removed.

The preliminary observations from live cell microscopy on *P. falciparum* stage V gametocytes were consistent with studies on *P. berghei* which showed that XA induced a rapid release of Ca^{2+} which appeared after a lag period of 10 seconds then peaked at the 10-12 second time point[210]. Addition of XA to live Fluo-4 loaded *P. falciparum* gametocytes resulted in a rapid release of Ca^{2+} ; however, it appeared to result in fluorescence almost immediately. This is slightly at odds to the 10 second lag phase seen in *P. berghei* strains expressing a GFP-Aequorin fusion protein[210]. This may represent differences in the species of *Plasmodium*, differences in experimental design or dynamics of the reporter system and acquisition and analysis of data. The data presented here are preliminary and were only achieved once. Attempts made to reproduce these data were unsuccessful because on subsequent attempts, fluorescence was already present in unstimulated gametocytes. As such, definitive conclusions were unable to be drawn from these data. There are a number of possible factors that may have contributed to this including Fluo-4 loading and cellular distribution (the fluo-4 may have entered cellular Ca^{2+} stores prior to activation), sample preservation leading to the unstimulated release of Ca^{2+} ,

namely challenges with maintaining unstimulated gametocytes at 37°C prior to activation and maintaining a temperature range sufficient for gametocyte activation to occur when stimulated (gametocyte samples may have cooled). This was due to the long distance required to transport the samples in order to image them using the confocal microscope and the very low temperature of the microscope room required for maintenance of equipment stored there. Although care was taken, unfavourable conditions for gametocytes during sample preparation may also be a contributing factor.

Interestingly, the majority of fluorescence observed in XA-stimulated gametocytes appeared to be found in circular foci towards both ends of each gametocyte. This pattern of fluorescence was consistent in all gametocytes observed in the sample. This pattern may be a reflection of the cytosolic space available (the nuclear material and haemozoin are often concentrated in the centre of the gametocyte). Or may possibly indicate a more specific localisation of the site of Ca²⁺ response. Fluo-3, a labelled calcium indicator with similar properties to Fluo-4 (Fluo-4 is an analogue of Fluo-3, with two chlorines replaced by two fluorine's resulting in higher fluorescent signals), is thought to concentrate mostly in the cytosol and this is likely to be the case for Fluo-4 also[268]. However, Fluo-3 can also compartmentalise into internal organelles in some cases. The fact that this pattern of fluorescence was seen only after addition of XA indicates that the foci observed are unlikely to be representing compartmentalisation of Fluo-4 into a Ca²⁺ store, but that it is likely to be a result of Ca²⁺ mobilisation from the store to elsewhere in the cell where the Fluo-4 is located on XA addition. Fluo-4-AM is able to cross membranes prior to esterification (this process removes the ester group preventing the Fluo-4 from crossing membranes and essentially traps the Fluo-4 within the cell's cytoplasm where it can then bind to Ca²⁺ released from internal stores), however on losing the AM ester, it should get trapped within the cell and is unlikely to be able to cross further membranes and, for example, enter organelles such as the ER. It would be hypothesised that XA would induce release of Ca²⁺ from the ER into the cytosol where the majority of the Fluo-4 would be predicted to be concentrated. This hypothesis is based on evidence that the IP₃ signalling pathway may be induced by XA stimulation in *P. berghei* gametocytes[200] and that there is evidence that the ER is involved in Ca²⁺ mobilisation[198]. It was very interesting to observe a possible second wave of fluorescence. This may have been due to an artefact such as movement of liquid across the sample disrupting the focus. If this second wave of fluorescence is due to a second wave of Ca²⁺ mobilisation, this would be highly interesting and may support the hypothesis presented earlier which suggests that there may be a first wave of PKG-dependent Ca²⁺ mobilisation, followed by a second PKG-independent but C2-sensitive Ca²⁺ release, possible requiring CDPK4. It would be

very interesting to optimise the conditions for this live cell microscopy experiment to look at XA-induced Ca^{2+} mobilisation in real time more closely. If conditions can be optimised, this possible second wave of fluorescence can be investigated more thoroughly and the use of both C2 which can inhibit both PKG and CDPK4 and MRT00207065 which will only target PKG (at low concentrations) in combination with the gatekeeper mutant line and a CDPK4-ko line, and possibly a CDPK4 gatekeeper mutant line, will all be useful tools in identifying if there is in fact another wave of Ca^{2+} release and whether there is a differing PKG-dependency for XA-induced Ca^{2+} mobilisation. This will also complement experiments suggested above which would aim to investigate the hypothesis that CDPK4 may be involved in the XA-induced Ca^{2+} response.

Data presented here and published[174] show that in *P. falciparum* schizonts, *Pf*PKG plays a role in regulating levels of phosphoinositol lipids. Zaprinst induced depletion of PIP_2 and its precursor PIP only when *Pf*PKG was inhibited indicating that phosphoinositide (lipid) levels can be regulated by activation of *Pf*PKG through PDE-induced changes in levels of cGMP. This has also been shown to be the case in motile ookinetes of the murine species *P. berghei*[174]. In both *P. berghei* and *P. falciparum* phospholipid analysis studies, in conjunction with gatekeeper mutant lines, were used to show that this phosphoinositide metabolism was PKG dependent. It would be useful to measure IP_3 levels in zaprinast-treated schizonts from both the 3D7a and *Pf*PKG_{T618Q} lines in the presence and absence of a PKG inhibitor and also in the presence and absence of a PLC inhibitor such as U73122. This would confirm what the data presented in this thesis indicates, that the changes in phospholipids induced by zaprinast lead to the hydrolysis of PIP_2 to produce the secondary messenger IP_3 and that this occurs via PLC in a *Pf*PKG-dependent manner. This would provide a nice link to Ca^{2+} mobilisation. To complement this, it would also be of interest to repeat Ca^{2+} release assays using a PLC inhibitor.

At a permissive temperature, XA has been shown to induce the hydrolysis of phosphoinositide (lipids) to produce IP_3 in *P. berghei* gametocytes and inhibition of PLC using the inhibitor U73122 reduced the initial XA-induced Ca^{2+} signal[200]. An analysis of the gametocyte lipidome by Electrospray-mass spectrometry to look at changes in levels of phospholipids in relation to *Pf*PKG inhibition using MRT00207065 would be interesting. This would give us insight into whether phospholipid synthesis and IP_3 production is involved in the generation of Ca^{2+} in mature *P. falciparum* gametocytes in response to zaprinast and XA stimulation. This would also complement work done in *P. berghei* gametocytes which showed that XA can trigger the hydrolysis of PIP_2 which is accompanied by the production of IP_3 and which results in a rapid release of Ca^{2+} [200]. The production of IP_3 and subsequent Ca^{2+} mobilisation can be inhibited by

a the PLC inhibitor U73122 in *P. berghei* gametocytes[200]. It would be interesting to measure levels of IP₃ in XA and zaprinast-induced *P. falciparum* gametocytes in the presence and absence of both C2 and MRT00207065 and also in the presence and absence of inhibitors of the IP₃ pathway including PI-PLC.

XA stimulation of gametogenesis is an important event in the parasite lifecycle, enabling the parasite to undergo a transformation leading to fertilisation and subsequent establishment of infection within the mosquito. A drug that could disrupt this process would block transmission and would be a valuable tool in tackling this devastating disease. Similarly, asexual blood stage merozoites egress is essential for parasite proliferation as a block in egress prevents the liberation of free merozoites, which are required to invade new erythrocytes and continue the lifecycle in the human host. Unlike disruption of the transmission stages which will not alleviate clinical symptoms but will prevent the host from being infectious to feeding mosquitoes, disruption of the asexual blood stage life cycle can treat the symptoms of malaria and save lives. Understanding the signalling pathways leading to events such as Ca²⁺ mobilisation during crucial stages of the life cycle such as schizogony and gametogenesis will help us to identify drug targets and novel ways to disrupt these parts of the parasite life cycle. Although there have been several really important findings in terms of understanding the signalling systems involved in driving these processes, including the identification of XA, thought to be the natural trigger for gametogenesis, understanding of cell signalling in plasmodium is still in its infancy and much more needs to be learnt. Understanding how XA actually induces gametogenesis, whether it binds to a receptor or perhaps interacts directly with a component of the signalling cascade such as a PDE and the elucidation of the order of downstream signalling events will greatly benefit our understanding of gametogenesis and this in turn will facilitate drug discovery progress.

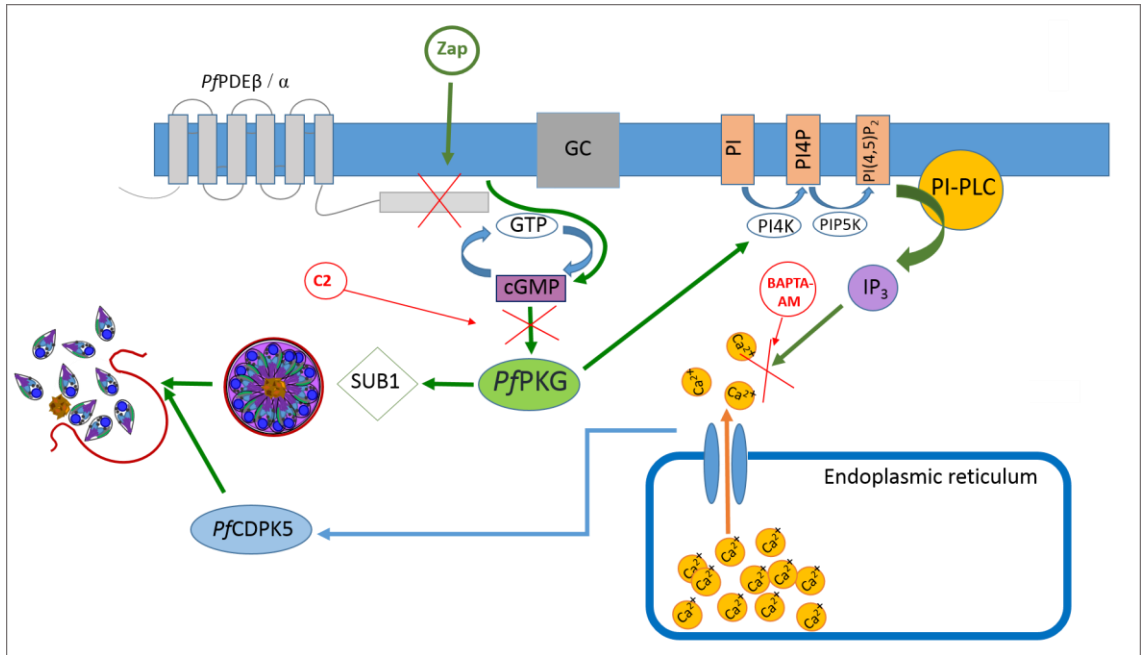


Figure 3.16. Schematic showing a model of signalling pathways induced by zaprinast involved in asexual blood stage merozoite egress. Zaprinast induces premature egress of merozoites (which are often non-invasive). Zaprinast inhibits cGMP-PDE activity (red cross), which leads to increased levels of cGMP and subsequent activation of PKG (signalling cascades downstream of PKG can be blocked by addition of the PKG inhibitor C2: red cross). PKG is required for the discharge of the serine protease SUB1 from exonemes which is required for the proteolytic processing of proteins such as SERA proteases and components of the MSP complex needed for egress and invasion. Activation of PKG also induces Ca^{2+} mobilisation via the phosphoinositide synthesis pathway leading to subsequent IP_3 production via PI-PLC by targeting the kinases that mediated the hydrolysis of phospholipids. Released Ca^{2+} activates CDPK5, which is independent of PKG-induced proteolytic processing but also required for egress. This can be blocked by addition of the Ca^{2+} chelator BAPTA-AM (red cross). The PKG inhibitor C2 inhibits both Ca^{2+} mobilisation and release of SUB1.

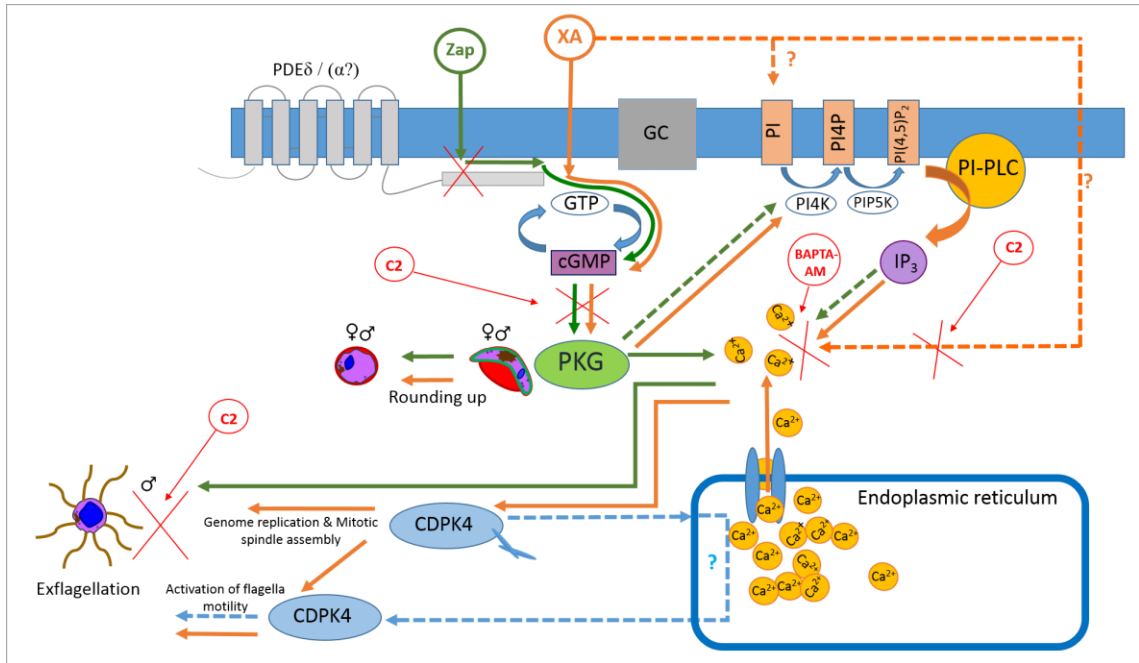


Figure 3.17. Schematic showing a model of signalling pathways activated by XA (orange arrows) and zaprinast (green arrows) that induce gametogenesis. Zaprinast induces rounding up of gametocytes by PDE inhibition (PDE δ and/or possibly PDE α) followed by an increase in cGMP, which activates PKG. This leads to rounding up of both male and female gametocytes in a non-Ca²⁺-dependent manner. Zaprinast induces Ca²⁺ mobilisation in gametocytes, which is required for exflagellation. This Ca²⁺ release is inhibited by C2 in the wildtype line but not by C2 or 065 in the gatekeeper mutant line *PfPKG*_{T618Q}. Indicating that zaprinast likely induces Ca²⁺ mobilisation in a *PfPKG*-dependent manner. As seen in schizonts, zaprinast may induce Ca²⁺ mobilisation via phosphoinositide metabolism leading to IP₃ production and subsequent Ca²⁺ release but this is currently not known. XA treatment increases levels of cGMP by a mechanism currently unknown (but may involve PDE inhibition or GC activation). This leads to PKG activation and PKG-dependent but non-Ca²⁺-dependent induction of rounding up. XA induces Ca²⁺ mobilisation via PKG and the phosphoinositide hydrolysis cascade leading to the production of IP₃ via PI-PLC likely resulting in Ca²⁺ release from the ER. XA-induced Ca²⁺ mobilisation leads to the activation of two isoforms of CDPK4 (myristoylated and non-myristoylated) which results in male exflagellation. A myristoylated isoform regulates genome replication and mitotic spindle assembly in the first 30 seconds of activation. A non-myristoylated isoform regulates flagella motility 9 minutes post XA-activation. Blue dotted arrows represent the hypothetical induction of Ca²⁺ mobilisation by the already PKG-dependent Ca²⁺-activated myristoylated isoform of CDPK4, which then leads to the Ca²⁺-dependent activation of the non-myristoylated isoform.

Chapter 4

Investigation into the role of phosphodiesterases in distinct stages of gametocyte development using genetic and pharmacological approaches

4.1. Introduction

Gametocyte-infected erythrocyte deformability and gametogenesis are essential parts of the parasite lifecycle and a requirement for transmission from the human host to the mosquito vector. Although there has been some progress in understanding the signalling pathways involved in these cellular events, they are still not currently well understood. Increased knowledge and understanding of what signalling pathways are required for gametocytes to develop, survive in the host and to transmit to the mosquito vector where fertilisation takes place, and the role that signalling molecules play in these processes, will help to identify possible drug targets in gametocyte stages. Cyclic nucleotide signalling plays an important role in several key stages of the parasite life cycle. Regulation of cyclic nucleotide levels by ACs, guanylyl cyclases (GCs) and PDEs is essential to maintaining normal cellular functions. As such, these enzymes are attractive targets to explore further. Drugs developed against mammalian PDEs, in particular have been used successfully for a number of medical conditions. Although *Plasmodium* PDEs show some similarity to their human homologues, it is thought that they are divergent enough in the catalytic domain to be selectively targeted and although many PDE inhibitors that target mammalian PDEs also target apicomplexan PDEs (such as sildenafil citrate, tadalafil and zaprinast), these compounds could potentially be used as a starting point to design drugs that specifically target apicomplexan PDEs and not mammalian ones. This will enable treatment of malaria infection (or prevention of malaria transmission) without adverse side effects. There has recently been a surge of interest in the targeting of *Plasmodium* PDEs because disruption of cyclic nucleotide signalling pathways through inhibition of *Pf*PDEs would be an important tool that can be used not only to treat clinical symptoms of malaria, but also to prevent transmission within a population and along with other interventions, will greatly aid the move towards malaria elimination.

This chapter therefore seeks to understand more about the effects of *Pf*PDE inhibition with the aim to determine the value of *Plasmodium* PDEs as drug targets in mature gametocyte stages. This will be achieved by using a combination of genetic and pharmacological approaches to investigate the impact of *Pf*PDE inhibition on gametocyte infected erythrocyte deformability,

gamete egress from the host erythrocyte and the mobilisation of Ca^{2+} from internal stores, events that are all required for transmission from the human host to the mosquito vector.

Mature *P. falciparum* gametocytes that have been released from sequestration in the bone marrow are able to avoid splenic clearance while circulating in the host blood stream. This is thought to be due to their ability to change from a stiff phenotype to a deformable one once they reach maturity at stage V. The mechanisms and cell signalling pathways mediating this switch are not fully understood; however, in collaboration with Catherine Lavazec (Institute Pasteur), deformability assays were carried out on a *PfPDE δ* -ko and a *PfPDE γ* -ko line. These data are presented below and formed part of a publication[25], the broader findings of which will be discussed in more detail in the discussion section.

The known signal that initiates gametogenesis, XA[26][258] has been shown to act through a *PfPKG*-dependent pathway[159], and this is thought to be mediated through the cGMP signalling pathway[126] to result in a rapid rise in cytosolic Ca^{2+} [210], which is required for the later stages of gametogenesis but not for the earlier stage of rounding up[159]. The effector protein, calcium-dependent protein kinase 4 (CDPK4) is essential for the later male specific stages of gametogenesis and this kinase is dependent upon the upstream mobilisation of Ca^{2+} [215][210]. There is currently no identified receptor for XA and the mechanism by which XA induces gametogenesis is unknown. Studies on mammalian cells have shown that XA can cross membranes and enter the ER of lens epithelial cells and directly interact with ER proteins[269]. There is therefore a possibility that in *P. falciparum*, XA could cross the erythrocyte and parasite vacuole membranes freely to enable it to associate with signalling molecules or receptors either on the parasite surface or within the parasite itself.

The cGMP *PfPDE* inhibitor zaprinast[159] and the PDE inhibitor sildenafil citrate (Cathy Taylor, PhD Thesis, 2007) can also induce gametogenesis independently of XA indicating that the pharmacological inhibition of cGMP-*PfPDE*s can lead to the induction of gametogenesis. The zaprinast-induced induction of gametogenesis, like XA, has also been shown to be *PfPKG* dependent[159] and to act upstream of Ca^{2+} [159]. In *P. falciparum*, the earlier stages of rounding up have therefore been shown to be *PfPKG* dependent (as XA or zaprinast-stimulated gametocytes will not round up in the presence of C1), but Ca^{2+} independent (gametes will still round up the presence of the Ca^{2+} chelator BAPTA-AM but emergence is greatly reduced and male gametes will not exflagellate[159]). This is interesting and could possibly indicate that XA may induce a similar or the same signalling pathways that zaprinast does. Work by Cathy Taylor

et al[130] indicated an essential role for *PfPDEδ* in gametogenesis, as a *PfPDEδ*-ko line was unable to emerge from the host erythrocyte in response to XA-stimulation. The published[25] work carried out on gametocyte infected erythrocyte deformability presented in this chapter revealed an unexpected role for *PfPDEδ* and *PfPDEγ* (the latter not included in the publication) in gametocyte deformability. This was linked to elevated levels of cAMP as a result of the absence of *PfPDEδ* leading to an inability of mature gametocytes to become deformable. In light of these findings, it was deemed important to re-evaluate the *PfPDEδ*-ko line phenotype observed by Cathy Taylor[130], (Cathy Taylor, PhD Thesis, 2007) because the theory was formed that perhaps this inability of the *PfPDEδ*-ko line to round up may be a consequence of cAMP-induced stiffness due to the absence of *PfPDEδ* rather than a cGMP-dependent effect as concluded by Taylor *et al*[130]. Alternatively, *PfPDEδ* may be required for the initiation of gametogenesis in this line, but the deformability phenotype complicates the use of this line in determining a role for *PfPDEδ* in gametogenesis. This was an important question to answer in order to progress in dissecting the signalling pathways involved in gametogenesis.

4.2. Results

4.2.1. Investigation into the effects of PDE inhibition on gametocyte deformability

Stage V gametocytes of the *PfPDE γ* -ko and *PfPDE δ* -ko lines show deformability defects

The role of *PfPDE γ* and *PfPDE δ* in host cell deformability was investigated. To achieve this, a nano-filtration technology was used in collaboration with Catherine Lavazec (Institute Pasteur)[25]. Purified samples of stage V gametocytes from the 3D7a, *PfPDE γ* -ko and *PfPDE δ* -ko lines were perfused through a microsphere matrix using a peristaltic pump in order to mimic splenic retention. Numbers of parasites in the flow through (deformable) were compared to numbers retained in the matrix (stiff) by light microscopy of paraformaldehyde-fixed samples (for more information see section 2.5.F of the methods).

The majority of stage V gametocytes of the wildtype 3D7a line (~ 70 %) filtered through the microsphere matrix with ~ 30 % remaining inside (Figure 4.1 and Table 4.1). This indicates that the majority of 3D7a stage V gametocytes were deformable.

By contrast, stage V gametocytes of the *PfPDE γ* -ko and *PfPDE δ* -ko lines were mostly retained with only ~ 10 % and ~20 % of parasites respectively being able to transverse the microsphere matrix (Figure 4.1 and Table 4.1). The difference in retention compared to the 3D7a wildtype control was significant for both *PfPDE γ* -ko ($P = <0.0001$) and *PfPDE δ* -ko ($P = 0.0116$) using a Welch's unpaired t test). The majority of gametocytes from these two lines were therefore retained and were thus non deformable, suggesting a likely role for *PfPDEs* in gametocyte-infected erythrocyte deformability.

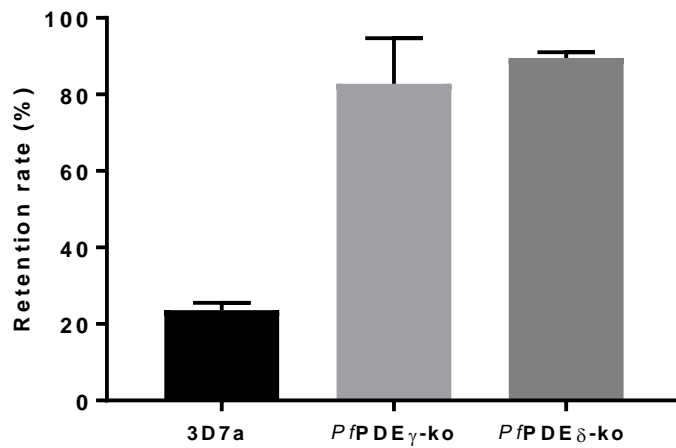


Figure 4.1. Retention rates of *PfPDE γ -ko* and *PfPDE δ -ko* stage V gametocytes filtered through a microsphere matrix. Data are an average of 3 experiments for both wildtype and the *PfPDE δ -ko* line and two experiments for the *PfPDE γ -ko* line, all carried out in triplicate. Presented as percentage retention rate of gametocytes passed through a microsphere matrix. Graph generated in GraphPad, Prism. Error bars represent SD.

Retention rate of stage V gametocytes \pm SD		
3D7a	<i>PfPDEδ-ko</i>	<i>PfPDEγ-ko</i>
23.65 \pm 1.93	82.81 \pm 11.89	89.50 \pm 1.55

Table 4.1. Percentage retention rate (\pm SD) of 3D7a, *PfPDE δ -ko* and *PfPDE γ -ko* stage V gametocytes passed through a microsphere matrix. Data are analysed in Excel and are an average of 3 experiments for both wildtype and *PfPDE δ -ko* lines and two experiments for *PfPDE γ -ko* line, all carried out in triplicate.

4.2.2. Investigation into the effect of phosphodiesterase inhibition on rounding up and emergence of *P. falciparum* gametocytes

To re-evaluate the involvement of *PfPDE*-regulated cGMP signalling in mature gametocyte emergence from the host cell erythrocyte, stage V gametocytes of the 3D7a, *PfPKG*_{T618Q}, *PfPDE* γ -ko and *PfPDE* δ -ko lines were stimulated with the known inducer of gametogenesis; XA, in the presence and absence of the *PfPKG* inhibitor C2. The aim of this was to confirm previous work done by Cathy Taylor (Cathy Taylor, PhD Thesis, 2007), which showed that in the absence of *PfPDE* δ , rounding up of gametocytes was reduced and emergence of gametocytes from the host erythrocyte was greatly reduced. The work in this chapter will also aim to confirm work done by McRobert *et al* on the *PfPKG*-specificity of rounding up and emergence[159].

Blood films were incubated with an antibody specific to a host erythrocyte membrane protein, Band 3, followed by incubation with an Alexa Fluor 594-conjugated secondary antibody and observation by confocal microscopy. Numbers of crescent-shaped (non-activated gametocytes) and rounded cells (activated gametocytes) were counted and staining of the host erythrocyte (non-emerged) and lack of staining (emerged) was recorded.

XA induces rounding up and emergence of stage V gametocytes in a *PfPKG*-dependent manner

3D7a stage V gametocytes rounded up and emerged in response to XA treatment in a *PfPKG*-dependent manner (Figures 4.2 and 4.3) consistent with previous findings[130],[159]. Parasites in the control (DMSO) sample remained as crescent shaped gametocytes surrounded by the host erythrocyte membrane, which was stained with the Band 3 antibody, characteristic of non-activated parasites (Figure 4.3). On addition of XA, ~90 % of parasites rounded up with no Band 3 staining detected, indicative of gamete emergence from the host cell (Figures 4.2 and 4.3). Rounding up and emergence of XA-induced mature gametocytes in the 3D7a line was reversed by addition of C2 with parasites retaining their characteristic crescent shape and host erythrocyte staining of Band 3 detected as seen in the DMSO control sample. A small number of gametocytes (~10 %) still rounded up and emerged in C2 treated samples (Figure 4.2).

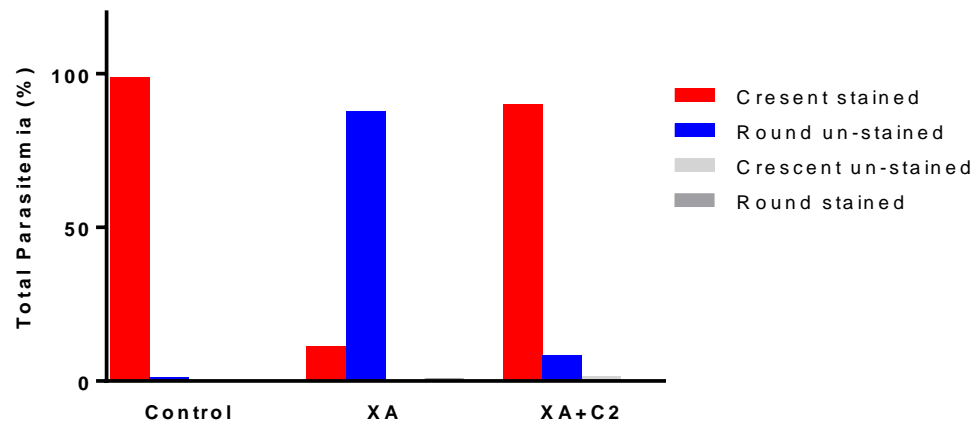


Figure 4.2. XA-induced rounding up and emergence in 3D7a gametocytes in the presence and absence of C2. XA-treated (100 μ M) stage V gametocyte samples were incubated for 30 minutes at RT in the presence or absence of C2 (2 μ M) and compared to an unstimulated control (0.05 % DMSO). Data are presented as percentage of total parasitemia and determined by counts of parasites from IFA samples prepared from blood films stained with Band 3 ab and imaged by confocal microscopy. Data are from a single count (~ 900cells counted per replicate) of one experiment analysed in Excel. The graph was generated in GraphPad, Prism.

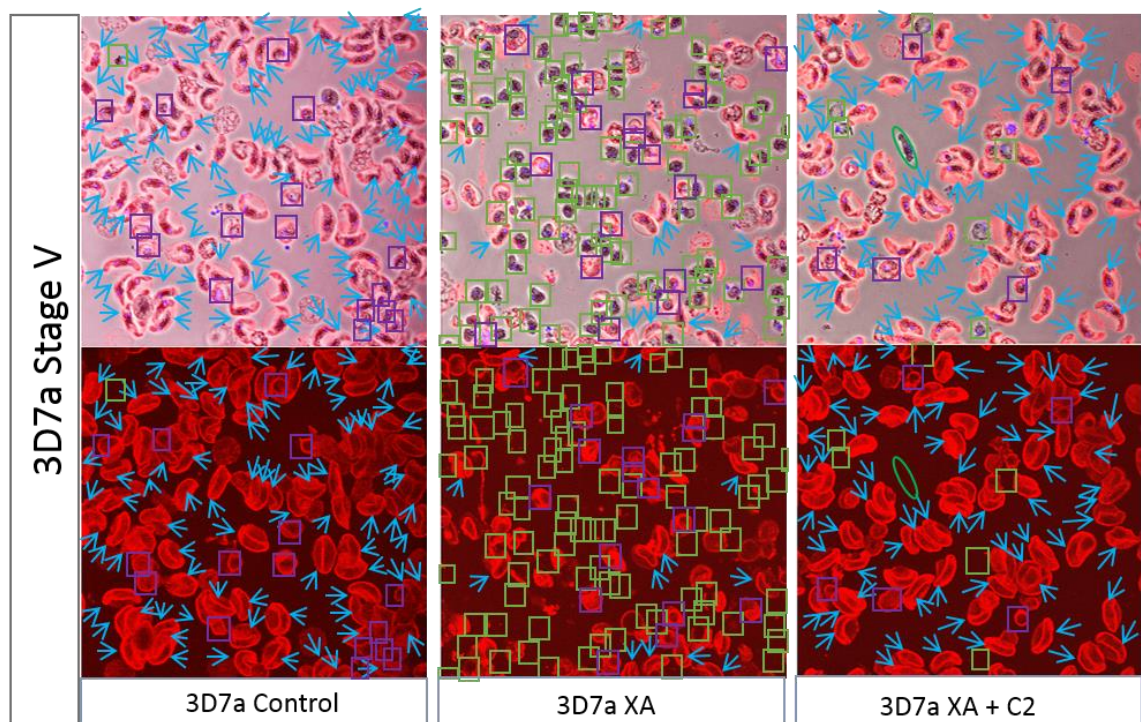


Figure 4.3. Confocal Images of XA-induced rounding up and emergence in the 3D7a line +/- C2 XA-treated (100 μ M) samples compared to an unstimulated control (0.05 % DMSO). Upper panels represent light image with Band 3 (red) and DAPI (blue) staining. Lower panels represent the same image with Band 3 staining only (red). Blue arrows indicate crescent shaped stage V gametocytes stained with Band 3 antibody (non-activated). Green boxes represent rounded up gametocytes with no Band 3 staining (activated). Purple boxes are parasites that appear round in morphology but have not emerged (Band 3 staining present).

Stage V gametocytes of the *Pf*PKG_{T618Q} line also rounded up and emerged in response to XA but this could not be reversed by C2 (Figures 4.4 and 4.5). Parasites in the control (DMSO) sample remained as crescent-shaped gametocytes surrounded by the host erythrocyte membrane, which was stained with Band 3 antibody, characteristic of non-activated parasites (Figure 4.5). On addition of XA, ~90 % of parasites rounded up with no Band 3 staining detected, indicative of host cell emergence (Figures 4.4 and 4.5).

On addition of C2 to XA-treated samples, unlike the 3D7a line, parasites did not retain their characteristic crescent shape and presented as rounded up cells with no Band 3 staining of the erythrocyte membrane, comparable to XA-treated samples (Figures 4.4 and 4.5). C2 could therefore not reverse XA activation of rounding up and emergence in this C2-resistant line indicating that XA induced rounding up and emergence are *Pf*PKG-dependent events.

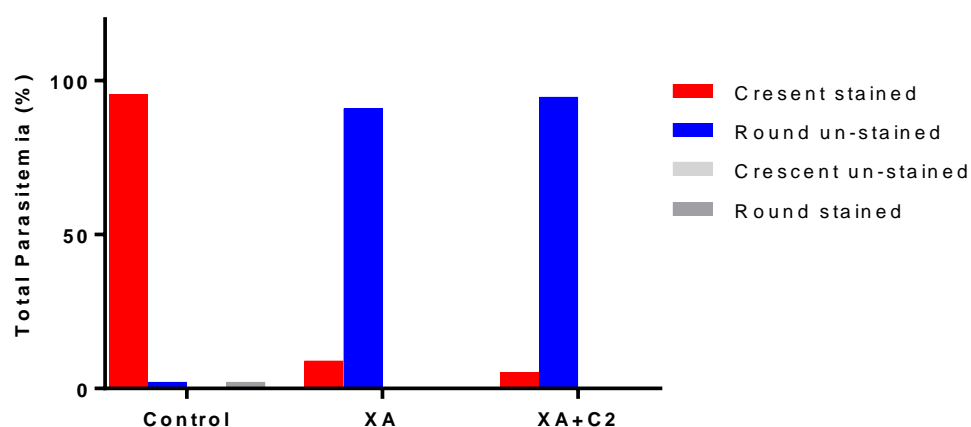


Figure 4.4. XA induced rounding up and emergence in the *Pf*PKG_{T618Q} line in the presence and absence of C2

XA-treated (100 μ M) samples incubated for 30 minutes/RT in the presence or absence of C2 (2 μ M) and compared to an unstimulated control (0.05 % DMSO). Data are presented as percentage of total parasitemia and determined by counts of parasites from IFA samples prepared from blood films stained with Band 3 ab and imaged by confocal microscopy. Data are a single count (~ 900cells counted per replicate) of one experiment analysed in Excel. Graph generated in GraphPad, Prism.

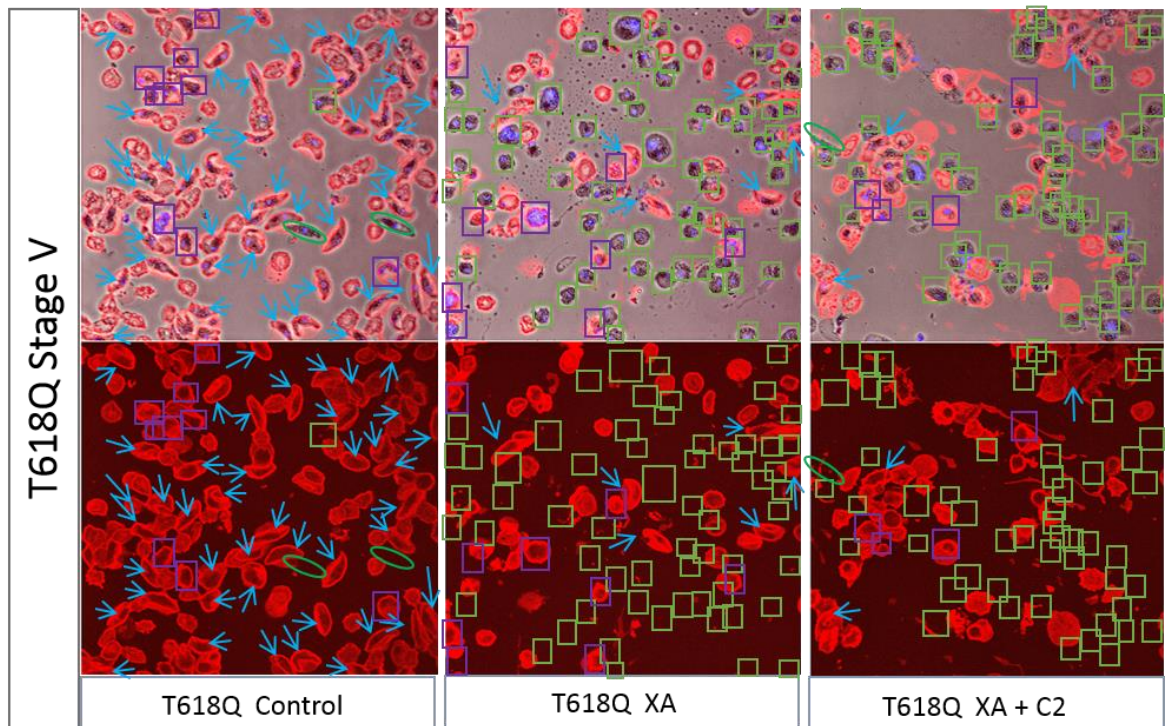


Figure 4.5. Confocal images of XA-induced rounding up and emergence in the *PfPKG*_{T618Q} line +/- C2. XA-treated (100 μ M) samples compared to an unstimulated control (0.05 % DMSO). Upper panels represent light image with Band 3 (red) and Dapi (blue) staining. Lower panels represent the same image with Band 3 staining only (red). Blue arrows indicate crescent shaped stage V gametocytes stained with Band 3 (non-activated). Green boxes represent rounded up gametocytes with no Band 3 staining (activated). Purple boxes are parasites that appear round in morphology but have not emerged (Band 3 staining present).

***Pf*PDE γ -ko line Stage V gametocytes round up and emerge normally in response to XA stimulation**

In light of the deformability data presented in section 4.2.1, It was of interest to attempt to reproduce emergence experiments carried out by Cathy Taylor (Cathy Taylor, PhD Thesis, 2007) on the *Pf*PDE γ -ko line, the reason being that hypothetically, gametocytes that present with a stiff phenotype (as the data in section 4.2.1. suggests is the case for *Pf*PDE γ -ko line gametocytes) are unlikely to be able to round up, and data presented by Cathy Taylor on gametocyte emergence is at odds with this and indicates that the *Pf*PDE γ -ko line appears to round up normally in response to XA stimulation compared to a wildtype line (Cathy Taylor, PhD Thesis, 2007).

Stage V gametocytes of the *Pf*PDE γ -ko line rounded up and emerged from the host erythrocyte in response to XA treatment in a *Pf*PKG-dependent manner comparable to what was seen in the wild type 3D7a line (Figures 4.2 and 4.6) and consistent with the findings of Cathy Taylor (Cathy Taylor, PhD Thesis, 2007). Parasites in the control (0.05 % DMSO) sample remained as crescent-shaped gametocytes surrounded by the host erythrocyte membrane, which was stained with the Band 3 antibody, characteristic of non-activated parasites (Figure 4.7). On XA addition, ~95 % of parasites rounded up with no Band 3 staining of the host erythrocyte detected, indicative of host cell emergence (Figures 4.6 and 4.7). Rounding up and emergence of XA-induced mature gametocytes in the *Pf*PDE γ -ko line was reversed by addition of C2 with parasites retaining their characteristic crescent shape and host erythrocyte staining with Band 3 detected as seen in the DMSO control samples indicating XA can induce rounding up in the absence of *Pf*PDE γ and that this is a *Pf*PKG-dependent event as seen in the wildtype 3D7a parasite line. In samples stimulated with XA in the presence of C2, a small number (~6 %) of parasites also appeared as crescent shaped gametocytes with no erythrocyte Band 3 staining detected (Figure 4.7, green ovals). These data mirror work carried out by Cathy Taylor (Cathy Taylor, PhD Thesis, 2007) demonstrating that *Pf*PDE γ -ko line stage V gametocytes will round up and emerge from the host erythrocyte in response to XA stimulation in comparable levels to that of the control line and that this occurs in a *Pf*PKG-dependent manner. This indicates that the absence of *Pf*PDE γ has no impact on the ability of gametocytes to respond to XA by rounding up and emerging and puts into question the results presented in section 4.2.1, which suggest that *Pf*PDE γ -ko line stage V gametocytes may present with a 'stiff' phenotype.

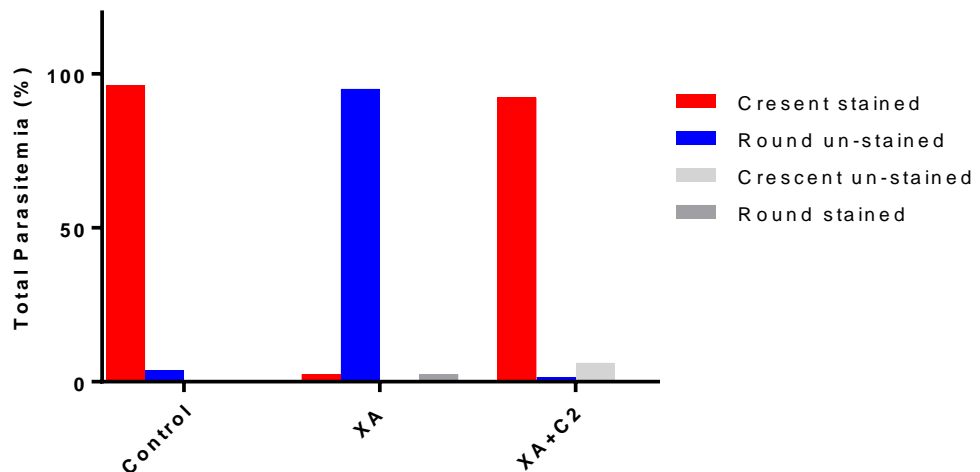


Figure 4.6. XA induced rounding up and emergence in the *PfPDEγ*-ko line in the presence and absence of C2. XA-treated (100 μM) samples incubated for 30 minutes/RT in the presence or absence of C2 (2 μM) and compared to an unstimulated control (0.05 % DMSO). Data are presented as percentage of total parasitemia and determined by counts of parasites from IFA samples prepared from blood films stained with Band 3 ab and imaged by confocal microscopy. Data are a single count (~ 900cells counted per replicate) of one experiment analysed in Excel. Graph generated in GraphPad, Prism.

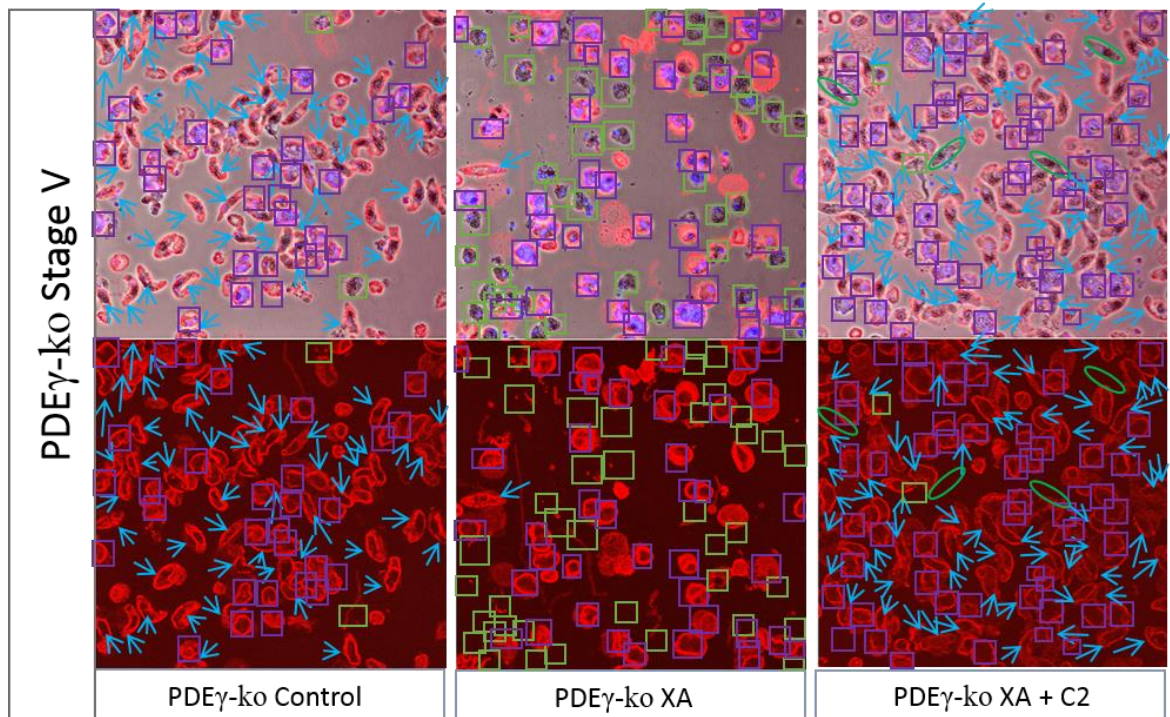


Figure 4.7. Confocal Images of XA-induced rounding up and emergence in the *PfPDEγ*-ko line +/- C2 XA-treated (100 μM) samples were compared to an unstimulated control (0.05 % DMSO). Upper panels represent light image with Band 3 (red) and Dapi (blue) staining. Lower panels represent the same image with Band 3 staining only (red). Blue arrows indicate crescent shaped stage V gametocytes stained with Band 3 (non-activated). Green boxes represent rounded up gametocytes with no Band 3 staining (activated). Purple boxes are parasites that appear round in morphology but have not emerged (Band 3 staining present). Green ovals represent crescent shaped stage V gametocytes that are not stained with Band 3.

***PfPDE δ* -ko line stage V gametocytes do not round up or emerge in response to XA stimulation**

In keeping with data produced by Cathy Taylor (Cathy Taylor, PhD Thesis, 2007) the majority of stage V gametocytes of the *PfPDE δ* -ko line do not emerge from the host erythrocyte in response to XA (Figures 4.8 and 4.9). DMSO treated parasites remained as crescent-shaped cells with host erythrocyte Band 3 staining detected. On addition of XA, ~85 % of cells retained their crescent shape and did not round up. Band 3 staining of the erythrocyte was still detected, indicative that these cells had not emerged from the host erythrocyte. This is slightly at odds with data presented by Cathy Taylor (Cathy Taylor PhD Thesis, 2007), which show that some cells do round up but that the majority of cells will not emerge, which suggests predominantly an emergence phenotype, whereas the data presented here indicates both a rounding up and emergence phenotype.

A small number (~15 %) of cells both rounded up and emerged from the host erythrocyte in response to XA (again this is at odds to Cathy Taylor's work). This was much lower than the ~90 % that rounding up in response to XA in the 3D7a wildtype line. In samples treated with both XA and C2, ~100 % of gametocytes retained their crescent shape and erythrocyte membrane Band 3 staining was still observed. Indicative that the small number of parasites that were able to round up and emerge in response to XA, did so in a *PfPKG*-dependent manner. This sample contained a proportion of asexual stages that remained surrounded by an erythrocyte membrane asexual stages were identified by the bright field image and the larger Dapi staining and were excluded from the final counts.

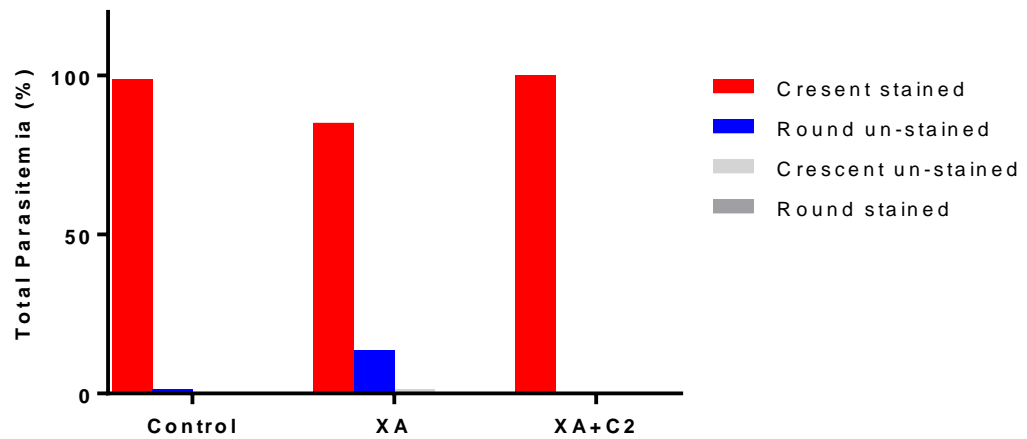


Figure 4.8. XA induced rounding up and emergence in the *PfPDEδ*-ko line in the presence and absence of C2. XA-treated (100 μ M) samples incubated for 30 minutes/RT in the presence or absence of C2 (2 μ M) and compared to an unstimulated control (0.05 % DMSO). Data are presented as percentage of total parasitemia and determined by counts of parasites from IFA samples prepared from blood films stained with band 3 ab and imaged by confocal microscopy. Data are a single count of one experiment analysed in Excel. Graph generated in GraphPad, Prism.

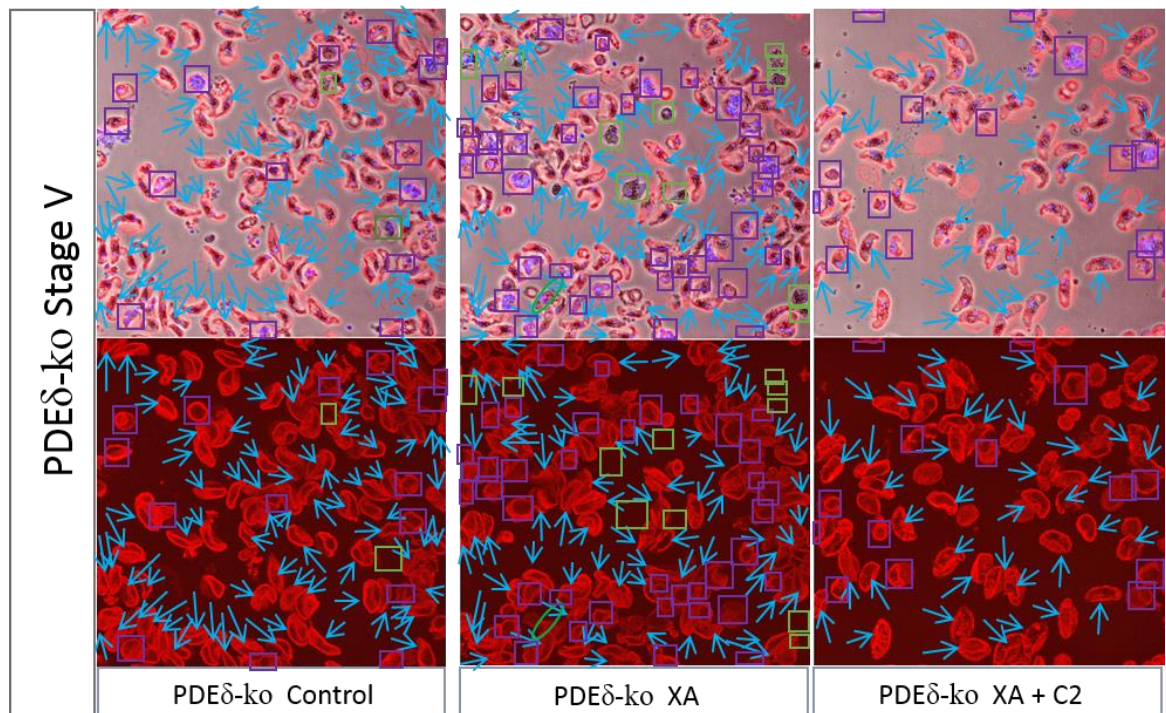


Figure 4.9. Confocal Images of XA-induced rounding up and emergence in the *PfPDEδ* -ko line +/- C2 XA-treated (100 μ M) samples compared to an unstimulated control (0.05 % DMSO). Upper panels represent light image with Band 3 (red) and Dapi (blue) staining. Lower panels represent the same image with Band 3 staining only (red). Blue arrows indicate crescent shaped stage V gametocytes stained with Band 3 (non-activated). Green boxes represent rounded up gametocytes with no Band 3 staining (activated). Purple boxes are parasites that appear round in morphology but have not emerged (Band 3 staining present). Green ovals represent crescent shaped stage V gametocytes that are not stained with Band 3.

4.2.3. Investigation into a possible link between the ‘stiff’ phenotype of the *PfPDEδ*-ko line and its inability to round up.

In light of published data presented in this thesis showing that in the absence of *PfPDEδ*, stage V gametocytes exhibit a ‘stiff’ phenotype (section 4.2.1), it was of huge interest to investigate whether this lack of deformability contributes to the absence of XA-induced rounding up and emergence observed in the *PfPDEδ*-ko line (section 4.2.2). The absence of XA-induced emergence in the *PfPDEδ*-ko line, and greatly reduced ability to round up was first observed by Cathy Taylor (Cathy Taylor, PhD Thesis, 2007). Deletion of *PfPDEδ* was shown to increase levels of cGMP (~2-fold, corresponding to a ~2-fold decrease in cGMP-PDE activity) in gametocytes[130] indicating that the absence of *PfPDEδ* disrupted cGMP signalling. cAMP levels were also measured in this study but levels were very low and unchanged compared to the control and so it was not clear whether they were beyond the detection limit of the cAMP ELISA used[130]. Unregulated cGMP levels were deduced as the cause of the aberrant gametogenesis observed in the *PfPDEδ*-ko line. As mentioned elsewhere in this thesis, *PfPDEδ* is expressed at the protein level in mature gametocytes[144] and likely plays an important role in regulating cGMP levels, which are required for the process of gametogenesis. *PfPDEδ* was therefore previously thought to be a cGMP-specific *PfPDE*. However, data published by Ramdani *et al*[25] (in which the deformability data presented in this thesis are included), have linked *P. falciparum* gametocyte infected erythrocyte deformability to the absence of *PfPDEδ* and subsequent activation of *PfPKA*. In the Ramdani study, in contrast to work by Taylor *et al*[130], the total intracellular cAMP concentration in *P. falciparum* gametocyte was shown to be elevated in the *PfPDEδ*-ko line compared to 3D7a in both immature and mature gametocytes[25]. These data, along with those linking the absence of *PfPDEδ* to cAMP-regulated gametocyte deformability, suggests that *PfPDEδ* may be dual specific (however, data presented in this thesis (Chapter 6, Section 6.2.5) and data from Cathy Taylor’s work suggests otherwise). Alternatively, the apparent influence of *PfPDEδ* on cAMP levels may be indirect. However this needs to be confirmed (see chapter 5 for data presented on *PfPDEδ* cyclic nucleotide specificity). It must be noted that the host erythrocyte PKA may be contributing wholly or partly to the deformability phenotype. The PKA-induced stiff phenotype of the *PfPDEδ*-ko line complicates investigations into the role of *PfPDEδ* in gametogenesis because a premature spike in cAMP/PKA signalling may have rendered the PDE- δ gametocytes unable to respond later to cGMP/PKG signalling that triggers rounding up and emergence. Therefore, in order to attempt to dissect the two questions of the role of *PfPDEδ* in deformability and the role of *PfPDEδ* in inducing rounding up and

emergence, PKA was inhibited in the *PfPDE δ* -ko line using three concentrations of the PKA inhibitor KT5720. This is a specific, cell permeable inhibitor of both human and parasite PKA (assumed) that does not target PKG (Sigma product information). In mammalian cells it is known to inhibitor PKA by competitively binding to the ATP binding site on the PKA catalytic subunit preventing PKA from phosphorylating target proteins[270]. It is important to note that PKA inhibition in this assay may affect the host-derived PKA, the parasite-derived PKA or both. PKA-inhibitor treated *PfPDE δ* -ko samples were observed for rounding up events in both non-stimulated (no PF9) and stimulated (plus PF9) samples. Samples were compared to a PKA-inhibitor treated wildtype control. PF9 is a potent PDE inhibitor that stimulates gametogenesis (see chapter 6).

At the highest concentration of KT5720 tested (10 μ M), a small proportion (\sim 9 % of the no PKA inhibitor control) of stage V gametocytes of the *PfPDE δ* -ko line rounded up in the absence of PF9 stimulation (Figure 4.10, control). This was completely reversed by the addition of the specific PKG inhibitor MRT00207065 indicating that the rounding up observed in this line when incubated with 10 μ M KT5720 is *Pf*PKG dependent. Addition of PF9 to samples pre-incubated with 10 μ M KT5720 (Figure 4.10, PF9) resulted in \sim 25 % of gametocytes rounding up compared to the non-PKA inhibitor-treated control. This was reversed almost completely by pre-incubation with MRT00207065 with only \sim 3 % of parasites rounding up, indicating that at this concentration of KT5720, gametocytes lacking *PfPDE δ* are able to respond to PF9 stimulation by rounding up in a *Pf*PKG-dependent manner. The data demonstrate that at this concentration, inhibition of PKA can reverse the inability of *PfPDE δ* -ko gametocytes to round up and that this may be due to reversing the deformability phenotype observed in this line. Not only this, but a small proportion (\sim 9 %) of PKA-inhibited parasites lacking *PfPDE δ* can also round up un-stimulated.

***PfPDE δ* -ko KT5720 10 μ M**

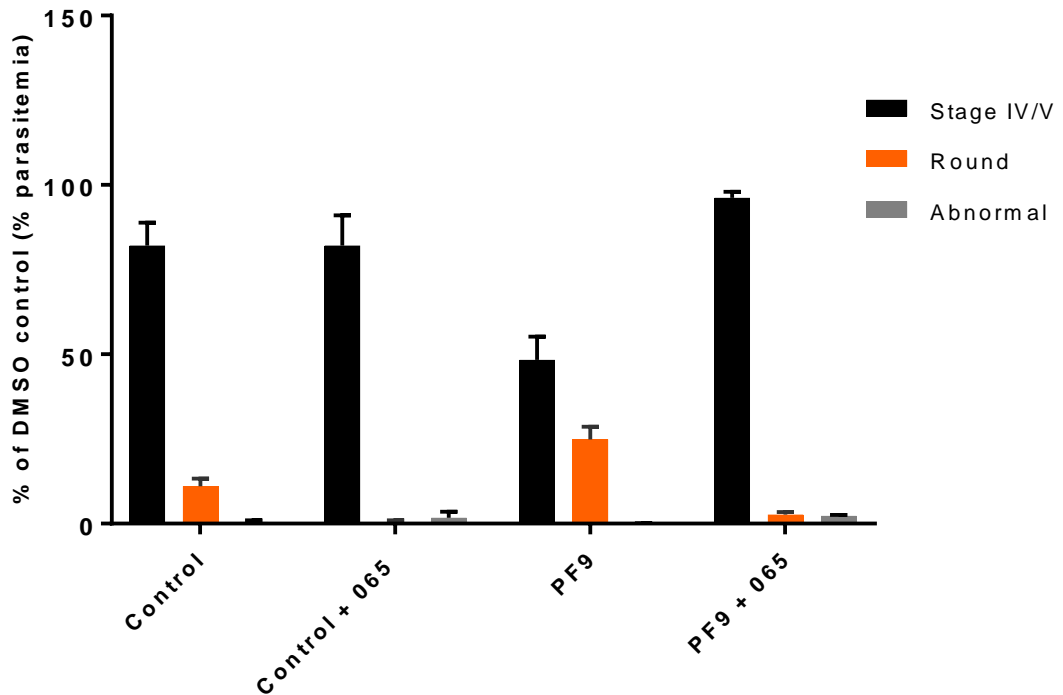


Figure 4.10. Rounding up of *PfPDE δ* -ko stage V gametocytes treated with 10 μ M KT5720. Samples were pre-incubated with KT5720 (10 μ M) in the presence and absence of MRT00207065 (1 μ M). After 3 hours incubation, samples were split and incubated for 20 minutes in the presence or absence of PF9 (10 μ M). Data are presented as percentage of the DMSO (0.05 %) control (no PKA inhibitor treatment see Figure 4.13 green star) generated by counts (number of parasites per 900 RBC's) of Giemsa stained blood films. Data are the average of 2 counts from 2 individual experiments. Graph generated in GraphPad, Prism. Error bars represent SD.

At 5 μ M KT5720, as seen with 10 μ M KT5720, a proportion of stage V gametocytes of the *PfPDE δ* -ko line rounded up unstimulated (Figure 4.11, control). Numbers of rounded up parasites were comparable to that of 10 μ M KT5720 treatment with ~ 9 % appearing as rounded up forms. The number of non-stimulated rounded-up parasites was completely reversed by *PfPKG* inhibition (Figure 4.11, control + 065) indicating that treatment with 5 μ M KT5720 can lead to rounding up of mature gametocytes in a *PfPKG*-dependent manner. This was also the case for PF9-stimulated mature gametocytes treated with 5 μ M KT5720 (Figure 4.11, PF9), which showed ~ 30 % rounding up compared to the non-PKA inhibited control. This was completely reversed by pre-incubation with MRT00207065.

***PfPDEδ*-ko KT5720 5 μ M**

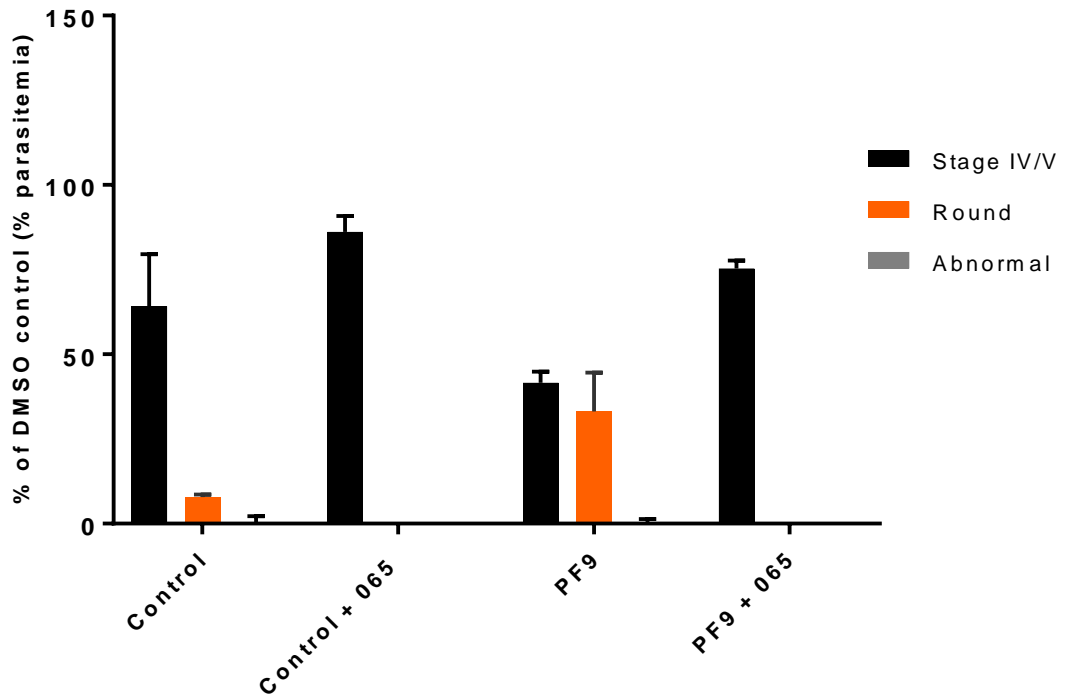


Figure 4.11. Rounding up of *PfPDEδ*-ko stage V gametocytes treated with 5 μ M KT5720. Samples were pre-incubated with KT5720 (5 μ M) in the presence and absence of MRT00207065 (1 μ M). After 3 hours incubation, samples were split and incubated for 20 minutes in the presence or absence of PF9 (10 μ M). Data are presented as percentage of the untreated DMSO (0.05 %) control (no PKA inhibitor treatment see Figure 4.13 green star) generated by counts (number of parasites per 900 RBC's) of Giemsa stained blood films. Data are the average of 2 counts from 2 individual experiments. Graph generated in GraphPad, Prism. Error bars represent SD.

Pre-incubation of *PfPDEδ*-ko line parasites with 1 μ M KT5720 did not result in un-stimulated rounding up as seen with 5 μ M and 10 μ M KT5720, although a very small number (~ 1 % of the non-PKA inhibited control) did round up (Figure 4.12). However, when stimulated with PF9, ~30 % of gametocytes rounded up compared to the DMSO control. This was completely reversed by pre-incubation with MRT00207065 (Figure 4.12) demonstrating that at the lowest concentration tested, although *PfPDEδ*-ko line gametocytes did not appear to round up un-stimulated as seen at the two higher PKG inhibitor concentrations, they were able to round up in a *PfPKG*-dependent manner when stimulated with PF9.

PfPDEδ-ko KT5720 1 μ M

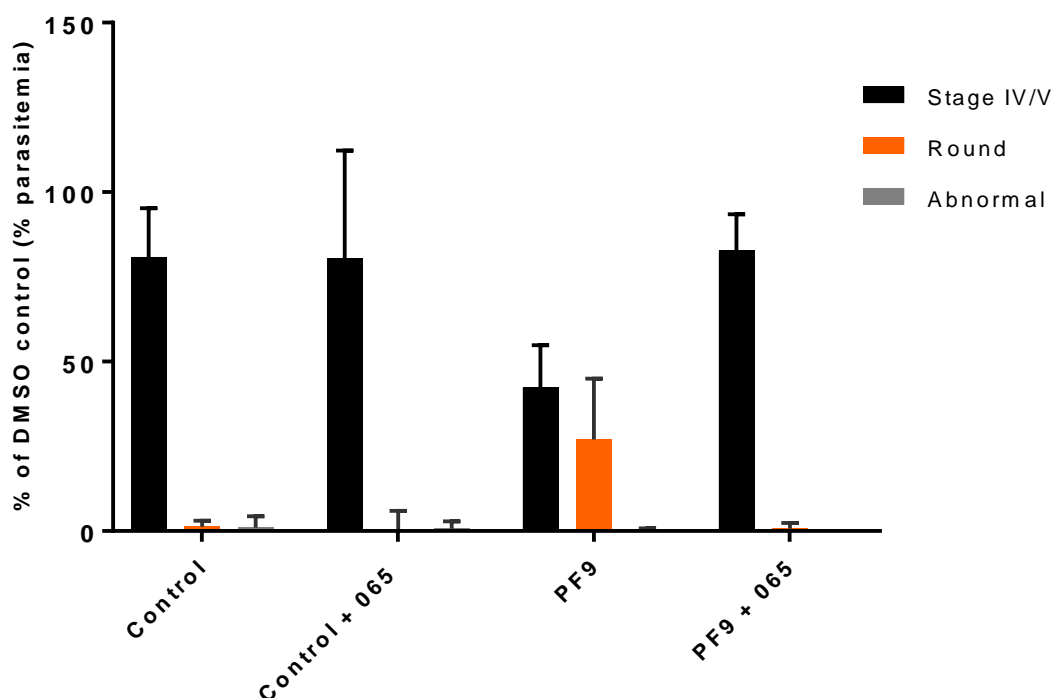


Figure 4.12. Rounding up of *PfPDEδ*-ko stage V gametocytes treated with 1 μ M KT5720. Samples were pre-incubated with KT5720 (1 μ M) in the presence and absence of MRT00207065 (1 μ M). After 3 hours incubation, samples were split and incubated for 20 minutes in the presence or absence of PF9 (10 μ M). Data are presented as percentage of the untreated DMSO (0.05 %) control (no PKA inhibitor treatment see Figure 4.13 green star) generated by counts (number of parasites per 900 RBC's) of Giemsa stained blood films. Data are the average of 2 counts from 2 individual experiments. Graph generated in GraphPad, Prism. Error bars represent SD.

Control samples (no PKA inhibition) of the *PfPDEδ*-ko line showed no un-stimulated rounding up (Figure 4.13). This demonstrates that in samples inhibited with KT5720, un-stimulated rounding up was likely to be due to PKA inhibition. These samples also showed ~15 % PF9-stimulated rounding up (Figure 4.13). However this was lower than seen in PKA inhibitor-treated samples and comparable levels to numbers seen in other experiments carried out on *PfPDEδ*-ko line parasites using PF9 (chapter 6 section 6.2.4.1). Again this indicated that the majority of PF9-induced rounding is likely to be a result of PKA inhibition. Some abnormal forms were observed in PF9-treated samples of the non-PKA-inhibited control but not in any of the KT5720-treated samples.

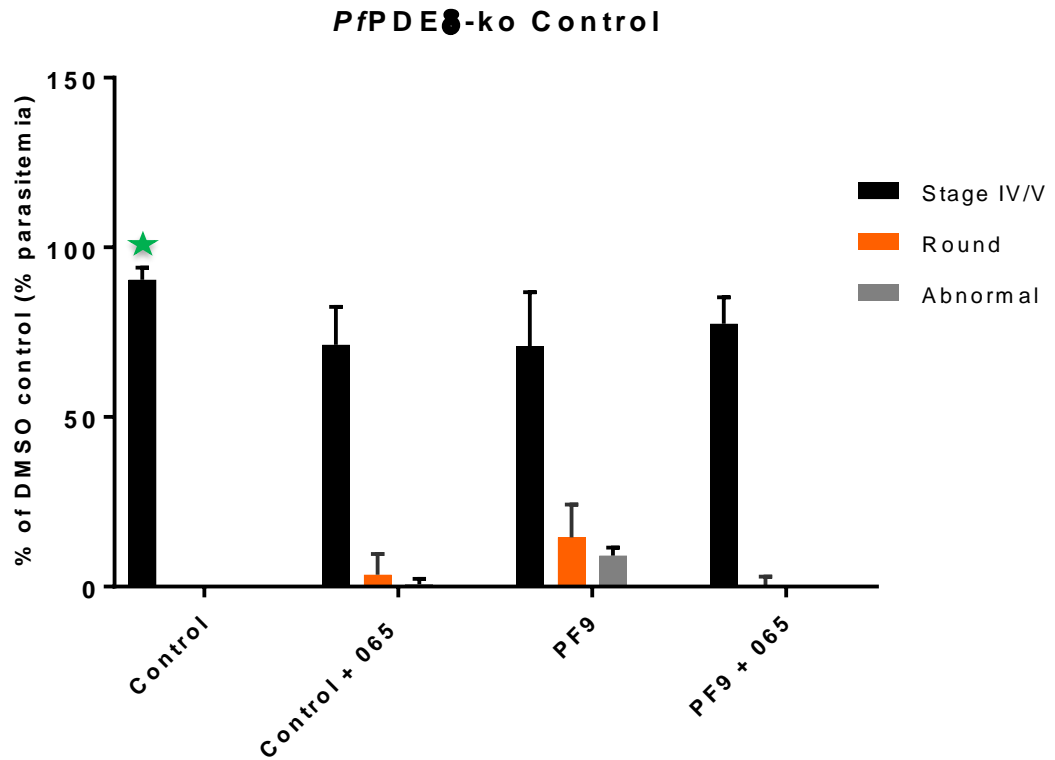


Figure 4.13. Rounding up of *PfPDE6*-ko stage V gametocytes with no PKA inhibition. Samples were pre-incubated with DMSO (0.05 %) in the presence and absence of MRT00207065 (1 μ M). After 3 hours incubation, samples were split and incubated for 20 minutes in the presence or absence of PF9 (10 μ M). Data are presented as percentage of the untreated DMSO (0.05 %) control (green star) generated by counts (number of parasites per 900 RBC's) of Giemsa stained blood films. Data are the average of 2 counts from 2 individual experiments. Graph generated in GraphPad, Prism. Error bars represent SD.

Addition of KT5720 to the 3D7a wildtype line does not affect gametocyte numbers or lead to un-induced rounding up.

To make sure that the PKA inhibitor KT5720 did not lead to any adverse effects on gametocytes, and to ensure that the rounding up seen in *PfPDEδ*-ko line gametocytes was due to the reversing of the stiff phenotype rather than rounding up induced by addition of the PKA inhibitor, increasing concentrations of KT5720 were incubated with 3D7a stage V gametocytes and samples observed for rounding up events or changes in total parasitemia.

Addition of 10 μ M, 5 μ M or 1 μ M KT5720 to wild type 3D7a stage V gametocytes did not result in un-stimulated rounding up as seen in the *PfPDEδ*-ko line (Figure 4.14). Stage V gametocyte numbers did not differ from the non-treated control when KT5720 was added. This indicates that KT5720 does not act to induce rounding up in the wildtype line. These data also indicate that all concentrations of KT5720 tested do not affect parasite numbers after 3 hours of incubation and are therefore unlikely to result in a toxic effect under the conditions of the assay.

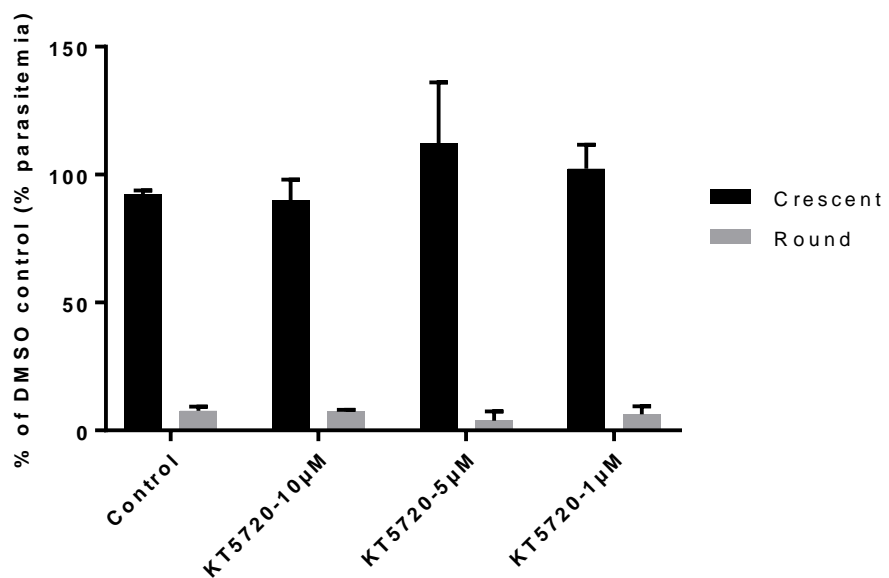


Figure 4.14. Addition of KT5720 to stage V gametocytes of the 3D7a line. Samples pre-incubated with 10 μ M, 5 μ M or 1 μ M KT5720 for 3 hours. Data are presented as percentage of the untreated DMSO (0.05 %) control generated by counts (number of parasites per 900 RBC's) of Giemsa stained blood films. Data are the average of 2 counts from 1 experiment. Graph generated in GraphPad, Prism. Error bars represent SD.

XA was also able to induce an increase in round forms in KT5720-treated samples

Addition of XA to stage V gametocytes of the *PfPDE δ -ko* line resulted in only a very small proportion (~ 5 %) of parasites rounding up from a crescent shaped to a rounded form (Figure 4.15). This proportion was increased when *PfPDE δ -ko* line gametocytes were treated for 12 hours with the PKA inhibitor KT5720 (Figure 4.16). ~25 % gametocytes rounded up in response to XA when PKA was inhibited. A small proportion (~ 9 %) of gametocytes of the *PfPDE δ -ko* line appeared to have rounded up in samples that had been incubated for 20 minutes with KT5720 but which had not been stimulated by XA (Figure 4.16). This proportion of rounded up cells was ~ 2.5 times lower than in XA treated samples, but was not seen in *PfPDE δ -ko* line samples not treated with KT5720 indicating that a small proportion of PKA-inhibited gametocytes can round up unstimulated. The XA response in the *PfPDE δ -ko* line was compared to that in the 3D7a wildtype line not treated with PKA inhibitors. ~ 51 % of 3D7a stage V gametocytes rounded up in response to XA (Figure 4.17).

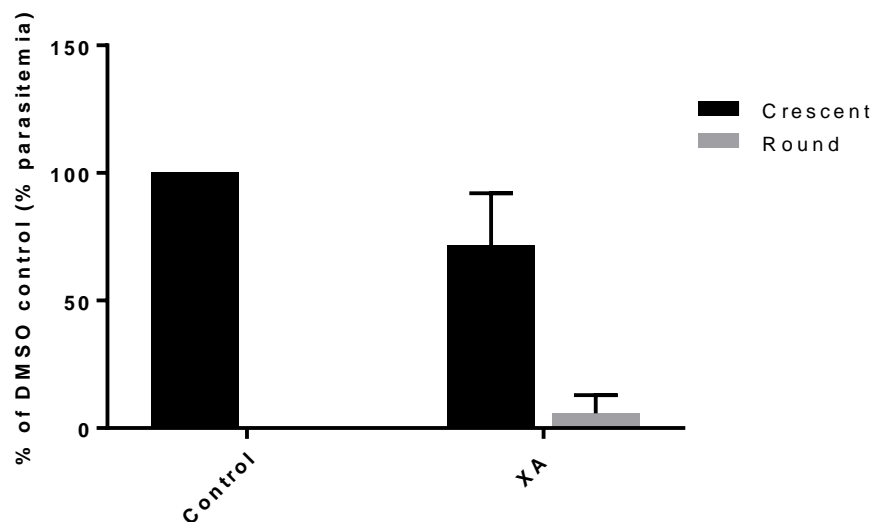


Figure 4.15. XA stimulation of *PfPDE δ -ko* gametocytes. *PfPDE δ -ko* line stage V gametocytes were incubated with XA (30 μ M) or 0.05 % DMSO (control) at RT for 30 minutes. Numbers of stage V (crescent) and rounded up parasites were counted from Giemsa stained blood films. Data are the average of 3 counts (parasites per ~900 RBC's counted) from 1 experiment. Graph generated in GraphPad, Prism. Error bars represent SD.

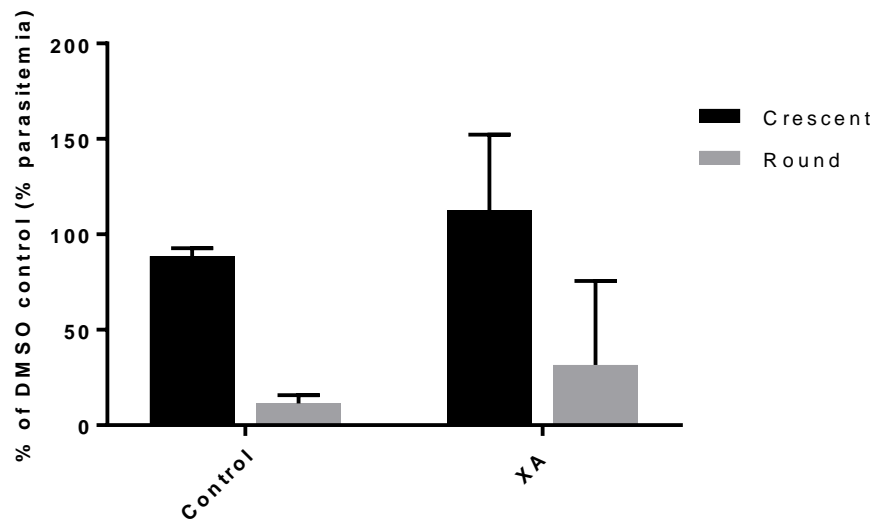


Figure 4.16. XA-stimulation of *PfpPDEδ*-ko gametocytes in the presence of KT5720. *PfpPDEδ*-ko line stage V gametocytes pre-incubated with 5 μ M KT5720 for 12 hours were then incubated with XA (30 μ M) or 0.05 % DMSO (control) at RT for 30 minutes. Numbers of stage V (crescent) and rounded up parasites were counted from Giemsa stained blood films. Data are the average of 3 counts (parasites per \sim 900 RBC's counted) from 1 experiment. Graph generated in GraphPad, Prism. Error bars represent SD.

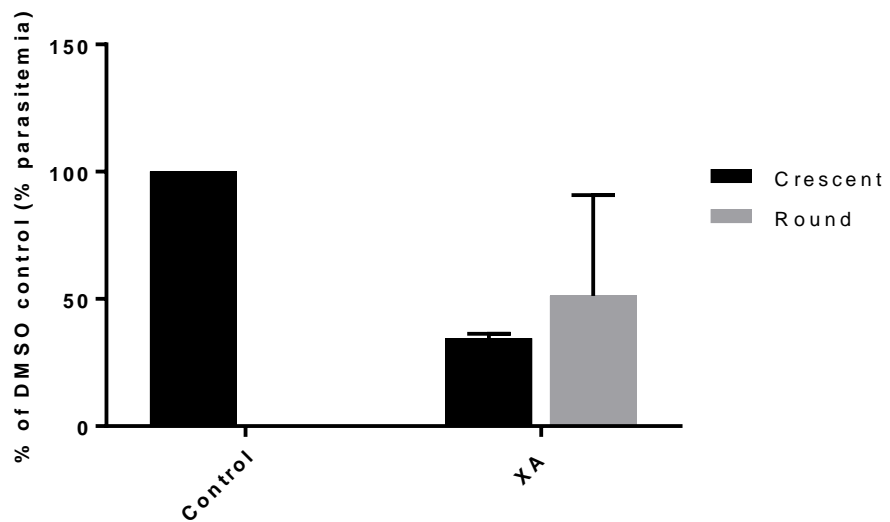


Figure 4.17. XA-stimulated 3D7a stage V gametocytes. 3D7a stage V gametocytes were incubated with XA (30 μ M) or 0.05 % DMSO (control) at RT for 30 minutes. Numbers of stage V (crescent) and rounded up parasites were counted from Giemsa stained blood films. Data are the average of 3 counts (parasites per \sim 900 RBC's counted) from 1 experiment. Graph generated in GraphPad, Prism. Error bars represent SD.

These data indicate that PKA inhibition of *PfPDEδ*-ko line gametocytes results in some non-induced rounding up and, more strikingly, an increase in both XA and PF9-induced rounding up. This suggests that if PKA-induced 'stiffness' is reversed, parasites are able to round up. However, this line still appears to exhibit greatly reduced XA-induced (and PF9) rounding up as previously described[130], suggesting that as previously hypothesised, *PfPDEδ* may play an important role in the processes of gametogenesis. In light of this it was of interest to investigate whether the absence of *PfPDEδ* could affect another important part of the gametogenesis process, the release of Ca^{2+} from internal stores, which is required for the later stages of gametogenesis.

4.2.4. Investigation into the effect of genetic and pharmacological phosphodiesterase disruption on Ca²⁺ mobilisation

XA-induced Ca²⁺ mobilisation in stage V gametocytes requires the presence of *PfPDEδ*.

It is known that gametogenesis involves Ca²⁺ release. It was therefore of interest to explore the role of *PfPDEs* that are potentially expressed in mature gametocyte stages at this crucial event of gametogenesis and to determine a possible link between Ca²⁺ mobilisation and cyclic nucleotide regulation through *PfPDEs*. As seen in chapter 3 (section 3.3.1), both XA and zaprinast can induce Ca²⁺ mobilisation in wild type stage V gametocytes and for zaprinast this is a *PfPKG*-dependent event, whereas in XA-induced Ca²⁺ mobilisation, although there is evidence of some *PfPKG* specificity, a proportion of the XA induced Ca²⁺ response appears not to be *PfPKG* dependent (chapter 3). The *PfPDEα*-ko, *PfPDEγ*-ko and *PfPDEδ*-ko lines were used in calcium release assays (see methods section 2.4.A) to determine the *PKG* specificity of the XA and zaprinast-induced Ca²⁺ responses in the absence of *PfPDEα*, *PfPDEγ* or *PfPDEδ*. The aim of this was to investigate the impact that the absence of these *PfPDEs* would have on the Ca²⁺ signalling response in mature gametocytes in the presence and absence of the *PKG* inhibitor C2.

Purified stage V gametocytes were loaded with Fluo-4-AM then treated with XA or zaprinast. In order to look at the *PKG* specificity of the Ca²⁺ response in these knockout lines, samples were treated in the presence or absence of C2. Levels of Ca²⁺ release from test samples were compared to an ionophore control that facilitates the transport of Ca²⁺ across membranes and therefore induced a rapid rise in intracellular Ca²⁺.

There is no evidence that deletion of *PfPDEy* alters the XA or zaprinast-induced Ca²⁺ response

Although data are preliminary and need repeating, the *PfPDEy*-ko line (Figure 4.18) appeared to behave as the wildtype line (Chapter 3, section 3.2.2, Figure 3.10 and also see Figure 4.21 for a comparison of the Ca²⁺ response in all parasite lines tested). In the absence of *PfPDEy*, parasites responded to both XA and zaprinast by releasing Ca²⁺. Ca²⁺ release induced by zaprinast was fully reversed by addition of C2. However, C2 only reversed XA induced Ca²⁺ mobilisation by ~50 % in XA-treated samples indicating that half of the XA-induced Ca²⁺ release is likely to be *PfPKG*-dependent but the other half of the Ca²⁺ response is likely to be induced through a signalling pathway that is not dependent upon *PfPKG* as C2 inhibition of *PfPKG* in this line does not fully reverse the Ca²⁺ release as previously observed (Chapter 3). This experiment is only one replicate and needs to be repeated and with an ionophore control.

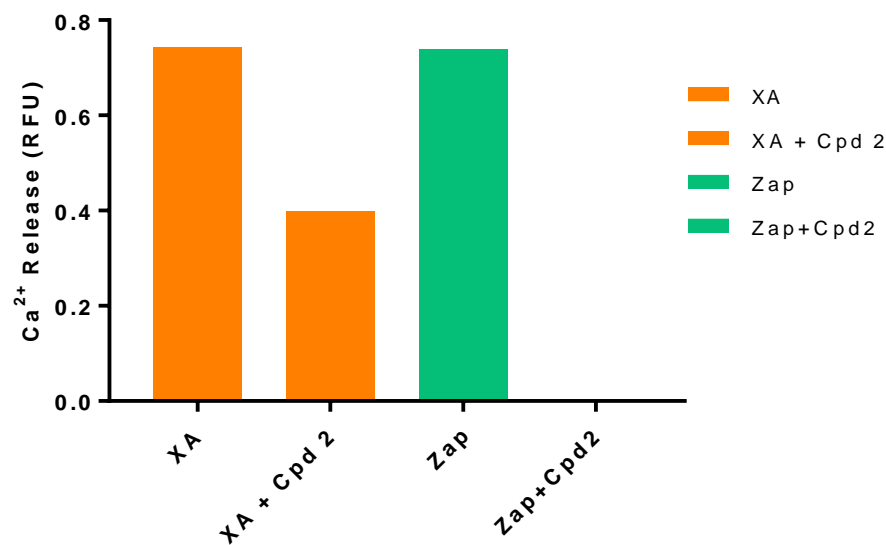


Figure 4.18. Ca²⁺ release in purified stage V gametocytes of the *PfPDEy*-ko line. Parasites were stimulated with 3 μ M XA and 100 μ M zaprinast in the presence and absence of 2 μ M C2. Fluorescence levels are presented as relative fluorescence units (RFU) minus the baseline fluorescence and fluorescence of the DMSO (0.05 %) control sample analysed in Excel. Graph generated in GraphPad, Prism. Data are from one experiment carried out in triplicate.

***PfPDEδ*-ko gametocytes are unable to respond to XA stimulation but can release Ca²⁺ in response to zaprinast**

Interestingly, stage V gametocytes of the *PfPDEδ*-ko line appeared completely unresponsive to XA-stimulation. No Ca²⁺ was detected at all in XA treated or XA + C2 samples and this result was reproducible (Figure 4.19).

Zaprinast induced ~20 % Ca²⁺ release in relation to the ionophore control (normalised to 100 %). All of the Ca²⁺ release seen in the zaprinast-treated sample was reversed by the addition of C2. This indicates that in the absence of *PfPDEδ*, Gametocytes cannot undergo Ca²⁺ release in response to XA stimulation. They can however respond to zaprinast stimulation and do so in a *PfPKG*-dependent manner.

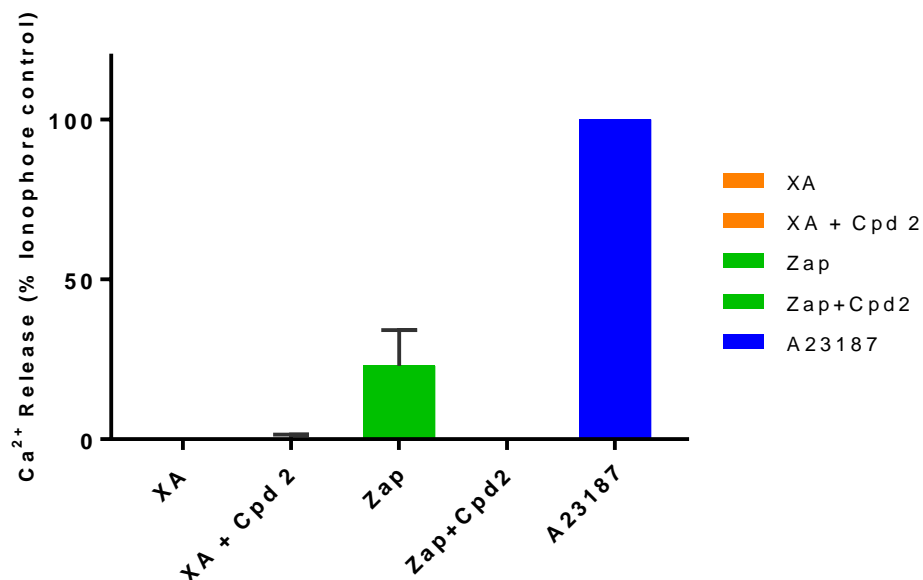


Figure 4.19. Ca²⁺ release in stage V *PfPDEδ*-ko gametocytes. Parasites were stimulated with XA (3 μM) and zaprinast (100 μM) in the presence and absence of 2 μM C2. Fluorescence levels are presented as percentage of ionophore control (A23187, 5 μM) minus the baseline fluorescence and fluorescence of the DMSO (0.05 %) control sample analysed in Excel and are the average of 2 separate experiments each carried out in triplicate. Graph generated in GraphPad, Prism. Error bars represent SD.

Absence of *Pf*PDE α appears to reduce the *Pf*PKG dependence of both the XA and zaprinast induced Ca²⁺ responses

Both XA and zaprinast stimulated Ca²⁺ release in parasites in which *Pf*PDE α had been knocked out (Figure 4.20). This indicates that in the absence of *Pf*PDE α , parasites can still respond to both XA and zaprinast stimulation to release Ca²⁺. Addition of C2 reduced the XA-induced Ca²⁺ response by only ~ 30 %. This reduction in the Ca²⁺ levels was shown to be not significant (Welch's unpaired t test, P = 0.0636).

Addition of C2 to the *Pf*PDE α -ko line reduced the zaprinast-induced Ca²⁺ response by ~ 60 %. This decrease in Ca²⁺ levels was also not significant (Welch's unpaired t test, P = 0.0763). However, the more specific PKG inhibitor MRT00702065 appeared to reduce both XA and zaprinast-induced Ca²⁺ release more than C2 with a ~ 60 % and a ~ 70 % decrease reduction compared to non-PKG inhibition, respectively. The decrease in Ca²⁺ release observed with addition of MRT00702065 was shown to be significant for both XA induced Ca²⁺ mobilisation (Welch's unpaired t test, P = 0.0440) and for zaprinast-induced Ca²⁺ mobilisation (Welch's unpaired t test, P = 0.0202). The data, although preliminary, suggest that when *Pf*PDE α is absent, the Ca²⁺ released in response to both XA and zaprinast is likely to be less PKG dependent compared to the wildtype 3D7a line (See figure 4.21 for a comparison) as C2 does not significantly reverse levels of Ca²⁺ compared to that stimulated by XA or zaprinast alone. However, the reduction in Ca²⁺ levels on addition of MRT00702065 is a significant decrease. However, this may be due to an off target effect at the concentration used.

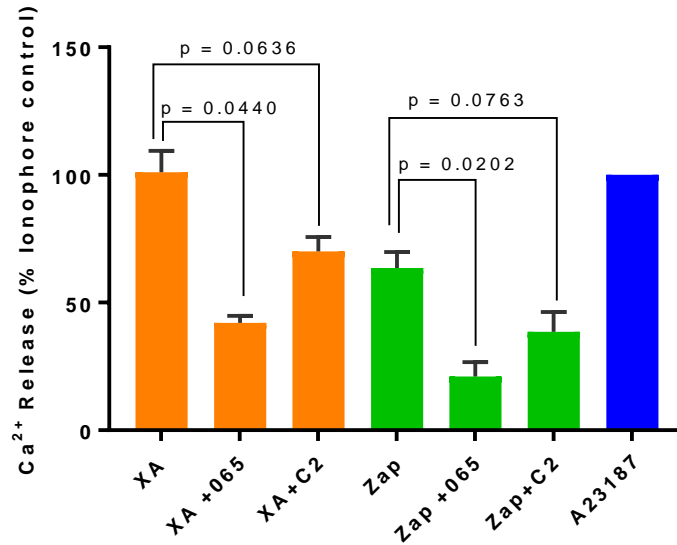


Figure 4.20. Ca²⁺ release in stage V *PfPDE*α-ko gametocytes. Parasites pre-incubated in the presence and absence of 2 μM C2 or 1 μM MRT00207065 were stimulated with XA (30 μM) and zaprinast (100 μM). Data are presented as Ca²⁺ release measured as percentage A23187 (positive control) minus the baseline fluorescence and fluorescence of the DMSO (0.05 %) control sample analysed in Excel. Bar chart was generated in GraphPad, Prism and shows the data from 1 experiment carried out in duplicate.

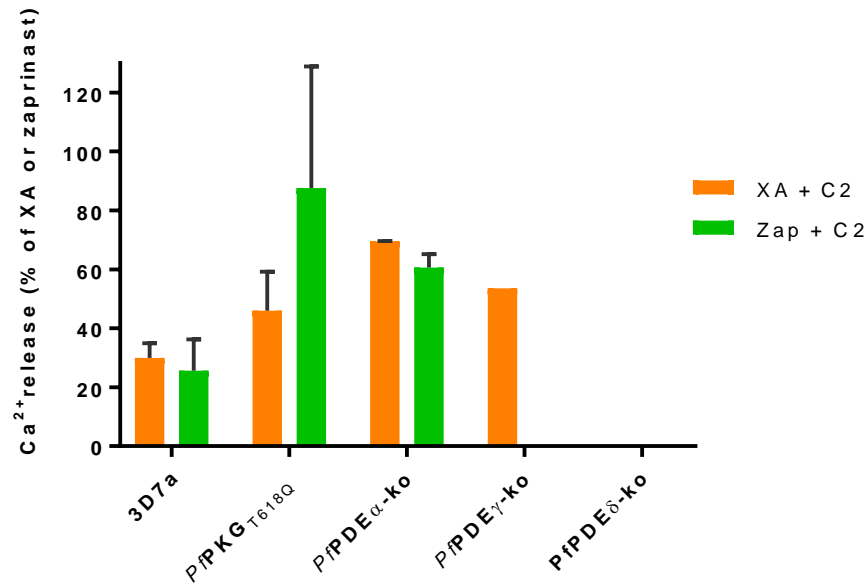


Figure 4.21. Comparison between parasite lines of the *PfPKG*-specificity of the XA and zaprinast-induced Ca²⁺ responses.

Data are from Figures 3.10, 3.11, 4.16, 4.17 and 4.18 collated and presented as percentage reduction of XA (30 μM-*PfPDE*α-ko and *PfPKG*_{T618Q}, 3 μM all other lines) or zaprinast (100 μM) induced Ca²⁺ levels on addition of C2. (Note, no XA-induced Ca²⁺ data included for *PfPDE*δ-ko). XA and zaprinast-induced Ca²⁺ release in the absence of C2 is normalised to 100 %. Bar chart was generated in GraphPad, Prism and shows the data from 3 experiments carried out in triplicate for 3D7a, 1 experiment carried out in duplicate for *PfPDE*α-ko and *PfPKG*_{T618Q}, 2 experiments carried out in triplicate for *PfPDE*δ-ko and 1 experiment carried out in triplicate for *PfPDE*γ-ko line. Error bars represent SD.

4.3. Discussion

Data presented in this chapter, although requiring further work, strongly indicate that *Pf*PDEs play an important role in regulating levels of cyclic nucleotides required for essential stages of gametogenesis including rounding up, emergence and Ca^{2+} mobilisation and also for gametocyte infected erythrocyte deformability, which is required for the circulation in the host blood stream of gametocytes primed for transmission and ready to be taken up in a blood meal.

There is evidence to suggest that *Pf*PDE δ may be essential for the process of gametogenesis (Cathy Taylor, PhD Thesis, 2007)[159]; however, the role of *Pf*PDE δ in gametocyte infected erythrocyte deformability complicates the use of this line in studies into the role of *Pf*PDE δ in subsequent processes such as rounding up and emergence from erythrocytes.

In gametocyte infected erythrocyte deformability assays, unlike the wildtype line that exhibited a deformable phenotype, stage V gametocytes of both the *Pf*PDE γ -ko and *Pf*PDE δ -ko lines were unable to pass through the microfiltration matrix. This demonstrates that these parasites were not deformable and likely exhibited a stiff phenotype. Accompanying data in this publication[25] indicated that this stiff phenotype was a result of increased levels of cAMP in the *Pf*PDE δ -ko line. Supporting this, authors showed that the overall concentration of cAMP in gametocyte infected erythrocytes decreases as parasites mature from early gametocytes to mature stage V gametocytes and that this correlates with increased deformability of these cells. In this study, a role for PDEs in deformability was shown in this process, with the PDE inhibitors sildenafil citrate and zaprinast elevating levels of cAMP in mature gametocytes and rendering them stiff. Cyclic GMP levels were also shown to be slightly elevated with these compounds. However, inhibition of *Pf*PKG using C2 did not alter retention rates of stage III or Stage V gametocytes. However, this doesn't rule out cross-talk between the cAMP and cGMP-signalling pathways which could lead to an indirect role for parasite cGMP signalling in gametocyte infected erythrocyte deformability. Cross talk between these two signalling pathways has been identified in mammalian systems and in human erythrocytes: levels of cAMP can be regulated by the cGMP-induced inhibition of the PDE that regulates cAMP, PDE3. Inhibition of PDE5, which regulates cGMP in these cells, leads to elevated levels of cAMP due to cGMP-induced inhibition of PDE3 and this leads to ATP release leading to vasodilation. This is interesting and as we predict that *Pf*PDE δ is likely to be cGMP-specific rather than dual-specific (see chapter 6 section 6.25) (despite the outcome of this publication[25]), it is tempting to speculate that perhaps the elevated levels of cGMP known to be a result of the pharmacological or genetic removal of

PfPDE δ in mature gametocyte stages, could indirectly elevate levels of cAMP (either host or parasite derived) to induce gametocyte stiffness, rather than *PfPDE δ* directly regulating levels of cAMP.

Data presented here on the deformability phenotype of the *PfPDE γ* -ko line were not included in the final manuscript[25]. These data suggest that the absence of *PfPDE γ* also impacts on the ability of gametocyte-infected erythrocytes to become deformable via direct or indirect regulation of cAMP levels. This was unexpected as *PfPDE γ* does not appear to be expressed at the mRNA level in gametocytes[25]. The ability of *PfPDE γ* to hydrolyse cAMP is not known, although there is evidence that *PfPDE γ* may hydrolyse cGMP. This was shown by a study on a transgenic line of *P. yoelii* in which *P γ PDE γ* was absent. Sporozoites of this line exhibited elevated levels (~ 18 fold higher than wildtype) of cGMP[142]. However confirmation of the deformability phenotype of the *PfPDE γ* -ko line requires further clarification. It is possible that parasites used in the assay may have been too young and were already exhibiting a stiff phenotype as a result of not reaching sufficient maturity to become deformable. Data presented in this chapter showing gamete egress assays demonstrate that stage V gametocytes lacking *PfPDE γ* can still round up and emerge normally in response to XA stimulation. This brings into doubt the evidence presented here that indicates that these parasites also show a lack of deformability. If this were the case, *PfPDE γ* -ko line gametocytes would not be expected to be able to round up in response to XA stimulation. This assay needs to be repeated and the *PfPDE γ* -ko parasite line checked.

Gamete egress assays confirmed Cathy Taylor's work (Cathy Taylor, PhD Thesis, 2007) showing that gametocytes cannot respond to XA by emerging from the host erythrocyte when *PfPDE δ* is absent (and that rounding up is also reduced). However, these data presented here show some differences to that of Cathy Taylor's work in that the majority of gametocytes (> 80 %) were unable to round up in response to XA. By contrast, data by Taylor *et al*[130], point towards an emergence phenotype rather than a rounding up phenotype (although rounding up is reduced) and show that depending on the day of induction and clonal line tested (three were tested), between ~50 % and ~80 % of *PfPDE δ* -ko line parasites will still round up in response to XA[130]. However, similarly to the results presented here, the same publication showed that the majority of gametes will not emerge[130]. This difference is interesting and may reflect the differences in the assays used to determine rounding up or possibly the clonal line or age of gametocytes used in these studies. However, despite the differences, both the work presented here and work carried out by Taylor *et al*, point towards a defect in emergence when *PfPDE δ* is absent.

Data presented in this chapter using the PKA inhibitor KT5720 have shown convincingly that if PKA is inhibited (inhibition by KT5720 is likely to target both host and parasite PKA, although, it is only assumed that it targets parasite PKA, this has not been confirmed experimentally) and it is not yet clear which is responsible for deformability) a greater proportion of the *PfPDE δ* -ko gametocytes can round up and emerge from the host erythrocyte in response to the PDE inhibitor PF9 and XA (although emergence is still greatly reduced). This suggests that the egress phenotype previously observed in this line is due in part to the inability of gametocytes to physically change their shape from a crescent to a rounded morphology and that this is due to PKA-induced stiffness as a result of the absence of *PfPDE δ* . Interestingly but unsurprisingly, a small proportion of *PfPDE δ* -ko mature gametocytes also rounded up un-stimulated when PKA was inhibited. This is unsurprising because given that *PfPDE δ* is absent in this line and it is known to have elevated levels of cGMP, it would be expected that the elevated levels of cGMP would lead to induction of gametogenesis and as a consequence, the phenotype of this line would be expected to be that of premature rounding up (with no induction) rather than no rounding up when induced with XA. Data showing induction of gametogenesis with pharmacological inhibition of PDEs (i.e. PF9 and zaprinast) support this and it has always been puzzling to observe a discrepancy between the phenotype of the *PfPDE δ* -ko line (no rounding up) and pharmacological PDE inhibition (induction of gametogenesis). This discrepancy may therefore be explained by these data presented here using PKA inhibition to prevent the 'stiff' phenotype, which suggests that when this block in deformability is removed, a proportion of *PfPDE δ* -ko stage V gametocytes can round up unstimulated. If the deformability phenotype resulting from the removal of *PfPDE δ* were not present, it may be expected that this line would round up unstimulated upon reaching maturity at stage V and perhaps it would be expected that a greatly reduced number of stage V gametocytes would be observed in cultures. It may also be expected, given other observations outlined in this report, that the absence of *PfPDE δ* would still exhibit a defect in the XA-induced response (see figure 4.22 for a schematic).

The number of *PfPDE δ* -ko line parasites rounding up un-stimulated was low. This likely reflects an essential role for *PfPDE δ* in gametogenesis and the majority of parasites may be unable to round up due to the absence of *PfPDE δ* . It may also reflect the maturity of the parasites and the subsequent requirement for other components of the cellular signalling cascade to be present in order for the signalling cascade to be complete, so rounding up may not be able to occur until gametocytes have reached full maturity. Or it may simply reflect the result of unregulated elevated levels of cGMP (or cAMP), which have essentially disrupted the parasites. It would be

interesting to observe these un-stimulated PKA-inhibited parasites over time to see if numbers of parasites rounding up increases temporally as parasites mature. It is important to note that although we know that KT5720 inhibits mammalian PKA[270] there is no concrete evidence that it will also target *Plasmodium* PKA and there is also a possibility that this inhibitor could be targeting other kinases. In mammalian cells it is known to target amongst others, the serine-threonine protein kinase Phosphoinositide-dependent kinase 1 (PDK1) which itself targets other kinases, and mitogen-activated protein kinase (MAPK)[270]. However, data presented here on the 3D7a line (Figure 4.14) indicate that this inhibitor will not induce rounding up in the wildtype line at the three concentrations tested. Therefore the rounding up that is seen in the *PfPDE* δ line is unlikely to be due to an off target effect but is likely to be a result of inhibitor-induced reversing of the 'stiff phenotype'.

Both un-stimulated and stimulated (XA and PF9) rounding up of *PfPDE* δ -ko gametocytes was reversed by pre-incubation with the PKG inhibitor MRT00207065. This indicates that both stimulated rounding up and un-stimulated rounding up in parasites devoid of *PfPDE* δ is a *PfPKG*-dependent process. This was also observed in XA treated samples and supports evidence presented in this chapter (and in the literature[159]) on rounding up and emergence. MRT00207065, although more specific for *PfPKG* than C2, may have off target effects if used at a concentration that is too high. This inhibitor is extremely active and has a low EC_{50} value of 2.1 nM, however, it's EC_{50} value on the *PfPKG*_{T618Q} parasite line (2.4 μ M), although much higher than the concentration required to inhibit the wildtype line, is still low and as such a concentration of 1 μ M may target other kinases. C2 on the other hand, has an EC_{50} value of 6 μ M on the *PfPKG*_{T618Q} parasite line so a concentration of 1 μ M C2 would be safer to use than 1 μ M MRT00207065. In light of this, it would be good to repeat these assays using a lower concentration of MRT00207065 to ensure that the potential *PfPKG*-specificity seen is real and not due to inhibition of another kinase.

Addition of PF9 or XA to PKA-inhibited samples induced a higher level of rounding up than seen in non-treated samples. In Chapter 6 (section 6.2.4.1), data are presented to demonstrate that PF9 can induce a small proportion of *PfPDE* δ -ko parasites to round up. This is very likely to be due to inhibition of a *PfPDE* other than *PfPDE* δ . This is predicted to be *PfPDE* α and it is possible that activation of PKA in this line is not 100 % sufficient to cause all parasites to become stiff and this is seen by the retention rates of the *PfPDE* δ -ko which showed ~80 % retention demonstrating that ~ 20 % of the parasites are still deformable. It is likely that this population

of cells are the ones able to round up when induced with PF9 in a PKG-dependent manner, as they are unlikely to exhibit the structural restraints that the 'stiff' cells do. In KT5720-treated *PfPDE δ* -ko gametocytes, this proportion of rounded up parasites is higher, suggesting that PKA inhibition allows more parasites to become deformable and therefore able to be induced by *PfPDE* inhibition (and PKG activation) to round up. This proportion of parasites able to round up in the PKA-inhibited *PfPDE δ* -ko line is much lower than seen in the 3D7a wildtype line with the same treatment. This is likely due to the fact that the *PfPDE δ* protein is absent from this line and is likely to be the predominant *PfPDE* required for gametogenesis (although this needs to be clarified) therefore, absence of *PfPDE δ* still significantly lowers the rounding up efficiency of gametocytes. This supports data from Cathy Taylor (Cathy Taylor, PhD, 2007) and points towards an essential role for *PfPDE δ* in the initial stages of gametogenesis. The observation of stimulated rounding up (of a small proportion of gametocytes) in the *PfPDE δ* -ko line suggests that the presence of one or more other *PfPDE*s may play a slight compensatory role (although not enough to reverse the phenotype observed). It is possible, although speculative, that *PfPDE α* may be the only other *PfPDE* expressed in the *PfPDE δ* -ko line at the protein level (although again, this requires confirmation) and may be able to help regulate levels of cGMP. It cannot be ruled out that gametogenesis could be *PfPDE δ* -regulated and involve both cGMP and cAMP and there is evidence in the literature that both of these cyclic nucleotides are elevated in the *PfPDE δ* -ko line in mature gametocytes (although elevated cAMP levels may be host derived)[130][25].

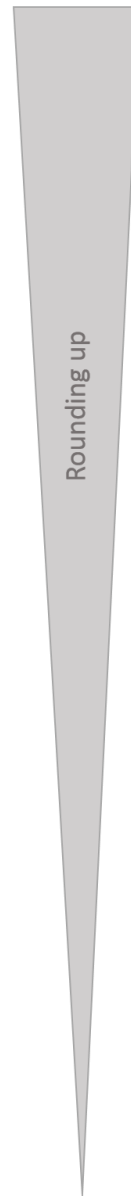
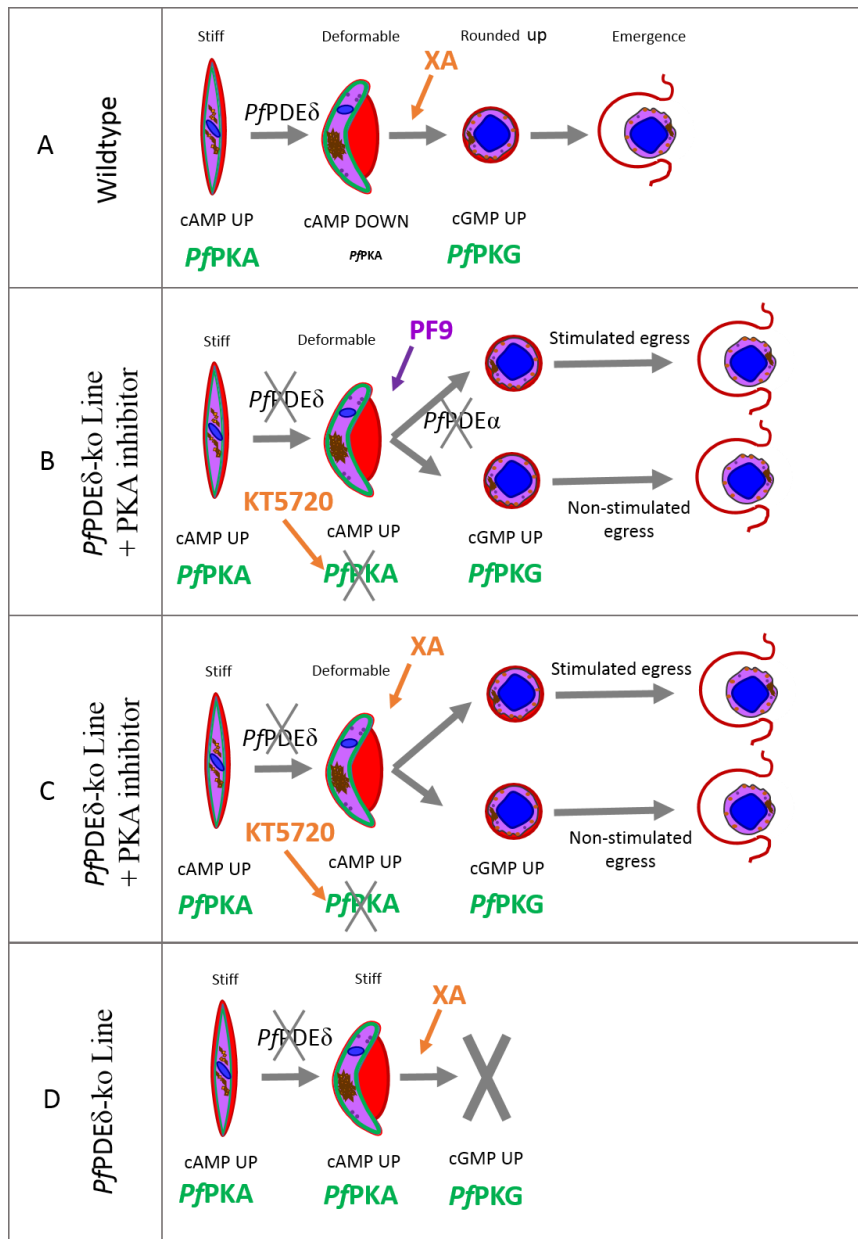


Figure 4.22. Schematic showing a model of the relationships between cyclic nucleotide signalling, *PfPDEδ*, gametocyte deformability and gametocyte rounding up and gamete emergence.

(A) In a wildtype situation, early gametocytes exhibit a 'stiff' phenotype maintained by elevated levels of cAMP, which keep *PfPKA* activated. When gametocytes reach maturity at stage V cAMP levels go down and *PfPKA* is no longer activated resulting in gametocytes becoming deformable. This is thought to require *PfPDEδ*. These parasites round up and emerge in response to XA, which stimulates elevation of cGMP levels leading to PKG activation. **(B)** and **(C)** In the *PfPDEδ*-ko line in the presence of the PKA inhibitor KT5720, both cAMP and cGMP levels remain high in stage V gametocytes. However, *PfPKA* is non-activated by the PKA inhibitor reversing the stiff phenotype. Elevated levels of cGMP leading to activation *PfPKG* as a result of the absence of the *PfPDEδ* lead to a small proportion of gametocytes rounding up unstimulated. A proportion of *PfPDEδ*-ko line gametocytes treated with KT5720 can also round up when stimulated with XA (C) or (B) PF9. PF9 likely inhibits *PfPDEα*, which may lead to rounding up via cAMP signalling. **(D)** In the *PfPDEδ*-ko line, *PfPDEδ* is absent leading to an increase in levels of both cAMP (by a *PfPDEδ*-mediated non-PKG-dependent pathway) and cGMP which do not go down once parasites reach maturity. Stage V gametocytes remain stiff and do not become deformable. This physical restriction prevents these parasites from rounding up in response to XA.

The relationship between cGMP signalling and Ca²⁺ mobilisation from internal stores in *P. falciparum* gametocytes is explored in chapter 3. The data presented in that chapter demonstrate that Ca²⁺ release in mature gametocytes can be stimulated by zaprinast in a *PfPKG*-dependent manner (and this is also seen in zaprinast-induced Ca²⁺ mobilisation in schizont stages). However, data in chapter 3 also identified that XA stimulation of Ca²⁺ release in gametocytes is more complicated and may involve both a *PfPKG*-dependent and a non-*PfPKG*-dependent component. On this basis, and particularly given the evidence that *PfPDE* inhibition by zaprinast leads to Ca²⁺ mobilisation, it was of interest to explore further the relationship between Ca²⁺ mobilisation and cGMP signalling by investigating the effect on Ca²⁺ release in mature gametocyte stages where the individual *PfPDEs* have been deleted. Observation of the absence of XA-induced Ca²⁺ mobilisation, but the presence of zaprinast-induced Ca²⁺ mobilisation in the *PfPDE*δ-ko line was very exciting. These data suggest that these two compounds may either act through different pathways or that XA may specifically require the presence of *PfPDE*δ to induce Ca²⁺ mobilisation in mature gametocytes and that zaprinast may bypass this initial interaction. Zaprinast is a broad spectrum PDE inhibitor, so in the absence of *PfPDE*δ, can induce Ca²⁺ release through inhibition of another *PfPDE* such as *PfPDE*α in a *PfPKG*-dependent manner. There is a possibility that *PfPDE*δ-ko parasites could be disrupted due to prolonged elevated levels of cGMP. The fact that zaprinast can trigger calcium release in *PfPDE*δ-ko means that the calcium release machinery is intact. However, if the proteomic data are considered, it is likely that *PfPDE*δ is only expressed at the protein level in mature gametocytes and not earlier. Therefore, if this is the case, levels of cGMP (in the *PfPDE*δ-ko line) would not likely have been elevated for long (or at all) prior to gametocytes reaching stage V. However, cAMP may be elevated for a prolonged period (possibly through synthesis by ACs) and it must be considered that parasites of the *PfPDE*δ-ko line may not be viable due to disruption. It would be of huge interest to test the viability of this line. It may be possible to do this using Alamar blue to determine whether the cells are metabolically active. It would also be of use to re-create this knockout line using a gametocyte luciferase expressing line as a background. Another interesting approach would be to make a conditional knock down line of *PfPDE*δ. This would hopefully decrease the length of time that parasite are exposed to unregulated elevated levels of cyclic nucleotides and may be a useful tool in investigating the role for *PfPDE*δ in gametocyte stages.

Elevated levels of cGMP (~2 fold and ~0.5 fold cGMP-PDE activity) have been recorded in *PfPDE*δ-ko parasites[130]. It was therefore interesting to see that *PfPDE*δ-ko line gametocytes

could respond to zaprinast by releasing Ca^{2+} . The presence of a zaprinast-induced Ca^{2+} response (which will elevate cGMP levels further) in this line indicates that these already elevated cGMP levels do not appear to affect the zaprinast response. The presence of another *PfpDE* such as the cGMP-*PfpDE*, *PfpDE* α , may reduce levels of cGMP to a low enough level that doesn't exceed the threshold required to activate *PfpPKG*. However, this is unlikely given that *PfpDE* δ -ko line gametocytes can round up un-stimulated in the presence of a PKA inhibitor (unless PKA suppresses PKG) But levels of cGMP may be reduced enough in the *PfpDE* δ -ko line that further increases in cGMP due to addition of zaprinast would still have an effect. In the *PfpDE* δ -ko line the zaprinast-induced Ca^{2+} mobilisation appeared to be *PfpPKG*-dependent as it was completely reversed by C2. It would be interesting to measure levels of cGMP in this line in the presence and absence of stimuli such as PF9, zaprinast and XA.

The absence of XA-induced Ca^{2+} mobilisation in the *PfpDE* δ -ko line is an exciting result but needs to be confirmed further. A serial dilution of XA addition to this line would identify whether this line may just require a higher concentration of XA than the wildtype line to induce a Ca^{2+} response. The concentration of XA used in this assay was very low (3 μM) and although this is the same concentration used to stimulate the wildtype line in which XA-induced Ca^{2+} mobilisation was observed, it would be of benefit to test XA on the *PfpDE* δ -ko line at a higher concentration. XA has been shown to only stimulate gametogenesis above 3 μM [26] so the concentration used should have been higher. The contrast observed between zaprinast and XA-induced Ca^{2+} release in the *PfpDE* δ -ko line was interesting and if further investigation does indeed confirm that the *PfpDE* δ -ko line cannot respond to XA-stimulation by releasing Ca^{2+} , this would suggest that the signalling components or pathways used by XA and zaprinast to induce Ca^{2+} release may differ or as suggested earlier, zaprinast may bypass the initial XA response, which is the more likely scenario. Hypothetically it may be that XA interacts specifically with *PfpDE* δ to induced Ca^{2+} release so when *PfpDE* δ is absent XA can have no effect, whereas zaprinast can inhibit *PfpDE*s other than *PfpDE* δ also, leading to Ca^{2+} mobilisation in the absence of *PfpDE* δ . This would be an extremely interesting finding. It would be interesting to use immunoprecipitated *PfpDE* δ from gametocyte stages to carry out interaction studies with XA to determine whether there is a direct interaction between *PfpDE* δ and XA. It would be also be of interest to carry out Ca^{2+} release assays on the *PfpDE* δ -ko line in the presence of the PKA inhibitor KT5720. It could be possible that the elevated levels of cAMP in the *PfpDE* δ -ko line are somehow suppressing the XA response.

As explored in other chapters in this thesis, the other *Pf*PDE predicted to be present in stage V gametocytes is *Pf*PDE α . Both XA and zaprinast induced Ca²⁺ release in parasites in which *Pf*PDE α had been deleted. This indicates that unlike *Pf*PDE δ , the presence of *Pf*PDE α is not required for the Ca²⁺ response induced by either of these compounds. Interestingly, both XA and zaprinast-induced Ca²⁺ release was reduced much less by C2 when *Pf*PDE α was absent. This assay was only carried out once and needs to be repeated to confirm the result observed, however, this preliminary data indicates that when *Pf*PDE α is absent the XA and zaprinast induced Ca²⁺ responses appear to show less *Pf*PKG dependence. This indicates that when the cGMP-specific PDE *Pf*PDE α is removed, so is most of the PKG-dependent Ca²⁺ response and that in the *Pf*PDE α -ko line, the majority of the Ca²⁺ release is not likely to be PKG-dependent, therefore XA and zaprinast ‘inhibition’ of the remaining *Pf*PDE (which is predicted to be *Pf*PDE δ based on PlasmDB data), does not result in Ca²⁺ release through a PKG-dependent pathway. This is unexpected as based on the literature[130] and data presented in this thesis (Chapter 6, section 6.2.5), it is predicted that *Pf*PDE δ is likely to be cGMP-specific and as yet there is no evidence that it directly hydrolyses cAMP. It would be interesting if possible to create a line in which both *Pf*PDE α and *Pf*PDE δ can be conditionally knocked down. In the *Pf*PDE α -ko line, the pattern of XA and zaprinast responses in regards to the effect of C2 addition were very comparable. This is interesting and may possibly reflect the differences in the way that zaprinast and XA induce gametogenesis. It would be interesting to speculate that zaprinast (which we believe likely inhibits all four *Pf*PDEs) will inhibit whatever PDEs are expressed at the protein level in stage V gametocytes to induce Ca²⁺ mobilisation, whereas XA will only specifically inhibit *Pf*PDE δ (assuming that the interaction with *Pf*PDE δ is to inhibit it). This hypothesis would account for the observation that in the *Pf*PDE α -ko line, where both compounds may only be targeting *Pf*PDE δ , the profile of XA and zaprinast-induced Ca²⁺ response is similar whereas in the *Pf*PDE δ -ko line where only zaprinast is targeting *Pf*PDE α the pattern is not comparable. MRT00207065 did significantly reduce the XA or zaprinast-induced Ca²⁺ mobilisation in the *Pf*PDE α -ko line. However, as stated earlier, this concentration may have been too high and as a consequence, could have had off-target effects. This compound needs to be used at a lower concentration in order to confirm the *Pf*PKG-specificity in this line.

Overall, these data indicate that despite the deformability phenotype clouding efforts to determine the importance of *Pf*PDE δ in rounding up of gametocytes, *Pf*PDE δ is still likely to be essential for critical events of gametogenesis such as rounding up and emergence and Ca²⁺ release (although this does require further work). Partially reversing (or fully reversing, the

effect is unknown) the 'Stiff' phenotype induced by the activation of PKA, allows a small proportion *PfPDEδ*-ko line gametocytes to round up un-stimulated and increases the number of parasites that can round up when stimulated by either XA or PDE inhibition. However, a large number of parasites are still unable to round up in response to XA or PF9 treatment when *PfPDEδ* is absent. This suggests that *PfPDEδ* may be important for this event to occur.

PfPDEs also appear to play an important role in Ca^{2+} mobilisation in mature gametocyte stages. This is particularly apparent with XA treatment and data point towards *PfPDEδ* playing an essential role in XA-induced Ca^{2+} release and interestingly, *PfPDEα*, although dispensable for both XA and zaprinast-induced Ca^{2+} mobilisation, appears to contribute to most of the *PfPKG* specificity of the Ca^{2+} response.

Although exciting data, much of this is speculative and more work needs to be done to dissect and understand more the role that *PfPDEs* play in the process of gametogenesis. However, this work has forced a spotlight onto *PfPDEδ* as a *PfPDE* that is worth investigating further.

Chapter 5

The mode of action of a gametocytocidal PDE inhibitor

5.1. Introduction

In the fight against malaria, it is essential that drug discovery efforts continue because although there are some promising clinical candidates undergoing testing, drug attrition rates are high. Understanding the biology of the parasites that cause malaria is essential to discovering new and unique drug targets that can result in production of new candidates to enter the drug discovery pipeline. The combined efforts of chemists, developing new compounds against these targets and of biologists, testing such compounds against the parasite, is an invaluable part of the drug discovery process.

PDE inhibitors have been used successfully as drugs to treat a number of medical issues in humans such as roflumilast to treat severe chronic obstructive pulmonary disease[271], pentoxifylline to treat muscle pain in patients with peripheral vascular disease[272] and Viagra to treat erectile dysfunction[273]. This success and the increasing literature emphasising the importance of cyclic nucleotide signalling in *Plasmodium* species has sparked a growing interest in *Plasmodium* PDEs as potential drug targets. Several human PDE inhibitors have been used as tools in numerous malaria parasite biology studies. IBMX (3-isobutyl-1-methylxanthine), a broad-spectrum human PDE inhibitor, has been reported to enhance exflagellation events[274]. Caffeine another broad-spectrum PDE inhibitor has been shown to induce both gametogenesis[275][276] and gametocytogenesis[277][243]. Despite these observations in sexual stages, investigations into the inhibition of *P. falciparum* PDE enzyme activity in both asexual and sexual stage parasite lysates showed little or no activity for either of these compounds (Ross Cummings, PhD Thesis, 2005). The lack of IBMX activity on *P. falciparum* PDEs has been further confirmed using ^3H incorporation assays on live parasites, with IBMX showing no activity ($>100\ \mu\text{M}$) against asexual stages (Laura Drought, PhD Thesis, 2014). This confirmed previous data by Yuasa *et al*, who found no inhibition of parasite growth of *P. falciparum* by IBMX even at $100\ \mu\text{M}$ [143]. Zaprinast was the first human PDE inhibitor identified as being active against malaria parasite PDEs and was shown to inhibit cGMP *Pf*PDE activity in membrane fractions of mixed asexual stages with an IC_{50} of $4\ \mu\text{M}$ [143]. This compound also showed good inhibitory properties against both cAMP *Pf*PDE enzyme activity (IC_{50} $12\ \mu\text{M}$) and cGMP *Pf*PDE enzyme activity (IC_{50} $3\ \mu\text{M}$) in schizont stages and good cGMP hydrolytic activity in ring stages

(3.5 μM)[143]. Unlike most other human PDE inhibitors tested, zaprinast also showed activity against *P. falciparum* gametocyte cGMP-PDE activity (34 μM) (Ross Cummings, PhD Thesis, 2005).

Since then, zaprinast has been shown to induce premature blood stage merozoite egress in *P. falciparum*[173]. It can also be used to induce gamete egress (gametogenesis) when added to *P. falciparum* stage V gametocytes with the whole process from rounding up and emergence to male exflagellation being observed, in the absence of XA[159]. Zaprinast also exhibits good inhibitory activity against PDEs of the related apicomplexan *T. gondii*[278]. From this collection of studies, zaprinast has emerged as a good PDE inhibitor that targets all blood stream stages of *P. falciparum*, and represents a good starting point to develop more effective *Plasmodium* PDE inhibitors.

Sildenafil citrate (known by the commercial name Viagra) targets human PDE5[273] and was originally developed to treat pulmonary heart disease[137]. It is now widely used to treat male erectile dysfunction. This PDE inhibitor and related inhibitors such as tadalafil which is also used to treat pulmonary arterial hypertension[279]:[280], have been shown to impact on *P. falciparum* gametocyte deformability?[25]:[281]. However, these inhibitors are less active than zaprinast on native gametocyte PDE activity (Ross Cummings, PhD Thesis, 2005)[25]. Sildenafil citrate (SC) is less effective at inducing rounding up with only $\sim 30\%$ rounding up in response to 400 μM SC treatment and 800 μM SC required to induce 70 % of rounding up. In similar assays, 400 μM of zaprinast induced $\sim 100\%$ of the wildtype line to round up (Cathy Taylor, PhD Thesis, 2007). Sildenafil citrate is also less effective at inducing egress in *P. falciparum* stage V gametocytes compared to XA (Cathy Taylor, PhD Thesis, 2007 and my data not included).

The PDE inhibitor BIPPO (5-benzyl-3-isopropyl-1H-pyrazolo[4,3-d]pyrimidin-7(6H)-one)[282] was developed along with several others based on the structures of existing human PDE1 and PDE9 inhibitors as these human PDEs (hPDEs) show greatest homology to *Plasmodium* PDEs. BIPPO was found to inhibit recombinant *Pf*PDE α with an IC_{50} value of 150 nM, a much more potent activity than the 5 μM IC_{50} of zaprinast. BIPPO was shown to have high activity (IC_{50} 0.4 μM) exceeding that of zaprinast on *P. falciparum* asexual blood stages. It also exhibited better inhibitory activity than zaprinast against tachyzoites of *T. gondii* with an IC_{50} of 2 μM [282]. As observed with zaprinast[283]:[173], BIPPO also induced egress of *T. gondii* tachyzoites and *P. falciparum* blood stage schizonts[282]. This inhibitor is an effective and useful tool for investigating cell signalling pathways and the related cellular events in both *P. falciparum* and *T. gondii*. However, as BIPPO has a higher potency against human PDEs (hPDE1, hPDE5, hPDE6 and hPDE9) with an IC_{50} value of 30 nM against recombinant hPDE9 and inhibition of 42 %, 66 % and

64 % at 1 μ M against recombinant hPDE1, hPDE5 and hPDE6 protein respectively[282], it cannot be used as a drug to treat patients with malaria. Nevertheless, the work carried out with zaprinast and BIPPO to identify their activity in apicomplexan parasites demonstrates that human PDEs are a good starting point for the design of drugs that specifically target apicomplexan PDEs. In fact, a good example of how compounds can be altered to develop similar compounds with slightly different properties is the work done by Beghyn *et al*, who altered the structure of tadalafil with the aim to produce new analogues with improved biochemical properties and selectivity for malaria parasites[284].

A very large number of PDE inhibitors have been developed by chemists at Pfizer. Five of these were selected to be tested against *P. falciparum* blood stages and exhibited sub- μ M inhibitory activity against asexual blood stages. One of these inhibitors exhibited potency of around 1000-fold higher than that of zaprinast (Laura Drought, PhD Thesis, 2014) against mixed *P. falciparum* asexual blood stages.

This chapter focuses on the testing of these five Pfizer PDE inhibitors against the gametocyte stages of *P. falciparum*. Elucidation of the mechanism of action against transmission stages, although not a priority for drug discovery in the past, has now emerged as an important focus of drug discovery efforts in the malaria elimination/eradication era. It has now been recognised that elimination/eradication cannot be seriously considered without breaking the cycle of transmission (also targeting the transmission stages). Currently available antimalarial drugs alleviate clinical symptoms of the disease by killing asexual blood stages. However, these drugs have no inhibitory effect on mature gametocytes, enabling these stages to continue the parasite life cycle through mosquitoes and back to a new human host, thus maintaining malaria transmission within the population. As noted in the introduction, primaquine is the only currently licenced antimalarial that targets mature gametocytes and use of this drug is limited due to its toxicity in people with G6PD deficiency[66] and its poor activity against *P. falciparum* blood stages[285].

5.2. Results

5.2.1. The human PDE inhibitor PF9 shows potent activity against mature *P. falciparum* gametocytes

The panel of five Pfizer human PDE inhibitors were tested against immature (stage II/III) and mature (IV/V) gametocytes from a 3D7a transgenic line (3D7*elo1-pfs16*-CBG99) expressing luciferase under the control of the sexual stage specific *pfs16*-gene promoter[264] in a gametocyte viability assay. Pfs16 is the earliest marker for the onset of gametocytogenesis and is expressed from the committed ring stage through to stage V gametocytes[286]. Separate assays were carried out on both purified stage II gametocytes and purified stage V gametocytes expressing luciferase. This luciferase (CBG99 from the click beetle *Pyrophorus plagiophthalmus*[264]) catalyses the oxidation of its substrate, D-luciferin, releasing photons in the visible light spectrum that can then be measured. As the luciferase expressed is dependent upon ATP to produce light, this assay can be used as an indicator of cell viability. This assay is further improved by the use of a D-luciferin substrate solution developed by L. Cevenini *et al*[264], which is nontoxic and does not cause cell lysis (see methods section 2.4.C for more details).

EC₅₀ values for inhibition of asexual blood stage replication had previously been determined for these compounds using a 72 hour ³[H] hypoxanthine assay which utilises incorporation of ³[H] into newly synthesised DNA in replicating cells[287] (Laura Drought, PhD Thesis, 2014). As gametocytes do not undergo DNA replication (until male gametogenesis in the mosquito), this gold standard assay, or any other assay based on DNA replication, cannot be used to determine gametocyte survival. Therefore, a luciferase expressing gametocyte-producing line[264] was used to determine possible gametocytocidal activity of these PDE inhibitors using measurement of luminescence (RLUs) as a quantitative indicator of cell survival.

Table 5.1 shows the EC₅₀ values (μM) of the 5 Pfizer compounds tested in the luciferase assay against both immature (II/III) and mature (IV/V) gametocyte stages. These values are compared in the table to the EC₅₀ values of the same compounds tested on asexual erythrocyte stages in a previous ³[H] assay (Laura Drought, PhD Thesis, 2014).

As shown in Figure 5.1, after 48 hours incubation, the compounds PF9, PF11, PF12 and PF14 showed no inhibition of immature stage gametocyte viability even at the highest concentration

tested (10 μ M). This indicates that *Pf*PDEs are either not expressed, not active or their activity not essential in immature stage gametocytes or that these drugs do not target the PDE(s) that are expressed at these stages. PF10 appeared to show a small amount of inhibition of early gametocyte stage viability (12.8 %) at 10 μ M (Figure 5.1 and Figure 5.2). However, this inhibition was only observed in one of the three experiments carried out on immature gametocyte stages. The only compound exhibiting inhibition of mature (stages IV/V) gametocyte viability was compound PF9 (Figures 5.3 and Figure 5.4). PF9 did not show any activity against immature stages but showed potent activity ($EC_{50} \sim 60$ nM) against mature gametocyte stages. Interestingly, this EC_{50} was almost three times lower than the EC_{50} against asexual stage parasites.

Overall, the data indicate that PF9 targets a *Pf*PDE that is essential in stages IV and/or V gametocytes. Both *Pf*PDE α and *Pf*PDE δ have been identified by proteomics in stage V gametocytes. Existing proteome data suggests that *Pf*PDE α is the most abundant protein in late gametocyte stages, whereas, transcriptomic data[145] indicates that *Pf*PDE δ is the most abundant isoform expressed in late gametocyte stages. However, as the proteomics are not absolutely quantitative, a higher spectral count does not necessarily imply that *Pf*PDE α is more abundant and the presence of mRNA transcripts does not necessarily indicate that translation occurs and in fact, transcripts can be translationally repressed in gametocytes and this is particularly apparent in female gametocytes[144]. This suggests that one or both of these *Pf*PDEs are the most likely targets of PF9 in mature sexual stages. The *Pf*PDE target of PF9 will be investigated in the next section.

Pfizer PDE Inhibitors Luciferase Assay EC ₅₀ values (μM)			
Compound	Average EC ₅₀ Asexual stages	Average EC ₅₀ Immature Gametocytes	Average EC ₅₀ Mature Gametocytes
	μM	μM	μM
PF-01273175 (PF9)	0.14	>10	0.0521 (± 0.412)
PF-05184913 (PF10)	0.16	>10	>10
PF-05225388 (PF11)	0.01	>10	>10
PF-00394183 (PF12)	0.08	>10	>10
PF-00388991 (PF14)	0.03	>10	>10

Table 5.1. EC₅₀ values (μM) of 5 Pfizer PDE inhibitors in a gametocyte viability assay. These were tested against both immature (stage II/III) gametocytes and mature (IV/V) gametocytes (of the 3D7*elo1*-*pfs16*-CBG99 parasite line) in a luciferase-based cell viability assay. The average of 3 technical replicates from 3 experiments are shown ± SD). EC₅₀ values were generated in GraphPad Prism and compared to EC₅₀ (μM) values on asexual blood stages in a ³[H] incorporation assay (Laura Drought, PhD Thesis, 2014). The compound showing activity against mature gametocytes is highlighted in grey.

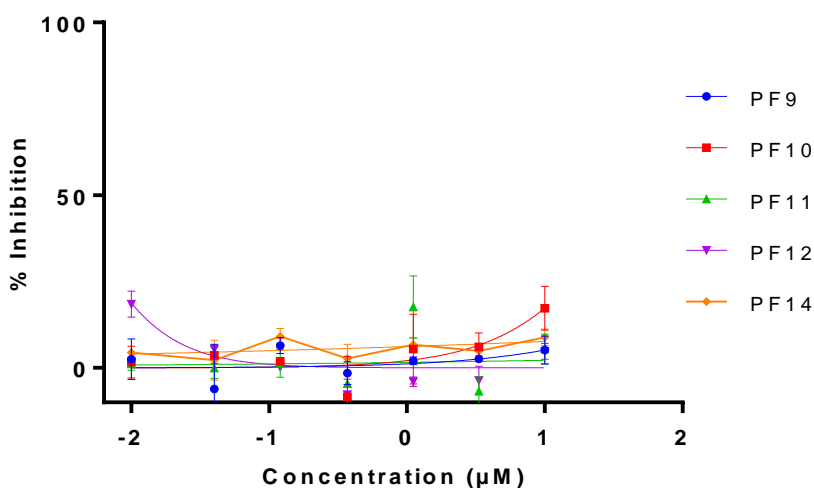


Figure 5.1. EC₅₀ (μM) values of Pfizer PDE inhibitors tested against immature *P. falciparum* 3D7*elo1*-*pfs16*-CBG99 gametocyte stages (II/III) in a gametocyte viability assay. EC₅₀ values measured from a (1:3) serial dilution in complete media from a starting concentration of 10 μM (stock diluted in DMSO). Data are transformed and presented as percentage inhibition of 3D7*elo1*-*pfs16*-CBG99 (luciferase expressing) *P. falciparum* parasites by the compounds relative to a no inhibitor (DMSO 0.05 %) control from a single biological replicate assay performed in triplicate (a representative experiment is presented). Percentage inhibition values calculated in Excel. The graph was generated in GraphPad Prism. Error bars represent SEM.

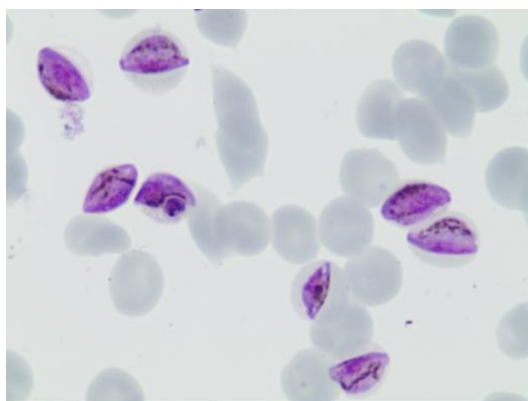


Figure 5.2. Representative image of a Giemsa-stained blood film taken prior to the start of an immature stage gametocyte luciferase assay. Parasites are the characteristic 'half-moon' shape of stage II.

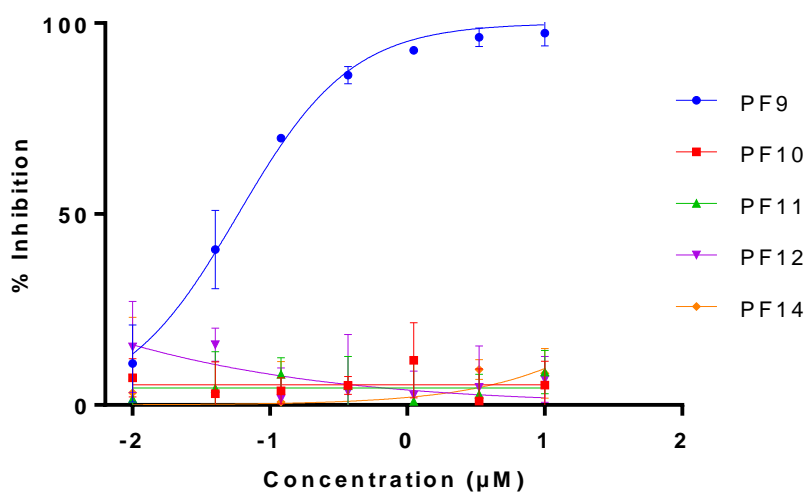


Figure 5.3. EC₅₀ (μM) values of Pfizer PDE inhibitors tested against mature *P. falciparum* 3D7elo1-pfs16-CBG99 gametocyte stages (IV/V) in a gametocyte viability assay. EC₅₀ values measured from a (1:3) serial dilution in complete media from a starting concentration of 10 μM (stock diluted in DMSO). Data are transformed and presented as percentage inhibition of 3D7elo1-pfs16-CBG99 (luciferase expressing) *P. falciparum* parasites by the compounds relative to a no inhibitor (DMSO 0.05 %) control from a single biological replicate assay performed in triplicate (a representative experiment is presented). Percentage inhibition values calculated in Excel. The graph was generated in GraphPad Prism. Error bars represent SEM.

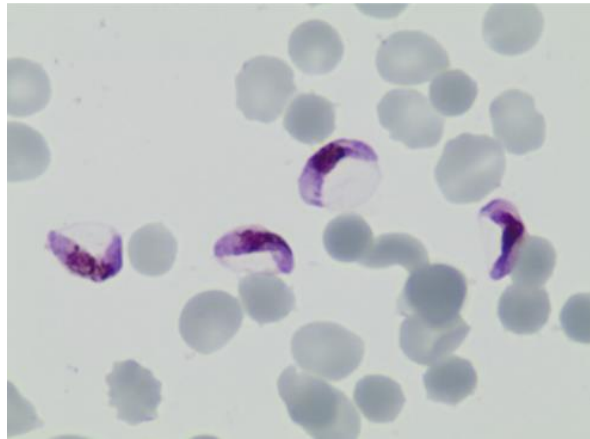


Figure 5.4. Representative image of a Giemsa-stained blood film taken prior to the start of a mature stage gametocyte viability assay. Parasites appear as the characteristic ‘crescent’ shape of stage V gametocytes.

5.2.2. Investigation of the PDE target of Pfizer 9

Data from section 5.2.1 show that PF9 targets mature gametocyte stages specifically. This leads to the question of which *Pf*PDE or *Pf*PDEs, this inhibitor targets in mature gametocyte stages. PF9 is known to target human PDE9 and current data suggest it targets both *Pf*PDE α and *Pf*PDE β in asexual blood stages (Laura Drought, PhD Thesis, 2014). These data were derived from comparing PDE inhibition data from the *Pf*PDE α -ko and wild type blood stage parasites and also from a *Pf*PDE β conditional knockout line (Drought, Flueck *et al.*, LSHTM, unpublished data), However, no experiments had been carried out to investigate the effects of PF9 on gametocyte stages from these lines or on gametocytes from the PDE δ -ko or *Pf*PDE γ -ko lines and so the *Pf*PDE target of PF9 in gametocytes is not known. Based on what we already know from the literature, we would hypothesise that the main target for PF9 in gametocytes is *Pf*PDE δ . This is because we know that *Pf*PDE δ is highly expressed in mature gametocytes at the mRNA level and more importantly, is detectable at the protein level[144] and there is evidence that *Pf*PDE δ is required for the process of gametogenesis[130]. However, this needs confirmation and currently, the role of other *Pf*PDEs in mature gametocyte stages cannot be ruled out. It has been shown that the *Pf*PDE α protein is present in gametocytes[144] and is known to specifically hydrolyse cGMP[141].[143]. However, gametocyte growth and development appear normal in a *Pf*PDE α

knock out line (my data, unpublished), indicative that *PfPDE α* alone is not essential for gametogenesis or gametocytogenesis to occur. Therefore, *PfPDE α* is unlikely to be the sole or main target of PF9 in mature gametocytes as PF9 targeting of *PfPDE α* alone would not be expected to result in the level of inhibition of gametocyte viability seen in luciferase assays (section 5.2.1). But that is not to say that inhibition of *PfPDE α* wouldn't contribute to the overall inhibitory activity of PF9 in the gametocyte and it does not rule out a role for *PfPDE α* in gametocyte stages. *PfPDE α* is also dispensable for asexual blood stage growth[141]. Another possible, but less likely candidate is *PfPDE γ* . *PfPDE γ* mRNA but not protein has been detected at low levels in gametocytes[145] and gametocytogenesis and gametogenesis are not affected in a *PfPDE γ* -ko line (Cathy Taylor PhD Thesis, 2007), suggesting that *PfPDE γ* is not essential in gametocyte stages. However, *PfPDE γ* has been shown to be important for *P. falciparum* sporozoite motility[142], so it may well be a dominant target for PF9 in sporozoite stages. This would be interesting to investigate in the future.

PF9 kills mature NF54 gametocytes in a PKG-dependent manner

To investigate the *PfPDE* target of PF9 in sexual stages, *PfPDE α* (Christian Flueck, LSHTM, unpublished), *PfPDE δ* and *PfPDE γ* knockout lines all with a 3D7a background (Cathy Taylor PhD Thesis, 2007) and an NF54 line were used in a PF9 dose response assay. Stage IV/V gametocytes were incubated for 12 hours with 0.2 μ M, 2 μ M and 20 μ M PF9. The *PfPKG* dependence (and therefore the cGMP specificity) of PF9 activity was also investigated using the *PfPKG* inhibitor compound 2 (C2). Percentage parasitaemia was calculated by counts of Giemsa stained blood films. Test samples were compared to a DMSO control.

In an NF54 control line, PF9 treatment resulted in an almost complete reduction in mature gametocyte numbers at the highest concentration of 20 μ M (Figures 5.5 and 5.9) with less than 5 % of stage V gametocytes counted when normalised to the DMSO control (Table 5.2). At a concentration of 2 μ M PF9 also showed a good reduction of gametocyte numbers in the NF54 line with an ~85 % reduction in gametocytemia after 12 hours (Figure 5.5 and Table 5.2). Remarkably, reduction in numbers of NF54 gametocytes at both 20 μ M and 2 μ M was almost completely reversed by adding the PKG inhibitor C2 (2 μ M) (see Figure 5.9 for a comparison of PF9 treatment on the four lines tested). This indicates that PF9 activity on the NF54 line is *PfPKG*

dependent and strongly suggests that that PF9 inhibits cGMP-specific *Pf*PDE activity in mature gametocytes to elevate cGMP levels and prematurely activate *Pf*PKG.

At the lower concentration of 0.2 μ M, PF9 did not appear to reduce NF54 stage V gametocytemia, with comparable numbers of crescent shaped gametocytes in the no DMSO control (Figure 5.5, Table 5.2). This was initially surprising given the IC_{50} value of ~ 0.060 μ M seen in luciferase assays. However, this may reflect strain specific differences or differences in experimental design i.e. length of exposure to the compound, but is likely to reflect the different read out of the two assays, i.e. cell viability in the luciferase assays by measurement of ATP verses the less sensitive method of quantification of counts of cells by microscopy which is not necessarily an indication of viability.

In all samples, a population of cells exhibiting an abnormal morphology (Figure 5.5 red bars) were present. From here on, these will be referred to as abnormal cells. Numbers of these abnormal cells were higher in samples treated with 0.2 μ M PF9 and 2 μ M PF9 (Figure 5.5). The percentages of abnormal cells in these samples were ~ 30 % and ~ 75 % respectively. C2 treatment appeared to reduce the numbers of abnormal cells observed. In samples treated with 20 μ M PF9, the % parasitaemia of abnormal cells was less than seen in samples treated with lower concentrations of PF9, but exceeded that of cells appearing with a normal morphology (stage IV/V gametocytes) with ~ 76 % of the total number of cells counted being abnormal. C2 did not appear to reduce the number of abnormal cells counted in samples treated with 20 μ M PF9.

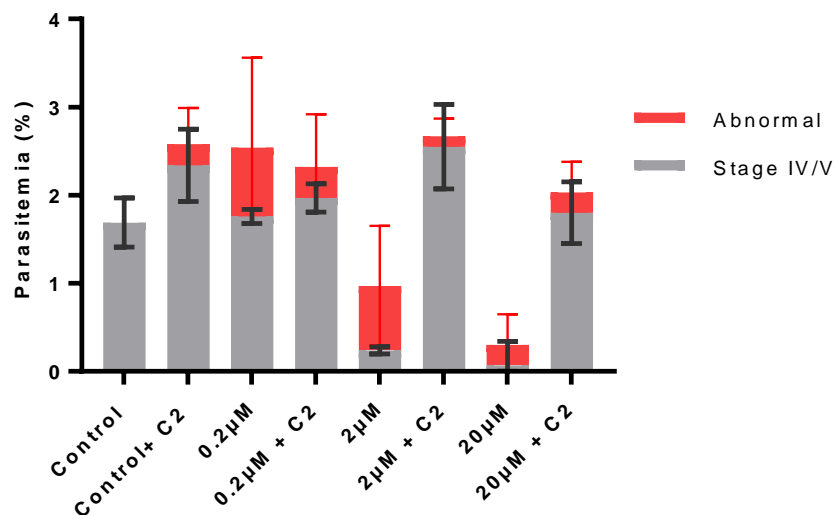


Figure 5.5. Parasitaemia of stage IV/V NF54 gametocytes treated with PF9. NF54 line samples incubated for 12 hours 37 °C/CO₂ with 20 μM, 2 μM and 0.2 μM PF9 +/- C2 (2 μM). Data are presented as percentage parasitaemia of stage IV/V gametocytes compared to unusual shaped gametocytes (abnormal). Numbers of abnormal cells in the control sample are subtracted from all other samples. Data analysed in Excel is 3 independent counts (900 cells counted per replicate) from one experiment. Graph is generated in GraphPad, Prism. Error bars represent SD.

PF9 kills *PfPDEγ*-ko gametocytes in a *PfPKG*-dependent manner

Addition of PF9 to mature *PfPDEγ*-ko gametocytes showed comparable results to those obtained with NF54 gametocytes (see Figure 5.9 for a comparison between lines). Both 20 μM and 2 μM concentrations of PF9 resulted in complete disappearance of stage V gametocytes from samples within 12 hours of incubation (Figure 5.6). 0.2 μM PF9 reduced the parasitaemia to ~ 70 % compared to the DMSO control. This is a higher reduction in parasitemia than seen in the NF54 line (Table 5.2) and may reflect differences between parasite lines since the *PfPDEγ*-ko line is derived from a 3D7a background. PF9 inhibition in the *PfPDEγ*-ko was shown to be *PfPKG* dependent as gametocytes survived in the presence of PF9 if the *PfPKG* inhibitor C2 was also present (Figures 5.6 and 5.9). The difference between PF9 treatment in the presence and absence of C2 was shown to be significant at 20 μM, 2 μM and 0.2 μM using the Holm-Sidak method (GraphPad, Prism), which gave P values of P=0.00000015, P=0.000043 and P=0.01444 respectively. This indicates that the absence of *PfPDEγ* in mature gametocyte stages appears to have no effect on PF9 activity and that PF9 is achieving its killing effect independently of *PfPDEγ*. A population of abnormal cells was observed in *PfPDEγ*-ko samples treated with PF9 (Figure 5.6 red bars). Numbers of abnormal cells were much lower than seen in the NF54 line. In samples

treated with 0.2 μM PF9, numbers of abnormal cells constituted less than $\sim 20\%$ of the total parasitaemia counted. In samples treated with 2 μM over half of cells counted were abnormal in morphology, constituting $\sim 59\%$ of the total parasitaemia. In samples treated with 20 μM PF9, the majority of cells counted were abnormal ($\sim 95\%$ of the total parasitaemia). In both the 2 μM and 20 μM treated samples, C2 completely reversed the presence of cells exhibiting an abnormal morphology. In contrast, C2 did not appear to alter the numbers of abnormal parasites observed in samples treated with 0.2 μM .

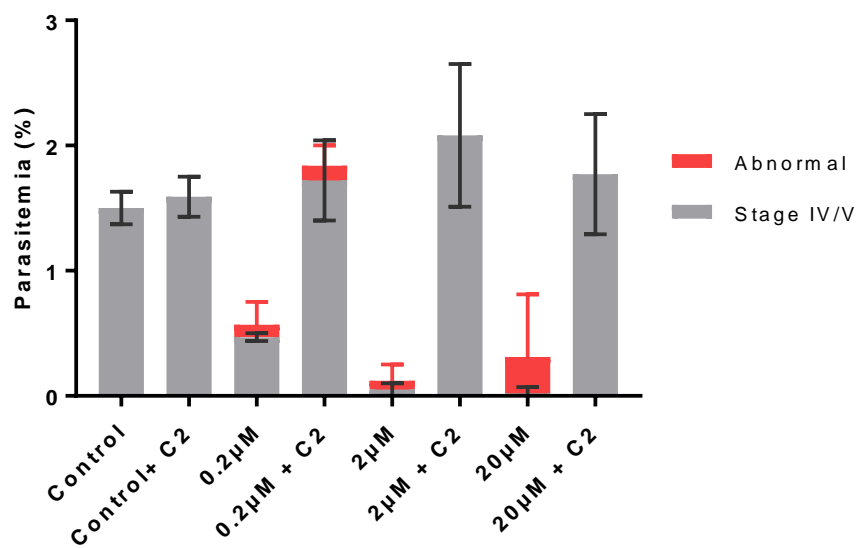


Figure 5.6. Parasitaemia of stage IV/V *PfPDE γ* -ko line gametocytes treated with PF9. *PfPDE γ* -ko line samples incubated for 12 hours 37 $^{\circ}\text{C}/\text{CO}_2$ with 20 μM , 2 μM and 0.2 μM PF9 +/- C2 (2 μM). Data is presented as percentage parasitaemia of stage IV/V gametocytes compared to unusual shaped gametocytes (abnormal). Number of abnormal cells in the control sample are subtracted from all other samples. Data analysed in Excel is the average of two experiments each with 3 independent counts (900 cells counted per replicate). Graph is generated in GraphPad, Prism. Error bars represent SD.

***PfPDE* α -ko gametocytes are apparently more sensitive to PF9 than the *PfPDE* γ -ko line, the *PfPDE* δ -ko line and NF54**

Stage V gametocytes of the *PfPDE* α -ko line showed high sensitivity to all concentrations of PF9 tested (Figure 5.7 and 5.9). This was particularly apparent at the lowest concentration of 0.2 μ M PF9, which resulted in complete disappearance of crescent-shaped cells with a small proportion (~0.1 % parasitemia) of abnormal forms remaining. Gametocyte numbers were reversed back to control levels by addition of C2. 2 μ M PF9 also resulted in complete disappearance of crescent shaped gametocytes and as seen at 0.2 μ M, this was reversed back to control levels by addition of C2. At a concentration of 20 μ M, numbers of crescent shaped gametocytes were reduced almost completely. However, in contrast to the lower concentrations of PF9 tested, this reduction in parasitemia was not reversed back to control levels by C2 indicating a possible toxic effect at this concentration in this line. C2 treatment reversed gametocyte numbers to ~ 30 % of the control.

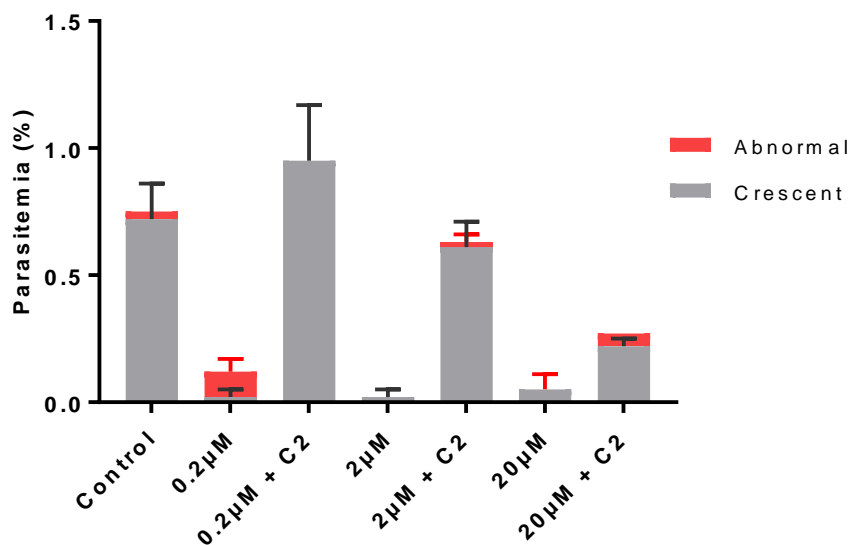


Figure 5.7. Parasitaemia of stage IV/V *PfPDE* α -ko line gametocytes treated with PF9. *PfPDE* α -ko line samples incubated for 12 hours 37 $^{\circ}$ C/CO₂ with 20 μ M, 2 μ M and 0.2 μ M PF9 +/- C2 (2 μ M). Data is presented as percentage parasitaemia of stage IV/V gametocytes compared to unusual shaped gametocytes (abnormal). Number of abnormal cells in the control sample are subtracted from all other samples. Data analysed in Excel is 3 independent counts (900 cells counted per replicate) from one experiment. Graph is generated in GraphPad, Prism. Error bars represent SD.

PF9 does not alter the parasitemia or morphology of stage V gametocytes of the *PfPDE δ* knockout line

Interestingly, in contrast to the results obtained with NF54 and *PfPDE γ* -ko cultures, mature *PfPDE δ* -ko gametocyte survival was very pronounced in the presence of PF9 (Figure 5.8, see Figure 5.9 for a comparison between lines). PF9 appeared to show some killing of *PfPDE δ* -ko gametocytes at both 20 μ M and 2 μ M (60 % and 70 % of parasites counted in PF9 treated samples respectively compared to the DMSO control normalised to 100 %). However, this decrease in parasitaemia in the PF9 treated samples was not significant in both cases using a Welch's unpaired t test, which was used to compare the percentage parasitaemia of PF9-treated samples to the percentage parasitaemia of the DMSO control with P values of P=0.1161 and P=0.0809 respectively. As seen with the data obtained from the NF54 line, no reduction in gametocyte numbers was observed at a PF9 concentration of 0.2 μ M (Figure 5.9). Very few gametocytes exhibiting an abnormal morphology were observed in *PfPDE δ* -ko line samples compared to the NF54 line and the *PfPDE γ* -ko line (Figure 5.9). The majority of all cells counted were normal looking crescent shaped gametocytes. Addition of C2 did not alter the parasitemia at any of the concentrations. Figure 5.9 shows a comparison of all lines at each concentration of PF9.

Overall, these data suggests that PF9 is much less effective at reducing the parasitemia of gametocyte samples when *PfPDE δ* is absent. This indicates that the presence of *PfPDE δ* is likely required for the majority of PF9 activity and may be the main target of PF9. It also demonstrates that the absence of *PfPDE γ* does not alter PF9 activity at all whereas, in the absence of *PfPDE α* , parasites become more sensitive to PF9. These data indicates that PF9 mediated killing of mature gametocytes is *PfPKG*-dependent.

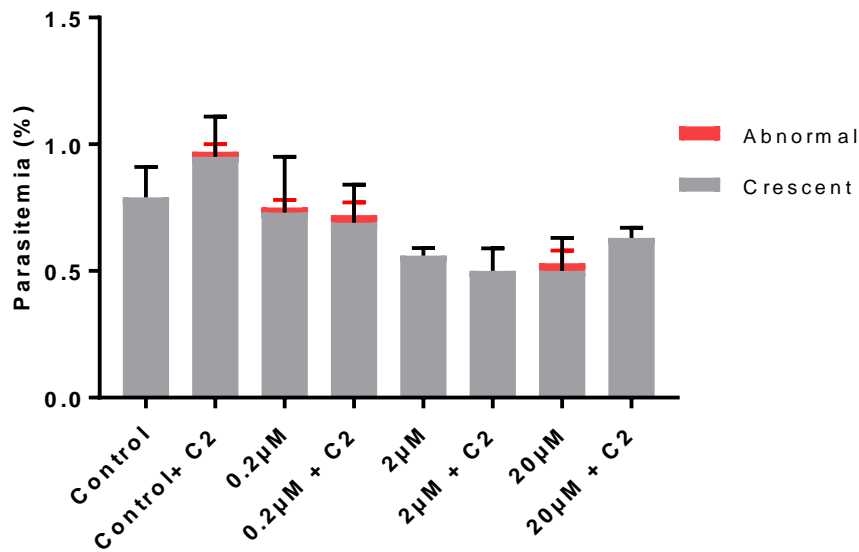


Figure 5.8. Parasitaemia of stage IV/V *PfPDEδ*-ko line gametocytes treated with PF9. *PfPDEδ*-ko line samples incubated for 12 hours 37 °C/CO₂ with 20 μM, 2 μM and 0.2 μM PF9 +/- C2 (2 μM). Data is presented as percentage parasitaemia of stage IV/V gametocytes compared to unusual shaped gametocytes (abnormal). Number of abnormal cells in the control sample are subtracted from all other samples. Data analysed in Excel is 3 independent counts (900 cells counted per replicate) from one experiment. Graph is generated in GraphPad, Prism. Error bars represent SD.

	Stage V gametocytes (% of Control ± SD)			
	NF54	<i>PfPDEγ</i> -ko	<i>PfPDEδ</i> -ko	<i>PfPDEα</i> -ko
	Average (SD)			
Control	100	100	100	100
Control + C2	160.05 ± 46.92	82.96 ± 15.75	135.60 ± 20.93	-
PF9 0.2 μM	106.94 ± 24.73	73.52 ± 24.67	103.71 ± 26.96	2.26 ± 3.92
PF9 0.2 μM + C2	118.14 ± 21.59	130.61 ± 60.48	97.72 ± 18.60	130.67 ± 6.84
PF9 2 μM	14.32 ± 0.92	0	59.63 ± 18.54	2.06 ± 3.56
PF9 2 μM + C2	151.24 ± 11.45	102.85 ± 20.93	59.17 ± 3.70	88.01 ± 31.64
PF9 20 μM	3.97 ± 4.77	0	72.29 ± 20.35	7.17 ± 1.89
PF9 20 μM + C2	107.80 ± 11.19	119.50 ± 30.37	92.01 ± 7.14	30.98 ± 4.46

Table 5.2. Counts of NF54, *PfPDEγ*-ko and *PfPDEδ*-ko gametocytes treated with PF9 ± C2. Data is the average and SD of 3 separate counts from one experiment presented as the percentage of the DMSO control normalised to 100 %. Values above 60 % of the control (little or no inhibition) represented in dark grey. Values below 20 % of the control (Good inhibition) represented in light grey.

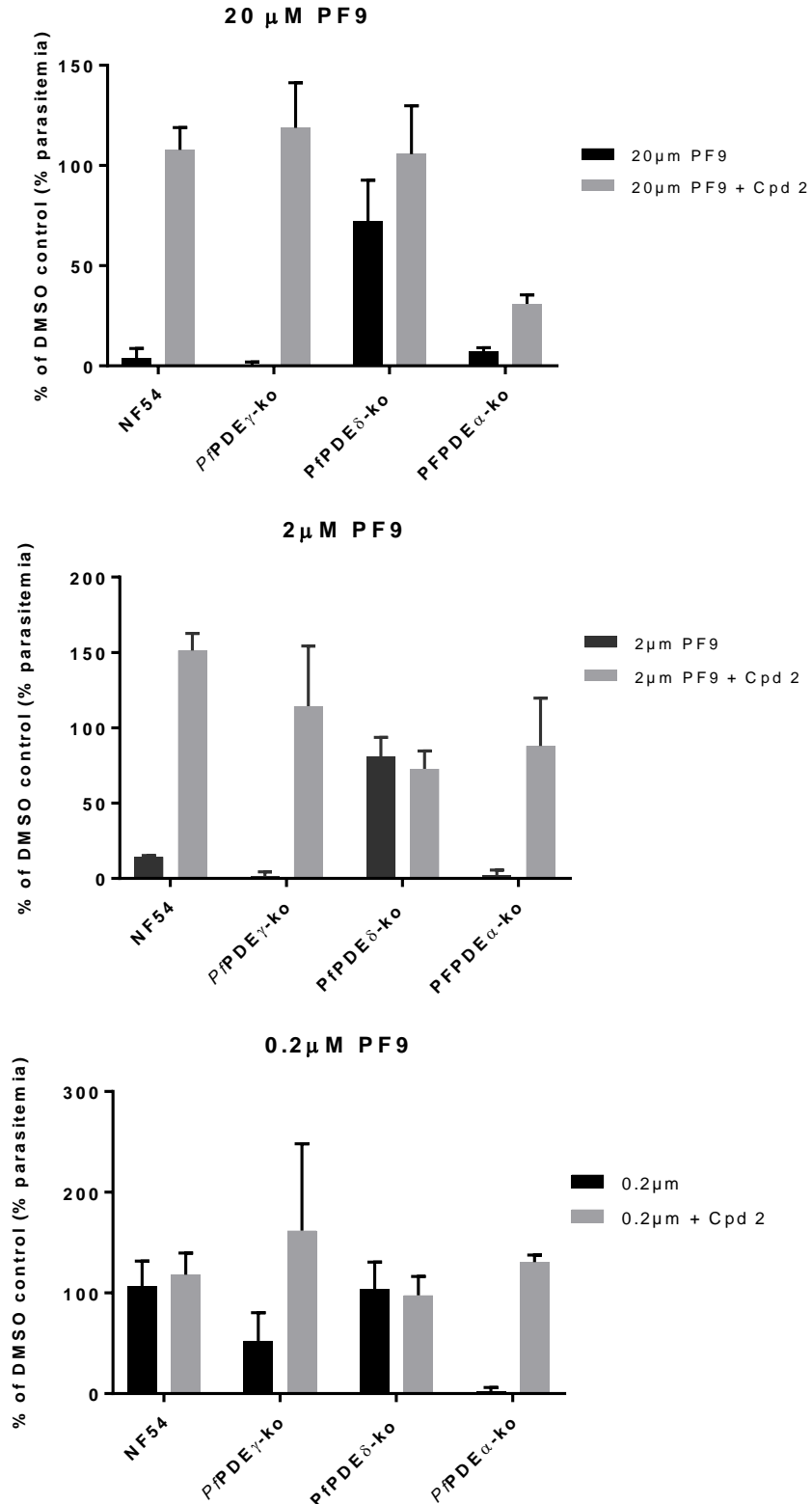


Figure 5.9. Reduction in number of stage V gametocytes treated with PF9 in the presence and absence of C2. Stage IV/V gametocytes from the NF54, *PfPDE α -ko*, *PfPDE γ -ko* and *PfPDE δ -ko* lines incubated for 12 hours 37 °C/5 % CO₂ with 20 μM, 2 μM or 0.2 μM PF9 +/- 2 μM C2. Data presented as percentage parasitaemia of parasites relative to a no inhibitor (DMSO 0.05 %) control (normalised to 100 %). Data analysed in Excel is 3 independent counts from 1 experiment for NF54, *PfPDE α -ko*, and *PfPDE δ -ko* lines and 3 counts from 2 experiments for *PfPDE γ -ko* line. 900 cells counted per replicate. Graph generated by GraphPad, Prism. Error bars represent SD.

5.2.3. PF9 causes rounding up of mature gametocytes and acts within 5 minutes of addition

In order to investigate the reduction in gametocyte numbers observed in the experiments above and to determine when the gametocytes disappear from samples, 3D7a stage V gametocytes were incubated in the presence or absence of PF9 for a 30-minute period and blood films prepared every 5 minutes. The numbers of stage V gametocytes (crescent shaped) in PF9 treated samples were counted from Giemsa-stained blood films and compared to the numbers of stage V gametocytes in DMSO-treated control samples.

Parasites in PF9-treated samples appeared as mostly round shaped cells at all time points with only a small number of parasites remaining as crescent-shaped cells (Figures 5.10 and 5.11). The numbers of rounded cells remained relatively constant over the 30 minute period. These 'rounded' forms were strikingly similar in morphology to that of gametocytes undergoing the initial stage of gametogenesis (rounding up) (Figure 5.11). This was a really interesting find and is investigated further in the next section. These data show that PF9 acts quickly and within 5 minutes of addition to mature gametocytes. The percentage parasitaemia of stage V gametocytes in PF9-treated samples was decreased at all time points by approximately one third (Figure 5.10). As demonstrated by images of Giemsa stained samples in Figure 5.11, this was not due to the presence of a population of 'abnormal' cells, but parasites have disappeared from the culture. Interestingly, the cells that were present in the PF9-treated samples appeared morphologically changed, presenting as rounded up forms characteristic of XA-induced gametocytes. These data leads to the exciting question of whether PF9 acts by inducing gametogenesis. This question will be explored in the next section.

Gametocytes in all DMSO-treated samples remained as crescent-shaped cells characteristic of non-induced stage V gametocytes (Figures 5.10 and 5.11). The numbers of crescent-shaped gametocytes in control samples remained relatively constant over the first 20 minutes. At the 30 minute time point, a small increase in a population of rounded cells appeared in the control sample (Figure 5.10). This experiment was carried out at room temperature, a temperature not favourable to gametocyte growth and survival, so this increase in rounded cells at this time point is likely to be due to the length of time that the gametocytes were exposed to a drop in temperature below 37 °C, and would likely represent a reduced gametocyte viability causing them to adopt a rounded morphology.

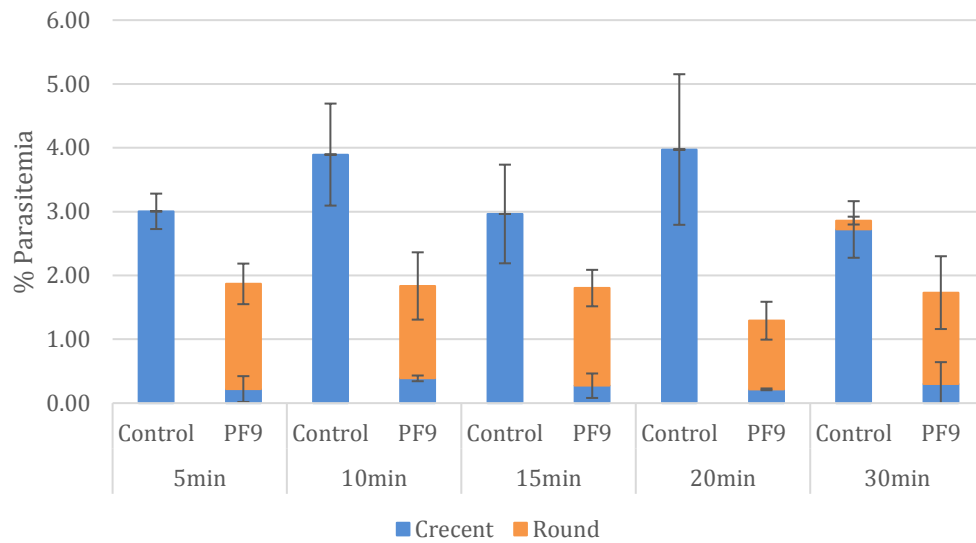


Figure 5.10. Time course of PF9 treatment of stage V gametocytes from the 3D7a line. Presented as percentage parasitaemia of parasites treated with PF9 (10 µM) over a 30 minute period compared to a no inhibitor (DMSO, 0.05 %) control. Counts are of crescent-shaped cells (blue) and rounded cells (orange) from Giemsa stained blood films. Data analysed in Excel is 3 independent counts from one experiment. Error bars represent SD.

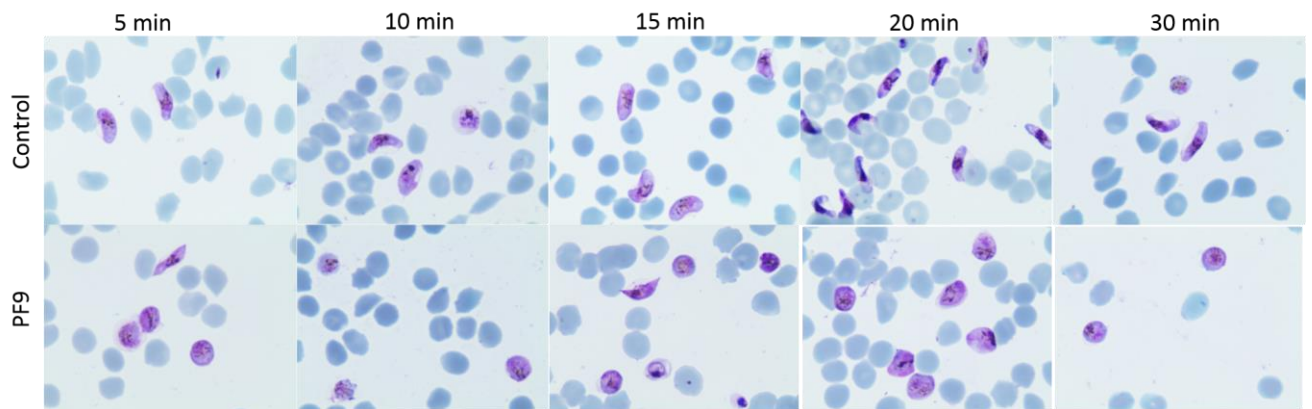


Figure 5.11. Images of Giemsa-stained blood films of 3D7a stage V gametocytes incubated ± PF9 PF9 concentration was 10 µM. Samples were taken over a period of 30 minutes at 5 minute time intervals.

5.2.4. Investigation into the mode of action of PF9

Data in the previous sections have shown that PF9 acts very quickly (within 5 minutes), that it is apparently more active when *PfPDE δ* is present and less active when it is absent, and that the majority of PF9 inhibition in the wildtype line is *PfPKG* dependent. We know from the literature that the initial stage of gametogenesis (rounding up) is a *PfPKG*-dependent process[159], and that the cGMP-PDE inhibitor zaprinast can induce gametogenesis *in vitro* in the absence of XA[130], indicative that *PfPDE* inactivation and subsequent *PfPKG* activation are important parts of the signalling cascade required for gametogenesis to occur. This led to the hypothesis that PF9 may act on mature gametocytes by inducing premature gametogenesis. This would be achieved as follows; PF9 inhibits *PfPDE* activity in the mature gametocyte. Inhibition of cGMP-specific *PfPDEs* (most likely from the evidence so far to be *PfPDE δ*) would abolish cGMP-*PfPDE* hydrolytic activity leading to elevated levels of cGMP. This in turn would activate *PfPKG*, which would then phosphorylate downstream protein targets leading to the initiation of gametogenesis (See Figure 5.28 in discussion section for schematic).

5.2.4.1. Pfizer 9 induces rounding up of wildtype stage V gametocytes

To determine whether PF9 can induce Stage V gametocytes to round up, the number of crescent shaped and round parasites were counted in Giemsa-stained blood smears from samples of wildtype (3D7a) parasites after treatment with PF9 and compared to a non-treated wildtype 3D7a control and a PF9-treated *PfPDE δ* -ko line sample.

After 15 minutes of incubation at room temperature, DMSO-treated wildtype (3D7a) parasites remained mostly crescent shaped, characteristic of non-activated gametocytes, with a small proportion appearing with a rounded morphology (~ 21 %) (Figure 5.12 and Table 5.3). PF9 treatment of the same line resulted in the majority of parasites rounding up, with ~ 20 % remaining as crescent-shaped cells.

By contrast, treatment of the *PfPDE δ* -ko line did not induce rounding up, with the majority of cells (~ 75 %) remaining crescent shaped reminiscent of the 3D7a non-treated control line (Figure 5.12 and Table 5.3). A relatively small proportion of *PfPDE δ* -ko line gametocytes (~25 %) did round up in response to PF9 treatment. But this is over 3 times less than seen in the 3D7a wildtype line.

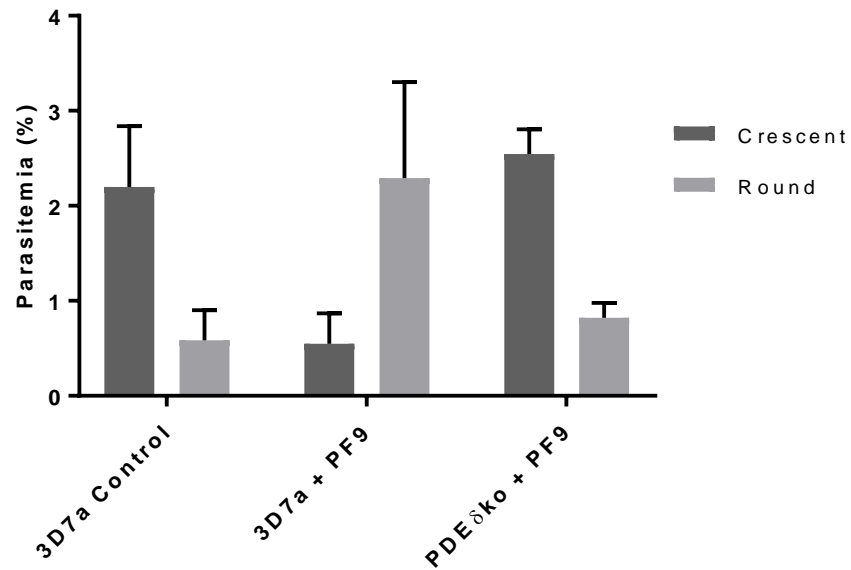


Figure 5.12. Comparison of PF9 treatment in wildtype (3D7a) and *PfPDE δ* -ko gametocytes. Gametocytes were treated for 15 minutes with PF9 (10 μ M) and compared to a DMSO (0.05 %) control. The numbers of non-activated (crescent) or activated (round) parasites were counted (a total of 900 parasites counted per replicate) from Giemsa-stained blood films. Data is the average of 3 counts from one experiment analysed in Excel and presented as percentage of total parasitaemia. Graph is generated in GraphPad, Prism. Error bars represent SD.

% Total parasitaemia \pm SD		
	Crescent	Round
3D7a control	78.93 \pm 8.93	21.06 \pm 8.93
3D7a + PF9	20.47 \pm 12.02	79.52 \pm 12.02
<i>PfPDEδ</i>ko + PF9	75.75 \pm 1.77	24.24 \pm 1.77

Table 5.3. Comparison of PF9 treatment in wildtype (3D7a) and *PfPDE δ* -ko gametocytes. Gametocytes were treated for 15 minutes with PF9 (10 μ M) and compared to a DMSO (0.05 %) control. The numbers of non-activated (crescent) or activated (round) parasites were counted (a total of 900 parasites counted per replicate) from Giemsa-stained blood films. Data is the average of 3 counts from one experiment analysed in Excel and presented as percentage of total parasitaemia. Graph is generated in GraphPad, Prism. Error bars represent SD.

To investigate PF9-induced rounding up of stage V gametocytes further, 3D7a stage V gametocytes were incubated with PF9 for 1 minute or 3 minutes and compared to incubation with XA under the same conditions. Samples were compared to a DMSO control. Blood films were prepared immediately after incubation and counts of non-activated (crescent shaped cells) and activated (rounded-up cells) were carried out to determine percentage of parasites activated and non-activated in each sample.

PF9 stimulated rounding up of wildtype 3D7a gametocytes (Figures 5.13 and 5.14). In the control sample (0.05 % DMSO) at both 1 minute and 3 minutes, cells remained crescent shaped (Figure 5.14). After 3 minutes, ~ 65 % of parasites in PF9 treated samples appeared morphologically rounded up with ~ 30 % of parasites remaining crescent shaped (Figure 5.13 and Table 5.4). This was comparable to the numbers of rounded up cells recorded in the XA-treated samples treated sample after 3 minutes (~ 55 %). After 1 minute incubation with PF9, the majority (~100 %) of wildtype cells remained crescent shape indicating that PF9 does not induce rounding up before 1 minute. This is comparable to XA-induced samples, which appeared mostly non-activated at the 1 minute time point with only ~10 % (Table 5.4) of parasites rounded up.

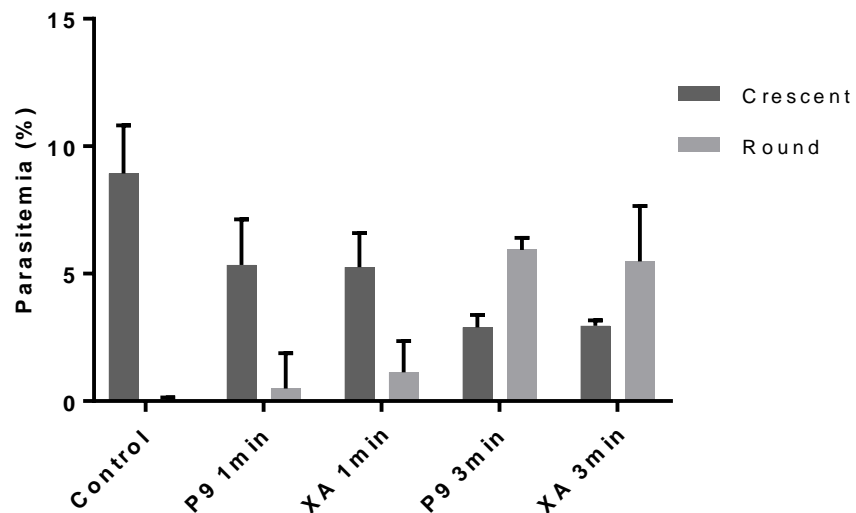


Figure 5.13. Comparison of XA and PF9 treatment of 3D7a stage V gametocytes. Samples treated for 1 minute or 3 minutes at room temperature with either PF9 (10 μ M) or XA (30 μ M). Numbers of non-activated (crescent) or activated (round) parasites counted from giemsa stained blood films. Data presented as percentage parasitemia and compared to a DMSO (0.05 %) control (incubated for 3 minutes). Data analysed in Excel is the average of 3 counts from one experiment (~900 cells counted per replicate). Error bars represent SD.

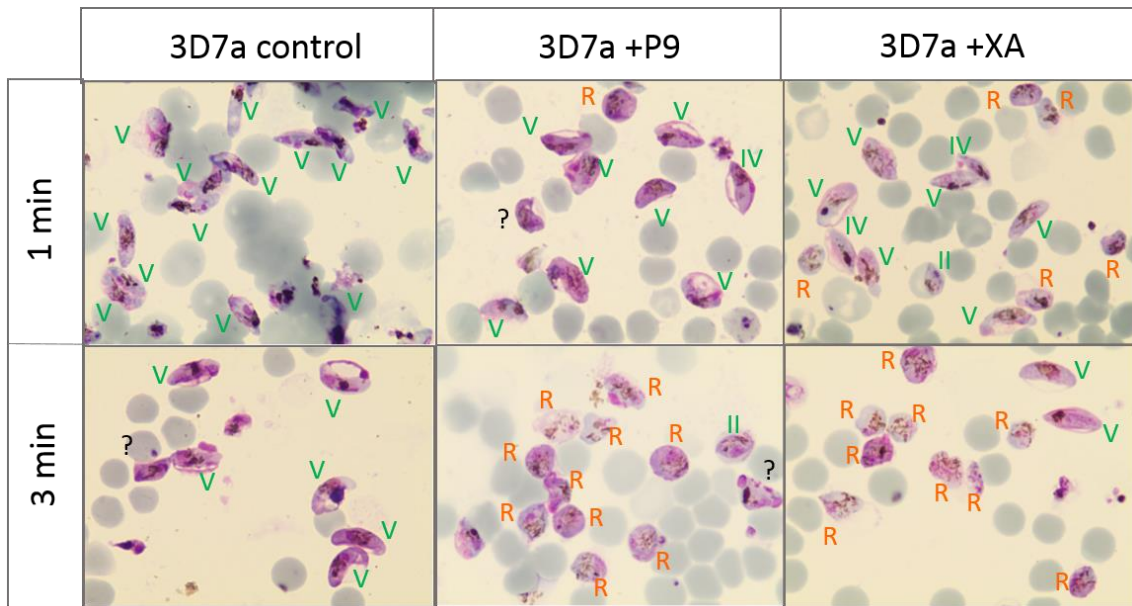


Figure 5.14. Morphology of 3D7a stage V gametocytes treated with either XA or PF9. Identified by Giemsa stained blood films. Samples treated for 1 minute or 3 minutes with 10 μ M PF9 (column 2) or 30 μ M XA (column 3) compared to a DMSO (0.05 %) control (column 1). Crescent-shaped Stage V (V) gametocytes (non-activated) and rounded-up (R) gametocytes (activated) identified by light microscopy.

Closer examination of Giemsa-stained blood films showed that the morphology of rounded-up gametocytes in the PF9-treated 3D7a gametocytes appear comparable to that following XA treatment (Figure 5.15).

Parasites appear rounded in shape with dissipated haemozoin pigment. Nuclear staining (pink) indicates nuclear material is visible by microscopy in all cells. Most cells appeared emerged from the erythrocyte with no apparent Giemsa staining of the erythrocyte membrane although some cells appear to have remnants of erythrocyte membrane still associated with the parasite and a small number have staining indicative that they are still at least partially retained inside the host erythrocyte (Figure 5.15 and 5.16).

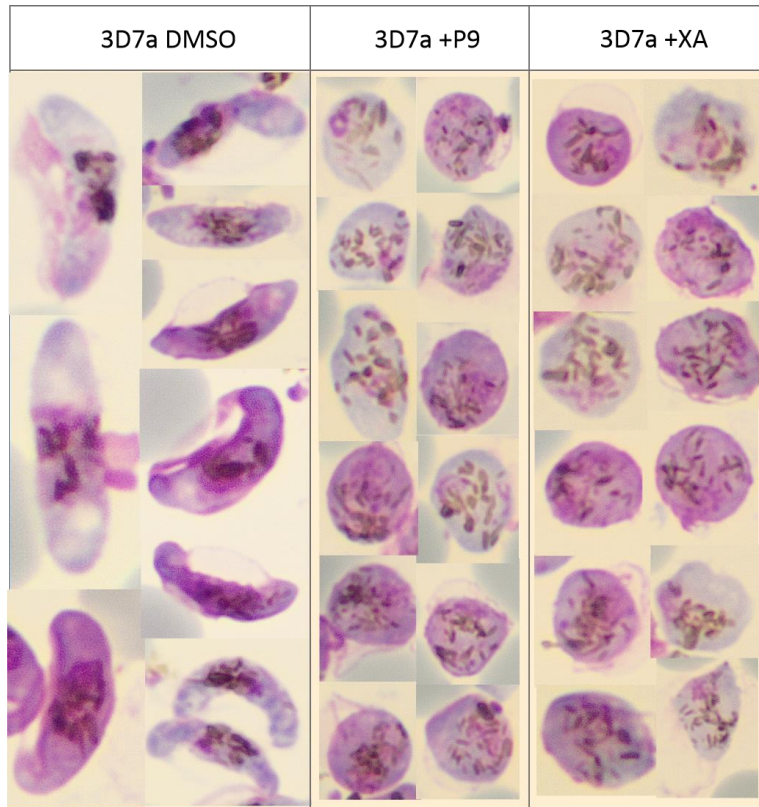


Figure 5.15: Comparison of morphology of PF9 (10 μ M) treated and XA-treated (30 μ M) 3D7a stage V gametocytes compared to a DMSO control (un-treated) after 3-min incubation at room temperature from a single experiment. Blood films stained with Giemsa. Note: sizes of individual parasites are not to scale in this figure.

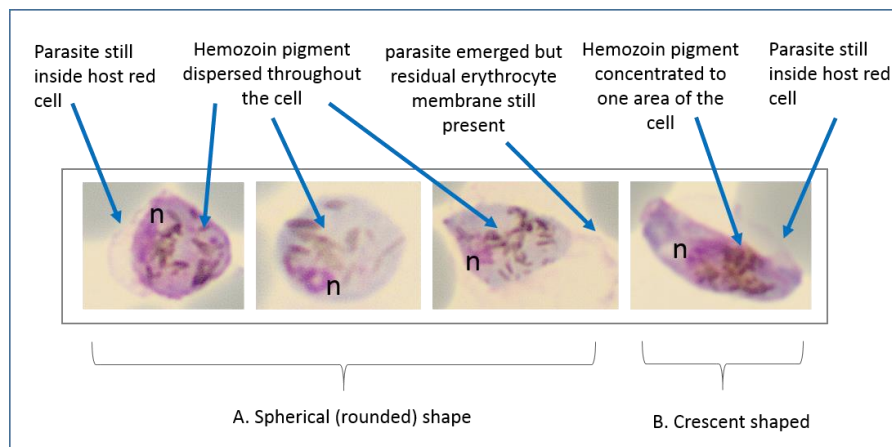


Figure 5.16. Features of rounded-up parasites (A) compared to non-activated parasites (B) identified in Giemsa-stained blood films from samples activated with XA or PF9 (A) or not treated (B). Nucleus (n) stained pink and cytoplasm stained pink/blue with Giemsa stain. In stage V female gametocytes, pigment usually relatively concentrated and close to the nucleus whereas in males, the pigment and nucleus is more diffuse.

PfPDEδ-ko line parasites treated with 0.05 % DMSO only had a comparable morphology to DMSO-treated 3D7a gametocytes (Figures 5.17 and 5.18) with ~100 % cells appearing crescent shaped after 3 minutes (Table 5.4). However, this line greatly differed in its response to both PF9 and XA compared to the 3D7a control line.

Following both 1 minute and 3 minute incubations with 10 μM PF9, the majority of gametocytes remained crescent shaped (~85 %, Table 5.4). A small number of *PfPDEδ*-ko parasites treated with PF9 rounded up (~ 15 %). This was the same number for both the 1-minute and 3-minute time points (Figures 5.17 and 5.18 and Table 5.4). At the 3 minute time point, the number of rounded-up cells was significantly lower in *PfPDEδ*-ko line samples treated with PF9 when compared to the 3D7a wildtype line ($P=0.0222$, Welch's paired t test). The numbers of rounded-up gametocytes in *PfPDEδ*-ko cultures treated with XA was also less than seen in the 3D7a line treated with XA, with only ~ 20 % of *PfPDEδ*-ko gametocytes rounding up after 3 minutes of XA incubation compared to ~55 % (Table 5.4) in the 3D7a line. No-rounded up parasites were seen in XA-treated samples at the 1 minute time point (Figure 5.17 and Table 5.4).

Overall, these data are in agreement with results presented in section 5.2.2 indicating that in the absence of *PfPDEδ*, PF9 is much less active. It also shows that in the 3D7a wildtype line, PF9 acts more quickly than XA and that it induces stage V gametocytes to round up in a manner that appears morphologically comparable to that of XA stimulation. It may be that PF9 is able to bypass the XA 'receptor' steps leading to elevated cGMP levels more quickly.

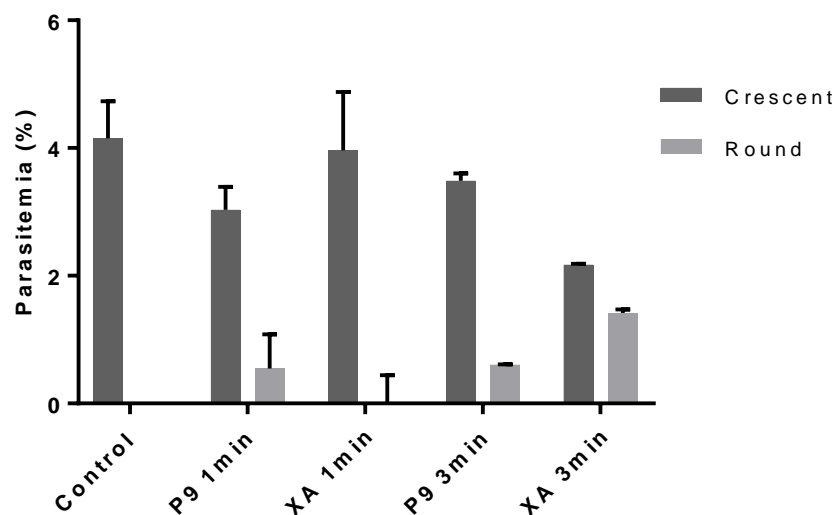


Figure 5.17. Comparison of XA and PF9 treatment of *PfPDEδ*-ko line stage V gametocytes. Samples treated for 1 minute or 3 minutes at room temperature with either PF9 (10 μM) or XA (30 μM). Numbers of non-activated (crescent) or activated (round) parasites counted from Giemsa stained blood films. Data presented as percentage parasitemia and compared to a DMSO (0.05 %) control (incubated for 3 minutes). Data analysed in Excel is the average of 3 counts (~900 cells counted per replicate). Error bars represent SD.

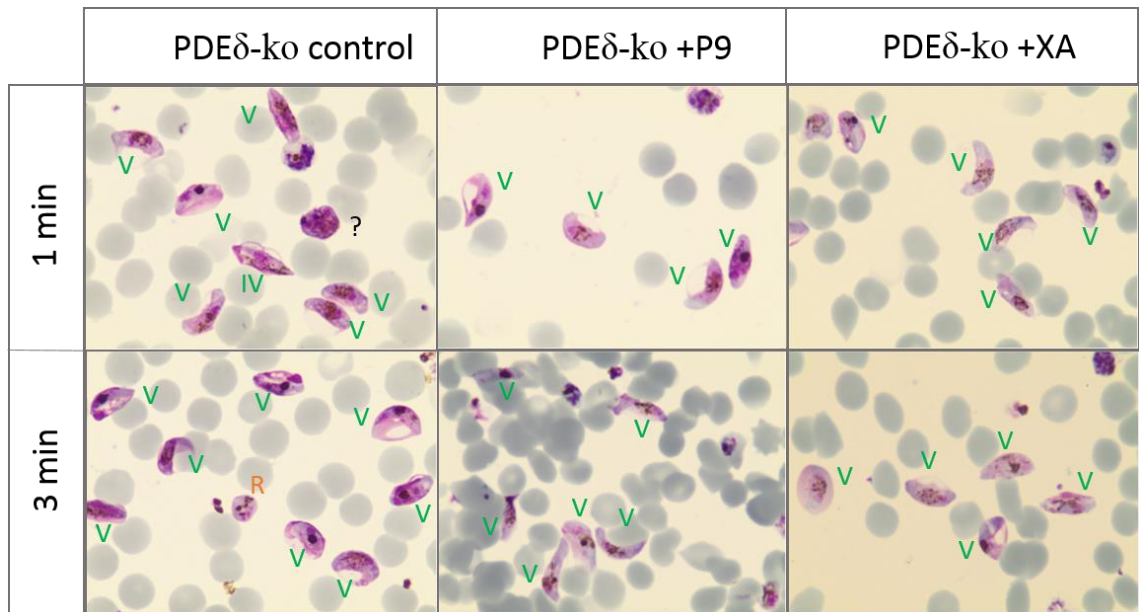


Figure 5.18. Morphology of *PfpDEδ*-ko stage V gametocytes treated with either XA or PF9 identified by Giemsa stained blood films. Samples treated for 1 minute or 3 minutes with 10 μ M PF9 (column 2) or 30 μ M XA (column 3) compared to a DMSO (0.05 %) control (column 1). Crescent-shaped stage V (V) gametocytes (non-activated) and rounded-up (R) gametocytes (activated) identified by light microscopy.

Percentage of Total parasitaemia \pm SD				
	3D7a		<i>PfpDEδ</i> -ko	
	Stage V	Round	Stage V	Round
Control	100	0.00	100	0.00
PF9 10 μ M 1min	106.45 \pm 38.72	0.00 \pm 38.72	85.02 \pm 14.16	14.98 \pm 14.16
XA 30 μ M 1min	88.21 \pm 20.62	11.79 \pm 20.62	103.19 \pm 11.25	0.00 \pm 11.25
PF9 10 μ M 3min	32.63 \pm 2.77	67.37 \pm 2.77	85.15 \pm 0.30	14.85 \pm 0.30
XA 30 μ M 3min	45.04 \pm 17.25	54.96 \pm 17.25	76.82 \pm 1.35	23.18 \pm 1.35

Table 5.4. Comparison of XA and PF9 treatment of 3D7a and *PfpDEδ*-ko line stage V gametocytes. Data as presented in Figures 5.13 and 5.17. Parasites incubated with PF9 (10 μ M) or XA (30 μ M) for 1 minute or 3 minutes and compared to a DMSO (0.05 %) control incubated for 3 minutes. Data presented as percentage of total number gametocytes (Including all crescent and rounded up cells but minus stages I-IV). Date is the average of 3 individual counts (~900 cells counted per replicate) from one experiment \pm SD. Values above 50 % of the control represented in dark grey, Values below 25 % of the control represented in light grey. Values between 50 % and 25 % of the control represented in white.

Pfizer 9 induces rounding up in the wildtype line in a PKG-dependent manner and more effectively than either zaprinast and XA

The previous data in section 5.2.4 show that PF9 induces rounding up of mature gametocytes and that it does so very quickly.

To investigate the PF9 activation of gametocytes further, PF9 treatment of 3D7a stage V gametocytes was compared to that of XA and zaprinast treatment. In section 5.2.2 the majority of PF9 activity was shown to be *Pf*PKG dependent. To further confirm this, the *Pf*PKG-specific inhibitor MRT00207065 was added to PF9-activated samples and compared to C2 treatment. Gametocyte activation was determined by counts (using Giemsa-stained blood films) comparing the number of crescent shaped parasites (non-activated) to the number of rounded up (activated) parasites in each sample. The same experiment was carried out on the *Pf*PDE δ -ko line in parallel.

In the 3D7a line, gametocytes in the DMSO control sample all remained as crescent-shaped cells with no rounded-up cells counted (Figure 5.19). This is the expected morphology for normal, non-activated gametocytes. After treatment with PF9, the majority (~90 %) of cells appeared to have rounded up, with only ~10 % remaining crescent shaped after 15 minutes of incubation (Figure 5.19). This is a higher proportion of rounded-up cells than was seen in the XA-treated samples (~70 % rounded up) and even more so for (100 μ M) zaprinast-treated samples (~20 % rounded up). This indicates that 10 μ M PF9 induces higher levels of rounding up than 30 μ M XA does in the same time period.

PF9 treatment in combination with C2 confirmed earlier data that PF9 induced rounding up is a *Pf*PKG-dependent process. This was further confirmed by the more potent (and more specific) PKG inhibitor MRT00207065 (1 μ M) (Baker *et al.*, 2017), which also reversed the activity of PF9 in a similar manner to C2. However a small number (~ 15 %) of parasites were still able to round up with PF9 stimulation in the presence of MRT00207065 (Figure 5.19). This was a similar level seen with C2 treatment.

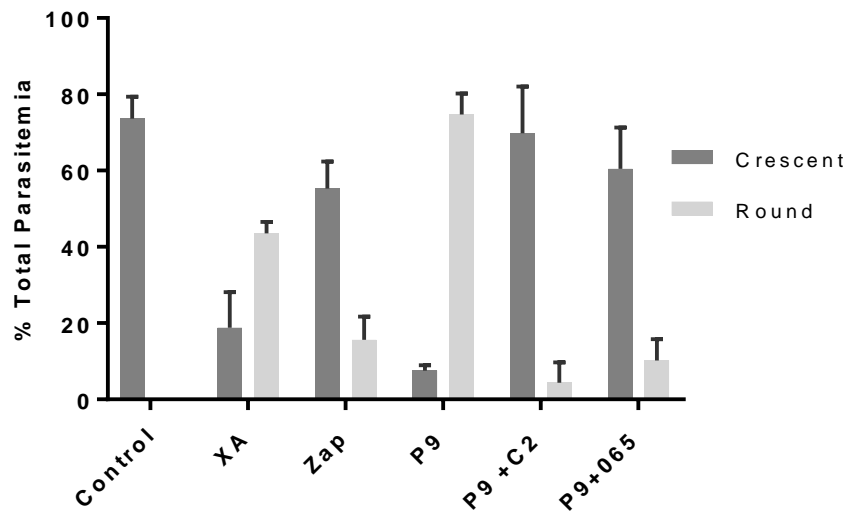


Figure 5.19. Comparison of PF9 treatment of 3D7a stage V gametocytes to XA and zaprinast treatment. Parasites treated with PF9 (10 μ M) in the presence and absence of C2 (2 μ M) or MRT00207065 (1 μ M). Compared to XA (30 μ M) or zaprinast (100 μ M) incubated at room temperature for 15 minutes. Data analysed in Excel are presented as percentage total parasitaemia from 3 separate counts from Giemsa stained blood films (~900 cells counted per replicate) from 1 experiment. Graph generated in GraphPad, Prism. Error bars represent SD.

The inactivity of PF9 against the *PfPDEδ*-ko line was further confirmed with only ~25 % of cells rounding up in response to PF9 compared to ~90 % in the 3D7a line (Figure 5.20). In the *PfPDEδ*-ko line, the small level of PF9 activity observed appears to be PKG dependent as it was completely reversed to control levels by both C2 and MRT00207065.

Only ~5 % of gametocytes rounded up in XA-treated samples in the *PfPDEδ*-ko line with ~90 % of parasites remaining crescent shaped (Figure 5.20). This is in agreement with data presented in Figure 5.17 and Table 5.4, which show that ~75 % of gametocytes from the *PfPDEδ*-ko line remain crescent shaped after 3 minutes of incubation with XA.

Parasites of the *PfPDEδ*-ko line treated with zaprinast also remained mostly crescent shaped (~90 %), (Figure 5.20).

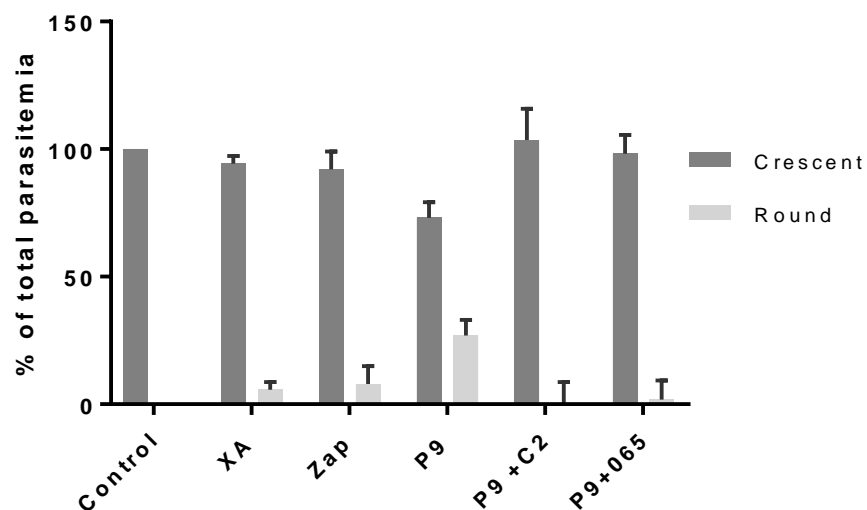


Figure 5.20. Comparison of PF9 treatment of *PfPDEδ*-ko line stage V gametocytes to XA and zaprinast treatment. Parasites treated with PF9 (10 μ M) in the presence and absence of C2 (2 μ M) or MRT00207065 (1 μ M), compared to XA (30 μ M) or zaprinast (100 μ M). All treatments were incubated at room temperature for 15 minutes. Data analysed in Excel is presented as percentage total parasitaemia from 3 separate counts from Giemsa stained blood films (~900 cells counted per replicate) from 1 experiment. Graph generated in GraphPad, Prism. Error bars represent SD.

5.2.4.2. Pfizer 9 induces emergence of gametes from the host erythrocyte

So far the data have shown convincingly that PF9 induces rounding up. However, this is only the first visible step of gametogenesis so it was important to determine whether PF9 could induce subsequent steps in the process of gametogenesis such as host erythrocyte emergence and male exflagellation. This would strengthen the data supporting the hypothesis that PF9 acts by inducing gametogenesis rather than just inducing a morphological change in the parasite which results in a phenotype resembling activated gametocytes.

In the above section, the morphology of rounded-up parasites induced by PF9 appears to indicate emergence from the erythrocyte in Giemsa-stained blood films (Figures 5.14 to 5.16). However, Giemsa staining alone cannot confirm emergence. This must be achieved by analysis of samples in which the host erythrocyte cell membrane has been stained. This enables identification of emerged (no erythrocyte staining) or non-emerged (erythrocyte staining) parasites.

To achieve this, live gametocyte samples were stained with an erythrocyte membrane stain conjugated to a fluorescent dye, Wheat Germ Agglutinin-Texas Red (WGA-TR). WGA is a lectin that specifically binds the sugars N-acetyl glucosamine and sialic acid and when conjugated to a fluorescent probe can be imaged by fluorescent microscopy. Gametocytes were also stained with a nuclear stain Hoechst 33342. Samples were then treated with PF9 in the presence and absence of C2 for 20 minutes after which they were immediately fixed in formaldehyde and imaged using a fluorescent microscope. This protocol was used to investigate whether the rounded-up gametocytes observed in Giemsa-stained blood films of PF9-activated samples have emerged from the host erythrocyte or not. This was done in the presence and absence of C2 to investigate the *Pf*PKG-specificity of PF9-induced emergence.

In control samples treated with DMSO, parasites remained crescent shaped, characteristic of non-activated gametocytes with positive erythrocyte staining (Figures 5.21 and 5.22). Addition of PF9 resulted in emergence of gametocytes from the host erythrocyte (Figures 5.21 and 5.22). Emerged parasites appeared rounded and lacking in erythrocyte membrane staining (Figure 5.22). Addition of C2 to PF9-treated samples reversed the effects of PF9 but not fully, with the majority of cells remaining crescent shaped and with erythrocyte staining present (Figures 5.21 and 5.22).

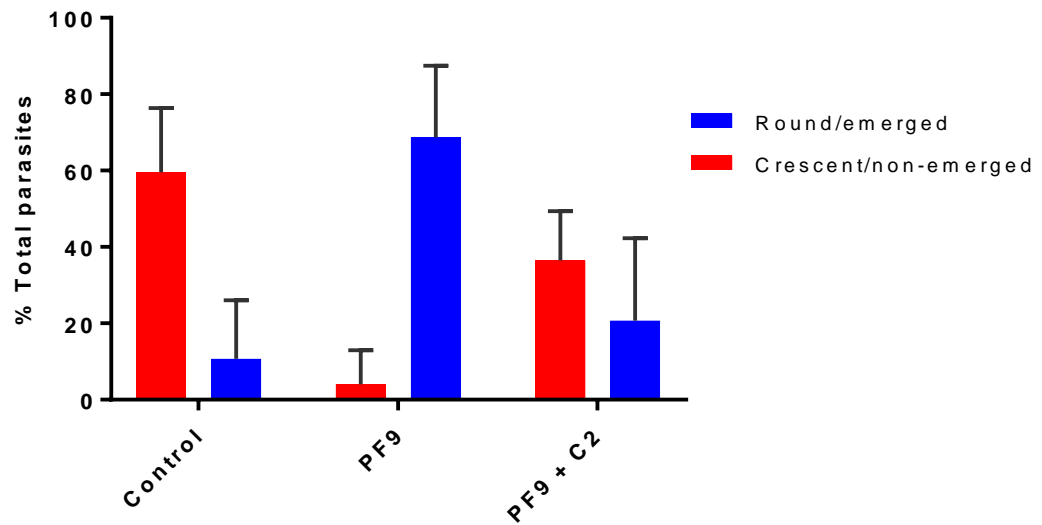


Figure 5.21. Levels of emergence from host erythrocytes in 3D7a gametocytes treated with PF9 in the presence and absence of C2.

WGA-Texas red (5 $\mu\text{g/ml}$) and Hoechst 33342 (20 μM) stained gametocytes incubated with PF9 (10 μM) \pm C2 (2 μM) for 20 minutes followed by formaldehyde fixation and imaged by fluorescent microscopy. (Data are presented as percentage of total number of gametocytes/gametes counted and are an average of 5 counts from a single experiment. Error bars represent SD.

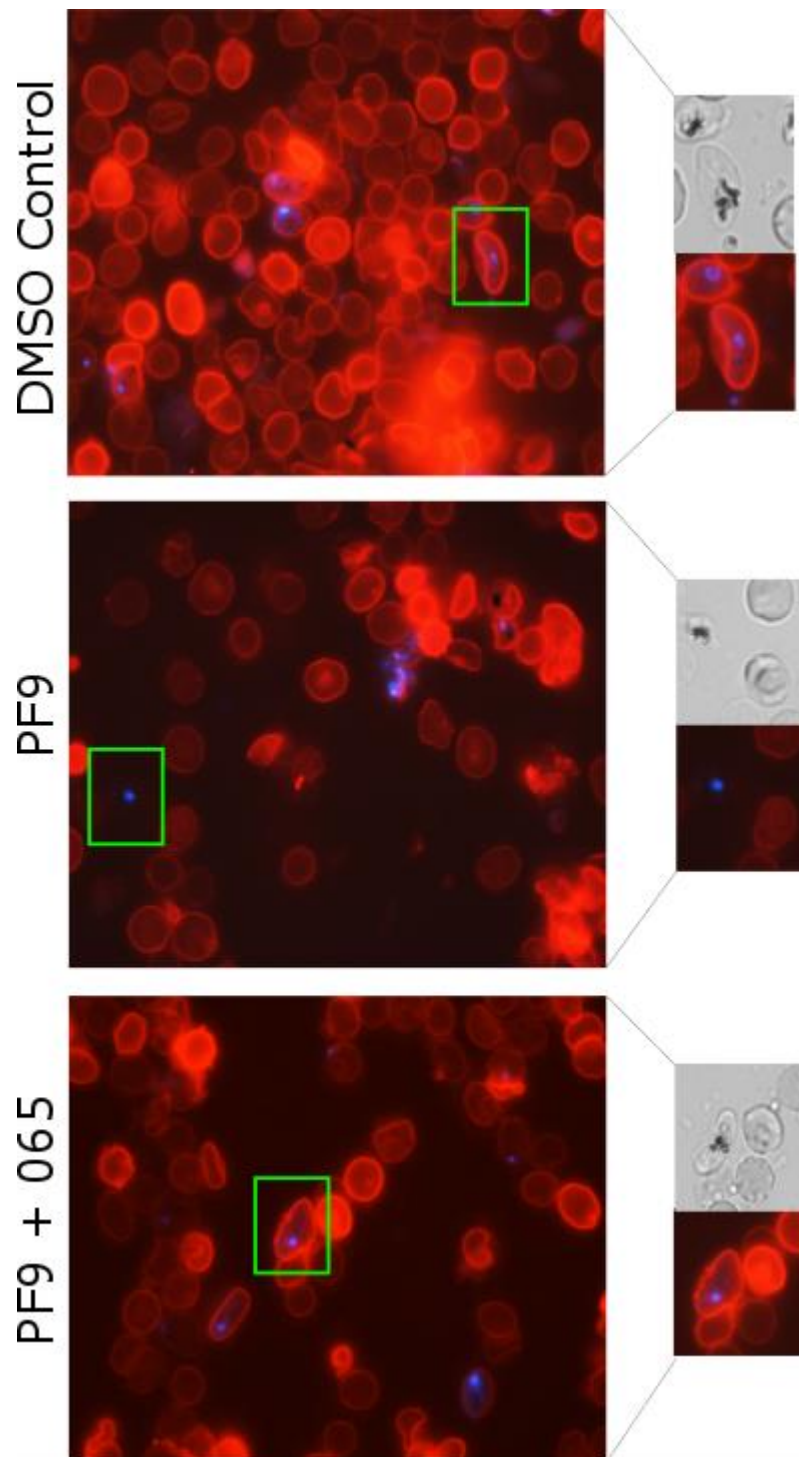


Figure 5.22. Representative images of 3D7a stage V gametocytes stained with WGA coupled to Texas Red to detect emergence of parasites from erythrocytes.

Nuclear material stained with Hoechst (blue), erythrocyte membrane stained with WGA-Texas Red (Red). Top panel is DMSO control (non-stimulated), middle panel is PF9-treated (10 μ M) stage V gametocytes (activated) and the bottom panel is treatment with PF9 (10 μ M) + MRT00207065 (1 μ M). Green boxes represent zoomed-in images presented on the right along with bright field images. Images generated from formaldehyde-fixed samples in suspension on an EVOS FL cell imaging system x 1000 objective.

5.2.4.3. Pfizer 9 induces exflagellation of 3D7a male gametes

The final stages of male gametogenesis involve, amongst other cellular events, the production of 8 highly motile flagella. This can be seen by light microscopy. Giemsa-stained blood films from PF9-treated samples of 3D7a stage V gametocytes were examined by light microscopy for exflagellation events.

Exflagellating forms were observed in both PF9 and XA-treated samples (Figure 5.23). These events were apparent after 15 minutes of incubation with 10 μ M PF9 and 30 μ M XA (not shown). No exflagellation events were observed in control (DMSO) samples (not shown).

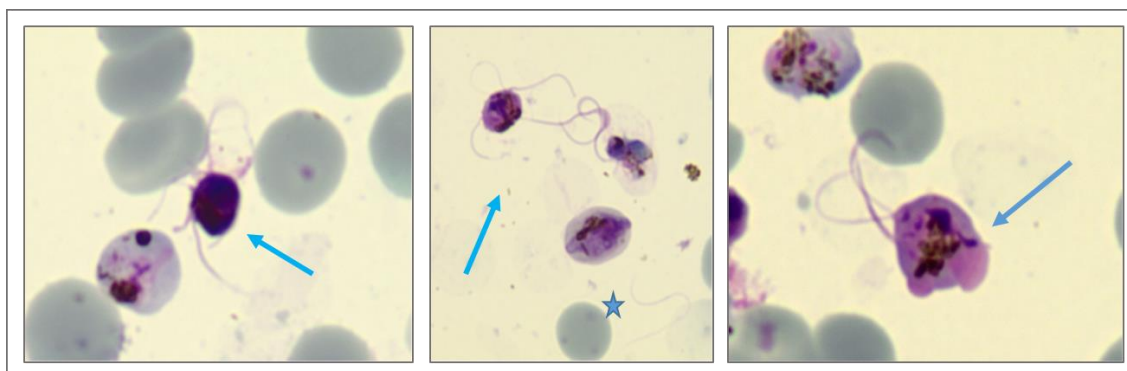


Figure 5.23. Exflagellating male gametocytes following treatment with PF9. Blue arrows indicate exflagellation events in Giemsa stained dried blood films from samples incubated for 15 minutes with PF9 (10 μ M). Blue star indicates a detached flagellum.

5.2.4.4. Pfizer 9 induces PKG-dependent Ca²⁺ release in stage V gametocytes of the 3D7a line.

The mobilisation of Ca²⁺ from internal stores is essential for the later stages of gametogenesis to occur. XA has been shown to induce Ca²⁺ release[210] and Ca²⁺ is required for the late stages of both XA- induced and zaprinast-induced gametogenesis[159]. Given this information and the fact that PF9 can induce gametocyte activation and exflagellation, it was therefore of interest to investigate whether PF9 could induce Ca²⁺ mobilisation in mature gametocytes. In order to do this, Ca²⁺ release was measured in 3D7a stage V gametocytes loaded with a Fluo-4-AM, which fluoresces upon binding to free Ca²⁺ (for method see section 2.4.A). Samples were treated with PF9, XA or zaprinast and levels of fluorescence compared to an ionophore control (A23187). This ionophore selectively binds to Ca²⁺ forming complexes and thus increases permeability of Ca²⁺ across membranes resulting in a rapid release of Ca²⁺ into the cytosol.

Treatment of 3D7a Stage V gametocytes with PF9 resulted in the release of Ca²⁺ (Figure 5.24). Levels of Ca²⁺ measured in the PF9-treated samples were comparable to those induced by the ionophore control and were much higher than the Ca²⁺ release measured in samples treated with both XA (~40 % of ionophore control) and zaprinast (~40 % of ionophore control). The majority of Ca²⁺ released in the PF9-treated samples (~80 %) was reversed by addition of C2. However ~20 % of the Ca²⁺ release measured in the PF9 treated sample was not reduced by C2 treatment.

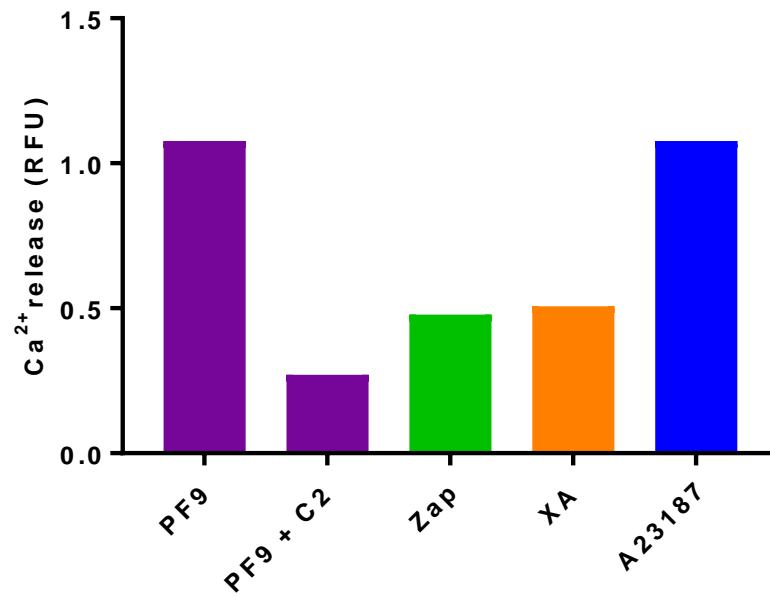


Figure 5.24. Ca²⁺ release in Fluo-4-AM-loaded 3D7a stage V gametocytes stimulated with PF9.

Stage V gametocytes treated with PF9 (10 μ M) in the presence and absence of C2 (2 μ M). Compared to zaprinast (100 μ M) and XA (10 μ M) treatment. Data are analysed in Excel and presented as Ca²⁺ release measured in relative fluorescent units minus the baseline fluorescence and fluorescence of the DMSO (0.05 %) control. The ionophore (A23187, 10 μ M) used as a positive control. Graph generated in GraphPad, Prism shows a single experiment carried out in triplicate.

5.3. Discussion

5.3.1. PF9 inhibition of gametocyte viability

Compounds that kill late gametocyte stages would be a valuable tool to reduce transmission of malaria and thus contribute to elimination efforts. To date, there is only one compound, primaquine that does this. However, this drug has safety issues and so there is a great need to develop additional drugs, which can target both asexual blood stages and gametocyte stages. PF9 was developed by Pfizer as an inhibitor of human PDE9. It has also been shown to have potent inhibitory activity against *P. falciparum* asexual blood stages (EC_{50} 143 nM) (Laura Drought, PhD Thesis, 2014).

Work carried out in this thesis further investigated the properties of PF9 on *P. falciparum* by focussing on its inhibition of gametocyte stages. This work has discovered that PF9 specifically targets mature gametocytes and not early gametocytes and that it exhibits potent activity against mature (stage V) gametocytes (EC_{50} value of $\sim 0.060 \mu\text{M}$) in a gametocyte viability assay. This EC_{50} value is ~ 2.5 times lower than that for asexual stages. This may reflect a difference in the types of assay used to measure viability, or more likely, it may indicate that this compound is more active in gametocytes than asexual stages, possibly in reflection of its mode of action. However, this assay needs to be repeated to confirm this result. None of the other four Pfizer compounds tested were active against gametocytes. It was previously shown that compounds PF11, PF12 and PF14 all specifically target *PfPDE β* in asexual blood stages, whereas PF9 targets both *PfPDE α* and *PfPDE β* (Laura Drought PhD Thesis, 2014) and it is predicted that it may target all *PfPDEs*. The potent activity of the Pfizer compounds against asexual blood stages is consistent with the fact that they all inhibit *PfPDE β* , which is the only essential *PfPDE* at these stages (Laura Drought, PhD Thesis, 2014, Christian Flueck, LSHTM, unpublished data). The results are also consistent with the fact that none of the compounds, apart from PF9, showed inhibition of gametocyte stages, as *PfPDE β* has not been detected in gametocyte stages[145] and does not appear to be required for sexual stage growth and development (my data unpublished). The lack of activity on early gametocyte stages suggests that perhaps *PfPDEs* are not expressed or are not required for early gametocyte stage growth and development. This is supported by the observations that gametocytes can grow and develop from stage I through to stage V in knock

out lines of *PfPDE* α (my data, unpublished), *PfPDE* γ [130] and *PfPDE* δ [130] and in a conditional knockdown line of *PfPDE* β (my data unpublished).

5.3.2. *PfPDE* target of PF9 in stage V gametocytes

Since PF9 showed good inhibition against mature gametocyte stages in viability assays, it was then of interest to try to determine the *PfPDE* target of this compound in stage V gametocytes. If the prediction that PF9 targets all *PfPDE*s is assumed correct, then the *PfPDE* specificity of PF9 would possibly give us insight into the *PfPDE*s required at this stage of the life cycle. Data using PF9 treatment on knock out lines of *PfPDE* α , *PfPDE* γ and *PfPDE* δ and also a wild type NF54 line, indicate that in the absence of *PfPDE* δ , PF9 treatment reduces gametocyte numbers much less effectively compared to loss of stage V gametocytes in the NF54 line and the *PfPDE* γ -ko and *PfPDE* α -ko lines. This was assessed by observation of numbers of stage V gametocytes exhibiting the characteristic crescent shape remaining after treatment compared to a non-treated DMSO control. In all lines, but particularly apparent in the NF54 line, a population of what has been referred to here as 'abnormal' forms were also counted. These were cells which did not present as having the normal stage IV or V gametocyte morphology or the characteristic morphology of rounded up cells. These abnormal forms were at higher numbers in PF9-treated samples and C2 treatment reduced the proportion of such forms. This indicates that these abnormal forms are present as a result of a PKG-dependent effect of PF9 treatment. The overall general parasitemia, including abnormal forms was significantly reduced in the NF54, *PfPDE* α -ko and *PfPDE* γ -ko lines in PF9-treated samples indicating that the general effect of this compound is by killing rather than inhibition of development because most parasites disappear from culture after 12 hours of incubation. Given that we now know that PF9 acts by inducing gametogenesis, it may be that the 'abnormal' forms observed are stages earlier than stage V which are affected by PF9 treatment but which do not have the cell signalling capacity for gametogenesis to be induced so they remain in the culture but do not appear morphologically as normal, healthy gametocytes. It would be useful to determine the viability of gametocytes remaining in PF9-treated samples and in samples treated with both PF9 and C2, particularly in the absence of *PfPDE* δ . It may be possible to knockout *PfPDE* δ in the luciferase expressing line using a similar method to that used by Cathy Taylor (Cathy Taylor, PhD Thesis, 2007) to produce the *PfPDE* δ -ko line that I have used in these studies. Luciferase conversion of its substrate requires ATP, which is only present in viable cells so repeating these assays on a luciferase expressing line lacking *PfPDE* δ would

indicate whether the cells that are present by microscopy are viable. It also may be possible to look at the effect on gametocyte viability of PF9 in the NF54 and *PfPDE α -ko* *PfPDE γ -ko* and *PfPDE δ -ko* lines by flow cytometry using a live-dead fluorescent stain such calcein-AM.

The lack of PF9 activity in the *PfPDE δ -ko* line initially suggested that PF9 targets *PfPDE δ* in mature gametocyte stages, as PF9 is much more active in the NF54, *PfPDE α* and *PfPDE γ -ko* lines where *PfPDE δ* protein is expected to be present based on proteomic data[144] compared to the knockout line where it is absent. The rationale being that if the target of PF9 is not present, then the inhibitor will be inactive. However as demonstrated in chapter 4 of this Thesis (section 4.2.3), the *PfPDE δ -ko* line appears unable to round up in response to PF9 due to its lack of deformability as a result of *PfPDE δ* -mediated cAMP/*PfPKA* activation and addition of a PKA inhibitor to this line can result in PF9-induced rounding up. This complicates work attempting to explore the role of *PfPDE δ* in gametogenesis and *PfPDE δ* as a target for PF9 as it may already be unable to undergo rounding up due to an earlier effect on deformability. A conditional knock down line of *PfPDE δ* would be a useful tool to look at the effect of PF9 on a line in which *PfPDE δ* is present until excision is induced. These data also suggest that the effects of PF9 appear to be *PfPKG*-specific and on target because they are reversed by the *PfPKG* inhibitors C2 and MRT00207065. The relatively small effect of PF9 on *PfPDE δ -ko* gametocytes, was shown to be not significant using statistical analysis.

Interestingly, the *PfPDE α -ko* line appeared to be more sensitive to PF9 treatment. The lowest concentration of 0.2 μ M completely inhibited this line. This was in contrast to NF54 in which gametocyte numbers were unchanged at this concentration. The *PfPDE α -ko* line also exhibited higher sensitivity at 0.2 μ M PF9 than the *PfPDE γ -ko* line. This indicates that in the absence of *PfPDE α* , PF9 is more active. This result may reflect a scenario whereby PF9 is targeting *PfPDE δ* which is likely to be the predominant *PfPDE* present in stage V gametocytes and required for gametocyte activation, but that it is also targeting *PfPDE α* , which is also present in mature gametocytes but is known not to play an essential role in the process of gametogenesis. It is not clear what the role of *PfPDE α* is as no phenotype has been observed in blood stages or gametocyte development. It is perhaps present to compensate for the loss of *PfPDE δ* or it may play an important role in vivo or later on during mosquito stage development, but this has not yet been defined. In the absence of *PfPDE α* , a lower concentration of PF9 is required to inhibit *PfPDE δ* and the compound is essentially more active. PF9 is predicted to bind both *PfPDE α* and *PfPDE δ* , therefore in the absence of *PfPDE α* there will be effectively more free PF9 to bind to *PfPDE δ* . In a wildtype situation where both *PfPDE α* and *PfPDE δ* are present, the presence of

PDE α provides an additional target for PF9 to bind to. The number of target molecules in a cell clearly influences the EC₅₀ value and so if there are fewer target molecules the EC₅₀ value will be lower and this appears to be what is seen in the *PfPDE α -ko* line, which shows a much higher sensitivity to PF9 compared to the wildtype line. The similarity observed between the PF9 responses in wildtype (3D7a) and *PfPDE γ -ko* line gametocytes may be due to the fact the *PfPDE γ* is not likely to be expressed at the protein level in mature gametocytes so as seen in the wildtype line, both targets, *PfPDE α* and *PfPDE δ* are present but *PfPDE γ* is absent. Therefore it is unlikely that *PfPDE γ* contributes to the EC₅₀ of PF9 in gametocytes.

The slight difference in sensitivity observed in the NF54 and *PfPDE γ -ko* lines may be due to strain specific differences as the background of the *PfPDE γ -ko* line is 3D7. Repeating this assay on the 3D7a line would provide a more useful comparison to the knockout lines that NF54.

The inability of C2 to reverse the effect of 20 μ M PF9 in the *PfPDE α -ko* line may be due to a toxic (off target, PKG-independent) effect at this concentration. Or it may be that as PF9 shows more activity when *PfPDE α* is absent (and therefore when the only *PfPDE* available for targeting is *PfPDE δ*), it may be reaching its *PfPDE* target more quickly than C2 is able to inhibit *PfPKG* so may therefore not be able to fully reverse the effects of PF9 at the higher concentration.

PF9 appeared not to require the presence of *PfPDE γ* for activity (i.e. *PfPDE γ* does not contribute to the EC₅₀ of PF9), as absence of the gene encoding *PfPDE γ* in the *PfPDE γ -ko* line did not alter PF9 activity on mature gametocytes when compared to the NF54 line. One explanation for this is that *PfPDE γ* is simply not a target for PF9. This is currently unknown. Another explanation is that *PfPDE γ* protein is absent from stage V gametocytes so it is not present as a target for PF9. *PfPDE γ* mRNA transcripts have been detected in *P. yoelii* sporozoites[142], but detected at only very low levels in gametocyte stages of *P. falciparum*[25],[145]; however, the presence of mRNA transcripts does not necessarily indicate that protein is present at these stages. A third explanation is that *PfPDE γ* protein is present in gametocyte stages but may not be active, so PF9 targeting of *PfPDE γ* would not affect gametocyte viability. However, if this were to be the case, the absence of *PfPDE γ* would likely present an effect of PF9, which reflects what was seen in the *PfPDE α -ko* line. *PfPDE γ* is not required for gametocyte or gamete development (Cathy Taylor, PhD Thesis, 2007) but it has been implicated as an essential PDE in *P. yoelii* sporozoite motility and subsequent infection of the mosquito salivary gland[142]. It may be that PF9 could affect parasite viability by targeting *PfPDE γ* at a later point in the insect stages of the life cycle. It would be interesting to test the activity of PF9 on sporozoite stages, or to test PF9 in native PDE inhibition assays using samples of epitope tagged *PfPDE γ* protein from pull down experiments

or from baculovirus expression studies. The most likely explanation for the PF9 activity seen in the *PfPDEy*-ko line is that the enzyme is simply not present or not active in stage V gametocytes because activity of this *PfPDE* is not required until later in the life cycle for sporozoite motility and subsequent salivary gland invasion[142].

5.3.3. PF9 mode of action on stage V gametocytes

Following the discovery of PF9 killing of mature *P. falciparum* gametocytes, it was then of interest to determine how quickly this compound acted. A time course experiment demonstrated that PF9 acts within 5 minutes of PF9 addition and interestingly, parasites treated with PF9 at all time points appeared to exhibit a round morphology. This phenotype is the same as that seen when gametogenesis is initiated in stage V gametocytes using a drop in temperature in combination with either the compound XA or a permissive increase in pH. This led to an investigation into whether PF9 induced gametogenesis and this resulted in confirmation that PF9 does indeed act by initiating gametogenesis. This was confirmed by observing rounding up, erythrocyte emergence and exflagellation in PF9-treated parasites of the 3D7a line.

PF9-activated gametocytes appeared morphologically indistinguishable by Giemsa staining from XA-activated gametocytes presenting as rounded-up forms. In both PF9 and XA-treated samples haemozoin pigment appeared dissipated in contrast to the concentrated area of haemozoin in non-activated gametocytes. In contrast to the 3D7a wild type line, gametocytes of the *PfPDEδ*-ko line did not round up or emerge from the host erythrocyte when treated with PF9, but retained the characteristic crescent shape of non-activated stage V gametocytes. This is reminiscent of what is seen in XA-induced gametocytes of the *PfPDEδ*-ko line and the inability of this line to round up and emerge from the host erythrocyte has been investigated in chapter 4 (section 4.2.3. p145). The inability of *PfPDEδ*-ko line gametocytes to round up in response to PF9 is likely to be largely due to PKA-mediated 'stiffness'. This needs to be explored further and use of a conditional knockdown line of *PfPDEδ* or possibly a better way of inhibiting PKA in the *PfPDEδ*-ko line (or an additional pharmacological targeting of PKA) may aid to separate the two questions of *PfPDEδ*-mediated deformability and the role of *PfPDEδ* in gametocyte rounding up and emergence. It would be of interest to study images of PF9-induced rounded up gametocytes in both the wildtype line and the *PfPDEδ*-ko line and look at the comparison to XA-induced rounded up gametocytes by electron microscopy to further confirm that these rounded up parasites have the same morphology.

In the wildtype line, rounding up of gametocytes treated with PF9 was inhibited by both C2 and MRT00207065, indicating that PF9 induces gametogenesis through a *Pf*PKG-dependent pathway (however, this experiment needs to be repeated with a lower concentration of MRT00207065 as the 1 μ M used in this study may have been too high leading to a possibility of off target effects). XA also initiates gametogenesis in a *Pf*PKG-dependent manner[159] and it is likely that PF9 may be stimulating gametogenesis through the same pathway, by bypassing the interaction of XA with its receptor to stimulate elevation of cGMP levels (as is thought to be the case with zaprinast). It would be of interest to measure levels of cGMP in response to PF9 treatment in stage V gametocytes. In light of the data presented in this chapter, indicating that PF9 activity is *Pf*PKG dependent, it would be expected that levels of cGMP would be elevated in response to PF9 treatment.

Further investigation using WGA-Texas red to visualise the presence/absence of the erythrocyte membrane of gametocyte-infected erythrocytes of the 3D7a line confirmed that the rounded-up parasites observed in PF9-treated samples had mostly emerged from the host erythrocyte. Observation that these morphologically-rounded parasites do in fact emerge from the host erythrocyte and that the rounded-up forms that are seen were not morphologically altered from the characteristic crescent shape due to another action of the compound, serves to further confirm that PF9 is acting by stimulating gametogenesis rather than by another inhibitory effect.

The icing on the cake in terms of confirming that PF9 acts by inducing gametogenesis, was the observation of exflagellation events in PF9-treated 3D7a wildtype samples. This confirmed further that this compound acts by initiating gametogenesis and also indicating that PF9 can induce the whole process of gametogenesis from rounding up through to exflagellation. These data also indicates that PF9 is not likely to act in a sex-specific manner as it clearly stimulates male gametocytes as exflagellation has been observed and the number of gametocytes stimulated to round up in response to PF9 is not likely to account for only male gametocytes especially given that the predicted ratio of males to females is around 1:4 and the data indicating that PF9 could induce rounding up of >90 % of wildtype gametocytes. Exflagellation assays need to be carried out to quantify the number of exflagellation centres in PF9-treated samples compared to XA-treated samples (in the presence and absence of C2 and/or MRT00207065 and in the *Pf*PKG_{T618Q} gatekeeper mutant line) and EC₅₀ values determined for induction of exflagellation and *Pf*PKG-specificity of PF9-induced exflagellation (which was shown by McRobert *et al*[159], to be likely to be a non-PKG-dependent event). We have now available,

another PF9-like compound, which has shown higher potency than PF9 on asexual blood stages. It would be good to test this compound for its activity in gametocyte stages and to also identify whether this compound will induce events of gametogenesis.

Interestingly, in the wildtype 3D7a line, ~ 15 % of parasites still rounded up in the presence of both PF9 and MRT00207065. This could mean that the majority of PF9 activity is *Pf*PKG dependent but that in addition, this compound can also induce rounding up of gametocytes through a different non-*Pf*PKG-dependent mechanism, which is not sensitive to *Pf*PKG inhibition (which is hypothesised to be the case with XA treatment based on evidence on Ca²⁺ mobilisation presented in chapter 4). It is highly unlikely that an off target effect would be seen with MRT00207065; however, this compound needs to be used at low concentrations to avoid an off target effect. This inhibitor is highly specific for *Pf*PKG and has an EC₅₀ value of 2 nM in a 72-hour hypoxanthine incorporation assay and was used at 1 μM in this assay, which in hindsight may have been too high. It would be useful to repeat these assays using MRT00207065 at a lower concentration in the nM range. PF9 was used at 10 μM, which is well above the EC₅₀ (143 nM) value of this compound. Another explanation is that it could be a product of experimental design. Both compounds were added simultaneously. It may be that PF9 is reaching its target more quickly than that of C2 in this assay, so a certain proportion of cells have rounded up before *Pf*PKG has been inhibited. Or it may reflect different dynamics of the actual inhibition process. Data in this thesis have indicated that PF9 acts very quickly, faster than is seen in XA induction. It would be of interest to pre-incubate cells with C2 prior to addition of PF9. It would also be useful to test PF9 on the *Pf*PKG_{T618Q} line in both the presence and absence of C2 and MRT00207065.

What is also interesting is that in the *Pf*PDEδ-ko line, ~ 25 % of cells still rounded up in response to PF9 in the absence of *Pf*PDEδ. This indicates PF9 can still induce rounding up in the absence of *Pf*PDEδ (and in the presence of activated *Pf*PKA leading to induced stiffness) but much less effectively than in the wildtype line. This activity in the *Pf*PDEδ-ko line was completely reversed by both C2 and MRT00207065, indicating that this is a *Pf*PKG-dependent event. An explanation for this is that PF9 is also targeting another *Pf*PDE, such as *Pf*PDEα that is present in mature gametocytes (though not essential) and that can hydrolyse cGMP. As the majority (two thirds) of activity is inhibited when *Pf*PDEδ is absent, this indicates that this other *Pf*PDE is unable to compensate fully for the loss of *Pf*PDEδ. And that the inhibition of this *Pf*PDE alone cannot induce gametocyte induction to levels as high as *Pf*PDEδ inhibition. The fact that these cells can still undergo rounding up in the presence of *Pf*PKA-induced stiffness likely indicates that absence of *Pf*PDEδ does not result in all cells becoming stiff and that a small proportion remain

deformable and can undergo gametogenesis when stimulated. This is supported by the deformability data presented in chapter 4 in which ~ 20 % of parasites of the *PfPDEδ*-ko line transcend the matrix indicating that this proportion of parasites still exhibit deformability in the absence of *PfPDEδ*. Another explanation may be that *PfPDEδ* is only present in one of the sexes i.e. in male gametocytes (as we see exflagellation). It would be interesting to repeat some of these rounding up assays using sex-specific antibodies such as α -tubulin II for male detection and Pfg377 for female detection.

Ca²⁺ mobilisation has been shown to play an important role in the process of gametogenesis[260][159][210]. Ca²⁺ has been shown to be required for both XA and zaprinast-induced exflagellation but not for rounding up[159]. It therefore appears not to be required for the initial step of gametogenesis and is thought to act downstream of *PfPKG* and *PfPDEs*[159]. As XA, zaprinast and PF9 have all been shown to stimulate gametogenesis in a *PfPKG*-dependent manner, it was therefore interesting to investigate whether PF9 also induces Ca²⁺ release in mature gametocytes.

Interestingly, PF9 induced Ca²⁺ mobilisation in stage V gametocytes at levels much higher than either XA or zaprinast. The majority of Ca²⁺ release appeared to be *PfPKG* dependent as it was reversed by C2. However, just over 20 % of the total Ca²⁺ released in PF9 treated samples was not reversed by C2. This mirrors what was seen in PF9-induced rounding up of the same line with MRT00207065 (~ 15 % rounding up) and indicates that PF9, although mostly inducing Ca²⁺ through a *PfPKG*-dependent pathway, might also induce Ca²⁺ mobilisation through an additional pathway that is not sensitive to *PfPKG* inhibition. This is what is observed in Ca²⁺ release assays in wildtype parasites in chapter 3 (section 3.2.2, p120). Again, this result may be explained simply by experimental design, as C2 and PF9 were added simultaneously in this assay and repeating this experiment using cells pre-incubated with C2 may confirm whether this result is just a case of PF9 reaching its target much quicker than C2. In the absence of this confirmation, it would be useful to repeat this experiment both using the more specific *PfPKG* inhibitor MRT00207065 at a lower concentration than used in this thesis, and the gatekeeper mutant *PfPKG*_{T618Q}, which is resistant to both C2 and MRT00207065. Based on work on other life cycle stages, zaprinast and XA are thought to induce Ca²⁺ mobilisation via PI-PLC induced release of IP₃. It may be that PF9 induces Ca²⁺ release through the same signalling pathways as both zaprinast and XA. It would be interesting to look at changes in levels of phosphoinositide lipids in PF9 treated gametocytes as we have done with zaprinast treated schizonts in chapter 3 (section 3.2, p116). It would be also of interest to look at changes in IP₃ levels with PF9 treatment. If pre-treatment of gametocytes

with MRT00207065 in both the wildtype and *Pf*PKG_{T618Q} still results in a population of cells that response to PF9 in the presence of *Pf*PKG inhibition, in terms of Ca²⁺ mobilisation and rounding up, it would be interesting to look at what other C2-sensitive protein (kinase) is responding to PF9-treatment in a *Pf*PKG-independent manner. *Pf*CDPK4 is a Ca²⁺-dependent protein kinase that is required for the late stages of gametogenesis[210]. An orthologue of *Pf*CDPK4 in *Eimeria* and *Toxoplasma* (the orthologue is known as CDPK1) has been shown to be sensitive to C1[159];[181]. It is therefore likely that *Pf*CDPK4 may be a secondary target of C2 in *P. falciparum* gametocytes. More work therefore needs to be done to confirm the specificity of the *Pf*PKG-dependent Ca²⁺ mobilisation induced by PF9. Data presented in chapter 4 (section 4.2.4, p157) indicate that the *Pf*PDE δ -ko line does not release Ca²⁺ in response to XA stimulation at all but does in response to zaprinast stimulation and in a *Pf*PKG-dependent manner. It would be interesting to test PF9 in a Ca²⁺ release assay on the *Pf*PDE δ -ko line to compare PF9 stimulation of Ca²⁺ mobilisation in this line to that of XA and zaprinast. This may give us an indication of which profile PF9 closely resembles and would therefore identify whether PF9 requires the presence of *Pf*PDE δ in order to stimulate Ca²⁺ release.

Evidence in the literature has shown that the cGMP-PDE inhibitor zaprinast can stimulate gametogenesis in the absence of XA[159]. This led to the hypothesis for PF9 action, which is described and depicted in Figure 5.26.

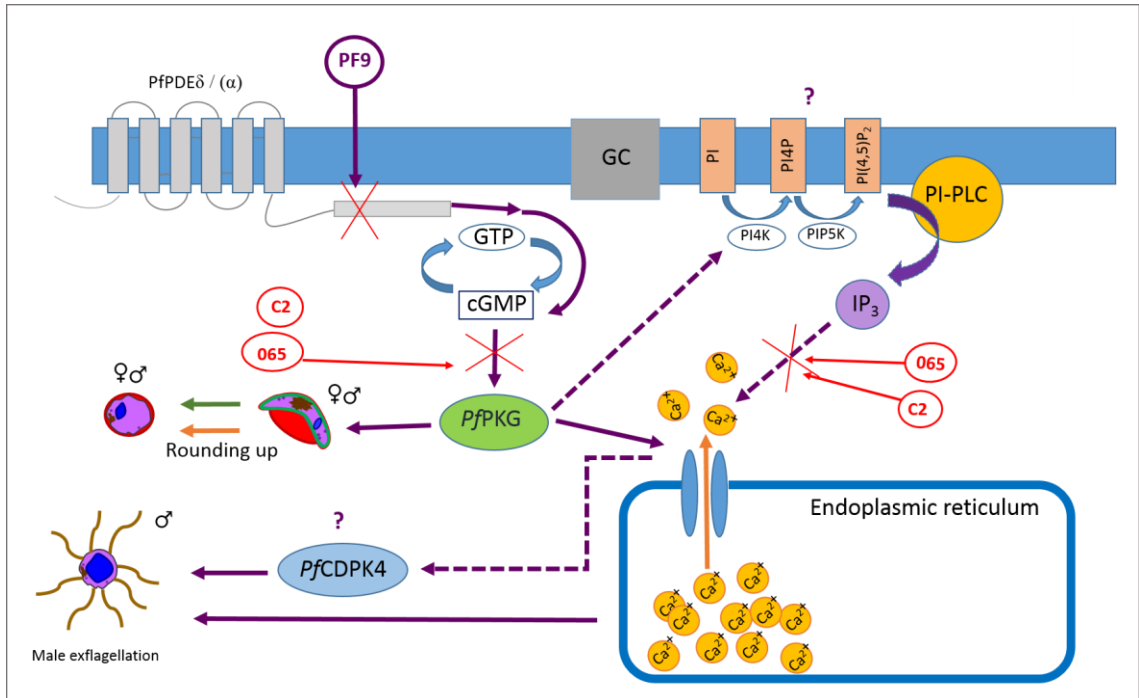


Figure 5.26. Schematic of predicted PF9-induced signalling pathways leading to gametogenesis in stage V gametocytes.

PF9 inhibits *PfpDEs* in mature gametocytes. It is likely to target *PfpDEδ* and *PfpDEα* but with targeting of *PfpDEδ* having a greater impact on gametogenesis. Inhibition of these *PfpDEs* is likely to result in elevated levels of cGMP and activation of *PfPKG*. This leads to activation of mature gametocytes leading to rounding up and emergence followed by the male specific exflagellation. This later stage of gametogenesis is dependent upon Ca^{2+} mobilisation and PF9 induces Ca^{2+} release. The signalling components between the PF9 signal and Ca^{2+} release are currently unknown but they may involve phosphoinositide lipid synthesis via PKG activation of phospholipid kinases and IP_3 -mediated Ca^{2+} mobilisation (dotted lines) as this is the likely pathway leading to Ca^{2+} release in XA and zaprinast-activated parasites. Rounding up, emergence and Ca^{2+} mobilisation induced by PF9 require *PfPKG* activation. Inhibition of *PfPKG* with either C2 or MRT00207065 inhibits all of these events. XA-induced Ca^{2+} release activates CDPK4, which leads to the later stages of male gametogenesis. PF9 treatment leads to both Ca^{2+} mobilisation and exflagellation but as yet there has not been evidence to link the two. PF9 may also induce exflagellation through Ca^{2+} - dependent activation of CDPK4 (dotted line) but this needs to be investigated. Rounding up of PF9-induced gametocytes is likely to be independent of Ca^{2+} release as observed in zaprinast and XA-induced gametocytes, however, this needs to be confirmed.

5.3.4. Discussion summary

Overall, the data described in this chapter were generated using a PDE inhibitor that targets both male and female mature gametocytes, by inducing gametogenesis in a *Pf*PKG-dependent manner. The target is likely to be *Pf*PDE δ , which is thought to be the predominant *Pf*PDE active in stage V gametocytes. This compound also induces mobilisation of Ca²⁺ from internal stores, a signalling event, which has been shown to be essential for the later stages of gametogenesis [260] [215][210] and an event which has been observed in PF9 induced gametocytes, indicating that this compound induces all the events of gametogenesis from rounding up through to exflagellation.

This mode of action and the evident fast speed at which this compound acts would have relevance in a clinical setting, as the premature initiation of gametogenesis in the human host would render gametocytes non-transmissible. Gamete emergence from the host erythrocyte into the harsh environment of the host blood stream where they are no longer protected inside a host cell would lead to quick removal by the spleen or the host immune system. Gametes need to be in the environment of the mosquito midgut for fertilisation to occur and in the absence of fertilisation, development through the mosquito stages of the life cycle to infectious sporozoites primed for transmission to a new human host will not occur. Premature gametocyte activation would quickly result in death of gametocytes in the host blood stream and it is not thought to be possible that these activated parasites would survive in the host blood stream to be taken up in a mosquito blood meal. Such a compound, which also exhibits good activity against asexual blood stages, would act to alleviate the clinical symptoms of the disease while also inhibiting transmission to the mosquito vector. This compound is a very good starting point to develop a compound that shows good inhibition against both asexual blood stages and gametocyte stages while not targeting any human PDEs. Such a drug would be an invaluable pharmacological intervention to reduce morbidity and mortality while also reducing the spread of malaria and could well be a new weapon in the arms race against malaria.

Chapter 6

Generation of a *PfPDEδ*-HA tagged transgenic line

6.1. Introduction

The putative metal ion-dependent 3'5'-cyclic nucleotide PDE *PfPDEδ* (PF3D7_1470500; located on chromosome 14) is a predicted 97.186 kDa (plasmodb.org) integral membrane protein as it contains 6 possible transmembrane helices. The membrane association of the *P. falciparum* PDE enzymes has been confirmed experimentally with PDE activity being associated with the membrane fractions of blood stage and gametocyte lysates but not the soluble fractions (Ross Cummings, PhD Thesis, 2005),[141]:[130]. These transmembrane domains are predicted to be located towards the N-terminus followed by a catalytic domain[141]. The catalytic domains of human PDEs contain the metal-ion binding sites (Zn^{2+} and one other presumed to be Mg^{2+}) required for activity and this domain is involved in cyclic nucleotide recognition and substrate binding. This domain is conserved in the four parasite PDEs. The functional importance of this domain suggests that it is likely to have most pharmacological relevance. Apart from its predicted membrane association, as yet there is no evidence regarding the specific cellular localisation of *PfPDEδ*. *PfPDEδ* mRNA transcripts have been detected in stage V gametocytes and ookinetes but only at low levels in other lifecycle stages[145] (see Figure 1.7, p49) of the Introduction for level of transcripts by Illumina sequencing), but this is not always an indication that the protein is expressed at a particular stage. This is a well-documented situation, female gametocytes transcribe many proteins which are translationally repressed until subsequent stages in the life cycle, usually in the insect stages when they are required[144]. However, *PfPDEδ* protein has been detected in stage V gametocyte lysates by proteome analysis of male and female gametocytes[144] and elevated levels of cGMP and correspondingly reduced cGMP-PDE hydrolytic activity have been measured in a *PfPDEδ*-ko transgenic line (Cathy Taylor, PhD Thesis, 2007) indicative that *PfPDEδ* is likely to be required in mature gametocyte stages. The cyclic nucleotide specificity of *PfPDEδ* has not been confirmed directly; however, the fact that elevated levels of cGMP but not cAMP have been measured in a *PfPDEδ*-ko line[130] suggests that this enzyme may be cGMP specific.

The aim of genetically modifying *PfPDEδ* with a triple (haemagglutinin) HA tag was to generate a tool to investigate further the role of *PfPDEδ* in gametocyte development and gametogenesis.

Such a line would be a useful tool firstly to confirm that the protein is present in gametocyte stages and also to determine its cellular localization and timing of expression. Immunoprecipitated protein would be pivotal to the study of protein-protein interactions and to determine the cyclic nucleotide specificity of *PfPDEδ* using a PDE assay. Observations of a defect in rounding up and emergence in the *PfPDEδ*-ko line originally pointed towards an essential role for *PfPDEδ* in gametogenesis. However, later work published on the PKA-regulated deformability of gametocyte infected erythrocytes[25] identified a role for *PfPDEδ* in maintaining a deformable phenotype to allow circulating mature gametocytes to avoid splenic clearance[25]. Interestingly, functional studies on *P. berghei* showed no phenotype in gametocytes or during gametogenesis in a *PbPDEδ*-ko line, but rather a role in ookinete stages where it regulates gliding motility. Work carried out in this thesis (chapter 4, p145) has identified that inhibition of PKA, (which becomes activated in the absence of *PfPDEδ*), can to some extent reverse the phenotype observed in *PfPDEδ*-ko parasites resulting in increased levels of XA and PF9-induced rounding up in this line. The observation that *PfPDEδ*-ko parasites will round up prematurely upon PKA inhibitor treatment is interesting and likely confirms that *PfPDEδ* does in fact play an important role in gametogenesis. However, more work needs to be done to investigate this further and the availability of a *PfPDEδ*-HA line will hopefully be a valuable tool to understand the role of this protein further.

6.2. Results

6.2.1. The design and generation of a transgenic *PfPDE δ* -HA tagged line using the CRISPR-Cas9 gene editing system.

The CRISPR-Cas9 gene editing system uses a small RNA sequence known as a guide RNA (gRNA), which specifically binds to the target sequence of interest and in doing so guides the enzyme bacterial CRISPR-associated protein-9 nuclease (Cas9) to the target sequence where it cuts at the desired site inducing a double strand break. This technique can be used to make precise changes to the parasite genome such as an insertion or deletion (see section 2.6.A to 2.6.J for a more detailed method). In collaboration with Christian Flueck (LSHTM) this technique was used to introduce a triple haemagglutinin (HA) tag at the C terminal end of *PfPDE δ* (Figure 6.1). In short, a ~700 bp synthetic repair template (ThermoFisher Scientific, see appendix (A1) for sequence) corresponding to a partly recodonised 3' end of *PfPDE δ* , a triple HA tag, and *PfPDE δ* 3' untranslated region (UTR) was inserted into the parental pL6_eGFP repair plasmid to yield pL6_ *PfPDE δ* -HA. pL6_ *PfPDE δ* -HA was verified by restriction digest and Sanger sequencing (Figure 6.2).

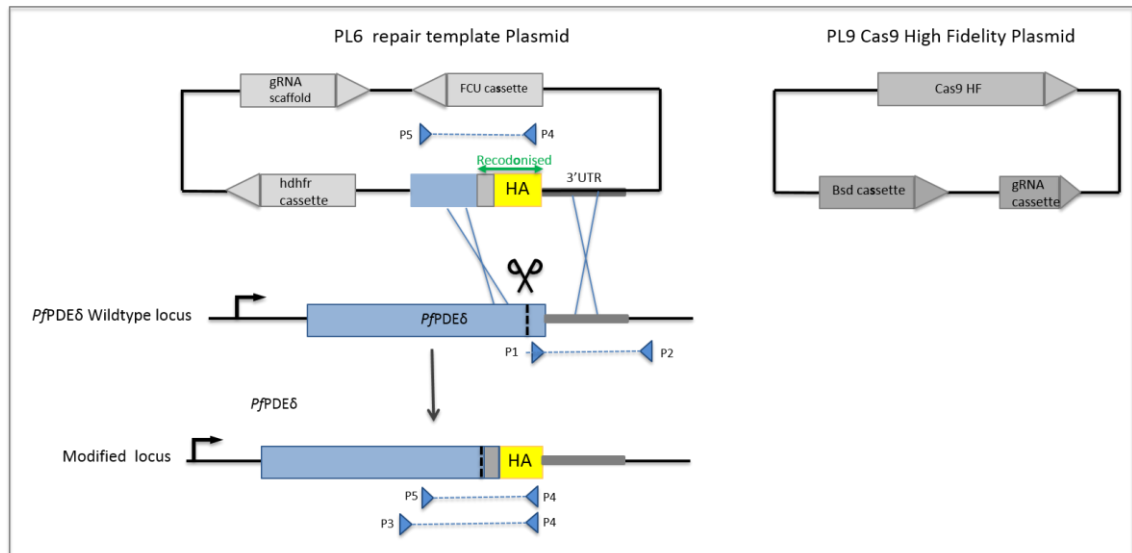


Figure 6.1. Schematic showing the strategy to introduce a C-terminal triple HA tag into the *PfpDEδ* locus. Representation of the pL9 cas9 high fidelity plasmid and the PL6 repair template plasmid before and after integration. A 700 bp synthetic repair template corresponding to a partly recodonised (grey) 3' end of *PfpDEδ* (blue), a triple HA tag (yellow) and a 3' UTR inserted into the pL6_GFP repair plasmid. The resulting pL6_*PfpDEδ*-HA plasmid was transfected simultaneously with a PL9 Cas9 high fidelity plasmid containing the gRNA sequence and a blasticidin (BSD) marker. This gRNA targets the cas9 to the target sequence where it cuts (black dotted line) and the triple HA tag is inserted into the wildtype locus. The primer pairs for integration PCR analysis are indicated by blue triangles (see appendix (A2) for sequences). Pair P1-P2-wildtype specific (expected size 226 bp), pair P3-P4 integration specific (expected size 761 bp) and P5-P4 for detection of the episome and integration of the modified locus (expected size 400 bp).

Selection of site-specific guide RNA

Selection of the most suitable guide RNA (gRNA) is crucial for efficient Cas9 targeting and subsequent repair using the provided repair template to introduce the triple HA tag. Poor guide RNA selection can lead to off target localisation of the Cas9 nuclease and induce a double strand break at the wrong location, which is potentially lethal. An initial attempt using a gRNA sequence predicted using the Protospacer software (<http://www.protospacer.com>), which predicts off-target activity but not on-target activity was used. After transfection of *P. falciparum* NF54 schizonts (Amaxa electroporation), a parasite population carrying both the pL6_ *PfPDE* δ -HA repair template plasmid (marker free, see Figure 6.1) containing the *PfPDE* δ -HA insert and the pUF1 Cas9 plasmid (selected for with DSM1) was selected, however, no modified *PfPDE* δ locus could be detected. The use of the Benchling software (<https://benchling.com>), which predicts both on-target and off-target gRNA activity revealed that the gRNA used exhibited poor on-target activity (score of 0.6 out of 100). As a result, this was repeated with a new gRNA with a high on-target activity score (31 out of 100) that was selected using this software (see Figure 6.1 for schematic) and a new transfection carried out as described below.

Introduction of a triple HA tag into the *PfPDE* δ -HA wildtype locus

The newly selected gRNA sequence was cloned into the pL9 Cas9-HF-bsd plasmid (Avnish Patel, LSHTM). For generation of a *PfPDE* δ -HA expressing line, *P. falciparum* NF54 ring stage parasites were transfected simultaneously with the circular pL6_ *PfPDE* δ -HA repair template plasmid and the pL9-HF-bsd plasmid (Cas9 high fidelity plasmid) plasmid containing the gRNA sequence and a blasticidin marker for plasmid selection (see Figure 6.1). Transfected parasites were treated with 2.5 μ g/ml blasticidin for 10 days and then monitored regularly until parasites were detectable by microscopy of Giemsa-stained blood films. Observations of parasite growth and development indicated that asexual blood stages of this transgenic line grow and develop normally through the cell cycle (data not included).

Confirmation of integration of the HA tagging plasmid into the *PfPDE* δ locus

A comprehensive PCR analysis was carried out on DNA extracted from *PfPDE* δ -HA cultures (Figure 6.2). This showed successful integration of the HA-tagging plasmid into the *PfPDE* δ locus. A band size of ~ 700 bp was detected using primers specific for integration of *PfPDE* δ -HA only in *PfPDE* δ -HA samples and not in the NF54 control (see appendix (A2) for primer sequences). This corresponded to the expected band size of 761 bp. The expected band size of 226 bp with wildtype-specific primers was detected only in the wildtype NF54 control sample and not in the *PfPDE* δ -HA sample showing that no wildtype parasites remained in the *PfPDE* δ -HA parasite population.

Together the data indicated that successful integration had occurred (Figure 6.2). Primers specific for both integrated and episomal *PfPDE* δ -HA detected an expected band size of ~ 400 bp. This was only detected in the *PfPDE* δ -HA sample and not the NF54 control. Primers specific for PKG were used as a DNA control and an expected band size of 711 bp was detected in both the *PfPDE* δ -HA and NF54 samples.

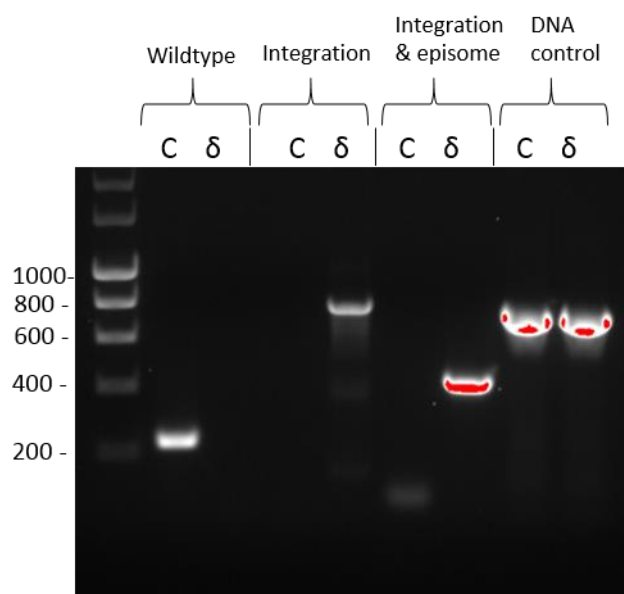


Figure 6.2. *PfPDE* δ -HA integration PCR. (For primer sequences see appendix). Wildtype-specific primer pair (P1-P2) detected a band only in the wildtype NF54 sample (C), Integration-specific pair (P3-P4) detected a band only in the *PfPDE* δ -HA line sample (δ). Integration and episome specific pair (P4-P5) detected a band only in the *PfPDE* δ -HA line sample. The DNA control primer pair (PKG, P6-P7) detected bands in both the wildtype and *PfPDE* δ -HA line samples.

On initiation of gametocytogenesis, the *PfPDE δ -HA* transgenic appeared to exhibit good gametocyte-producing capabilities, with comparable numbers of gametocytes observed when compared to an NF54 control line (data not included). Gametocytes appeared to develop normally to stage V and rounding up assays indicated a normal (rounding up) response to XA (Figure 6.3).

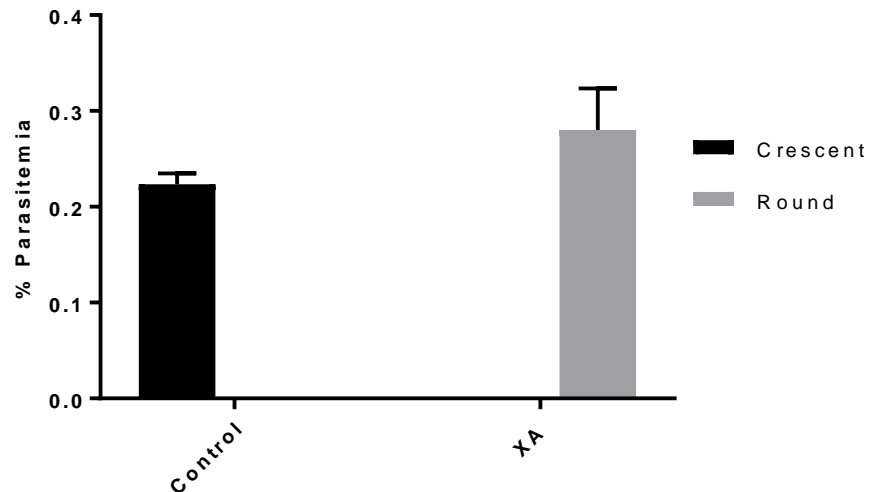


Figure 6.3. XA-induced rounding up in the *PfPDE δ -HA* transgenic line. Stage V gametocytes treated with 10 μ M XA or 0.05 % DMSO (control) for 30 minutes at room temperature. Presented as percentage parasitemia from counts of Giemsa stained blood films. Data analysed in Excel is the average of 3 counts (900 RBCs counted per sample) from one experiment. Graph generated in GraphPad, Prism. Error bars represent SD.

6.2.2. *PfPDEδ*-HA gives a faint signal by immunofluorescence assay

Determination of the localisation of a protein can provide information on its function. Detection of *PfPDEδ*-HA by immunofluorescence assay using a rat α -HA antibody and an α -rat Alexa Fluor 594 secondary antibody, on 4 % formaldehyde-fixed and cold methanol-fixed dried blood smears was not initially successful when carried out in the absence of detergent (data not shown). High levels of background were seen in the wild type NF54 control samples. This experiment was carried out prior to the successful immunoprecipitation of *PfPDEδ*-HA. However, on achieving purified *PfPDEδ*-HA protein by pull down from samples of stage IV/V gametocytes (see section 6.2.4), it was clear that the tagged protein is present in mature gametocytes. It is possible that the HA tag is not easily accessible to the α -HA antibody due to the folding of the protein or it may form part of a complex and this makes it harder for the antibody to access the HA tag. This assay was therefore repeated but including 0.05 % Tween 20 with the aim to make the HA tag more accessible. Two different conditions were tested. Firstly, a rat α -HA antibody followed by α -rat Alexa Fluor 594 secondary antibody. Secondly, a rat α -HA antibody followed by an α -rat-biotin antibody followed by Alexa Fluor 488-conjugated streptavidin with the aim to increase sensitivity. Preliminary data revealed faint levels of fluorescence with both the conditions (Figures 6.4 and 6.5). At this stage (in the absence of negative controls using the antibodies individually) it is not clear whether the fluorescence seen represents the localisation of *PfPDEδ*-HA protein or whether it is background fluorescence. However, the fluorescence levels observed in the wild type NF54 control gametocyte samples (using both primary and secondary antibodies) were much lower than in the transgenic line (Figure 6.6). Fluorescence in NF54 samples appeared to be lower in the α -rat-biotin antibody samples (Figure 6.5).

The faint fluorescence appeared to show a punctate pattern. Interestingly, this pattern of fluorescence is similar to the pattern of localisation of osmiophilic bodies using a transgenic line expressing Pfg377 fused to a reporter protein[288]. This is intriguing as osmiophilic bodies are thought to be involved in egress of female gametocytes and *PfPDEδ* is also thought to be required for egress. The conditions of this assay need to be improved to visualise the HA-tagged *PfPDEδ* protein and to minimise any background fluorescence and unspecific binding resulting in a better signal to noise ratio. It will be important to investigate whether the fluorescence seen corresponds to specific binding of HA antibody to the tagged *PfPDEδ* rather than non-specific binding.

*Pf*PDE δ -HA

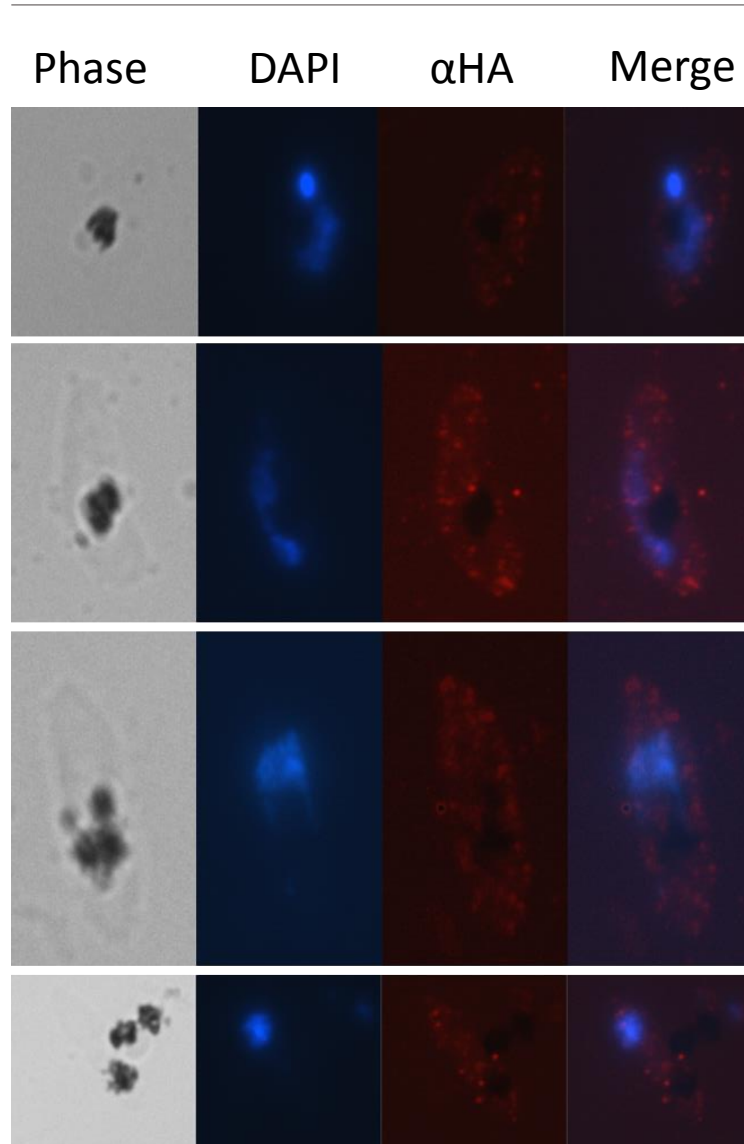


Figure 6.4. Immunofluorescence assay of *Pf*PDE δ -HA mature gametocytes. Dried blood smears of *Pf*PDE δ -HA stage V gametocytes were fixed with 4 % formaldehyde and incubated with α -HA antibody (rat) followed by a α -rat Alexa Fluor 594 secondary antibody (red), followed by addition of Vector shield containing DAPI (blue). Samples were imaged using an EVOS FL fluorescent cell imaging system.

*Pf*PDE δ -HA

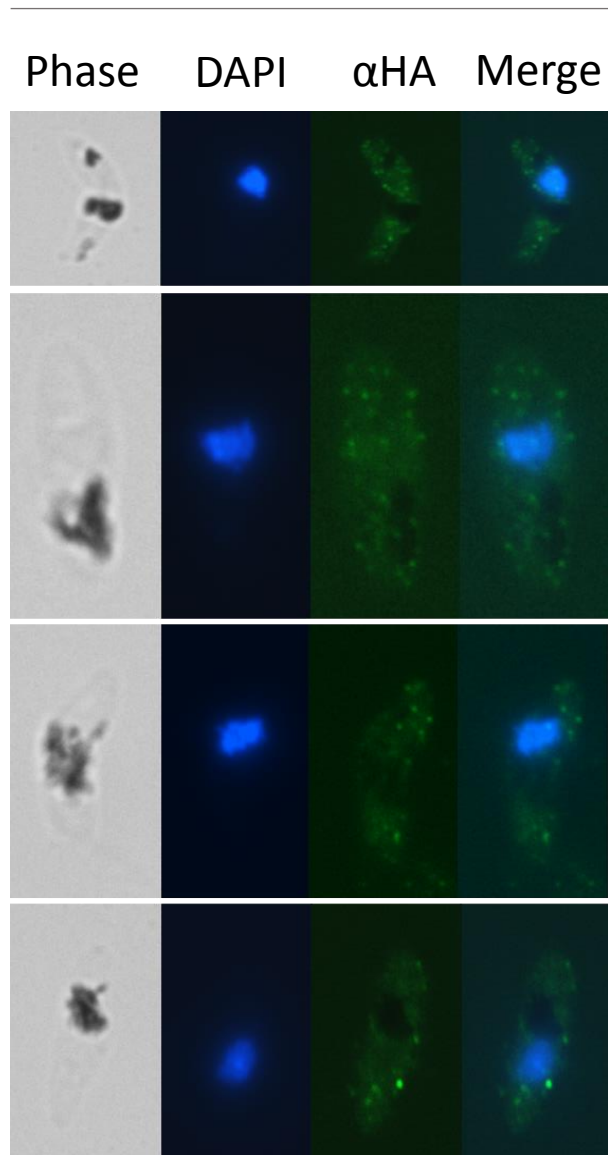


Figure 6.5. Immunofluorescence assay of *Pf*PDE δ -HA mature gametocytes. Dried blood smears of *Pf*PDE δ -HA stage V gametocytes fixed with 4 % formaldehyde and incubated with rat α -HA antibody (and 0.05 % Tween 20) followed by α -rat biotin antibody coupled to Alexa Fluor 488 conjugated streptavidin (green) followed by addition of Vector shield containing DAPI (blue). Samples were imaged using an EVOS FL fluorescent cell imaging system.

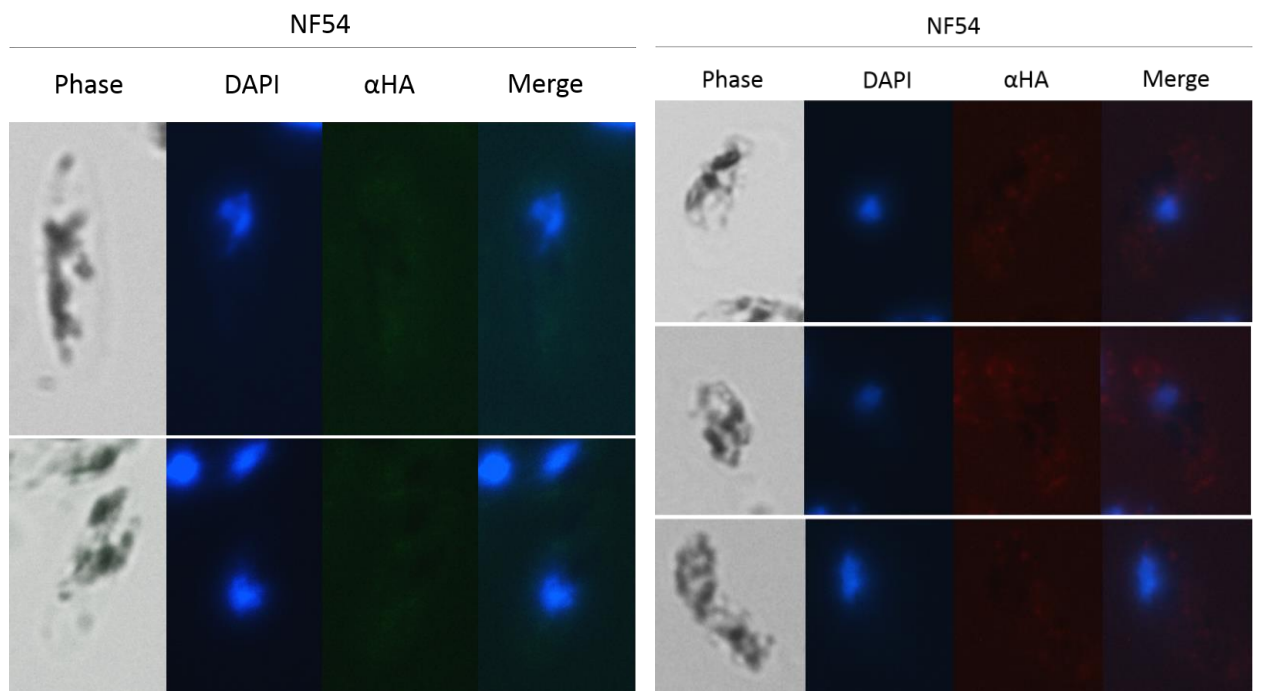


Figure 6.6. Immunofluorescence assay of NF54 mature gametocytes. Control samples for figures 6.4 and 6.5 (assays done in parallel). Dried blood smears of *PfPDE δ -HA* stage V gametocytes fixed with 4 % formaldehyde and incubated with α -HA antibody (rat) (and 0.05 % Tween 20) followed by a α -rat Alexa Fluor 594 secondary antibody (right) or with α -rat biotin antibody coupled to Alexa Fluor 488 conjugated streptavidin (left), both followed by addition of Vector shield containing DAPI (blue). Samples were imaged using an EVOS FL fluorescent cell imaging system.

6.2.3. *Pf*PDE δ -HA partially co-localises with the Golgi marker ERD2

Given the interesting pattern of fluorescence in HA-tagged stage V *Pf*PDE δ gametocytes (Figures 6.4 and 6.5), which suggests a possible osmiophilic body localisation, it was of interest to determine whether the pattern of fluorescence seen would co-localise with a marker for the Golgi. This is because osmiophilic bodies are thought to be derived from the Golgi[288] and accumulate in female gametocytes reaching higher densities as gametocytes mature. These data are very preliminary and the experiment needs to be repeated with the appropriate controls. However, a densely punctuate pattern was obtained in both cases and there appears to be some co-localisation of the α -HA and α -ERD2 antibodies, indicating that the location of *Pf*PDE δ may overlap somewhat with the Golgi protein ERD2 (Figure 6.7). This partial overlap may reflect the location of osmiophilic bodies. It would be interesting to investigate this further.

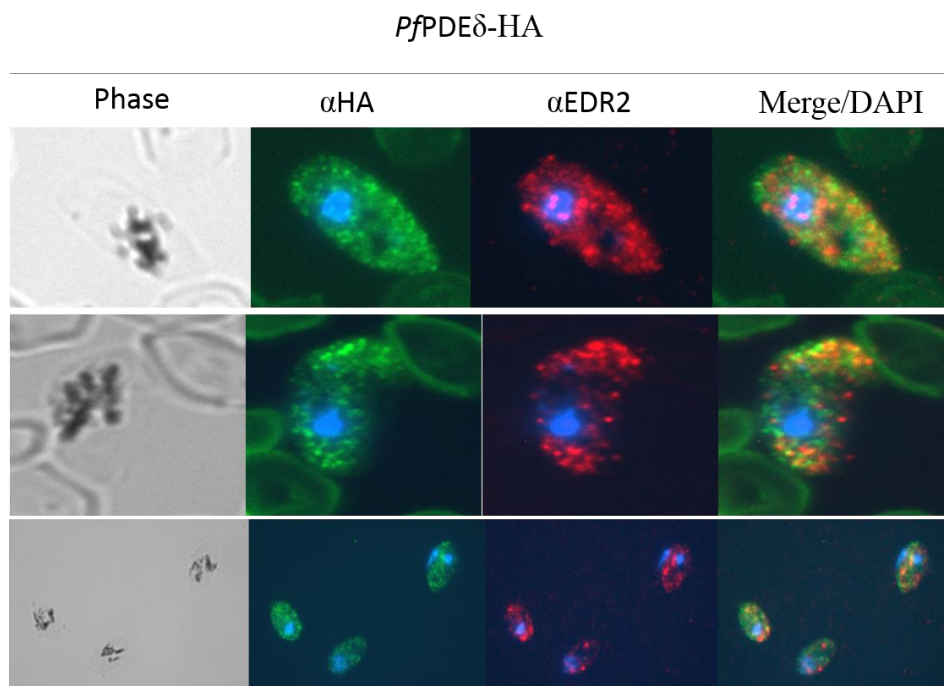


Figure 6.7. Immunofluorescence assay of *Pf*PDE δ -HA mature gametocytes. Dried blood smears of *Pf*PDE δ -HA stage V gametocytes fixed with 4 % formaldehyde. For detection of *Pf*PDE δ -HA, samples incubated with α -HA antibody followed by a α -rat Alexa Fluor 588 secondary antibody (green). For detection of ERD2, samples incubated with a rabbit α ERD2 (1:1000) antibody followed by α -rabbit Alexa Fluor 549 secondary antibody (red). Vector shield containing DAPI (blue) was added to both samples. Samples were imaged using an EVOS FL fluorescent cell imaging system.

6.2.4. Purification of HA tagged *PfPDE δ* by immunoprecipitation from gametocyte lysates

Immunoprecipitation (IP) assays were performed on stage IV/V gametocyte lysates from the *PfPDE δ* -HA transgenic line. An intense band size of ~ 90 kDa by western blotting was detected in the input sample, and also very strongly in the sample eluted from the anti-affinity matrix (Figure 6.8). This size is close to the expected size of *PfPDE δ* -HA, (97.168 kDa, plasmodb.org). The expected size of the triple HA tag is 3.17 kDa, making the whole protein size a predicted 100.33 kDa; this likely indicates that the protein detected on the Western blot is full length *PfPDE δ* . A much fainter band corresponding to *PfPDE δ* -HA was detected in the unbound sample, but the majority of protein appeared to have been immunoprecipitated indicating that this protein can be pulled down very efficiently (Figure 6.8). This was in contrast to the positive control (*PfPDE β* -HA from a *P. falciparum* blood stage culture) sample in which a strong band was still seen in the unbound sample indicative that not all of the *PfPDE β* -HA protein was bound to the beads with a large amount of protein remaining in the unbound fraction. These data indicates that a large amount of *PfPDE δ* can be pulled down from stage IV/V gametocytes, consistent with proteomics data[144] indicating the presence of *PfPDE δ* protein at stage V by mass spectrometry. No protein was detected in the 3D7a negative control sample in any of the fractions, indicative that this assay only detected HA-tagged protein.

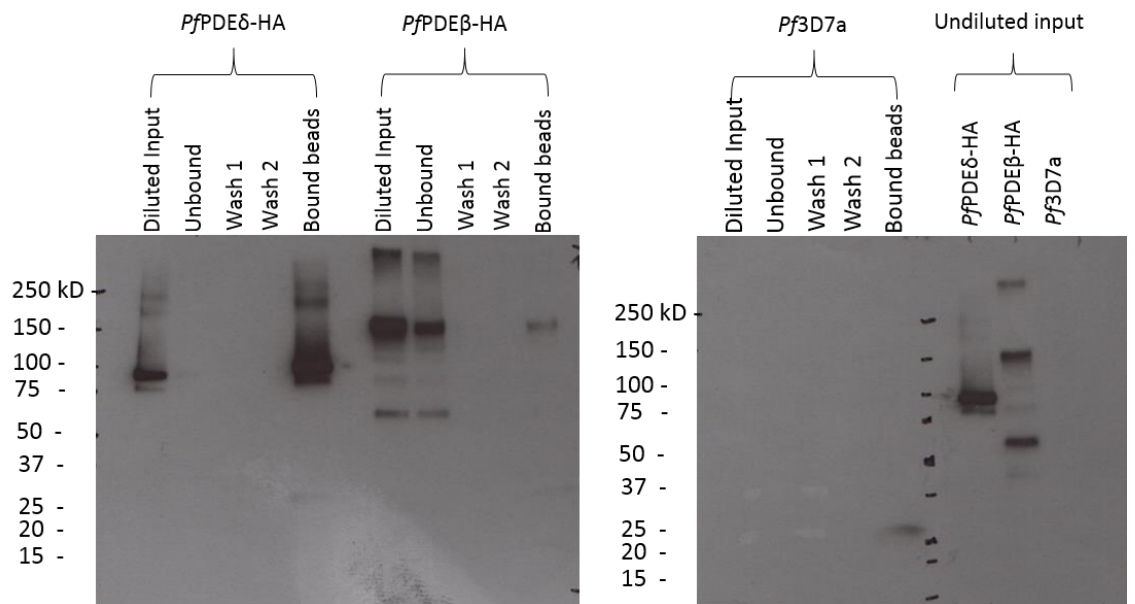


Figure 6.8: Western blot of immunoprecipitated *PfPDEδ*-HA from stage IV/V gametocyte lysates. *PfPDEδ*-HA compared to a positive control (*PfPDEβ*-HA from mature schizont lysates) and a negative control (3D7a schizont lysates). HA-tagged protein was pulled down using an Anti-HA Affinity matrix. HA-tagged protein detected using an α -HA high affinity rat monoclonal antibody. Undiluted input represents HA-tagged protein in parasite lysates prior to immunoprecipitation. Samples were diluted (diluted input) then detected in subsequent washes (unbound, wash 1 and wash 2). HA-tagged protein bound to the Anti-HA Affinity matrix (immunoprecipitated) and detected protein (bound beads).

6.2.5 cGMP (but not cAMP) hydrolytic activity is detected in immunoprecipitated *Pf*PDE δ -HA protein from stage IV/V gametocyte lysate.

The cyclic nucleotide specificity of native *Pf*PDE δ has not been measured directly. However, elevated levels of cGMP have been measured in a *Pf*PDE δ -ko line[130] and reduced cGMP but not cAMP hydrolytic activity has been measured in gametocyte lysates from the *Pf*PDE δ -ko line[130]. As such, *Pf*PDE δ is predicted to be a cGMP-specific PDE.

To measure the cyclic nucleotide specificity of *Pf*PDE δ directly, the immunoprecipitated protein eluted from the anti-affinity matrix (see Figure 6.8) was used to perform a PDE assay (see section 2.5.G, p90 for more details of the method). The cyclic nucleotide hydrolysing activity of *Pf*PDE δ was compared to that of *Pf*PDE β , which was shown to be dual specific in assays carried out by Laura Drought (Laura Drought, PhD Thesis, 2014).

Data from the assay showed as expected that *Pf*PDE β hydrolyses both cAMP and cGMP and was therefore a good positive control for the assay (Figure 6.9). *Pf*PDE δ on the other hand, showed only cGMP hydrolysing activity. No cAMP hydrolysing activity was detected. This is in keeping with data on gametocyte lysates, which showed cGMP hydrolysing activity but not cAMP activity and confirms that *Pf*PDE-delta is a cGMP-specific PDE[130].

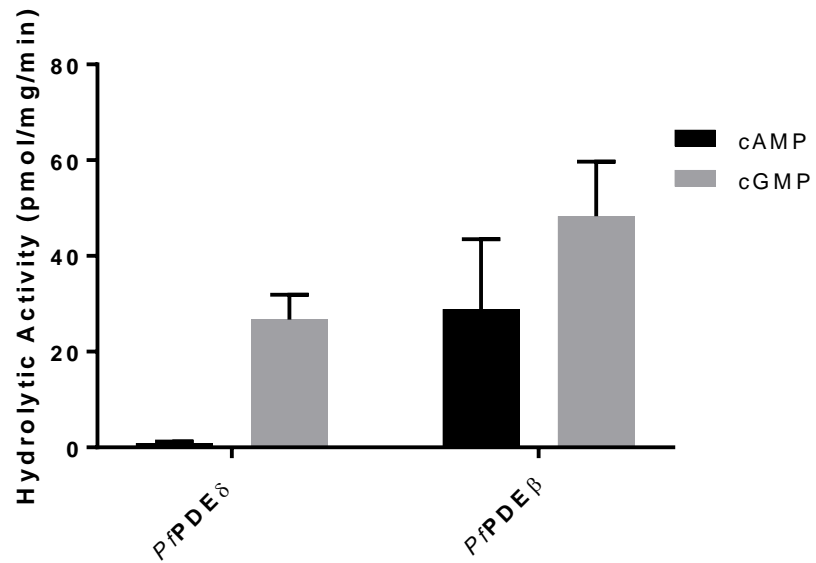


Figure 6.9: Cyclic nucleotide hydrolysing activity of immunoprecipitated *PfPDE* δ protein. Assays were carried out on *PfPDE* δ and *PfPDE* β protein pulled down by immunoprecipitation. Cyclic nucleotide hydrolytic activity was compared to that of *PfPDE* β protein. Levels of tritiated labelled cAMP and cGMP were measured by scintillation counting. Means of triplicate wells are presented. Data were analysed in Excel and the graph generated in GraphPad, Prism. Error bars represent SD.

6.2.6 PDE inhibition reduces both cAMP and cGMP hydrolytic activity in mature gametocyte stages.

Given the potent activity of the Pfizer PDE inhibitor PF9 on gametocytes (see chapter 5) and the observation that the *PfPDEδ*-ko line was unable to release Ca^{2+} in response to XA stimulation (chapter 4, section 4.24, p155), it was hypothesised that XA may interact with *PfPDEδ* either directly or indirectly to possibly turn off *PfPDEδ* leading to elevated levels of cGMP. It was of interest to test these compounds on immunoprecipitated (IP) HA-tagged *PfPDEδ* protein to determine whether they could inhibit cGMP hydrolytic activity. PF9 has already been tested on immunoprecipitated HA-tagged *PfPDEβ* protein and on asexual parasite lysates from a wildtype (3D7) and a *PfPDEα*-ko line. This compound reduced both the cAMP and cGMP hydrolytic activity in blood stage parasite lysates and showed some activity against immunoprecipitated HA-tagged *PfPDEβ* protein. The interpretation was that PF9 is a broad specificity PDE inhibitor that targets both *PfPDEα* and *PfPDEβ* (Laura Drought, PhD Thesis, 2014).

Addition of 5 μ M PF9 to purified HA-tagged *PfPDEδ* protein reduced cGMP hydrolysis by \sim 50 %, and this was shown to be significant (Welchs unpaired t test, $P = 0.0287$) (Figure 6.10). However, the lower concentration of 200 nM did not reduce levels of cGMP hydrolysis. Interestingly, addition of 1 μ M and 10 μ M XA to samples of *PfPDEδ* protein did not reduce the cGMP hydrolytic activity but appeared to increase it by 40-50 %. However, this was shown to be not significant (Welchs unpaired t test $P=0.0878$ and $P = 0.3333$ respectively).

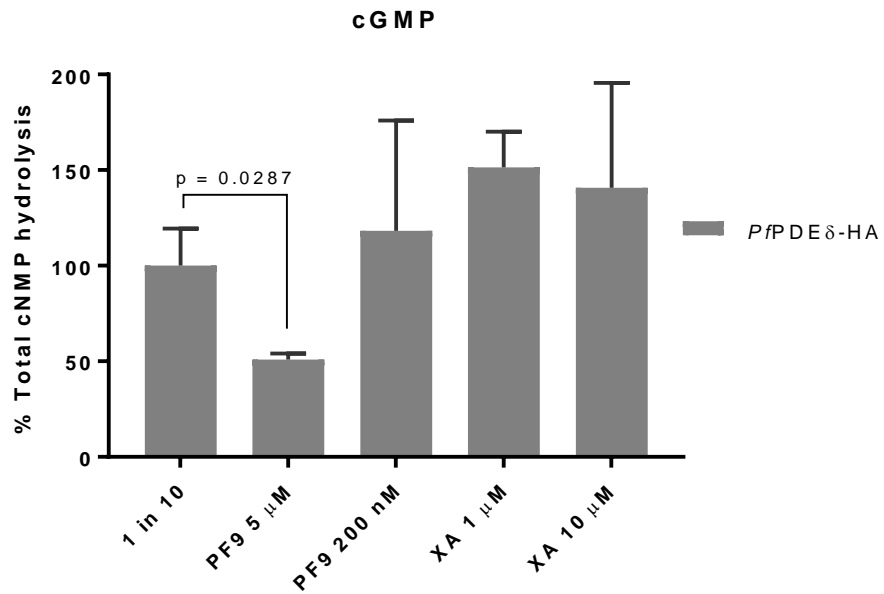


Figure 6.10. The effect of PF9 and XA on *PfPDE* δ -HA cGMP hydrolysing activity. Immunoprecipitated HA-tagged *PfPDE* δ protein incubated with PF9 (5 μ M and 200 nM) and XA (1 μ M and 10 μ M) presented as percentage of the control sample (1 in 10 dilution in PDE assay buffer) normalised to 100 %. Data is from one experiment carried out in triplicate and analysed in Excel. The graph was generated in GraphPad, Prism. Error bars represent SD.

PF9 is active against both *Pf*PDE β cAMP and cGMP hydrolysis

Addition of the Pfizer inhibitor PF9 to immunoprecipitated *Pf*PDE β protein reduced both the cAMP and cGMP hydrolytic activity. Addition of 5 μ M PF9 almost completely abolished the cAMP hydrolysis by *Pf*PDE β protein with only ~ 7 % of activity remaining ($P = 0.0024$). The lower concentration of PF9 (200 nM) also reduced PDE β cAMP hydrolysis by ~ 75 % (Figure 6.11) this was also shown to be significant (Welchs unpaired t test, $P = 0.0004$).

*Pf*PDE β cGMP hydrolytic activity was also reduced by PF9 but only at the highest concentration of 5 μ M, which reduced the hydrolytic activity by ~ 70 %. This was shown to be significant (Welchs unpaired t test, $P = 0.0287$). However, levels of cGMP hydrolysis by *Pf*PDE β were not altered by addition of the lower concentration (200 nM) of PF9 (Figure 6.12).

Interestingly, addition of 1 μ M XA appeared to reduced levels of cAMP hydrolysis by immunoprecipitated HA-tagged *Pf*PDE β protein by ~ 40 % (Figure 6.11), this was shown to be significant (Welchs unpaired t test, $P = 0.0033$). Levels of cGMP hydrolysis did not appear reduced with XA addition (Figure 6.12), in fact, *Pf*PDE β cGMP hydrolytic activity appeared higher in XA-treated samples reflected by a ~ 50 % increase in activity. However, this was shown to be not significant (Welchs unpaired t test $P = 0.1718$).

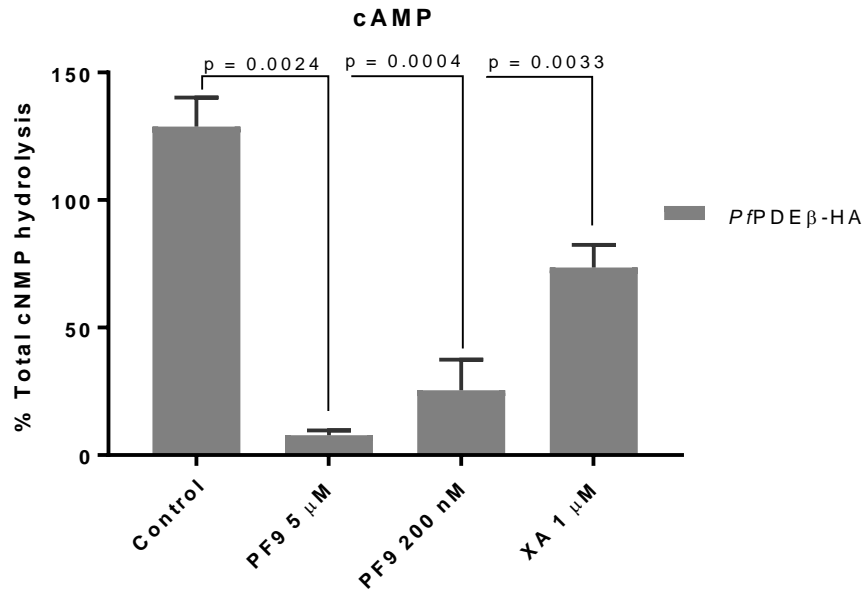


Figure 6.11. The effect of PF9 and XA on *PfPDE* β -HA cAMP hydrolysing activity. Immunoprecipitated HA tagged *PfPDE* β protein incubated with PF9 (5 μ M and 200 nM) and XA (1 μ M) presented as percentage of the control sample (1 in 10 dilution in PDE assay buffer) normalised to 100 %. Data are from one experiment carried out in triplicate analysed in Excel. Graph generated in GraphPad, Prism. Error bars represent SD.

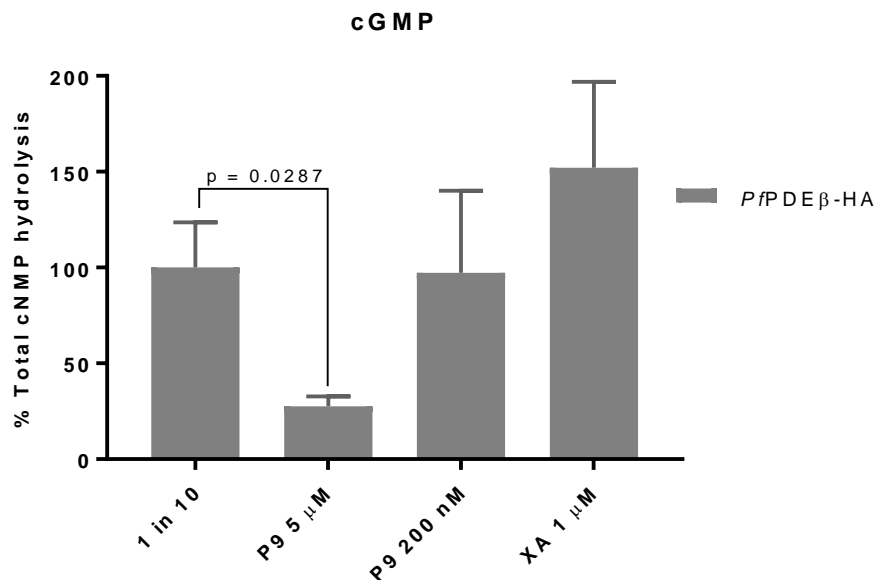


Figure 6.12. The effect of PF9 and XA on *PfPDE* β -HA cGMP hydrolysing activity. Immunoprecipitated HA tagged *PfPDE* β protein incubated with PF9 (5 μ M and 200 nM) and XA (1 μ M) presented as percentage of the control sample (1 in 10 dilution in PDE assay buffer) normalised to 100 %. Data are from one experiment carried out in triplicate analysed in Excel. Graph generated in GraphPad, Prism. Error bars represent SD.

6.3. Discussion

The success of producing a HA-tagged *PfPDE δ* line was confirmed by a PCR with a diagnostic primer set that showed clearly that integration had occurred and that the population did not contain any wildtype parasites. The tagging of *PfPDE δ* did not appear to affect the growth and development of asexual or sexual stages, indicating that this genetic modification did not disrupt normal growth and development.

Interestingly the possible *PfPDE δ* -HA protein localisation showed similarity to the localisation of osmiophilic bodies, these are electron dense organelles mostly specific to female gametocyte stages. These organelles accumulate in female gametocytes where they localise under the gametocyte surface and are involved in female gamete egress[289]-[288]. It would be interesting to repeat this assay with both the α -HA antibody and an antibody against the female-specific protein Pfg377, as this protein has been shown to localise to the osmiophilic bodies[288]. This would help determine whether *PfPDE δ* is localised in osmiophilic bodies or not. It would also be of interest to test an antibody against the male specific α -tubulin in parallel to determine whether male gametocytes exhibit this pattern of staining (or any staining). Osmiophilic bodies can also be found in male gametocytes but at a much lower number and it may be that in these cells no staining will be observed (as Pfg377 is not present and if *PfPDE δ* is also absent, so no staining for either proteins will be seen). Osmiophilic bodies are thought to be derived from the Golgi[288] so it was of interest to see a degree of co-localisation of antibodies against *PfPDE δ* and the Golgi protein ERD2. This was preliminary data but strengthens the hypothesis that *PfPDE δ* may be associated (or likely located within) osmiophilic bodies. In female gametocytes, the pattern of Pfg377 localisation changes as gametocytes emerge. If *PfPDE δ* is shown to co-localise with Pfg377, It would be interesting to carry out rounding up experiments on the *PfPDE δ* -HA line using XA (and PF9) and staining with sex-specific antibodies (including Pfg377) and an α -HA antibody to determine whether the localisation of *PfPDE δ* changes when egress occurs.

The possible association of *PfPDE δ* to osmiophilic bodies is an interesting observation since *PfPDE δ* is thought to have a role in gametocyte rounding up and gamete emergence/egress[130]. The sex ratio of females to males differs between parasite lines. However, the ratio leans in favour of females with an average ratio of $\sim 1:4$ [254]. Therefore if *PfPDE δ* were required for female egress only, the effect of deletion of *PfPDE δ* would still impact

significantly the egress/rounding up phenotype of a mixed culture as only ~ 25 % of parasites (depending on the sex ratio) would be expected to still be able to egress/round up in the absence of *PfPDEδ* and this could account for the male population. This appears to be reflected in egress assays presented in this thesis, carried out on the *PfPDEδ*-ko line, which in the presence of PKA inhibitors show that ~ 15/25 % of parasites can still round up in the absence of *PfPDEδ*. This may reflect the male population, with females still being unable to round up and egress in the absence of *PfPDEδ* despite the PKA inhibition, but males being able round up once the PKA-induced stiff phenotype has been removed. Interestingly, Ca^{2+} assays carried out on mature gametocyte stages appeared to show both a PKG-dependent and PKG-independent response. This may also reflect a sex- specific difference in the XA and zaprinast induced Ca^{2+} response in this line and would be an interesting question to explore further.

PfPDEδ-HA was successfully immunoprecipitated using an anti-HA affinity matrix. This method produced a good yield of *PfPDEδ* protein with very little protein remaining in the unbound fraction. This was a very welcomed result as large amounts of gametocyte material are hard to produce due to the long development time of gametocytes to stage V which takes up to 14 days, and the much lower parasitemias compared to asexual stages. The ability to pull down a good sized sample of *PfPDEδ* means that smaller starting gametocyte lysate samples can be used in the future, therefore saving a lot of time and resources. This yield also indicates that there is likely to be large amounts of *PfPDEδ* protein in stage IV/V gametocytes. The fact that there was a mixture of stage IV and V gametocytes in the sample used to produce the immunoprecipitated *PfPDEδ* protein may indicate that stage IV gametocytes also contain *PfPDEδ*. It would be interesting to carry out IFAs of gametocyte samples and Western blots from parasite lysates on all five stages of gametocytes to look at whether the *PfPDEδ* protein can be detected in stages other than stage V where it has been shown to be present by mass spectrometry.

The immunoprecipitated *PfPDEδ*-HA protein was used to determine the cyclic nucleotide specificity of *PfPDEδ*. Although PDEδ has historically been thought to be cGMP specific, work by Ramdani *et al*, have identified a role for *PfPDEδ* in cAMP-regulated deformability[25] which had raised the possibility that this PDE could be dual specific. Authors in this paper measured elevated levels of both cAMP and cGMP in *PfPDEδ*-ko line gametocytes. However it was unclear whether cAMP levels were regulated by *PfPDEδ* directly or indirectly. Therefore confirmation of the hydrolytic activity was important. The PDE assay presented here was only carried out once in triplicate and this needs to be repeated to confirm the result. However, the data presented here mirrors previous findings[130] and suggests that only cGMP hydrolytic activity is present

in the purified *Pf*PDE δ protein samples, suggesting that any elevation of cAMP levels in the PDE δ knockout must be achieved indirectly.

The observation that PF9 reduced cyclic nucleotide hydrolytic activity of purified PDE δ further confirmed our earlier observations that this PDE inhibitor has broad specificity in relation to the malaria parasite PDEs and further supports results presented in chapter 5 showing that PF9 induces gametogenesis and that it is likely to target PDE δ . PF9 has previously been shown to reduce the cyclic nucleotide hydrolytic activity of HA-tagged *Pf*PDE β (Laura Drought, PhD, 2014).

The HA-tagged *Pf*PDE δ line is a useful tool that can be used in further studies to confirm the localisation of *Pf*PDE δ and to answer the interesting question of a possible sex-specific function for this enzyme. It will also enable us to look at possible interactions of *Pf*PDE δ with other proteins in a membrane-bound signalling complex and to pinpoint the role of *Pf*PDE δ in the essential process of gametogenesis and gametocyte-infected erythrocyte deformability. This line may also prove useful in studies designed to determine the relationship between XA and *Pf*PDE δ in the process of gametogenesis and to determine whether XA directly interacts with *Pf*PDE δ .

Chapter 7

General discussion

7.1. Project overview

PDEs are essential enzymes that function in cyclic nucleotide signalling events that govern many stages of the malaria parasite's complex life cycle. These enzymes have been shown to be good drug targets in humans as several PDE inhibitors have been developed to successfully treat diseases. *Plasmodium* PDE catalytic domains show 24-28 % identity and ~50 % similarity to the 11 member family of human homologues, however, they are thought to be sufficiently divergent in their catalytic domain to make selective inhibitor generation feasible. Cyclic GMP signalling has been shown in several studies to coincide with the release of Ca^{2+} from internal stores and c Ca^{2+} -dependent protein kinase (CDPK) function, to regulate essential cellular processes in the parasite. CDPKs have been shown to be good potential drug targets in *P. falciparum*[290][291][292]. This project aimed to investigate the relationship between cGMP signalling and Ca^{2+} in blood stage schizonts and gametocytes and to also investigate the role of PDEs in the process of gametogenesis with particular focus on *Pf*PDE δ which has been indicated in the literature to be essential in the process of gametogenesis. A small panel of human PDE inhibitors developed by Pfizer that showed good activity on asexual blood stages (Laura Drought, PhD Thesis, 2014) were tested as part of my PhD project for gametocytocidal properties. Data generated through the investigation into the biology of *Pf*PDEs has emphasised the importance of PDEs as novel drug targets in the malaria parasite. Not only do these data reflect the value of targeting cyclic nucleotide signalling, (which will disrupt several parts of the parasite life cycle), but it demonstrates that since it is often closely associated with Ca^{2+} signalling, that this essential signalling pathways might also be blocked as a result of targeting cyclic nucleotide signalling pathways.

7.2. A relationship between cGMP signalling and calcium mobilisation

In schizont stages the relationship between cGMP signalling and zaprinast-induced Ca^{2+} release appears to be clear and some of the evidence presented in this thesis has been published in collaboration with Mathieu Brochet[174]. Zaprinast induces an increase in Ca^{2+} levels and a concomitant depletion of key phospholipid intermediates in the generation of IP_3 . Using the PKG inhibitor C2 and the *Pf*PKG_{T618Q} transgenic line, both of these signalling events were shown to be PKG dependent. Although zaprinast is not the natural trigger of these events, these data strongly imply that the inhibition of *Pf*PDE activity by zaprinast leads to increased levels of cGMP, which activate *Pf*PKG. This results in Ca^{2+} mobilisation from internal stores through phosphorylation of phosphoinositides and activation of PI-PLC to produce the secondary messenger IP_3 . Although not included in this report, XA was also tested on schizont stages in a Ca^{2+} release assay at increasing concentrations and no increases in Ca^{2+} levels were detected (see appendix A3).

In mature gametocyte stages, the relationship between zaprinast-induced Ca^{2+} release and cGMP signalling appears to mirror what is seen in schizont stages with zaprinast inducing Ca^{2+} mobilisation through a PKG-dependent pathway in *P. falciparum* gametocytes. Changes in levels of phospholipids were not investigated and this would be a useful question to address in future, to determine whether as seen in schizont stages, zaprinast (and XA) stimulates Ca^{2+} mobilisation through the IP_3 signalling pathway. In *P. berghei*, XA has been shown to trigger $\text{PI}(4,5)\text{P}_2$ hydrolysis[200]. Again zaprinast is not the natural trigger of gametogenesis and it is clear from the data presented here that the relationship between cGMP and Ca^{2+} release is more complicated in XA-stimulated gametocytes. The fact that C2 reduces XA-induced elevated Ca^{2+} levels indicates that C2 is targeting a protein kinase involved in the Ca^{2+} response. The fact that C2 does not fully reverse levels of Ca^{2+} could either be a result of experimental design (XA reaching its target to induce Ca^{2+} release before C2 can reach its target to inhibit it), or that Ca^{2+} release in gametocytes is complicated and involves both a C2-sensitive response and a non-C2-sensitive response. However, these assays need to be repeated to determine this. In a *P. berghei* transgenic line expressing the Ca^{2+} -dependent photoprotein Aequorin, XA was shown to induce Ca^{2+} release in a PKG-dependent manner[174]. The difference may reflect species-specific differences or differences in experimental design.

In the C2-resistant gatekeeper mutant line, the Ca^{2+} response was still reduced by ~ 50 % by C2. The likely explanation for this is that C2 can target another kinase the activation of which can also induce Ca^{2+} mobilisation but that the remaining 50 % of the Ca^{2+} response is still PKG

dependent (as it cannot be reversed by C2 in the *PfPKG_{T618Q}* line). This is interesting and based on the literature, a likely candidate for this non-PKG-dependent Ca^{2+} release is CDPK4. This protein kinase also has a small gatekeeper residue and is sensitive to C1 and C2[172] and is essential for the later stages of male specific gametogenesis[210][215]. This also raises the interesting question of whether this complicated Ca^{2+} response that we see could be a sex-specific one. For example could XA stimulate female gametocytes to release Ca^{2+} through a PKG-dependent pathway and males through a non-PKG-dependent pathway or vice versa? Or perhaps XA induces Ca^{2+} mobilisation in only one sex? The inhibitory effects of many new compound types have been shown to differ between male and female gametocytes with male gametocytes often exhibiting greater sensitivity. This may point to differences in metabolism and potentially sex-specific pathways in gametocyte stages[293]. It may be that only male gametocytes require Ca^{2+} for activation, as exflagellation is known to be Ca^{2+} dependent and is a male-specific event and there is currently no published data indicating a role for Ca^{2+} in female gametocytes. Data demonstrating that gametocytes will round up in the presence of the Ca^{2+} chelator BAPTA-AM but will not exflagellate supports this[159]. However, this does not rule out that female gametocytes (or gametes as emergence is not Ca^{2+} dependent) could release Ca^{2+} to activate male gametocytes once they are ready to be fertilised. This would be a very interesting question to answer but could only be achieved through separation of male and female gametocytes possibly using distinct colour reporters to differentiate the sexes in transgenic lines. This has been achieved in *P. berghei*[294]. Another possible theory is based on work done by Fang *et al*[215] who identified that in *P. berghei*, two forms of CDPK4 are responsible for the male specific events of gametogenesis. A myristoylated and non-myristoylated form. Both require Ca^{2+} for activation and are involved in distinct events leading to exflagellation. It may be possible that a first wave of Ca^{2+} activates the myristoylated form (which presumably is membrane bound) leading to the first events of male exflagellation and to a second wave of Ca^{2+} release, which may be through CDPK4 itself (so non-PKG dependent) that activates the non-myristoylated form to induce flagella motility. Preliminary live cell imaging data presented in this thesis is suggestive of a possible double wave of Ca^{2+} release but this needs further investigation. Published data on the PKG specificity of exflagellation also indicate that this event is not likely to be fully PKG dependent as changes in levels of exflagellation with C1 inhibition did not differ between a wildtype line and *PfPKG_{T618Q}* and it was suggested in this publication that a candidate for this could be CDPK4[159].

The fact that we don't see any evidence of a non-PKG-dependent Ca^{2+} response in zaprinast-treated stage V gametocytes suggests that zaprinast may be able to bypass the initial XA response including the non-PKG-dependent Ca^{2+} mobilisation but still induce all constitutive events of gametogenesis. The fact that zaprinast induces Ca^{2+} mobilisation in mature gametocytes implicates cGMP PDE activity in the Ca^{2+} response. This is supported by evidence in the literature demonstrating that zaprinast can induce gametogenesis in the absence of XA[159]. Data presented here measured clear and paralogue-specific changes in the Ca^{2+} response when individual *Pf*PDEs were deleted. The most striking example of this was the absence of any XA-induced Ca^{2+} response in a transgenic line in which *Pf*PDE δ was absent due to gene deletion. This was an extremely exciting result and led to the hypothesis that XA-induced Ca^{2+} release requires the presence of *Pf*PDE δ (however the concentration of XA used was low and this assay needs to be repeated with a higher concentration).

However, zaprinast was able to induce a *Pf*PKG-dependent Ca^{2+} response in the *Pf*PDE δ -ko line (which was completely reversed by C2) indicative that this line could respond to zaprinast stimulation and release Ca^{2+} through inhibition of a cGMP-PDE that is not *Pf*PDE δ . This was interesting given the concerns that this line may be disrupted due to dysregulated levels of cyclic nucleotides and the evidence that this line could respond to zaprinast and release Ca^{2+} is suggestive that parasites could respond to a signal leading to the induction of the cGMP signalling pathway and this provides evidence that the Ca^{2+} release machinery is at least partially intact.

The absence of *Pf*PDE γ appeared not to affect either the XA-induced or zaprinast-induced Ca^{2+} response (although these data is preliminary and needs confirmation). However, Ca^{2+} release assays carried out on a *Pf*PDE α -ko line revealed that the absence of this PDE resulted in a reduced *Pf*PKG-dependent Ca^{2+} response to both XA and zaprinast. This suggests that *Pf*PDE α may contribute to (the majority of) the *Pf*PKG-dependent response and this supports a hypothesis that the zaprinast-induced Ca^{2+} mobilisation seen in the *Pf*PDE δ -ko line may be due to zaprinast inhibition of *Pf*PDE α .

No receptor for XA has been identified in *P. falciparum* and the signalling events between entry of XA into the cell and providing the initial XA signal are unknown (XA may be able to diffuse into the cell or it may require a receptor binding interaction on the surface of the cell to either enter the cell or to initiate the pathway). Given the evidence we have for zaprinast outlined above and the inability of the *Pf*PDE δ -ko line to respond to XA by releasing Ca^{2+} (or rounding up), it is tempting to speculate that *Pf*PDE δ could be a receptor for XA. Or that XA could bind to *Pf*PDE δ and directly inhibit it leading to elevated levels of cGMP (elevated cGMP levels have been

measured in this line[130]). Immunoprecipitation of the epitope-tagged *Pf*PDE δ has been achieved in this project and the next step will be to determine whether XA can directly bind to *Pf*PDE δ . Using radiolabelled XA and immunoprecipitated *Pf*PDE δ protein it may be possible to carry out in vitro binding or association studies to determine whether there is an interaction between XA and *Pf*PDE δ . Preliminary data, however, suggest that XA does not inhibit PDE δ activity and in fact showed a stimulatory effect. A model of the predicted *Pf*PDE δ protein structure has been generated by a sequence alignment of *Pf*PDE δ with the closest human homologue, PDE9A (appendix A4). The aim of this is to attempt to dock XA into the protein structure of *Pf*PDE δ in order to predict whether XA can bind.

There are several studies in the literature indicating a role for cyclic nucleotide signalling as well the release of Ca²⁺ from internal stores and activation of stage-specific Ca²⁺-dependent protein kinases (CDPKs) at several stages of the parasite life cycle. These are presented in Figure 7.1. This schematic demonstrates the importance of these two signalling pathways throughout the complex life cycle of the malaria parasite and emphasises the impact that targeting of these signalling pathways would have on disruption of the parasite through selective inhibition.

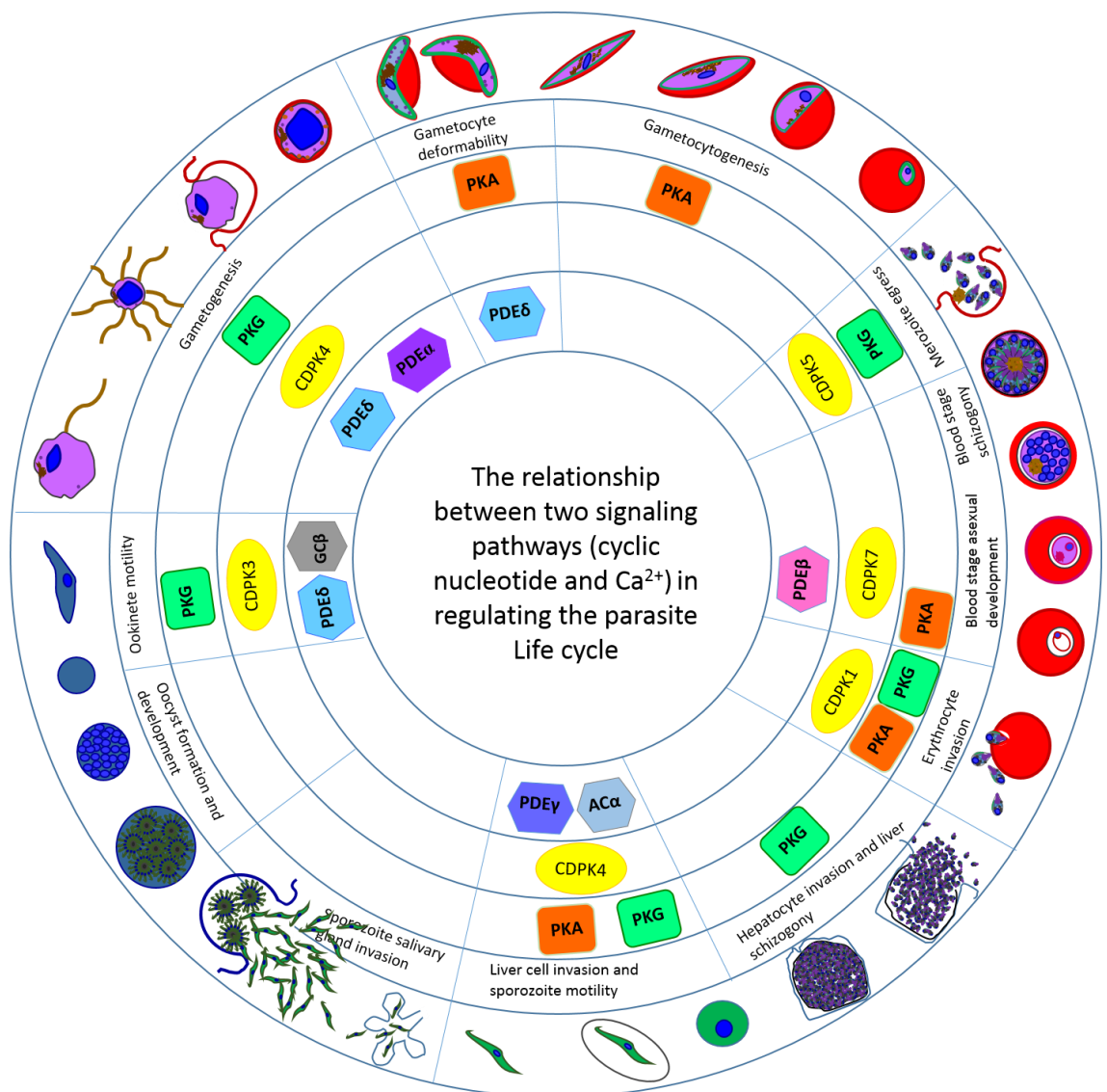


Figure 7.1. Schematic presenting the relationship between cyclic nucleotide signalling molecules and Ca^{2+} -dependent signalling proteins throughout the parasite lifecycle.

7.3. Generation of a *PfPDEδ* haemagglutinin-tagged transgenic line for use as a tool to study the role of *PfPDEδ* in gametocyte stages

Given the interest in *PfPDEδ* initiated by data produced by Cathy Taylor (Cathy Taylor, PhD thesis, 2007) suggesting that this *PfPDE* plays an essential role in gametogenesis, and evidence presented in this report further indicating its potential importance in gametocyte deformability, it was deemed worthwhile to investigate the role of this *PfPDE* in gametocyte stages further. The cellular localisation and cyclic nucleotide specificity of *PfPDEδ* has not been documented. In order to attempt to produce a tool to address these questions, a triple haemagglutinin (HA) tag was introduced at the C-terminal end of *PfPDEδ* using the CRISPR Cas9 system in a good gametocyte producing line (NF54). This double crossover event was successful and integration confirmed by locus-specific PCR.

Preliminary results using this line to determine the cellular localisation have not shown strong staining with an α -HA antibody and some background has been seen in control (NF54) samples, however fluorescence detected in the wildtype (NF54) α -HA antibody control samples was much lower than seen in the *PfPDEδ*HA line. Interestingly, the faint staining pattern that was observed appeared to show similarity to the localisation of Pfg377 which is located in osmiophilic bodies which are membrane bound (derived from Golgi vesicles) [288]. *PfPDEδ* (which has six predicted transmembrane domains and has been detected in membrane fractions of gametocyte lysates, and so is predicted to be membrane associated) could be anchored to the membrane with its catalytic domain facing the cytosol rather than the lumen of the osmiophilic body, however more work needs to be done to confirm the cellular localisation of *PfPDEδ*. The use of an antibody against the female specific protein Pfg377, which is found in osmiophilic bodies, may determine whether the pattern that we see in the *PfPDEδ* tagged line corresponds with these organelles. Osmiophilic bodies are female-specific organelles (or at least very highly enriched in females) that increase in number as the gametocyte matures and are associated with the mature gametocyte subpellicular membrane and are involved in female gamete egress[288]. If co-localisation were detected this would be a very exciting result and would indicate that *PfPDEδ* may play a predominantly female-specific role in gamete egress (as males may contain some *PfPDEδ*). The subpellicular membrane localisation would be interesting in terms of the role already established by Ramdani *et al*[25], for *PfPDEδ* in gametocyte infected erythrocyte deformability.

The *PfPDEδ*-HA line was successfully used to immunoprecipitate *PfPDEδ* protein. This was an important result, because it confirmed that this protein is present in mature gametocyte stages

despite low levels of immunofluorescence detectable by IFA. It also demonstrated that a good amount of protein could be produced using this method. This parasite line is therefore useful for future studies requiring *PfPDE* δ protein such as XA interaction studies and also for pull down assays to determine whether *PfPDE*-delta exists as part of a signalling protein complex.

Importantly, a PDE assay carried out on immunoprecipitated HA-tagged *PfPDE* δ protein demonstrated that *PfPDE* δ can only hydrolyse cGMP (this confirmed previous work by Cathy Taylor[130]), and provided the first direct measurement of cGMP specificity for this enzyme. No cAMP hydrolytic activity was detected in parallel assays which was also in keeping with previous work[130].

The possibility of a relationship between XA and *PfPDE* δ is an interesting avenue for further study. XA showed no significant impact on *PfPDE* δ cGMP hydrolytic activity of the immunoprecipitated (IP) tagged *PfPDE* δ enzyme in a PDE assay. The PDE inhibitor PF9, however, reduced the cGMP hydrolytic activity of the IP tagged-*PfPDE* δ by ~ 50 %. This preliminary data could be suggestive that XA does not directly interact with *PfPDE* δ to prevent hydrolysis of cGMP (whereas PF9, as expected, does). This may point to an indirect (or one not involving PDE enzyme inhibition) association with *PfPDE* δ to induce events of gametogenesis and may explain the differences seen in XA and zaprinast in terms of the ability to trigger a Ca²⁺ response. However, this requires further investigation.

7.4. A role for *Pf*PDE δ in gametocyte infected erythrocyte deformability

Data presented in this report and in the literature[130], indicate that *Pf*PDE δ is likely to be a cGMP-specific PDE rather than a dual specific enzyme (which is the case for *Pf*PDE β) as the HA-tagged protein did not show detectable cAMP hydrolytic activity. Although confirming previous work that suggested *Pf*PDE δ might be cGMP specific, this result raises questions concerning the published gametocyte-infected erythrocyte deformability data[25], which show elevated cAMP (and cGMP) levels in *Pf*PDE δ -ko line parasite lysates and a role for *Pf*PDE δ in the deformability phenotype. The authors of this study provide data that suggests that the changes in deformability are mediated by cAMP signalling and regulation of PKA and indicate using both pharmacological and genetic approaches that it is the parasite PKA that likely contributes to this response and not the host PKA. If *Pf*PDE δ is not dual specific and can only hydrolyse cGMP (as suggested in this thesis), then it cannot contribute to the deformability response by directly hydrolysing cAMP. However, levels of cGMP have been shown by different groups to be elevated in this knock out line[25][130] and it could be conceivable that *Pf*PDE δ may induce elevated levels of cAMP indirectly. Cross talk between the cGMP and cAMP signalling pathways has been demonstrated in mammalian cells and there is evidence that in *P. falciparum*, *Pf*AC β is phosphorylated in a PKG-dependent manner at S1572[172]. In mature gametocytes of the *Pf*PDE δ -ko line, there is evidence that the absence of *Pf*PDE δ leads to elevated levels of cGMP[130]. It could be hypothesised that activated PKG (as a result of these elevated levels of cGMP), may phosphorylate AC β leading to elevated levels of cAMP (elevated levels have been documented[25]), leading to activation of PKA which phosphorylates proteins involved in maintaining a stiff phenotype (see Figure 7.2 scenario B, grey arrows). In immature wildtype gametocytes, evidence suggests that PKG is not active (C2 will not block early gametocytes but will block gametogenesis in stage V gametocytes). Therefore, the maintenance of a stiff phenotype in immature wildtype gametocytes through elevated cAMP levels must be via a non-PKG-dependent pathway leading to PKA activation. However, when these parasites reach maturity at stage V, *Pf*PDE δ is involved in inducing deformability by indirectly lowering cAMP levels and 'switching off' PKA through cGMP hydrolysis subsequently reversing the stiff phenotype (see Figure 7.2 scenario A, grey arrows). In support of this hypothesis, data in chapter 4 (section 4.2.3) indicates that a proportion of *Pf*PDE δ -ko stage V gametocytes were able to round up unstimulated when treated with a PKA inhibitor (see Figure 7.2 scenario C, grey arrows) and this was reversed completely by PKG-inhibition (see Figure 7.2 scenario D, grey arrows).

It is thought that protein phosphatases are involved in the dephosphorylation of PKA targets to reverse the stiff phenotype of gametocytes when they reach maturity. In fact, the serine/threonine phosphatase inhibitor Calyculin A has been shown to prevent the action of phosphatases resulting in increased retention rates of mature gametocytes due to a lack of deformability[25].

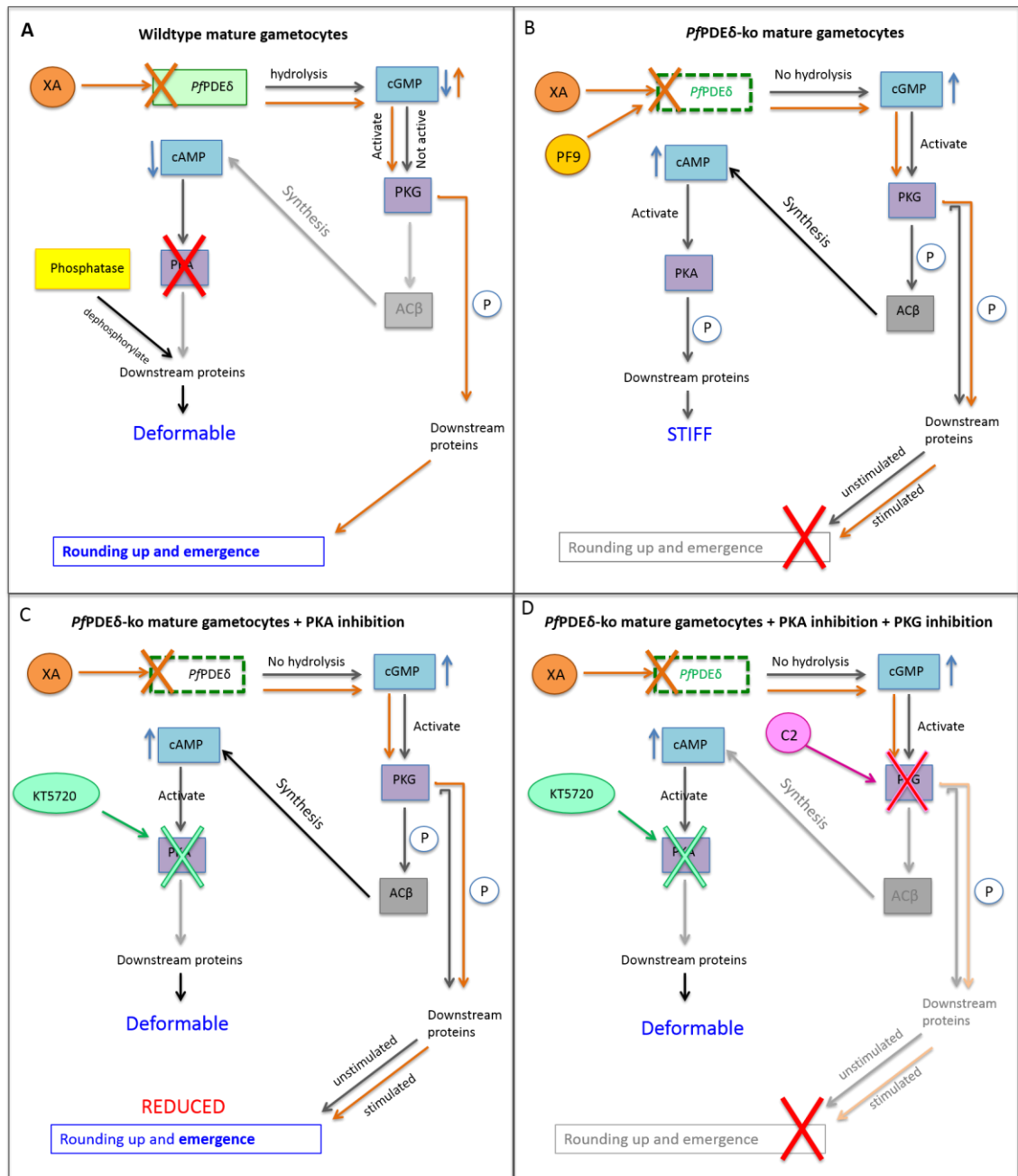


Figure 7.2. The predicted cell signalling pathways in gametocyte infected erythrocyte deformability and gametogenesis. (A). In a wildtype situation, in mature gametocytes, *PfPDEδ* is present and active, reducing cGMP levels by hydrolysis resulting in no PKG or PKA (indirect) activation (dark grey arrows) resulting in deformability. Phosphatases may act to dephosphorylate proteins phosphorylated by PKA to

induce stiffness in immature stages. When XA or PF9 is added (orange arrows) *PfPDE δ* is inhibited (possibly indirectly by XA) leading to elevated levels of cGMP and PKG activation leading to phosphorylation of downstream target proteins and the induction of gametogenesis. Downstream proteins still remain dephosphorylated maintaining the deformable phenotype. **(B)**. In the *PfPDE δ* -ko line, mature gametocytes, *PfPDE δ* is absent, leading to prematurely elevated levels of cGMP and PKG activation. PKG phosphorylates AC β leading to increased levels of cAMP and activation of PKA, which phosphorylates downstream target proteins, resulting in a stiff phenotype. Elevated levels of PKG, which would usually result in both stimulated and unstimulated rounding up in this line is unable to occur due to the lack of deformability. **(C)**. When the PKA inhibitor KT5720 is added to *PfPDE δ* -ko line mature gametocytes, it partially reverses the stiff phenotype by preventing PKA from phosphorylating downstream proteins that result in structural events to make the gametocyte infected erythrocytes stiff. This leads to a deformable phenotype as seen in the wildtype situation. However, elevated levels of cGMP due to the absence of *PfPDE δ* in this line lead to PKG activation, which phosphorylates downstream target proteins leading to the unstimulated induction of gametogenesis. XA (and PF9) can also further increase numbers of parasites undergoing gametogenesis by leading to further elevated levels of cGMP and PKG activation. However, rounding up is greatly reduced in the absence of *PfPDE δ* , possibly as a result of only females being unable to round up in the absence of *PfPDE δ* **(D)**. In PKA inhibited *PfPDE δ* -ko line parasites treated with the PKG inhibitor C2, cells are deformable due to the absence of PKA-induced stiffness (PKA is inhibited). Absence of *PfPDE δ* leads to elevated levels of cGMP. However PKG cannot phosphorylate downstream target to induce rounding up due to inhibition by C2. Gametocytes are therefore unable to round up unstimulated or stimulated.

7.5. A possible sex-specific role for *PfPDEδ* in gametogenesis

One of the questions addressed in this thesis was whether the defect in rounding up and emergence seen in the *PfPDEδ*-ko line was due to a cGMP-dependent direct effect on gametogenesis (as predicted by Taylor *et al*[130]), or whether the *PfPDEδ*-ko line can simply not round up due to the physical restraints imposed on the parasite by PKA-induced stiffness or both.

Studies presented in this report on *PfPDEδ*-ko mature gametocytes show that in *PfPDEδ*-ko line samples only ~ 5 % of parasites will round up in response to XA. This is increased to ~25 % with PKA inhibition. XA induction of rounding up in the wildtype line in this experiment was ~ 50 % (which was quite low and would normally be expected to be ~80 % in a culture containing mainly stage V gametocytes). This indicates that XA-induced rounding up is significantly increased when PKA is inhibited. This means that in the absence of *PfPDEδ*, ~ 25 % of parasites can still round up but that ~ 50 % less can round up compared to the wildtype line in which *PfPDEδ* is present. This does not rule out a rounding up phenotype in the *PfPDEδ*-ko line and an important role of *PfPDEδ* in gametogenesis, although the absence of *PfPDEδ* does not lead to a complete block in rounding up. It would be interesting to look at emergence of XA-induced/PKA inhibited *PfPDEδ*-ko line gametocytes to determine whether the phenotype is at the point of egress as observed by Cathy Taylor[130], rather than at the rounding up stage as observed here. It must be noted that these parasites may have been disrupted due to prolonged elevated levels of both cyclic nucleotides and as such are not competent to undergo gametogenesis. Viability assays would be required to determine this and a conditional knockout line of *PfPDEδ* would be a useful tool to investigate the function of *PfPDEδ* in gametogenesis without the issue of viability of the line. In such a line, excision of the gene encoding *PfPDEδ* both early (to look at deformability) and late (to look at gametogenesis) may help to dissect these two separate events and the involvement of *PfPDEδ*. It would also be of interest to look at other events of gametogenesis such as exflagellation and Ca^{2+} release in XA-induced/PKA inhibited *PfPDEδ*-ko line gametocytes. In addition to this, retention rates/deformability of the *PfPDEδ*-ko line in the presence and absence of KT5720 would indicate the percentage change in retention (which is expected to reduce significantly as seen in KT5720 treated immature gametocytes[25] when PKA is inhibited. This will be important to check the reason that the remaining parasites that will not round up in response to XA, to eliminate the possibility that a large percentage of parasites still remain stiff.

The fact that only 15 % - 25 % of *PfPDEδ*-ko line gametocytes treated with PKA will round up in response to XA or PF9 treatment may indicate a sex specific involvement. This is particularly interesting in light of the IFA results, which although preliminary, show a staining pattern that

exhibits similarity to the localisation of Pf377 in osmiophilic bodies. This would suggest a female-specific role for *PfPDEδ* in egress and would account for the ~85 % to 75 % population of PKA-treated *PfPDEδ*-ko line gametocytes that will still not round up in response to PF9 or XA (the 15 % - 25 % of gametocytes that can round up would be expected to be males which presumably would not require the presence of *PfPDEδ* but are able to round up when the stiff phenotype is reversed by PKA inhibition). It would be very interesting to use antibodies to sex-specific proteins such as *Pfg377* and α -tubulin in these assays to investigate this. Interestingly, work on *PfPKG* carried out by Christine Hopp, LSHTM (Christine Hopp, PhD Thesis 2011) using a rabbit α -human PKG antibody (that reacts strongly with *PfPKG* but not with human red cell PKG) showed that in gametocytes, *PfPKG* also exhibits a similar pattern of fluorescence to that of *PfPDEδ* presented in this thesis. This is extremely interesting and could indicate that *PfPKG* and *PfPDEδ* may form part of a complex that is localised to osmiophilic bodies in mature gametocyte stages. Interestingly, the protease subtilisin 2 (*PfSUB2*) has also been shown to localise to the osmiophilic bodies in female gametocytes[295]. In schizont stages the related *PfSUB1*, is a key player in merozoite egress[220] and is released from specialised organelles called exonemes in a PKG-dependent manner. It is tempting to speculate that *PfSUB2* might be released from the osmiophilic bodies in a PKG-dependent manner in mature gametocytes to induce egress.

There may also be a sex-specific role in the release of Ca^{2+} in response to XA and zaprinast. This would be interesting to explore. It may be that the possible PKG specificity and non-PKG specificity of the Ca^{2+} response seen in gametocytes may reflect the different responses in male and female gametocytes. It would be very interesting to carry out Ca^{2+} release assays on separated male and female gametocytes to see whether the Ca^{2+} response to XA and zaprinast differs. Given the possibility that *PfPDEδ* may be specific to females, the lack of a XA-induced Ca^{2+} response in the *PfPDEδ*-ko line may be due to the fact that without *PfPDEδ*, female gametocytes are unable to respond to XA and as the concentration of XA used was very low, it may be that the male response (which may require *PfPDEα*) is undetectable in that assay. A caveat to the sex-specific theory is that the absence of *PfPDEδ* results in a greatly reduced number of exflagellation events in XA-treated samples[130]. This indicates that *PfPDEδ* is likely required for the majority of XA-induced exflagellation. However, exflagellation is a Ca^{2+} -dependent event and this may be explained possibly by a female involvement (through *PfPDEδ*) in the Ca^{2+} response required to initiate exflagellation.

Given what we know about the involvement of cGMP and PKG in gametogenesis, the expected phenotype of *PfPDEδ*-ko mature gametocytes would be unstimulated or premature rounding

up/gametogenesis (rather than an absence of rounding up/gametogenesis). This is because, in the absence of *PfPDEδ* (presuming that there is no stiff phenotype preventing cells from physically rounding up), the elevated levels of cGMP induced by the absence of *PfPDEδ* would lead to activation of PKG and subsequent rounding up and emergence. The observation that a small proportion of parasites rounded up un-stimulated in PKA-treated *PfPDEδ*-ko gametocyte cultures is very interesting and supports this as in the absence of PKA inhibition, it is likely that parasites cannot physically round up due to PKA-induced stiffness. The fact that we don't see this premature rounding up phenotype in the *PfPDEδ*-ko line (with no PKA inhibition) supports this. A conditional knockout line of *PfPDEδ* as suggested above would be a very useful tool to determine whether the real phenotype is one of premature rounding up/egress. In a conditional knockout line, removal of *PfPDEδ* at stage V (in the presence of a PKA inhibitor) may be expected to result in un-stimulated rounding up of gametocytes as soon as they reach maturity (when the appropriate cell signalling components are ready) and as such, greatly reduced numbers of stage V gametocytes would be expected to be observed in cultures (see Figure 7.2 for a schematic). This is what is seen with pharmacological inhibition of PDEs in wildtype mature gametocyte stages, for example the addition of PF9 (discussed below) will induce rounding up of mature gametocytes within 5 minutes of addition and this is what would be hypothesised to happen in the unstimulated *PfPDEδ*-ko line. This hypothesis presumes that *PfPDEδ* is the predominant PDE involved in gametogenesis (because if it is female specific so a larger proportion of the gametocyte population is dependent upon this protein for gametogenesis to occur). The observation that XA can induce rounding up (at low levels) in the *PfPDEδ*-ko line may reflect the male population that may be able to round up in response to XA stimulation in the absence of *PfPDEδ* (possibly through *PfPDEα* hydrolysis of cGMP).

Data using the PDE inhibitor PF9 supports a theory for *PfPDEδ* being the predominant PDE involved in gametogenesis (discussed below). It may be that another *PfPDE* is involved or can partly compensate for the absence of *PfPDEδ* and respond to XA by inducing a small number of cells to round up or it may be that another *PfPDE* for example *PfPDEα* (the only other PDE expressed at the protein level in gametocytes) may be required for male gametogenesis while *PfPDEδ* is required for female gametogenesis. This hypothesis suggesting a sex-specific role for PDEs in gametogenesis is supported by proteomic data, which detected more *PfPDEα* protein in mature male gametocytes than mature female gametocytes[144] and this hypothesis would also be strengthened by confirmation of an osmiophilic body localisation for *PfPDEδ*. However, this hypothesis is very speculative and requires further experimental confirmation.

7.6. The Pfizer human PDE inhibitor, PF9, as a gametocytocidal compound

Data presented in this thesis have shown gametocytocidal activity in a human PDE inhibitor obtained from Pfizer, PF9, and demonstrated that this compound specifically kills mature gametocyte stages and not immature stages. Further investigation revealed that PF9 acts by inducing gametogenesis. Furthermore, this compound was shown to act quickly (within 5 minutes) and in a *PfPKG*-dependent manner and interestingly, appeared to not be active against *PfPDEδ*-ko line gametocytes (as assessed by their ability to round up, emerge and disappear over time) but showed greatest activity in the absence of *PfPDEα*. The hypothesis generated for this result is that the main PDE required for the process of gametogenesis (possible in females only) is *PfPDEδ* (PF9 is predicted to target all *PfPDEs*). In a wildtype situation when both *PfPDEα* and *PfPDEδ* are present in gametocytes, PF9 will bind to both PDEs. This leaves less available compound to target *PfPDEδ*. However, when *PfPDEα* is absent, a lower concentration is required to inhibit the parasite, as the only target present is *PfPDEδ*. This initial interpretation of the data (that *PfPDEδ* was the primary target for PF9), was questioned by data in Chapter 4 that has strongly suggested that this transgenic line is unable to complete the physical action of rounding up due to PKA-induced stiffness and this led to a re-evaluation of the initial interpretation. The observations that a small (~ 25 %) number of *PfPDEδ*-ko line parasites could round up when stimulated with PF9 (with PKA inhibition) rather than a large number rounding up, and the possible localisation of *PfPDEδ* to the osmiophilic bodies suggests that this ratio of rounded up parasites may reflect the male population and that the majority of parasites cannot round up, not because *PfPDEδ* is the main target, but because the majority of gametocytes are female (reflecting a predicted sex ratio of 4:1) and absence of *PfPDEδ* prevents this larger proportion of the population from rounding up. PF9 targeting of the *PfPDEδ*-ko line would presumably inhibit *PfPDEα* (as it is predicted to target all PDEs) and this would lead to gametogenesis in male gametocytes. It would be interesting to use antibodies against sex specific markers in the *PfPDEδ*-ko line in the presence and absence of PKA inhibition to determine the sex specificity of gametocytes that will round up in the absence of *PfPDEδ* both in the presence and absence of PKA inhibitors.

PF9 also induced Ca^{2+} mobilisation in 3D7a stage V gametocytes and induced high levels of Ca^{2+} compared to XA or zaprinast at the concentrations used. This coupled with the observation that exflagellation was also stimulated by PF9 in wildtype mature gametocytes was further

confirmation that this compound induced more than one essential event of gametogenesis and that its inhibitory effects were via stimulation of the pathway required for gametogenesis.

The premature initiation of gametogenesis in the human host would be an excellent strategy to block transmission, as emerged gametes would not survive long in the host blood stream and as such the life cycle would be cut short with no progression through the insect stages. As predicted for zaprinast, it is thought that PF9 may bypass the natural trigger of gametogenesis. It is likely that XA induces gametogenesis via an upstream event that causes activation of GCs or inhibition of PDEs leading to elevated levels of cGMP and PKG activation. Data in this thesis point towards the inhibition of PDEs in the XA-induced response, rather than GC activation.

7.7. General summary of discussion

Overall, data in this thesis strongly suggest that in line with previous work[130], *PfPDE δ* is still likely to be an important PDE involved in gametogenesis; however, more work needs to be done to confirm whether its absence impacts on two distinct events during sexual development (one in the human hosts and one in the insect vector). There is a possible indication that this PDE could play a sex-specific role in female gametogenesis. The discovery of a compound that will target *PfPDEs* and inhibit transmission stages by prematurely induce gametogenesis is an exciting result.

One of the target product profiles outlined by MMV in a proposal to optimise malaria control efforts in 2013 was a product with activity against asexual blood stages in combination with a second product to target the transmission stages[68][67]. PF9 is an example of a compound that can do both. PF9 can target asexual blood stage PDEs (*PfPDE β*) to disrupt invasion and early ring stages (cell cycle progression) and transmission stage PDEs (*PfPDE δ*) to prevent the essential transmission event. Not only this, but it would be predicted to also prevent the deformability of mature gametocyte-infected erythrocytes increasing splenic clearance of circulating gametocytes. *PfPDE α* and *PfPDE δ* are both predicted, based on evidence in this thesis, to be involved in gametogenesis. PF9 is known to target both. This means that despite the predicted sex specificity of *PfPDE δ* , PF9 can kill both male and female gametocytes by inducing premature gametogenesis. *PfPDEs* are novel targets because none of the current antimalarials target PDEs and so resistant parasite populations would be expected to be fully sensitive to a PDE inhibitor. Plans are currently underway in the Baker group at LSHTM (grant application submitted), partly based on data from this thesis, in partnership with Salvensis and MMV to optimise the PF9 chemical series to provide in vivo proof of concept for *PfPDEs* as antimalarial targets.

References

1. Maurice DH, Ke H, Ahmad F, Wang Y, Chung J, Manganiello VC. 2014 Advances in targeting cyclic nucleotide phosphodiesterases. *Nat. Rev. Drug Discov.* **13**, 290–314. (doi:10.1038/nrd4228)
2. World Health Organization. 2016 World Malaria Report 2016. *World Heal. Organ.* (doi:10.1071/EC12504)
3. World Health Organization. 2014 World Malaria Report 2014. *World Heal. Organ.*
4. Lim KG, Singh B. 2013 Zoonotic malaria in Malaysia. *Med. J. Malaysia* **68**, 4–5. (doi:10.1186/1475-2875-11-284)
5. William T, Rahman HA, Jelip J, Ibrahim MY, Menon J, Grigg MJ, Yeo TW, Anstey NM, Barber BE. 2013 Increasing Incidence of Plasmodium knowlesi Malaria following Control of *P. falciparum* and *P. vivax* Malaria in Sabah, Malaysia. *PLoS Negl. Trop. Dis.* **7**. (doi:10.1371/journal.pntd.0002026)
6. Cox-Singh J, Davis TME, Lee K-S, Shamsul SSG, Matusop A, Ratnam S, Rahman H a, Conway DJ, Singh B. 2008 Plasmodium knowlesi malaria in humans is widely distributed and potentially life threatening. *Clin. Infect. Dis.* **46**, 165–71. (doi:10.1086/524888)
7. Mecheri S. 2012 Contribution of allergic inflammatory response to the pathogenesis of malaria disease. *Biochim. Biophys. Acta - Mol. Basis Dis.* **1822**, 49–56. (doi:10.1016/j.bbadis.2011.02.005)
8. In press. centers for Disease control and prevention. <http://www.cdc.gov/malaria/about/disease.html>. See <http://www.cdc.gov/malaria/about/disease.html>.
9. Collins WE, Jeffery GM. 2007 Plasmodium malariae: Parasite and disease. *Clin. Microbiol. Rev.* **20**, 579–592. (doi:10.1128/CMR.00027-07)
10. Markus MB. 2011 Malaria: Origin of the Term ‘Hypnozoite’. *J. Hist. Biol.* **44**, 781–786. (doi:10.1007/s10739-010-9239-3)
11. Campo B, Vandal O, Wesche DL, Burrows JN. 2015 Killing the hypnozoite - drug discovery approaches to prevent relapse in Plasmodium vivax. *Pathog. Glob. Health*

- 109**, 107–22. (doi:10.1179/2047773215Y.0000000013)
12. Ashley EA, Recht J, White NJ. 2014 Primaquine: the risks and the benefits. *Malar. J.* **13**, 418. (doi:10.1186/1475-2875-13-418)
 13. Cunha CB, Cunha BA. 2008 Brief history of the clinical diagnosis of malaria: From hippocrates to Osler. *J. Vector Borne Dis.* **45**, 194–199.
 14. Smith DC, Sanford LB. 1985 Laveran's germ: The reception and use of a medical discovery. *Am. J. Trop. Med. Hyg.* **34**, 2–20.
 15. Muscatello U. 2007 Golgi's contribution to medicine. *Brain Res. Rev.* **55**, 3–7. (doi:10.1016/j.brainresrev.2007.03.007)
 16. Ross R. 2002 The role of the mosquito in the evolution of the malarial parasite: the recent researches of Surgeon-Major Ronald Ross, I.M.S. 1898. *Yale J. Biol. Med.* **75**, 103–105.
 17. Manson P. 2002 Experimental proof of the mosquito-malaria theory. 1900. *Yale J. Biol. Med.* **75**, 107–112. (doi:10.1136/bmj.2.2074.949)
 18. Cox FE. 2010 History of the discovery of the malaria parasites and their vectors. *Parasit. Vectors* **3**, 5. (doi:10.1186/1756-3305-3-5)
 19. Tavares J, Formaglio P, Thiberge S, Mordelet E, Van Rooijen N, Medvinsky A, Ménard R, Amino R. 2013 Role of host cell traversal by the malaria sporozoite during liver infection. *J. Exp. Med.* **210**, 905–15. (doi:10.1084/jem.20121130)
 20. Pouvelle B, Buffet P A, Lépolard C, Scherf A, Gysin J. 2000 Cytoadhesion of Plasmodium falciparum ring-stage-infected erythrocytes. *Nat. Med.* **6**, 1264–1268. (doi:10.1038/81374)
 21. Bannister L, Mitchell G. 2003 The ins, outs and roundabouts of malaria. *Trends Parasitol.* **19**, 209–213. (doi:10.1016/S1471-4922(03)00086-2)
 22. Baker D A. 2010 Malaria gametocytogenesis. *Mol. Biochem. Parasitol.* **172**, 57–65. (doi:10.1016/j.molbiopara.2010.03.019)
 23. Sinden RE. 1982 Gametocytogenesis of Plasmodium falciparum in vitro: an electron

- microscopic study. *Parasitology* **84**, 1–11.
24. Rogers NJ, Hall BS, Obiero J, Targett G A. T, Sutherland CJ. 2000 A Model for Sequestration of the Transmission Stages of Plasmodium falciparum: Adhesion of Gametocyte-Infected Erythrocytes to Human Bone Marrow Cells. *Infect. Immun.* **68**, 3455–3462. (doi:10.1128/IAI.68.6.3455-3462.2000)
 25. Ramdani G, Naissant B, Thompson E, Breil F, Lorthiois A, Dupuy F, Cummings R, Duffier Y, Corbett Y, Mercereau-Puijalon O, Vernick K, Taramalli D, Baker D A, Langley G, Lavazec C. 2015 cAMP-Signalling Regulates Gametocyte-Infected Erythrocyte Deformability Required for Malaria Parasite Transmission. *PLOS Pathog.* **11**, e1004815. (doi:10.1371/journal.ppat.1004815)
 26. Billker O, Lindo V, Panico M, Etienne A E, Paxton T, Dell A, Rogers M, Sinden RE, Morris HR. 1998 Identification of xanthurenic acid as the putative inducer of malaria development in the mosquito. *Nature* **392**, 289–92. (doi:10.1038/32667)
 27. Garcia GE, Wirtz RA, Rosenberg R. 1997 Isolation of a substance from the mosquito that activates Plasmodium fertilization. *Mol. Biochem. Parasitol.* **88**, 127–135. (doi:10.1016/S0166-6851(97)00086-8)
 28. Sinnis P, Zavala F. 2012 The skin: Where malaria infection and the host immune response begin. *Semin. Immunopathol.* **34**, 787–792. (doi:10.1007/s00281-012-0345-5)
 29. World Health Organization. 2015 World Malaria Report 2015. *World Health* , 243. (doi:ISBN 978 92 4 1564403)
 30. Clyde DF, McCarthy VC, Miller RM, Woodward WE. 1975 Immunization of man against falciparum and vivax malaria by use of attenuated sporozoites. *Am. J. Trop. Med. Hyg.* **24**, 397–401. (doi:0.3891/acta.chem.scand.25-3616)
 31. Nussenzweig RS, Vanderberg J, Most H, Orton C. 1967 Protective immunity produced by the injection of x-irradiated sporozoites of plasmodium berghei. *Nature* **216**, 160–162. (doi:10.1038/216160a0)
 32. Marsh K, Kinyanjui S. 2006 Immune effector mechanisms in malaria. *Parasite Immunol.* **28**, 51–60. (doi:10.1111/j.1365-3024.2006.00808.x)
 33. Bull PC, Lowe BS, Kortok M, Molyneux CS, Newbold CI, Marsh K. 1998 Parasite antigens

on the infected red cell surface are targets for naturally acquired immunity to malaria. *Nat. Med.* **4**, 358–60. (doi:10.1038/nm0398-358)

34. Partnership SCT. 2015 *New England Journal*. , 1863–1875.
35. Greenwood B. 2017 New tools for malaria control – using them wisely. *J. Infect.* **74**, S23–S26. (doi:10.1016/S0163-4453(17)30187-1)
36. Mordmüller B, Surat G, Lagler H, Chakravarty S, Ishizuka A, Lalremruata A, Gmeiner M, Campo J J, Esen M, Ruben A J, Held J, Lamsfus Calle C, Mengue J B, Gebru T, Ibanez J, Sulyok M, James E R, Billingsley P F, KC N, Manoj A, Murshedkar T, Gunasekera A, Eappen A G, Li T, Stafford R E, Li M, Felgner P L, Seder R A, Richie T L, Kim Lee Sim B, Hoffman S L, Kremsner P G. 2017 Sterile protection against human malaria by chemoattenuated PfSPZ vaccine. *Nature* **542**, 445–449. (doi:10.1038/nature21060)
37. Thera MA, Doubo O K, Coulibaly D, Laurens M B, Ouattara A, Kone A K, Guindo A B, Traore K, Traore I, Kouriba B, Diallo D A, Diarra I, Daou M, Dolo A, Tolo Y et al. 2011 A field trial to assess a blood-stage malaria vaccine. *N. Engl. J. Med.* **365**, 1004–13. (doi:10.1056/NEJMoa1008115)
38. Ogutu BR, Apollo O J, McKinney D, Okoth W, Siangla J, Dubovsky F, Tucker K, Waitumbi J N, Diggs C, Wittes J, Malkin E, Leach A, Soisson L A, Milman J B, Otieno L et al. 2009 Blood stage malaria vaccine eliciting high antigen-specific antibody concentrations confers no protection to young children in Western Kenya. *PLoS One* **4**. (doi:10.1371/journal.pone.0004708)
39. Genton B, Betuela I, Felger I, Al-Yaman F, Anders R F, Saul A, Rare L, Baisor M, Lorry K, Brown G V, Pye D, Irving D O, Smith T A, Beck H, Alpers M P. 2002 A Recombinant Blood-Stage Malaria Vaccine Reduces *Plasmodium falciparum* Density and Exerts Selective Pressure on Parasite Populations in a Phase 1–2b Trial in Papua New Guinea. *J. Infect. Dis.* **185**, 820–827. (doi:10.1086/339342)
40. Cachat M, Lurati F, Soe S, Leroy O, Corradin G, Druilhe P. 2005 Phase I Malaria Vaccine Trial with a Long Synthetic Peptide Derived from the Merozoite Surface Protein 3 Antigen Re. *Society* **73**, 8017–8026. (doi:10.1128/IAI.73.12.8017)
41. El Sahly HM, Patel SM, Atmar RL, Lanford TA, Dube T, Thompson D, Sim BKL, Long C, Keitel WA. 2010 Safety and immunogenicity of a recombinant nonglycosylated

erythrocyte binding antigen 175 region II malaria vaccine in healthy adults living in an area where malaria is not endemic. *Clin. Vaccine Immunol.* **17**, 1552–1559.

(doi:10.1128/CVI.00082-10)

42. Horii T, Shirai H, Jie L, Ishii K J, Palacpac N Q, Tougan T, Hato M, Ohta N, Bobogare A, Arakaki N, Matsumoto Y, Namazue J, Ishikawa T, Ueda S, Takahashi M. 2010 Evidences of protection against blood-stage infection of *Plasmodium falciparum* by the novel protein vaccine SE36. *Parasitol. Int.* **59**, 380–386. (doi:10.1016/j.parint.2010.05.002)
43. Crosnier C, Bustamante L Y, Bartholdson S J, Bei A K, Theron M, Uchikawa M, Mboup S, Ndir O, Kwiatkowski D P, Duraisingh M T, Rayner J C. 2011 Basigin is a receptor essential for erythrocyte invasion by *Plasmodium falciparum*. *Nature* **480**, 534–7. (doi:10.1038/nature10606)
44. Takala SL, Coulibaly D, Thera M A, Batchelor A H, Cummings A P, Escalante A A, Ouattare A, Traore K, Niangaly A, Djimde A A, Doumbo O K, Plowe C V. 2009 Extreme Polymorphism in a Vaccine Antigen and Risk of Clinical Malaria: Implications for Vaccine Development. *Sci Transl med* **1**, 1–21. (doi:10.1126/scitranslmed.3000257.Extreme)
45. Curtis CF, Maxwell CA, Magesa SM, Rwegoshora RT, Wilkes TJ. 2006 Insecticide-Treated Bed-Nets for Malaria Mosquito Control. *J. Am. Mosq. Control Assoc.* **22**, 501–506. (doi:10.2987/8756-971X(2006)22[501:IBFMMC]2.0.CO;2)
46. Raghavendra K, Barik TK, Reddy BPN, Sharma P, Dash AP. 2011 Malaria vector control: From past to future. *Parasitol. Res.* **108**, 757–779. (doi:10.1007/s00436-010-2232-0)
47. Protopopoff N, Matowo J, Malima R, Kavishe R, Kaaya R, Wright A, West P A, Kleinschmidt I, Kisinza F W, Rowland M. 2013 High level of resistance in the mosquito *Anopheles gambiae* to pyrethroid insecticides and reduced susceptibility to bendiocarb in north-western Tanzania. *Malar. J.* **12**, 149. (doi:10.1186/1475-2875-12-149)
48. Hargreaves K, Hunt RH, Brooke BD, Mthembu J, Weeto MM, Awolola TS, Coetzee M. 2003 *Anopheles arabiensis* and *An. quadriannulatus* resistance to DDT in South Africa. *Med. Vet. Entomol.* **17**, 417–422.
49. Asia S, January O, Province J, Prov- J, Appendix S, Asia S, Nu E, Appendix S. 2017 Emergence of Indigenous Artemisinin-Resistant *Plasmodium falciparum* in Africa. , 1–3.

50. Achan J, Talisuna AO, Erhart A, Yeka A, Tibenderana JK, Baliraine FN, Rosenthal PJ, D'Alessandro U. 2011 Quinine, an old anti-malarial drug in a modern world: role in the treatment of malaria. *Malar. J.* **10**, 144. (doi:10.1186/1475-2875-10-144)
51. Nzila A. 2006 The past, present and future of antifolates in the treatment of Plasmodium falciparum infection. *J. Antimicrob. Chemother.* **57**, 1043–1054. (doi:10.1093/jac/dkl104)
52. Jensen M, Mehlhorn H. 2009 Seventy-five years of Resochin in the fight against malaria. *Parasitol. Res.* **105**, 609–627. (doi:10.1007/s00436-009-1524-8)
53. Nájera J a, González-Silva M, Alonso PL. 2011 Some lessons for the future from the Global Malaria Eradication Programme (1955-1969). *PLoS Med.* **8**, e1000412. (doi:10.1371/journal.pmed.1000412)
54. Payne D. 1987 Spread of chloroquine resistance in Plasmodium falciparum. *Parasitol. Today* **3**, 241–246. (doi:10.1016/0169-4758(87)90147-5)
55. Meshnick SR, Dobson MJ. In press. The History of Antimalarial Drugs. , 15–26.
56. WHO. 2016 Artemisinin and artemisinin-based combination therapy resistance. , 1–8.
57. WHO. 2013 WHO world malaria report 2013.
58. Phyto AP, Nkhoma S, Stepniewska K, Ashley E A, Nair S, McGready R, Ler Moo C, Al-Saai S, Dondorp A M, Iwin K M, Singhasivanon P, Day N P, White N J, Anderson T J, Nosten F. 2012 Emergence of artemisinin-resistant malaria on the western border of Thailand: A longitudinal study. *Lancet* **379**, 1960–1966. (doi:10.1016/S0140-6736(12)60484-X)
59. Arieu F, Witkowski B, Amaratunga C, Beghain J, Ma L, Lim P, Leang R, Duong S, Sreng S. 2016 A molecular marker of artemisinin-resistant Plasmodium falciparum malaria. *Nature* **505**, 50–55. (doi:10.1038/nature12876.A)
60. Buckling A, Ranford-Cartwright LC, Miles A, Read A F. 1999 Chloroquine increases Plasmodium falciparum gametocytogenesis in vitro. *Parasitology* **118** (Pt 4, 339–346. (doi:10.1017/S0031182099003960)
61. Buckling A, Crooks L, Read A. 1999 Plasmodium chabaudi: effect of antimalarial drugs on gametocytogenesis. *Exp. Parasitol.* **93**, 45–54. (doi:10.1006/expr.1999.4429)

62. Puta C, Manyando C. 1997 Enhanced gametocyte production in Fansidar-treated Plasmodium falciparum malaria patients: implications for malaria transmission control programmes. *Trop. Med. Int. Health* **2**, 227–9.
63. Price RN, Nosten F, Luxemburger C, Ter Kuile FO, Paiphun L, Chongsuphajaisiddhi T, White NJ. 1996 Effects of artemisinin derivatives on malaria transmissibility. *Lancet* **347**, 1654–1658. (doi:10.1016/S0140-6736(96)91488-9)
64. Who. 2012 Updated WHO policy recommendation: Single dose primaquine as a gametocytocide in Plasmodium falciparum malaria. *October, 2012* , 1.
65. AlKadi HO. 2007 Antimalarial drug toxicity: a review. *Chemotherapy* **53**, 385–91. (doi:10.1159/000109767)
66. Howes RE, Battle KE, Satyagraha AW, Baird JK, Hay SI. 2013 *G6PD deficiency: global distribution, genetic variants and primaquine therapy*. Elsevier. (doi:10.1016/B978-0-12-407826-0.00004-7)
67. Burrows JN, Hooft van Huijsduijnen R, Möhrle JJ, Oeuvray C, Wells TN. 2013 Designing the next generation of medicines for malaria control and eradication. *Malar. J.* **12**, 187. (doi:10.1186/1475-2875-12-187)
68. Burrows JN, Duparc S, Gutteridge WE, Hooft van Huijsduijnen R, Kaszubska W, Macintyre F, Mazzuri S, Möhrle JJ, Wells TNC. 2017 New developments in anti-malarial target candidate and product profiles. *Malar. J.* **16**, 26. (doi:10.1186/s12936-016-1675-x)
69. Goodman CD, McFadden GI. 2013 Targeting apicoplasts in malaria parasites. *Expert Opin. Ther. Targets* **17**, 167–77. (doi:10.1517/14728222.2013.739158)
70. Rieckmann KH, Powell RD, McNamara J V., Willerson D, Lass L, Frischer H, Carson PE. 1971 Effects of tetracycline against chloroquine-resistant and chloroquine-sensitive Plasmodium falciparum. *Am. J. Trop. Med. Hyg.* **20**, 811–815.
71. Dahl EL, Shock JL, Shenai BR, Gut J, DeRisi JL, Rosenthal PJ. 2006 Tetracyclines specifically target the apicoplast of the malaria parasite Plasmodium falciparum. *Antimicrob. Agents Chemother.* **50**, 3124–3131. (doi:10.1128/AAC.00394-06)
72. Tan KR, Magill AJ, Parise ME, Arguin PM. 2011 Doxycycline for malaria

- chemoprophylaxis and treatment: Report from the CDC expert meeting on malaria chemoprophylaxis. *Am. J. Trop. Med. Hyg.* **84**, 517–531. (doi:10.4269/ajtmh.2011.10-0285)
73. R.P.P.Soaes. 2006 Evaluation of antimalarial and fluoroquinolone combinations against *Plasmodium falciparum* in vitro. *Int. J. Antimicrob. Agents* **28**, 271–272. (doi:10.1016/j.ijantimicag.2006.04.009)
 74. Tang Girdwood S C, Nenortas E, Shapiro T A. 2015 Targeting the gyrase of *Plasmodium falciparum* with topoisomerase poisons. *Biochem Pharmacol* **95**, 227–237. (doi:10.1016/j.bbamem.2015.02.010.Cationic)
 75. Georgiev SV. 1994 Management of Toxoplasmosis. *Drugs* **48**, 179–188. (doi:10.2165/00003495-199448020-00005)
 76. Seaberg LS, Parquette AR, Gluzman IY, Phillips GW, Brodasky TF, Krogstad DJ. 1984 Clindamycin Activity Against Chloroquine-Resistant *Plasmodium falciparum*. *J. Infect. Dis.* **150**, 904–911. (doi:10.1093/infdis/150.6.904)
 77. Perera RK, Nikolaev VO. 2013 Compartmentation of cAMP signalling in cardiomyocytes in health and disease. *Acta Physiol.* **207**, 650–662. (doi:10.1111/apha.12077)
 78. Restrepo D, Teeter JH, Schild D. 1996 Second messenger signaling in olfactory transduction. *J. Neurobiol.* **30**, 37–48. (doi:10.1002/(SICI)1097-4695(199605)30:1<37::AID-NEU4>3.3.CO;2-M)
 79. An S-Q, Chin K, Febrer M, McCarthy Y, Yang J, Liu C, Swarbreck D, Rogers J, Dow J M, Chou S, Ryan R P. 2013 A cyclic GMP-dependent signalling pathway regulates bacterial phytopathogenesis. *EMBO J.* **32**, 2430–8. (doi:10.1038/emboj.2013.165)
 80. Wiersma HI, Galuska SE, Tomley FM, Sibley LD, Liberator P A, Donald RGK. 2004 A role for coccidian cGMP-dependent protein kinase in motility and invasion. *Int. J. Parasitol.* **34**, 369–80. (doi:10.1016/j.ijpara.2003.11.019)
 81. Hartmann A, Arroyo-Olarte RD, Imkeller K, Hegemann P, Lucius R, Gupta N. 2013 Optogenetic modulation of an adenylate cyclase in *Toxoplasma gondii* demonstrates a requirement of the parasite cAMP for host-cell invasion and stage differentiation. *J. Biol. Chem.* **288**, 13705–13717. (doi:10.1074/jbc.M113.465583)

82. Kurokawa H, Kato K, Iwanga T, Sugi T, Sudo A, Kobayashi K, Gong H, Takemae H, Recuenco F C, Horimoto T, Akashi H. 2011 Identification of *Toxoplasma gondii* cAMP dependent protein kinase and its role in the tachyzoite growth. *PLoS One* **6**. (doi:10.1371/journal.pone.0022492)
83. Gurnett AM, liberator P A, Dulski P M, Salowe S P, Donald R G K, Anderson J W, Wiltsie J, Diaz C A, harris G, chang B, darkin-Rattray S J, Nare B, Crumley T, Blum P S, Misura A S, Tamas T, Sardana M K, Yuan J, Biftu T, Schmatz D M . 2002 Purification and molecular characterization of cGMP-dependent protein kinase from Apicomplexan parasites. A novel chemotherapeutic target. *J. Biol. Chem.* **277**, 15913–15922. (doi:10.1074/jbc.M108393200)
84. Rybalkina IG, Tang X-B, Rybalkin SD. 2010 Multiple affinity states of cGMP-specific phosphodiesterase for sildenafil inhibition defined by cGMP-dependent and cGMP-independent mechanisms. *Mol. Pharmacol.* **77**, 670–677. (doi:10.1124/mol.109.062299)
85. Chuang AT, Strauss JD, Murphy RA, Steers WD. 1998 Sildenafil, a type-5 CGMP phosphodiesterase inhibitor, specifically amplifies endogenous cGMP-dependent relaxation in rabbit corpus cavernosum smooth muscle in vitro. *J. Urol.* **160**, 257–261. (doi:10.1016/S0022-5347(01)63100-8)
86. Terrett NK, Bell AS, Brown D, Ellis P. 1996 Sildenafil (Viagra(TM)), a potent and selective inhibitor of type 5 CGMP phosphodiesterase with utility for the treatment of male erectile dysfunction. *Bioorganic Med. Chem. Lett.* **6**, 1819–1824. (doi:10.1016/0960-894X(96)00323-X)
87. Love BL, Johnson A, Smith LS. 2014 Linaclotide: A novel agent for chronic constipation and irritable bowel syndrome. *Am. J. Heal. Pharm.* **71**, 1081–1091. (doi:10.2146/ajhp130575)
88. Hatzelmann A, Morcillo EJ, Lungarella G, Adnot S, Sanjar S, Beume R, Schudt C, Tenor H. 2010 The preclinical pharmacology of roflumilast - A selective, oral phosphodiesterase 4 inhibitor in development for chronic obstructive pulmonary disease. *Pulm. Pharmacol. Ther.* **23**, 235–256. (doi:10.1016/j.pupt.2010.03.011)
89. Kamenetsky M, Middelhaufe S, Bank EM, Levin LR, Steegborn C. 2013 Tale of Two

Systems. **362**, 623–639. (doi:10.1016/j.jmb.2006.07.045.Molecular)

90. Buck J, Sinclair ML, Schapal L, Cann MJ, Levin LR. 1999 Cytosolic adenylyl cyclase defines a unique signaling molecule in mammals. *Proc. Natl. Acad. Sci. U. S. A.* **96**, 79–84. (doi:10.1073/pnas.96.1.79)
91. Chen Y, Cann M J, Litvin T N, Lourgenko V, Sinclair M L, levin L R, Buck J. 2000 Soluble adenylyl cyclase as an evolutionarily conserved bicarbonate sensor. *Science* **289**, 625–8. (doi:10.1126/science.289.5479.625)
92. Litvin TN, Kamenetsky M, Zarifyan A, Buck J, Levin LR. 2003 Kinetic properties of ‘soluble’ adenylyl cyclase: Synergism between calcium and bicarbonate. *J. Biol. Chem.* **278**, 15922–15926. (doi:10.1074/jbc.M212475200)
93. Sadana R, Dessauer CW. 2009 Physiological roles for G protein-regulated adenylyl cyclase isoforms: Insights from knockout and overexpression studies. *NeuroSignals* **17**, 5–22. (doi:10.1159/000166277)
94. Zimmermann G, Zhou D, Taussig R. 1998 Mutations uncover a role for two magnesium ions in the catalytic mechanism of adenylyl cyclase. *J. Biol. Chem.* **273**, 19650–19655. (doi:10.1074/jbc.273.31.19650)
95. Sunahara RK, Taussig R. 2002 Isoforms of mammalian adenylyl cyclase: multiplicities of signaling. *Mol. Interv.* **2**, 168–184. (doi:10.1124/mi.2.3.168)
96. Steegborn C. 2014 Structure, mechanism, and regulation of soluble adenylyl cyclases - similarities and differences to transmembrane adenylyl cyclases. *Biochim. Biophys. Acta - Mol. Basis Dis.* **1842**, 2535–2547. (doi:10.1016/j.bbadis.2014.08.012)
97. Mitterauer T, Hohenegger M, Tang WJ, Nanoff C, Freissmuth M. 1998 The C2 catalytic domain of adenylyl cyclase contains the second metal ion (Mn²⁺) binding site. *Biochemistry* **37**, 16183–16191. (doi:10.1021/bi981441m)
98. Ishikawa Y, Iwatsubo K, Tsunematsu T, Okumura S. 2005 Genetic manipulation and functional analysis of cAMP signalling in cardiac muscle: implications for a new target of pharmacotherapy. *Biochem. Soc. Trans.* **33**, 1337–40. (doi:10.1042/BST20051337)
99. Appukuttan A, Kasseckert SA, Kumar S, Peter Reusch H, Ladilov Y. 2013 Oxysterol-induced apoptosis of smooth muscle cells is under the control of a soluble adenylyl

- cyclase. *Cardiovasc. Res.* **99**, 734–742. (doi:10.1093/cvr/cvt137)
100. Ramos LS, Zippin JH, Kamenetsky M, Buck J, Levin LR. 2008 Glucose and GLP-1 stimulate cAMP production via distinct adenylyl cyclases in INS-1E insulinoma cells. *J. Gen. Physiol.* **132**, 329–38. (doi:10.1085/jgp.200810044)
101. Flacke JP, Flacke H, Appukuttan A, Palisaar RJ, Noldus J, Robinson BD, Reusch HP, Zippin JH, Ladilov Y. 2013 Type 10 soluble adenylyl cyclase is overexpressed in prostate carcinoma and controls proliferation of prostate cancer cells. *J. Biol. Chem.* **288**, 3126–3135. (doi:10.1074/jbc.M112.403279)
102. Lin GG, Scott JG. 2012 NIH Public Access. **100**, 130–134. (doi:10.1016/j.pestbp.2011.02.012.Investigations)
103. Linder JU, Schultz JE. 2003 The class III adenylyl cyclases: Multi-purpose signalling modules. *Cell. Signal.* **15**, 1081–1089. (doi:10.1016/S0898-6568(03)00130-X)
104. Baker DA. 2004 Adenylyl and guanylyl cyclases from the malaria parasite *Plasmodium falciparum*. *IUBMB Life* **56**, 535–540. (doi:10.1080/15216540400013937)
105. Weber JH, Vishnyakov A, Hambach K, Schultz A, Schultz JE, Linder JU. 2004 Adenylyl cyclases from *Plasmodium*, *Paramecium* and *Tetrahymena* are novel ion channel/enzyme fusion proteins. *Cell. Signal.* **16**, 115–125. (doi:10.1016/S0898-6568(03)00129-3)
106. Muhia DK, Swales CA, Eckstein-Ludwig U, Saran S, Polley SD, Kelly JM, Schaap P, Krishna S, Baker DA. 2003 Multiple splice variants encode a novel adenylyl cyclase of possible plastid origin expressed in the sexual stage of the malaria parasite *Plasmodium falciparum*. *J. Biol. Chem.* **278**, 22014–22022. (doi:10.1074/jbc.M301639200)
107. Read LK, Mikkelsen RB. 1991 Comparison of adenylate cyclase and cAMP-dependent protein kinase in gametocytogenic and nongametocytogenic clones of *Plasmodium falciparum*. *J. Parasitol.* **77**, 346–52.
108. Ono T, Cabrita-Santos L, leitao R, Bettiol E, Purcell L A, Diaz-Pulido O, Andrews L B, Tadakuma T, Bhanot P, Mota M M, Rodriguez A. 2008 Adenylyl cyclase α and cAMP signaling mediate *Plasmodium* sporozoite apical regulated exocytosis and hepatocyte infection. *PLoS Pathog.* **4**. (doi:10.1371/journal.ppat.1000008)

109. Bozdech Z, Llinás M, Pulliam BL, Wong ED, Zhu J, DeRisi JL. 2003 The transcriptome of the intraerythrocytic developmental cycle of *Plasmodium falciparum*. *PLoS Biol.* **1**, 85–100. (doi:10.1371/journal.pbio.0000005)
110. Le Roch KG, Zhou Y, Blair P L, Grainger M, Moch J K, Haynes J D, De la Vega P, Holder A A, Batalov S, Carucci D J, Winzeler E A. 2003 Discovery of gene function by expression profiling of the malaria parasite life cycle. *Science (80-)*. **301**, 1503–1508. (doi:10.1126/science.1087025)
111. Salazar E, Bank EM, Ramsey N, Hess KC, Deitsch KW, Levin LR, Buck J. 2012 Characterization of *Plasmodium falciparum* Adenylyl Cyclase-?? and its role in Erythrocytic stage parasites. *PLoS One* **7**, 1–8. (doi:10.1371/journal.pone.0039769)
112. Hardman JG, Sutherland EW. 1969 Guanyl cyclase, an enzyme catalyzing the formation of guanosine 3',5'-monophosphate from guanosine triphosphate. *J. Biol. Chem.* **244**, 6363–6370.
113. White AA, Aurbach GD. 1969 Detection of guanyl cyclase in mammalian tissues. *Biochim. Biophys. Acta* **191**, 686–697. (doi:10.1016/0005-2744(69)90362-3)
114. Kamisaki Y, Saheki S, Nakane M, Palmieri J A, Kuno T, Chang BY, Waldman S A, Murad F. 1986 Soluble guanylate cyclase from rat lung exists as a heterodimer. *J. Biol. Chem.* **261**, 7236–7241.
115. Koesling D, Russwurm M, Mergia E, Mullershausen F, Friebe A. 2004 Nitric oxide-sensitive guanylyl cyclase: Structure and regulation. *Neurochem. Int.* **45**, 813–819. (doi:10.1016/j.neuint.2004.03.011)
116. Ignarro LJ, Degnan JN, Baricos WH, Kadowitz PJ, Wolin MS. 1982 Activation of purified guanylate cyclase by nitric oxide requires heme comparison of heme-deficient, heme-reconstituted and heme-containing forms of soluble enzyme from bovine lung. *BBA - Gen. Subj.* **718**, 49–59. (doi:10.1016/0304-4165(82)90008-3)
117. Ignarro LJ, Adams JB, Horwitz PM, Wood KS. 1986 Activation of soluble guanylate cyclase by NO-hemoproteins involves NO-heme exchange. Comparison of heme-containing and heme-deficient enzyme forms. *J. Biol. Chem.* **261**, 4997–5002.
118. Budworth J, Meillerais S, Charles I, Powell K. 1999 Tissue distribution of the human

- soluble guanylate cyclases. *Biochem. Biophys. Res. Commun.* **263**, 696–701.
(doi:10.1006/bbrc.1999.1444)
119. Potter LR. 2011 Guanylyl cyclase structure, function and regulation. *Cell. Signal.* **23**, 1921–6. (doi:10.1016/j.cellsig.2011.09.001)
 120. Kuhn M. 2003 Structure, Regulation, and Function of Mammalian Membrane Guanylyl Cyclase Receptors, With a Focus on Guanylyl Cyclase-A. *Circ. Res.* **93**, 700–709.
(doi:10.1161/01.RES.0000094745.28948.4D)
 121. Tesmer JJ, Sunahara RK, Gilman A G, Sprang SR. 1997 Crystal structure of the catalytic domains of adenylyl cyclase in a complex with G α .GTP γ S. *Science* **278**, 1907–1916. (doi:10.1126/science.278.5345.1907)
 122. Dickey DM, Dries DL, Margulies KB, Potter LR. 2012 Guanylyl cyclase (GC)-A and GC-B activities in ventricles and cardiomyocytes from failed and non-failed human hearts: GC-A is inactive in the failed cardiomyocyte. *J. Mol. Cell. Cardiol.* **52**, 727–732.
(doi:10.1016/j.yjmcc.2011.11.007)
 123. Collection S. 2016 HHS Public Access. **8**, 583–592. (doi:10.1002/aur.1474.Replication)
 124. Carucci DJ, Witney A A, Warhurst D C, Schaap P, Meima M, Li J, Taylor M C, Kelly J M, Baker D A. 2000 Guanylyl cyclase activity associated with putative bifunctional integral membrane proteins in *Plasmodium falciparum*. *J. Biol. Chem.* **275**, 22147–56.
(doi:10.1074/jbc.M001021200)
 125. Linder JU, Engel P, Reimer A, Krüger T, Plattner H, Schultz A, Schultz JE. 1999 Guanylyl cyclases with the topology of mammalian adenylyl cyclases and an N-terminal P-type ATPase-like domain in *Paramecium*, *Tetrahymena* and *Plasmodium*. *EMBO J.* **18**, 4222–4232. (doi:10.1093/emboj/18.15.4222)
 126. Muhia DK, Swales C A, Deng W, Kelly JM, Baker D A. 2001 The gametocyte-activating factor xanthurenic acid stimulates an increase in membrane-associated guanylyl cyclase activity in the human malaria parasite *Plasmodium falciparum*. *Mol. Microbiol.* **42**, 553–60.
 127. Young J A, Fivelman QL, Blair PL, De la Vega P, Le Roch KG, Zhou Y, Carucci DJ, Baker D a, Winzeler E A. 2005 The *Plasmodium falciparum* sexual development transcriptome: a

- microarray analysis using ontology-based pattern identification. *Mol. Biochem. Parasitol.* **143**, 67–79. (doi:10.1016/j.molbiopara.2005.05.007)
128. Moon RW, Taylor CJ, Bex C, Schepers R, Goulding D, Janse CJ, Waters AP, Baker DA, Billker O. 2009 A cyclic GMP signalling module that regulates gliding motility in a malaria parasite. *PLoS Pathog.* **5**, e1000599. (doi:10.1371/journal.ppat.1000599)
129. Hirai M, Arai M, Kawai S, Matsuoka H. 2006 PbGC β is essential for Plasmodium ookinete motility to invade midgut cell and for successful completion of parasite life cycle in mosquitoes. *J. Biochem.* **140**, 747–757. (doi:10.1093/jb/mvj205)
130. Taylor CJ, McRobert L, Baker D A. 2008 Disruption of a Plasmodium falciparum cyclic nucleotide phosphodiesterase gene causes aberrant gametogenesis. *Mol. Microbiol.* **69**, 110–8. (doi:10.1111/j.1365-2958.2008.06267.x)
131. Francis SH, Turko I V., Corbin JD. 2001 Cyclic nucleotide phosphodiesterases: relating structure and function. *Prog. Nucleic Acid Res. Mol. Biol.* **65**, 1–52. (doi:10.1016/S0079-6603(00)65001-8)
132. Francis SH, Blount M A, Corbin JD. 2011 Mammalian cyclic nucleotide phosphodiesterases: molecular mechanisms and physiological functions. *Physiol. Rev.* **91**, 651–690. (doi:10.1152/physrev.00030.2010)
133. Zaccolo M, Movsesian MA. 2007 cAMP and cGMP signaling cross-talk: Role of phosphodiesterases and implications for cardiac pathophysiology. *Circ. Res.* **100**, 1569–1578. (doi:10.1161/CIRCRESAHA.106.144501)
134. Bender AT, Beavo JA. 2006 Cyclic nucleotide phosphodiesterases: molecular regulation to clinical use. *Pharmacol. Rev.* **58**, 488–520. (doi:10.1124/pr.58.3.5)
135. Miki N, Baraban JM, Keirns JJ, Boyce JJ, Bitensky MW. 1975 Purification and properties of the light-activated cyclic nucleotide phosphodiesterase of rod outer segments. *J. Biol. Chem.* **250**, 6320–7.
136. Morin F, Lugnier C, Kameni J, Voisin P. 2001 Expression and role of phosphodiesterase 6 in the chicken pineal gland. *J. Neurochem.* **78**, 88–99. (doi:10.1046/j.1471-4159.2001.00407.x)
137. Kuschner WG. 2005 Sildenafil citrate therapy for pulmonary arterial hypertension. *N.*

Engl. J. Med. **354**, 1091-3-3.

138. Cote RH. 2004 Characteristics of Photoreceptor PDE (PDE6): similarities and differences to PDE5. *Int. J. Impot. Res.* **16**, S28–S33. (doi:10.1038/sj.ijir.3901212)
139. Page CP, Spina D. 2011 Phosphodiesterase inhibitors in the treatment of inflammatory diseases. *Handb Exp Pharmacol* , 391–414. (doi:10.1007/978-3-642-17969-3_17)
140. Howard BL, Thompson PE MD. 2011 Active site similarity between human and Plasmodium falciparum phosphodiesterases: considerations for antimalarial drug design. *J Comput Aided Mol Des* **25**, 753–62.
141. Wentzinger L, Bopp S, Tenor H, Klar J, Brun R, Beck HP, Seebeck T. 2008 Cyclic nucleotide-specific phosphodiesterases of Plasmodium falciparum: PfPDEalpha, a non-essential cGMP-specific PDE that is an integral membrane protein. *Int. J. Parasitol.* **38**, 1625–37. (doi:10.1016/j.ijpara.2008.05.016)
142. Lakshmanan V, Fishbaugher ME, Morrison B, Baldwin M, Macarulay M, Vaughan AM, Mikolajczak S A, Kappe HI. 2015 Cyclic GMP Balance Is Critical for Malaria Parasite Transmission from the Mosquito to the Mammalian Host. **6**, 1–10. (doi:10.1128/mBio.02330-14.Editor)
143. Yuasa K, Mi-Ichi F, Kobayashi T, Yamanouchi M, Kotera J, Kita K, Omori K. 2005 PfPDE1, a novel cGMP-specific phosphodiesterase from the human malaria parasite Plasmodium falciparum. *Biochem. J.* **392**, 221–9. (doi:10.1042/BJ20050425)
144. Lasonder E, Rijpma S R, van Schaijk B C L, Hoeijmakers W A M, Kensche P R, Grenigt M S, Italiaander A, Vos M W, Woestenenk R, Bousema T, Mair G R, Khan S M, Janse C J, Bartfai R, Sauerwein R W. 2016 Integrated transcriptomic and proteomic analyses of P. Falciparum gametocytes: Molecular insight into sex-specific processes and translational repression. *Nucleic Acids Res.* **44**, 6087–6101. (doi:10.1093/nar/gkw536)
145. López-Barragán MJ, Lemieux J, Quinones M, Williamson K C, Molina-Cruz A, Cui K, Barillas-Mury C, Zhao K, Su X. 2011 Directional gene expression and antisense transcripts in sexual and asexual stages of Plasmodium falciparum. *BMC Genomics* **12**, 587. (doi:10.1186/1471-2164-12-587)
146. Kebaier C, Vanderberg JP. 2010 Initiation of Plasmodium sporozoite motility by albumin

is associated with induction of intracellular signalling. *Int. J. Parasitol.* **40**, 25–33.
(doi:10.1016/j.ijpara.2009.06.011)

147. Francis SH, Busch JL, Corbin JD, Sibley D. 2010 cGMP-dependent protein kinases and cGMP phosphodiesterases in nitric oxide and cGMP action. *Pharmacol. Rev.* **62**, 525–63.
(doi:10.1124/pr.110.002907)
148. Kaupp UB, Seifert R. 2002 Cyclic nucleotide-gated ion channels. *Physiol. Rev.* **82**, 769–824. (doi:10.1152/physrev.00008.2002)
149. de Rooij J, Zwartkruis FJ, Verheijen MH, Cool RH, Nijman SM, Wittinghofer A, Bos JL. 1998 Epac is a Rap1 guanine-nucleotide-exchange factor directly activated by cyclic AMP. *Nature* **396**, 474–477. (doi:10.1038/24884)
150. Wang P, Liu Z, Chen H, Ye N, Cheng X, Zhou J. 2017 Exchange proteins directly activated by cAMP (EPACs): Emerging therapeutic targets. *Bioorganic Med. Chem. Lett.* **27**, 1633–1639. (doi:10.1016/j.bmcl.2017.02.065)
151. Haijun Chen, Christopher Wild, Xiaobin Zhou, Na Ye XC and JZ. 2014 Recent advances in the Discovery of Small Molecules targeting Exchange proteins Directly Activated by cAMP (EPAC). *J Med Chem* **57**, 3651–3665. (doi:10.1007/s11103-011-9767-z.Placid)
152. Dawn A, Singh S, More KR, Siddiqui FA, Pachikara N, Ramdani G, Langsley G, Chitnis CE. 2014 The Central Role of cAMP in Regulating Plasmodium falciparum Merozoite Invasion of Human Erythrocytes. *PLoS Pathog.* **10**, e1004520.
(doi:10.1371/journal.ppat.1004520)
153. Sutherland E.W, Rall T W. 1957 Fractionation and characteriestion of a Cyclic adenine ribonucleotide formed by tissue particles.
155. Ashman DF, Lipton R, Melicow MM, Price TD. 1963 Isolation of adenosine 3',5'-monophosphate and guanosine 3',5'-monophosphate from rat urine. *Biochem. Biophys. Res. Commun.* **11**, 330–334. (doi:10.1016/0006-291X(63)90566-7)
156. Baillie GS. 2009 Compartmentalized signalling: Spatial regulation of cAMP by the action of compartmentalized phosphodiesterases. *FEBS J.* **276**, 1790–1799.
(doi:10.1111/j.1742-4658.2009.06926.x)
157. Beraldo FH, Almeida FM, da Silva AM, Garcia CRS. 2005 Cyclic AMP and calcium

- interplay as second messengers in melatonin-dependent regulation of *Plasmodium falciparum* cell cycle. *J. Cell Biol.* **170**, 551–7. (doi:10.1083/jcb.200505117)
158. Falae A, Combe A, Amaladoss A, Carvalho T, Menard R, Bhanot P. 2010 Role of *Plasmodium berghei* cGMP-dependent protein kinase in late liver stage development. *J. Biol. Chem.* **285**, 3282–8. (doi:10.1074/jbc.M109.070367)
159. McRobert L, Taylor CJ, Deng W, Fivelman QL, Cummings RM, Polley SD, Billker O, Baker D A. 2008 Gametogenesis in malaria parasites is mediated by the cGMP-dependent protein kinase. *PLoS Biol.* **6**, e139. (doi:10.1371/journal.pbio.0060139)
160. Taylor HM, McRobert L, Grainger M, Sicard Aa., Dluzewski A. R, Hopp CS, Holder A. A., Baker D A. 2009 The Malaria Parasite Cyclic GMP-Dependent Protein Kinase Plays a Central Role in Blood-Stage Schizogony. *Eukaryot. Cell* **9**, 37–45. (doi:10.1128/EC.00186-09)
161. Clapham DE. 2007 Calcium signaling. *Cell* **131**, 1047–58. (doi:10.1016/j.cell.2007.11.028)
162. Shi Y. 2009 Serine/Threonine Phosphatases: Mechanism through Structure. *Cell* **139**, 468–484. (doi:10.1016/j.cell.2009.10.006)
163. Ahrens H, Paul AK, Kuroda Y SR. 1982 Adrenocortical cyclic GMP-dependent protein kinase: purification, characterisation, and modification of its activity by calmodulin, and its relationship with steroidogenesis. *Arch Biochem Biophys* **215**, 597–609.
164. Deng W, Baker DA. 2002 A novel cyclic GMP-dependent protein kinase is expressed in the ring stage of the *Plasmodium falciparum* life cycle. **44**, 1141–1151.
165. Zhang YW, Rudnick G. 2011 Myristoylation of cGMP-dependent protein kinase dictates isoform specificity for serotonin transporter regulation. *J. Biol. Chem.* **286**, 2461–2468. (doi:10.1074/jbc.M110.203935)
166. Hofmann F. 2005 The biology of cyclic GMP-dependent protein kinases. *J. Biol. Chem.* **280**, 1–4. (doi:10.1074/jbc.R400035200)
167. Corbin JD, Stein D. 1983 Studies of Two Different Intrachain cGMP-binding Sites of cGMP- dependent Protein Kinase *. **258**, 11391–11397.

168. Donald RGK, Liberator P A. 2002 Molecular characterization of a coccidian parasite cGMP dependent protein kinase. *Mol. Biochem. Parasitol.* **120**, 165–75.
169. Kim JJ, Flueck C, Franz E, Sanabria-Figueroa E, Thomposn E, Lorenze R, Bertinetti D, Baker D A, Herberg F W, Kim C. 2015 Crystal Structures of the Carboxyl cGMP Binding Domain of the Plasmodium falciparum cGMP-dependent Protein Kinase Reveal a Novel Capping Triad Crucial for Merozoite Egress. *PLoS Pathog.* **11**, 1–22. (doi:10.1371/journal.ppat.1004639)
170. Deng W, Parbuh-Patel A, Meyer DJ, Baker DA. 2003 The role of two novel regulatory sites in the activation of the cGMP-dependent protein kinase from Plasmodium falciparum. *Biochem. J.* **374**, 559–565. (doi:10.1042/bj20030474)
171. Salowe SP, Wiltsie J, Liberator PA, Donald RGK. 2002 The role of a parasite-specific allosteric site in the distinctive activation behavior of Eimeria tenella cGMP-dependent protein kinase. *Biochemistry* **41**, 4385–4391. (doi:10.1021/bi0156658)
172. Alam MM, Solyakov L, Bottrill A R, Flueck C, Siddiqui F A, Shilija S, Mistry S, Viskduraki M, lee K, Hopp C S, Chitnis C E, Doerig C, Moon R W, Green J L, Holder A A, Baker D A, Tobin A B. 2015 Phosphoproteomics reveals malaria parasite Protein Kinase G as a signalling hub regulating egress and invasion. *Nat. Commun.* **6**, 7285. (doi:10.1038/ncomms8285)
173. Collins CR, Hackett F, Strath M, Penzo M, Withers-Martinez C, Baker DA, Blackman MJ. 2013 Malaria Parasite cGMP-dependent Protein Kinase Regulates Blood Stage Merozoite Secretory Organelle Discharge and Egress. *PLoS Pathog.* **9**. (doi:10.1371/journal.ppat.1003344)
174. Brochet M, Collins M O, Smith T K, Thomposn E, Sebastian S, Volkmann K, Schwach F, Chappell L, Gomes A R, Berriman M, Ryner J C, Baker D A, Choudhary J, Bilker O . 2014 Phosphoinositide metabolism links cGMP-dependent protein kinase G to essential Ca²⁺ signals at key decision points in the life cycle of malaria parasites. *PLoS Biol.* **12**, e1001806. (doi:10.1371/journal.pbio.1001806)
175. Dvorin JD, Martyn D C, Patel S D, Grinley J S, Collins C R, Hopp C S, Bright A T, Westenberger S, Winzeler E, Blackman M J, Baker D A, Wandless T J, Duraisingh M T. 2010 A plant-like kinase in Plasmodium falciparum regulates parasite egress from

- erythrocytes. *Science* **328**, 910–2. (doi:10.1126/science.1188191)
176. Hopp CS, Flueck C, Solyakov L, Tobin A, Baker D A. 2012 Spatiotemporal and functional characterisation of the Plasmodium falciparum cGMP-dependent protein kinase. *PLoS One* **7**, e48206. (doi:10.1371/journal.pone.0048206)
 177. Schwappacher R, Weiske J, Heining E, Ezerski V, Marom B, Henis YI, Huber O, Knaus P. 2009 Novel crosstalk to BMP signalling: cGMP-dependent kinase I modulates BMP receptor and Smad activity. *EMBO J.* **28**, 1537–1550. (doi:10.1038/emboj.2009.103)
 178. Donald RGK, Allocco J, Singh SB, Nare B, Salowe SP, Wiltsie J, Liberator P A. 2002 Toxoplasma gondii Cyclic GMP-Dependent Kinase: Chemotherapeutic Targeting of an Essential Parasite Protein Kinase. *Eukaryot. Cell* **1**, 317–328. (doi:10.1128/EC.1.3.317-328.2002)
 179. Diaz C A, Allocco J, Powles MA, Yeung L, Donald RGK, Anderson JW, Liberator P A. 2006 Characterization of Plasmodium falciparum cGMP-dependent protein kinase (PfPKG): antiparasitic activity of a PKG inhibitor. *Mol. Biochem. Parasitol.* **146**, 78–88. (doi:10.1016/j.molbiopara.2005.10.020)
 180. Biftu T, Feng D, Fisher M, Liang G, Qian X, Scribner A, Dennis R, Lee S, Liberator P A, Brown C, Gurnett A, Leavitt P S, Thompson D, Mathew J, Misura A, Samaras S, Tamas T, Sina J F, McNulty K A, McKnight C G, Schmatz D M, Wyvratt M. 2006 Synthesis and SAR studies of very potent imidazopyridine antiprotozoal agents. *Bioorganic Med. Chem. Lett.* **16**, 2479–2483. (doi:10.1016/j.bmcl.2006.01.092)
 181. Donald RGK, Zhong T, Wiersma H, Nare B, Yao D, Lee A, Allocco J, Liberator PA. 2006 Anticoccidial kinase inhibitors: Identification of protein kinase targets secondary to cGMP-dependent protein kinase. *Mol. Biochem. Parasitol.* **149**, 86–98. (doi:10.1016/j.molbiopara.2006.05.003)
 182. Nare B, Allocco JJ, Liberator PA, Donald RGK. 2002 Evaluation of a cyclic GMP-dependent protein kinase inhibitor in treatment of murine toxoplasmosis: Gamma interferon is required for efficacy. *Antimicrob. Agents Chemother.* **46**, 300–307. (doi:10.1128/AAC.46.2.300-307.2002)
 183. Li J, Cox LS. 2000 Isolation and characterisation of a cAMP-dependent protein kinase catalytic subunit gene from Plasmodium falciparum. *Mol. Biochem. Parasitol.* **109**, 157–

- 163.
184. Wong W, Scott JD. 2004 AKAP signalling complexes: focal points in space and time. *Nat. Rev. Mol. Cell Biol.* **5**, 959–970. (doi:10.1038/nrm1527)
185. Lomas O, Zaccolo M. 2014 Phosphodiesterases maintain signaling fidelity via compartmentalization of cyclic nucleotides. *Physiology (Bethesda)*. **29**, 141–9. (doi:10.1152/physiol.00040.2013)
186. Reimann EM, Brostrom CO, Corbin JD, King CA KE. 1971 No TitleSeparation of regulatory and catalytic subunits of the cyclic 3',5'-adenosine monophosphate-dependent protein kinase(s) of rabbit skeletal muscle. *Biochem Biophys Res Commun* **Jan 22**, 187–94.
187. Merckx A, Nivez MP, Bouyer G, Alano P, Langsley G, Deitsch K, Thomas S, Doerig C, Egée S. 2008 Plasmodium falciparum regulatory subunit of cAMP-dependent PKA and anion channel conductance. *PLoS Pathog.* **4**. (doi:10.1371/journal.ppat.0040019)
188. Syin C, Parzy D, Traincard F, Boccaccio I, Joshi M B, Lin D T, Yang X, Assemat K, Doering C, Langsley G. 2001 The H89 cAMP-dependent protein kinase inhibitor blocks Plasmodium falciparum development in infected erythrocytes. *Eur. J. Biochem.* **268**, 4842–4849. (doi:10.1046/j.1432-1327.2001.02403.x)
189. Sudo A, Kato K, Kobayashi K, Tohya Y, Akashi H. 2008 Susceptibility of Plasmodium falciparum cyclic AMP-dependent protein kinase and its mammalian homologue to the inhibitors. *Mol. Biochem. Parasitol.* **160**, 138–142. (doi:10.1016/j.molbiopara.2008.03.011)
190. Saito-Ito A, He S, Kimura M, Matsumura T TK. 1995 Cloning and structural analysis of the gene for cAMP-dependent protein kinase catalytic subunit from Plasmodium yoelii. *Biochim Biophys Acta* **19**, 1–5.
191. Harrison T, Samuel BU, Akompong T, Hamm H, Mohandas N, Lomasney JW, Haldar K. 2012 Erythrocyte G Protein – Coupled Receptor Signaling in Malarial Infection. **1734**. (doi:10.1126/science.1089324)
192. Leykauf K, Treeck M, Gilson PR, Nebel T, Bräulke T, Cowman AF, Gilberger TW, Crabb BS. 2010 Protein kinase a dependent phosphorylation of apical membrane antigen 1 plays

- an important role in erythrocyte invasion by the malaria parasite. *PLoS Pathog.* **6**.
(doi:10.1371/journal.ppat.1000941)
193. Lasonder E, Green JL, Camarda G, Talabani H, Holder AA, Langsley G, Alano P. 2012 The plasmodium falciparum schizont phosphoproteome reveals extensive phosphatidylinositol and cAMP-protein kinase A signaling. *J. Proteome Res.* **11**, 5323–5337. (doi:10.1021/pr300557m)
 194. Himschoot E, Beeckman T, Friml J, Vanneste S. 2015 Calcium is an organizer of cell polarity in plants. *Biochim. Biophys. Acta* (doi:10.1016/j.bbamcr.2015.02.017)
 195. Gehlert S, Bloch W, Suhr F. 2015 Ca²⁺-dependent regulations and signaling in skeletal muscle: from electro-mechanical coupling to adaptation. *Int. J. Mol. Sci.* **16**, 1066–95. (doi:10.3390/ijms16011066)
 196. Nagamune K, Moreno SN, Chini EN, Sibley LD. 2008 Calcium Regulation and signalling in Apicomplexan Parasites. In *Molecular mechanisms of parasite Invasion*,
 197. Zhao F, Li P, Chen SR, Louis CF, Fruen BR. 2001 Dantrolene inhibition of ryanodine receptor Ca²⁺ release channels. Molecular mechanism and isoform selectivity. *J. Biol. Chem.* **276**, 13810–6. (doi:10.1074/jbc.M006104200)
 198. Alves E, Bartlett PJ, Garcia CRS, Thomas AP. 2011 Melatonin and IP₃-induced Ca²⁺ release from intracellular stores in the malaria parasite Plasmodium falciparum within infected red blood cells. *J. Biol. Chem.* **286**, 5905–12. (doi:10.1074/jbc.M110.188474)
 199. Jones ML, Cottingham C, Rayner JC. 2009 Effects of calcium signaling on Plasmodium falciparum erythrocyte invasion and post-translational modification of gliding-associated protein 45 (PfGAP45). *Mol. Biochem. Parasitol.* **168**, 55–62. (doi:10.1016/j.molbiopara.2009.06.007)
 200. Raabe AC, Wengelnik K, Billker O, Vial HJ. 2011 Multiple roles for Plasmodium berghei phosphoinositide-specific phospholipase C in regulating gametocyte activation and differentiation. **13**, 955–966. (doi:10.1111/j.1462-5822.2011.01591.x)
 201. Nagamune K, Hicks LM, Fux B, Brossier F, Chini EN, Sibley LD. 2008 Abscisic acid controls calcium-dependent egress and development in Toxoplasma gondii. *Nature* **451**, 207–10. (doi:10.1038/nature06478)

202. Leef J L, Carlson P S. 1999 Caratenoid synthesis inhibiting herbicides and fatty acid synthesis inhibiting oxime herbicides as antiapicomplexa protozoan parasite agents.
203. Prole DL, Taylor CW. 2011 Identification of intracellular and plasma membrane calcium channel homologues in pathogenic parasites. *PLoS One* **6**, e26218. (doi:10.1371/journal.pone.0026218)
204. Chandran V, Stollar EJ, Lindorff-Larsen K, Harper JF, Chazin WJ, Dobson CM, Luisi BF, Christodoulou J. 2006 Structure of the regulatory apparatus of a calcium-dependent protein kinase (CDPK): a novel mode of calmodulin-target recognition. *J. Mol. Biol.* **357**, 400–10. (doi:10.1016/j.jmb.2005.11.093)
205. Wernimont AK, Artz J D, Finerty Jr P, Lin Y, Amani M, Allali-Hassani A, Senisterra G, Vedadi M, Tempel W, Mackenzie F, Chau I, Lourido S, Sibley D L, Hui R. 2010 Structures of apicomplexan calcium-dependent protein kinases reveal mechanism of activation by calcium. *Nat. Struct. Mol. Biol.* **17**, 596–601. (doi:10.1038/nsmb.1795)
206. Brochet M, Billker O. 2016 Calcium signalling in malaria parasites. *Mol. Microbiol.* **100**, 397–408. (doi:10.1111/mmi.13324)
207. Bansal A, Singh S, More KR, Hans D, Nangalia K, Yogavel M, Sharma A, Chitnis CE. 2013 Characterization of *Plasmodium falciparum* calcium-dependent protein kinase 1 (PfCDPK1) and its role in microneme secretion during erythrocyte invasion. *J. Biol. Chem.* **288**, 1590–602. (doi:10.1074/jbc.M112.411934)
208. Ishino T, Orito Y, Chinzei Y, Yuda M. 2006 A calcium-dependent protein kinase regulates *Plasmodium* ookinete access to the midgut epithelial cell. *Mol. Microbiol.* **59**, 1175–84. (doi:10.1111/j.1365-2958.2005.05014.x)
209. Siden-Kiamos I, Ecker A, Nybäck S, Louis C, Sinden RE, Billker O. 2006 *Plasmodium berghei* calcium-dependent protein kinase 3 is required for ookinete gliding motility and mosquito midgut invasion. *Mol. Microbiol.* **60**, 1355–63. (doi:10.1111/j.1365-2958.2006.05189.x)
210. Billker O, Dechamps S, Tewari R, Wenig G, Franke-fayard B, Brinkmann V. 2004 Calcium and a Calcium-Dependent Protein Kinase Regulate Gamete Formation and Mosquito Transmission in a Malaria Parasite. **117**, 503–514.

211. Kumar R, Musiyenko A, Oldenburg A, Adams B, Barik S. 2004 Post-translational generation of constitutively active cores from larger phosphatases in the malaria parasite, *Plasmodium falciparum*: implications for proteomics. *BMC Mol Biol* **5**, 6. (doi:10.1186/1471-2199-5-6)
212. Gazarini ML, Garcia CRS. 2004 The malaria parasite mitochondrion senses cytosolic Ca²⁺ fluctuations. *Biochem. Biophys. Res. Commun.* **321**, 138–44. (doi:10.1016/j.bbrc.2004.06.141)
213. Rohrbach P, Friedrich O, Hentschel J, Plattner H, Fink RHA, Lanzer M. 2005 Quantitative calcium measurements in subcellular compartments of *Plasmodium falciparum*-infected erythrocytes. *J. Biol. Chem.* **280**, 27960–27969. (doi:10.1074/jbc.M500777200)
214. Moreno SNJ, Zhong L. 1996 Acidocalcisomes in *Toxoplasma gondii* tachyzoites. **659**, 655–659.
215. Fang H, Klages N, Baechler B, Hillner E, Yu L, Pardo M, Brochet M, Team PM. 2017 Multiple short windows of Calcium-Dependent Protein Kinase 4 activity coordinate distinct cell cycle events during *Plasmodium* gametogenesis. , 1–23. (doi:10.7554/eLife.26524)
216. Hotta CT, Gazarini ML, Beraldo FH, Varotti FP, Lopes C, Markus RP, Pozzan T, Garcia CR. 2000 Calcium-dependent modulation by melatonin of the circadian rhythm in malarial parasites. *Nat. Cell Biol.* **2**, 466–8. (doi:10.1038/35017112)
217. Doi Y, Shinzawa N, Fukumoto S, Okano H, Kanuka H. 2011 Calcium signal regulates temperature-dependent transformation of sporozoites in malaria parasite development. *Exp. Parasitol.* **128**, 176–80. (doi:10.1016/j.exppara.2011.02.011)
218. Govindasamy K, Jebiwott S, Jaijyan DK, Davidow A, Ojo KK, Van Voorhis WC, Brochet M, Billker O, Bhanot P. 2016 Invasion of hepatocytes by *Plasmodium* sporozoites requires cGMP-dependent protein kinase and calcium dependent protein kinase 4. *Mol. Microbiol.* **102**, 349–363. (doi:10.1111/mmi.13466)
219. Blackman MJ, Fujioka H, Stafford WHL, Sajid M, Clough B, Fleckt SL, Aikawa M, Grainger M, Hackett F. 1998 A subtilisin-like protein in secretory organelles of *Plasmodium falciparum* merozoites. *J. Biol. Chem.* **273**, 23398–23409. (doi:10.1074/jbc.273.36.23398)

220. Yeoh S, O'Donnell R, Koussis K, Dluzewski A R, Ansell K H, Osborne S A, Hackett F, Withers-Martinez C, Mitchell G H, Bannister L H, Bryans J S, Kettleborough C A, Blackman M J. 2007 Subcellular discharge of a serine protease mediates release of invasive malaria parasites from host erythrocytes. *Cell* **131**, 1072–83. (doi:10.1016/j.cell.2007.10.049)
221. Miller SK, Good R T, Drew D R, Delorenzi M, Sanders P R, Hodder A N, Speed T P, Cowman A F, de Koning-Ward T F, Crabb B S. 2002 A subset of Plasmodium falciparum SERA genes are expressed and appear to play an important role in the erythrocytic cycle. *J. Biol. Chem.* **277**, 47524–47532. (doi:10.1074/jbc.M206974200)
222. Pang XL, Mitamura T, Horii T. 1999 Antibodies reactive with the N-terminal domain of Plasmodium falciparum serine repeat antigen inhibit cell proliferation by agglutinating merozoites and schizonts. *Infect. Immun.* **67**, 1821–1827.
223. Arastu-Kapur S, Ponder E L, Fonovic U P, Yeoh S, Yuan F, Fonovic M, Grainger M, Phillips C I, Powers J C, Bogyo M. 2008 Identification of proteases that regulate erythrocyte rupture by the malaria parasite Plasmodium falciparum. *Nat. Chem. Biol.* **4**, 203–13. (doi:10.1038/nchembio.70)
224. Glushakova S, Lizunov V, Blank PS, Melikov K, Humphrey G, Zimmerberg J. 2013 Cytoplasmic free Ca²⁺ is essential for multiple steps in malaria parasite egress from infected erythrocytes. *Malar. J.* **12**, 41. (doi:10.1186/1475-2875-12-41)
225. Carruthers VB, Sibley LD. 1999 Mobilization of intracellular calcium stimulates microneme discharge in Toxoplasma gondii. *Mol. Microbiol.* **31**, 421–8.
226. Lovett JL, Marchesini N, Moreno SNJ, Sibley LD. 2002 Toxoplasma gondii microneme secretion involves intracellular Ca²⁺ release from inositol 1,4,5-triphosphate (IP₃)/ryanodine-sensitive stores. *J. Biol. Chem.* **277**, 25870–6. (doi:10.1074/jbc.M202553200)
227. Bannister LH, Dluzewski AR. 1990 The ultrastructure of red cell invasion in malaria infections: a review. *Blood Cells* **16**, 257. (doi:10.1073/pnas.1007653107/-/DCSupplemental.www.pnas.org/cgi/doi/10.1073/pnas.1007653107)
228. Triglia T. 2000 Apical membrane antigen 1 plays a central role in erythrocyte invasion by Plasmodium species. *Mol. Microbiol.* **38**, 706–718.

229. Mitchell GH, Thomas A W, Margos G, Dluzewski A R, Bannister LH. 2004 Apical Membrane Antigen 1 , A Major Malaria Vaccine Candidate , Mediates the Close Attachment of Invasive Merozoites to Host Apical Membrane Antigen 1 , A Major Malaria Vaccine Candidate , Mediates the Close Attachment of Invasive Merozoites to Host Red B. **72**, 154–158. (doi:10.1128/IAI.72.1.154)
230. Jeffrey Mital, Markus Meissner, Dominique Soldati and GEW. 2005 Conditional expression of Toxoplasma gondii Apical Membrane Antigen-1 (TgAMA1) Demonstrates that TgAMA1 Plays a critical Role in host cell Invasion. *Mol. Biol. Cell* **16**, 4341–4349. (doi:10.1091/mbc.E05)
231. Soldati AK and D. 2004 The glideosome: a molecular machine powering motility and host-cell invasion by Apicomplexa. *Trends Cell Biol.* **14**, 528–532. (doi:10.1016/j.tcb.2004.08.001)
232. Alexander DL, Arastu-Kapur S, Dubremetz JF, Boothroyd JC. 2006 Plasmodium falciparum AMA1 binds a rhoptry neck protein homologous to TgRON4, a component of the moving junction in Toxoplasma gondii. *Eukaryot. Cell* **5**, 1169–1173. (doi:10.1128/EC.00040-06)
233. Harris PK, Yeoh S, Dluzewski AR, O'Donnell RA, Withers-Martinez C, Hackett F, Bannister LH, Mitchell GH, Blackman MJ. 2005 Molecular identification of a malaria merozoite surface sheddase. *PLoS Pathog.* **1**, 0241–0251. (doi:10.1371/journal.ppat.0010029)
234. Balaji S, Madan Babu M, Iyer LM, Aravind L. 2005 Discovery of the principal specific transcription factors of Apicomplexa and their implication for the evolution of the AP2-integrase DNA binding domains. *Nucleic Acids Res.* **33**, 3994–4006. (doi:10.1093/nar/gki709)
235. Fivelman QL, McRobert L, Sharp S, Taylor CJ, Saeed M, Swales C A, Sutherland CJ, Baker D A. 2007 Improved synchronous production of Plasmodium falciparum gametocytes in vitro. *Mol. Biochem. Parasitol.* **154**, 119–23. (doi:10.1016/j.molbiopara.2007.04.008)
236. Carter R, Miller LH. 1979 Evidence for environmental modulation of gametocytogenesis in Plasmodium falciparum in continuous culture. *Bull. World Health Organ.* **57**, 37–52.
237. Trager W, Gill GS. 1992 Enhanced gametocyte formation in young erythrocytes by Plasmodium falciparum in vitro. *J. Protozool.* **39**, 429–432. (doi:10.1111/j.1550-

7408.1992.tb01476.x)

238. Lingnau A, Margos G, Maier WA, Seitz HM. 1993 The effects of hormones on the gametocytogenesis of *Plasmodium falciparum* in vitro. *Appl. Parasitol.* **34**, 153–60.
239. Maswoswe SM, Peters W, Warhurst DC. 1985 Corticosteroid stimulation of the growth of *Plasmodium falciparum* gametocytes in vitro. *Ann Trop Med Parasitol* **79**, 607–616.
240. Cornelissen A W C A, Walliker D. 1985 Gametocyte development of *Plasmodium chabaudi* in mice and rats: evidence for host induction of gametocytogenesis. *Parasitol. Res.* **71**, 297–303. (doi:10.1007/BF00928331)
241. Kaushal DC, Carter R, Miller LH KG. 1980 Gametocytogenesis by malaria parasites in continuous culture. *Nature Jul* **31**, 490–2.
242. Hertelendy F, Toth M, Fitch CD. 1979 Malaria enhances cyclic AMP production by immature erythrocytes in vitro. *Life Sci.* **25**, 451–455. (doi:10.1016/0024-3205(79)90578-2)
243. Brockelman CR. 1982 Conditions Favoring Gametocytogenesis in the Continuous Culture of *Plasmodium falciparum*. *J Protozool* **29**, 454–8.
244. Flueck C, Bartfai R, Volz J, Niederwieser I, Salcedo-Amaya A M, Alko B T F, Ehlgren F, Ralph S A, Cowman A F, Bozdech Z, Stunnenberg H G, Voss T S. 2009 *Plasmodium falciparum* heterochromatin protein 1 marks genomic loci linked to phenotypic variation of exported virulence factors. *PLoS Pathog.* **5**. (doi:10.1371/journal.ppat.1000569)
245. Brancucci NMB, Berschi N L, Zhu L, Niederwieser I, Chin W H, Wampfler R, Freymond C, Rottmann M, Felger I, Bozdech Z, Voss T S. 2014 Heterochromatin protein 1 secures survival and transmission of malaria parasites. *Cell Host Microbe* **16**, 165–176. (doi:10.1016/j.chom.2014.07.004)
246. Cortés A, Crowley VM, Vaquero A, Voss TS. 2012 A View on the Role of Epigenetics in the Biology of Malaria Parasites. *PLoS Pathog.* **8**. (doi:10.1371/journal.ppat.1002943)
247. Iwanaga S, Kaneko I, Kato T, Yuda M. 2012 Identification of an AP2-family Protein That Is Critical for Malaria Liver Stage Development. *PLoS One* **7**. (doi:10.1371/journal.pone.0047557)

248. Yuda M, Iwanaga S, Shigenobu S, Mair GR, Janse CJ, Waters AP, Kato T, Kaneko I. 2009 Identification of a transcription factor in the mosquito-invasive stage of malaria parasites. *Mol. Microbiol.* **71**, 1402–1414. (doi:10.1111/j.1365-2958.2009.06609.x)
249. Yuda M, Iwanaga S, Shigenobu S, Kato T, Kaneko I. 2010 Transcription factor AP2-Sp and its target genes in malarial sporozoites. *Mol. Microbiol.* **75**, 854–863. (doi:10.1111/j.1365-2958.2009.07005.x)
250. Kafsack B F C, Rovira-Graells N, Clark T G, Bancells C, Crowley V M, Campina S G, Williams A E, Drought L G, Kwiatkowski D P, Baker D A, Cortes A, Llinas M. 2014 A transcriptional switch underlies commitment to sexual development in malaria parasites. *Nature* **507**, 248–52. (doi:10.1038/nature12920)
251. Day K P, Karamalis F, Thompson J, Barnes D A, Peterson C, Brown H, Brown G V, Kemp DJ. 1993 Genes necessary for expression of a virulence determinant and for transmission of *Plasmodium falciparum* are located on a 0.3-megabase region of chromosome 9. *Proc. Natl. Acad. Sci. U. S. A.* **90**, 8292–6. (doi:10.1073/pnas.90.17.8292)
252. Bruce M C, Alano P, Duthie S, Carter R. 1990 Commitment of the malaria parasite *Plasmodium falciparum* to sexual and asexual development. *Parasitology* **100 Pt 2**, 191–200. (doi:10.1017/S0031182000061199)
253. Smith T G, Lourenço P, Carter R, Walliker D, Ranford-Cartwright L C. 2000 Commitment to sexual differentiation in the human malaria parasite, *Plasmodium falciparum*. *Parasitology* **121**, 127–133. (doi:10.1017/S0031182099006265)
254. Schall J J C N. 1989 The sex ratio of *Plasmodium* gametocytes. *Parasitol.* **98**, 343–350. (doi:10.1017/S0031182000061412)
255. de Koning-Ward TF *et al.* 2008 The role of osmiophilic bodies and Pfg377 expression in female gametocyte emergence and mosquito infectivity in the human malaria parasite *Plasmodium falciparum*. *Mol. Microbiol.* **67**, 278–90. (doi:10.1111/j.1365-2958.2007.06039.x)
256. Sinden R E, Smalley M E. 1979 Gametocytogenesis of *Plasmodium falciparum* in vitro: the cell-cycle. *Parasitology* **79**, 277–296. (doi:10.1017/S003118200005335X)

257. Carter R, Ranford-cartwright L. 1998 Has the ignition key been found ? **392**, 227–228.
258. Garcia G E, Wirtz R A, Barr J R, Woolfitt A, Rosenberg R. 1998 Xanthurenic acid induces gametogenesis in Plasmodium, the malaria parasite. *J. Biol. Chem.* **273**, 12003–5.
259. Truscott R J, Elderfield A J. 1995 Relationship between serum tryptophan and tryptophan metabolite levels after tryptophan ingestion in normal subjects and age-related cataract patients. *Clin. Sci.* **89**, 591–9.
260. Kawamoto F, Alejo-Blanco R, Fleck S L, Kawamoto Y, Sinden R E. 1990 Possible roles of Ca²⁺ and cGMP as mediators of the exflagellation of Plasmodium berghei and Plasmodium falciparum. *Mol. Biochem. Parasitol.* **42**, 101–108. (doi:10.1016/0166-6851(90)90117-5)
261. Ponnudurai T, Leeuwenberg AD, Meuwissen J H. 1981 Chloroquine sensitivity of isolates of Plasmodium falciparum adapted to in vitro culture. *Trop. Geogr. Med.* **33**, 50–4.
262. Walliker D, Quakyi I, Wellems T, McCutchan T, Szarfman A, London W, Corcoran L, Burkot T, Carter R. 1987 Genetic analysis of the human malaria parasite Plasmodium falciparum. *Science (80-.)*. **236**, 1661–1666. (doi:10.1126/science.3299700)
263. Society A. 2005 Trager and Jensen — Continuous P . Falciparum Culture. *Society* **91**, 484–486.
264. Cevenini L, Camarda G, Michelini E, Siciliano G, Calabretta M M, Bona R, Kumar T R S, Cara A, Branchini B R, Fidock D A, Roda A, Alano P. 2014 Multicolor bioluminescence boosts malaria research: Quantitative dual-color assay and single-cell imaging in Plasmodium falciparum parasites. *Anal. Chem.* **86**, 8814–8821. (doi:10.1021/ac502098w)
265. Singh S, Alam M M, Pal-Bhowmick I, Brzostowski J A, Chitnis CE. 2010 Distinct external signals trigger sequential release of apical organelles during erythrocyte invasion by malaria parasites. *PLoS Pathog.* **6**, e1000746. (doi:10.1371/journal.ppat.1000746)
266. Tawk L, Payrastra B, Vial H J, Roy C, Wengelnik K. 2010 Phosphatidylinositol 3-Phosphate , an Essential Lipid in Plasmodium , Localizes to the Food Vacuole Membrane and the Apicoplast □ †. **9**, 1519–1530. (doi:10.1128/EC.00124-10)
267. Ojo KK, Eastman R T, Vidadala R, Zhang Z, Rivas K L, Choi R, Lutz J D, Reid M C, Fox A M

- W, Hulverson M A, Kennedy M, Isoherranen N, Kim L M, Comess K M, Kempf D J, Verlinde C L M, Su X, Kappe S H I, Maly D J, Fan E, Van Voorhis W C. 2014 A specific inhibitor of pfcdpk4 blocks malaria transmission: Chemical-genetic validation. *J. Infect. Dis.* **209**, 275–284. (doi:10.1093/infdis/jit522)
268. Kao J P Y, Harootunian AT, Tsien R Y. 1989 Photochemically generated cytosolic calcium pulses and their detection by fluo-3. *J. Biol. Chem.* **264**, 8179–8184.
269. Malina H Z. 1999 Xanthurenic acid provokes formation of unfolded proteins in endoplasmic reticulum of the lens epithelial cells. *Biochem. Biophys. Res. Commun.* **265**, 600–5. (doi:10.1006/bbrc.1999.1716)
270. Murray A J. 2008 Pharmacological PKA inhibition: all may not be what it seems. *Sci. Signal.* **1**, re4. (doi:10.1126/scisignal.122re4)
271. Giembycz M A, Field SK. 2010 Roflumilast: First phosphodiesterase 4 inhibitor approved for treatment of COPD. *Drug Des. Devel. Ther.* **4**, 147–158. (doi:10.2147/DDDT.S7667)
272. Salhiyyah K, Senanayake E, Abdel-Hadi M, Booth A, Michaels J A. 2012 Pentoxifylline for intermittent claudication. *Cochrane database Syst. Rev.* **1**, CD005262. (doi:10.1002/14651858.CD005262.pub2)
273. Moreland R B, Goldstein I, Kim N N. 1999 Sildenafil Citrate , A Selective Phosphodiesterase Type 5 Inhibitor : Research and Clinical Implications in Erectile Dysfunction. **10**, 97–104.
274. Parasitology B, Parasitology C, Biology A. 1990 Possible roles of Ca²⁺ and cGMP as mediators of the exflagellation of Plasmodium berghei and Plasmodium falciparum. *Mol. Biochem. Parasitol.* **42**, 101–108.
275. Martin SK. 1978 Exflagellation. **242**, 239–242.
276. Ogwan'g R, Mwangi J, Gachihi G, Nwachukwu A, Roberts CR, Martin SK. 1993 Use of pharmacological agents to implicate a role for phosphoinositide hydrolysis products in malaria gamete formation. *Biochem. Pharmacol.* **46**, 1601–1606. (doi:10.1016/0006-2952(93)90329-U)
277. Ono T, Nakabayashi T. 1989 Gametocytogenesis induction in cultured Plasmodium falciparum and further development of the gametocytes to ookinetes in prolonged

- culture*. *Parasitol Res* **75**, 348–352. (doi:10.1007/BF00931129)
278. Zoraghi R, Kunz S, Gong K, Seebeck T. 2001 Characterization of TbPDE2A, a Novel Cyclic Nucleotide-specific Phosphodiesterase from the Protozoan Parasite *Trypanosoma brucei*. *J. Biol. Chem.* **276**, 11559–11566. (doi:10.1074/jbc.M005419200)
279. Arif SA, Poon H. 2011 Tadalafil: A long-acting phosphodiesterase-5 inhibitor for the treatment of pulmonary arterial hypertension. *Clin. Ther.* **33**, 993–1004. (doi:10.1016/j.clinthera.2011.06.008)
280. Kukreja RC, Salloum FN, Das A, Koka S, Ockaili RA, Xi L. 2011 Emerging new uses of phosphodiesterase-5 inhibitors in cardiovascular diseases. *Exp. Clin. Cardiol.* **16**, 30–35.
281. Naissant B, Dupuy F, Duffier Y, Lorthiois A, Duez J, Scholz J, Buffet P, Merckx A, Bachmann A, Lavazec C. 2016 Plasmodium falciparum STEVOR phosphorylation regulates host erythrocyte deformability enabling malaria parasite transmission. *Blood* **127**, blood-2016-01-690776. (doi:10.1182/blood-2016-01-690776)
282. Howard BL, Harvey K L, Stewart R, Azevedo M F, Crabb B S, Jennings I G, Sanders P R, Manallack D T, Thompson P E, Tonkin C J, Gilson P R. 2015 Identification of potent phosphodiesterase inhibitors that demonstrate cyclic nucleotide-dependent functions in apicomplexan parasites. *ACS Chem. Biol.* **10**, 1145–1154. (doi:10.1021/cb501004q)
283. Lourido S, Tang K, Sibley L D. 2012 Distinct signalling pathways control *Toxoplasma* egress and host-cell invasion. *EMBO J.* **31**, 4524–34. (doi:10.1038/emboj.2012.299)
284. Beghyn T, Hounsou C, Deprez BP. 2007 PDE5 inhibitors: An original access to novel potent arylated analogues of tadalafil. *Bioorganic Med. Chem. Lett.* **17**, 789–792. (doi:10.1016/j.bmcl.2006.10.069)
285. Baird JK, Hoffman SL. 2004 Primaquine therapy for malaria. *Clin. Infect. Dis.* **39**, 1336–1345. (doi:10.1086/424663)
286. Dechering K J, Thompson J, Dodemont HJ, Eling W, Konings RN. 1997 Developmentally regulated expression of pfs16, a marker for sexual differentiation of the human malaria parasite *Plasmodium falciparum*. *Mol. Biochem. Parasitol.* **89**, 235–244. (doi:S0166-6851(97)00123-0 [pii])
287. Desjardins R E, Canfield C J, Haynes J D, Chulay J D. 1979 Quantitative assessment of

- antimalarial activity in vitro by a semiautomated microdilution technique. *Antimicrob. Agents Chemother.* **16**, 710–718. (doi:10.1128/AAC.16.6.710)
288. Sannella A R, Olivieri A, Bertuccini L, Ferrè F, Severini C, Pace T, Alano P. 2012 Specific tagging of the egress-related osmiophilic bodies in the gametocytes of *Plasmodium falciparum*. *Malar. J.* **11**, 88. (doi:10.1186/1475-2875-11-88)
289. Lawrence H Bannister GM and JMH. 2005 Making a home for *Plasmodium* Post-genomics: Ultrastructural organisation of the blood stages. In *Molecular Approaches to Malaria*, pp. 24–29.(doi:10.1111/j.1462-2920.2007.01529.x)
290. Green JL, Moon R W, Whalley D, Bowyer P W, Wallace C, Rochani A, Nageshan R K, Howell S A, Ggrainger M, Jones H M, Ansell K H, Chapman T M, Taylor D L, Osborne S A, Baker D A Tatu U, Holder A A. 2016 Dependent Protein Kinase 1 Also Target Cyclic GMP-Dependent Protein Kinase and Heat Shock Protein 90 To Kill the Parasite at Different Stages of Intracellular Development. **60**, 1464–1475. (doi:10.1128/AAC.01748-15.Address)
291. Vidadala R S R, Ojo K K, Johnson S M, Zhang Z, Leonard S E, Mitra A, Choi R, Reid M C, Keyloun K R, Fox A M W, Kennedy M, Silver-Brace T, Hume J C C, Kappe S, Verlinde C L M J, Fan E, merritt E A, Voorhis W C V, maly D J. 2014 Development of potent and selective *Plasmodium falciparum* calcium-dependent protein kinase 4 (PfCDPK4) inhibitors that block the transmission of malaria to mosquitoes. *Eur. J. Med. Chem.* **74**, 562–73. (doi:10.1016/j.ejmech.2013.12.048)
292. Chapman TM, Osborne S A, Wallace C, Birchall K, Bouloc N, Jones H M, Ansell K H, Taylor D L, Clough B, Green J L, Holder A A. 2014 Optimization of an imidazopyridazine series of inhibitors of *plasmodium falciparum* calcium-dependent protein kinase 1 (PfCDPK1). *J. Med. Chem.* **57**, 3570–3587. (doi:10.1021/jm500342d)
293. Delves MJ, Ruecker A, Straschil U, Lelievre J, Marques S, Lopez-Barragan MJ, Herreros E, Sinden RE. 2013 Male and female *Plasmodium falciparum* mature gametocytes show different responses to antimalarial drugs. *Antimicrob. Agents Chemother.* **57**, 3268–3274. (doi:10.1128/AAC.00325-13)
294. Khan SM, Franke-Fayard B, Mair GR, Lasonder E, Janse CJ, Mann M, Waters AP. 2005 Proteome analysis of separated male and female gametocytes reveals novel sex-specific

Plasmodium biology. *Cell* **121**, 675–87. (doi:10.1016/j.cell.2005.03.027)

295. Suárez-Cortes P, Sharma V, Bertuccini K, Costa G, Bannerman N L, Sannella A R, Williamson K, Klemba M, Ievashina E A, Lasonder E, Alano P. 2016 Comparative proteomics and functional analysis reveal a role of *P. falciparum* osmiophilic bodies in malaria parasite transmission. *Mol. Cell. Proteomics* (doi:10.1074/mcp.M116.060681)